

PHASE INVERSION OF LIQUID-LIQUID DISPERSIONS
PRODUCED BY SHEAR OR TURBULENCE

by

IRINI EFTHIMIADU

Submitted to the Faculty of Engineering of the
University of Birmingham
for the degree of
DOCTOR OF PHILOSOPHY

School of Chemical Engineering
The University of Birmingham
Birmingham

April 1990

UNIVERSITY OF
BIRMINGHAM

University of Birmingham Research Archive

e-theses repository

This unpublished thesis/dissertation is copyright of the author and/or third parties. The intellectual property rights of the author or third parties in respect of this work are as defined by The Copyright Designs and Patents Act 1988 or as modified by any successor legislation.

Any use made of information contained in this thesis/dissertation must be in accordance with that legislation and must be properly acknowledged. Further distribution or reproduction in any format is prohibited without the permission of the copyright holder.

SYNOPSIS

The purpose of the research was the investigation of the phase-inversion phenomenon in liquid-liquid dispersions by examining the various parameters that could affect it, trying to understand its mechanism and draw some general conclusions on the behaviour of liquid-liquid dispersions in relation to it.

The experimental investigation of phase inversion was done by using two different methods to produce the liquid-liquid dispersions. In the first method, the dispersions were produced by shearing the liquids between two parallel plates, one rotating and the other being stationary. In the second method, the dispersions were produced by the turbulent flow of the liquids in a horizontal tube. Phase inversion was examined in relation to the properties of the liquids and the experimental conditions. It was observed visually in the first method and by examining the electrical conductivity of the dispersions in the second method.

Following a general introduction to the phenomenon of phase inversion, a literature review of previous research work on the phenomenon is presented first, together with some theoretical aspects related to it. A detailed description of the experimental methods and materials used is presented next, followed by a brief theoretical analysis of the mode of flow of the liquids in the two different methods used. Finally, the results and correlations obtained from the experimental investigation of phase inversion are presented, followed by a detailed discussion and the conclusions drawn.

To my Mother and the Memory of my Father

ACKNOWLEDGEMENTS

This thesis was submitted for the degree of Doctor of Philosophy. The experimental work was carried out in the laboratories of the School of Chemical Engineering at the University of Birmingham, during the period October 1986-June 1989.

I would like to acknowledge the help and support of a number of people:

- I would like to thank Dr. Iain P.T. Moore for the supervision of the work.
- I also thank all the technical staff who helped me, and the following in particular:

Mr. Peter Martin and Mr. Stan Ward for building the equipment;

Mr. Stan Clabon for making the glass parts of the equipment;

Mr. Bob Badham for taking the viscosity measurements;

Mrs Kate Dyster for helping me in general and with the interfacial tension measurements in particular;

Miss Gill Wheeler for helping me with the photographs taken;

Mr. Sid Chatwin for his general help and support in the lab.

- My special thanks to those of the Academic staff who helped me, and the following in particular:

Professor Alvin W. Nienow and the late Dr. Andrew Gilchrist for their critical suggestions;

Dr. Stuart Guy for his help in designing the settler;

Dr. K. Thyaniathy for his help with the computer-aided drawing package used.

- I thank the State Scholarships Foundation in Greece for sponsoring my postgraduate studies in the U.K.

I would also like to give my special thanks to my mother, my sister and my friend Georges for their love and constant support.

CONTENTS

	Page
1. INTRODUCTION	1
2. LITERATURE REVIEW	4
2.1. Theories on the Stability of Liquid-Liquid Dispersions and the Mechanism of Phase Inversion	4
2.2. Factors Affecting the Droplet Size of the Dispersed Phase in Liquid-Liquid Dispersions	8
2.2.1. Dispersed-Phase Droplet Size of Dispersions Produced by Shear	9
2.2.2. Dispersed-Phase Droplet Size of Dispersions Produced by Turbulence	10
2.3. Factors Affecting Phase Inversion of Liquid-Liquid Dispersions	12
2.3.1. Volumetric Ratio of the Liquids in Relation to the Mode of Preparation of the Dispersed System	14
2.3.2. Agitation or Rotational Speed	17
2.3.3. Density and Viscosity Differences between the Phases	18
2.3.4. Wettability of the Container Surfaces	22
2.3.5. Interfacial Tension	23
2.3.6. Temperature	25
2.3.7. Type and Concentration of the Emulsifying Agent	26
2.4. Mathematical Models of the Phase-Inversion Process	28
3. EXPERIMENTAL METHODS AND MATERIALS	37
3.1. Introduction	37
3.2. Description of the Apparatus and the Procedure	38
3.2.1. Parallel Shearing Plates	38
3.2.2. Horizontal Glass Tube	43
3.3. Materials and Operating Conditions	49
3.4. Measurement of the Physical Properties of the Liquid Phases	53
3.4.1. Interfacial Tension Measurement	53
3.4.2. Viscosity Measurement	56
3.4.3. Contact Angle Measurement	57
4. MODE OF FLOW OF LIQUIDS	61
4.1. Introduction	61
4.2. Flow Between Parallel Shearing Plates	61
4.2.1. Reynolds and Taylor Numbers	61
4.2.2. Shear Rate	65
4.2.3. Hydrodynamic Instabilities	66

	Page
4.3. Flow in a Horizontal Tube	69
4.3.1. Reynolds Number	69
4.3.2. Flow Patterns	70
5. RESULTS	72
5.1. Introduction	72
5.2. Effect of Different Factors on Phase-Inversion of Liquid-Liquid Dispersions Produced between Parallel Shearing Plates	72
5.3. Phase Inversion of Liquid-Liquid Dispersions Produced in the Horizontal Glass Tube	80
5.3.1. Effects of Total Flow Rate and Method of Introducing the Liquids at the Inlet of the Tube for the Liquid-Liquid Systems used	80
5.3.2. Comparison with Predictive Mathematical Models	82
6. DISCUSSION OF PHASE-INVERSION RESULTS	89
6.1. Introduction	89
6.2. Method of Parallel Shearing Plates	89
6.2.1. Effect of Viscosity Difference between the Liquids	89
6.2.2. Effects of Rotational Speed and Gap Width between the Plates	93
6.2.3. Effects of Interfacial Tension, Addition of an Emulsifying Agent and Density Difference between the Liquids	99
6.2.4. Effect of Wettability of the Material of Plates by the Liquid Phases	103
6.3. Method of the Horizontal Glass Tube	106
6.3.1. Effect of Total Flow Rate	106
6.3.2. Effects of Addition of an Emulsifying Agent and Density Difference between the Liquids	109
6.3.3. Effect of Wettability of the Horizontal Glass Tube by the Liquids	110
6.4. Comparison between the Two Methods	116
7. CONCLUSIONS	121
TABLES	126
FIGURES	147
APPENDICES	179
A1. Calibrations	180

	Page
A2. Equations	187
A2.1. Derivation of Equation 3.1	187
A2.2. Derivation of Equation 4.4	187
A3. Calculations	189
A3.1. Example of Calculation of Interfacial Tension Measured by the Drop-Weight Method	189
A3.2. Example of Calculation of Shear Stress at a Given Shear Rate from the Contraves Rheomat 30 Rheogram for the Estimation of Viscosity	190
A3.3. Calculation of Mean Value and Standard Deviation of Φ_i between the Parallel Shearing Plates	196
A3.4. Calculation of Mean Values and Standard Deviations of Φ_i and Total Flow Rate at the Point of Inversion in the Horizontal Glass Tube	198
A3.5. Calculation of the Factor $\cos\theta We^{-0.5} Re^{0.15}$ using Phase-Inversion Results in the Horizontal Glass Tube	201
NOTATION	203
REFERENCES	205
PLATES	

LIST OF TABLES

	Page
Table 1. Physical Properties of the Liquid-Liquid Systems used (Room Temperature) in the Parallel Shearing Plates Method.	127
Table 2. Physical Properties of the Liquid-Liquid Systems used (Room Temperature) in the Horizontal Glass Tube Method.	128
Table 3. Contact Angles of the Liquids used with the Materials of the Parallel Shearing Plates.	128
Table 4. Contact Angles of the Liquid-Liquid Systems used with the Materials of the Parallel Shearing Plates (Measured through the Aqueous Phase).	129
Table 5. Range of Reynolds Numbers for the Liquids used in the Parallel Shearing Plates Method.	130
Table 6. Range of Taylor Numbers for the Liquids used in the Parallel Shearing Plates Method.	131
Table 7. Shear Rates used in the Parallel Shearing Plates Method.	132
Table 8. Range of Reynolds Numbers for the Liquids used in the Horizontal Glass Tube Method.	132
Table 9. Volume Fraction of the Organic Phase at Inversion at Different Rotational Speeds and Various Gap Widths between Parallel Shearing Perspex Plates for the Liquid Paraffin-Water System.	133
Table 10. Volume Fraction of the Organic Phase at Inversion at Different Rotational Speeds and Various Gap Widths between Parallel Shearing Stainless Steel Plates for the Liquid Paraffin-Water System.	133
Table 11. Volume Fraction of the Organic Phase at Inversion at Different Rotational Speeds and Various Gap Widths between Parallel Shearing Glass Plates for the Liquid Paraffin-Water System.	134
Table 12. Volume Fraction of the Organic Phase at Inversion at Different Rotational Speeds and Various Gap Widths between Parallel Shearing Perspex Plates for the Liquid Paraffin - 60 ppm Tween 80 in Water System.	134
Table 13. Volume Fraction of the Organic Phase at Inversion at Different Rotational Speeds and Various Gap Widths between Parallel Shearing Perspex Plates for the Liquid Paraffin - 200 ppm Tween 80 in Water System.	135

	Page
Table 14. Volume Fraction of the Organic Phase at Inversion at Different Rotational Speeds and Various Gap Widths between Parallel Shearing Stainless Steel Plates for the Liquid Paraffin - 60 ppm Tween 80 in Water System.	135
Table 15. Volume Fraction of the Organic Phase at Inversion at Different Rotational Speeds and Various Gap Widths between Parallel Shearing Stainless Steel Plates for the Liquid Paraffin - 200 ppm Tween 80 in Water System.	136
Table 16. Volume Fraction of the Organic Phase at Inversion at Different Rotational Speeds and Various Gap Widths between Parallel Shearing Stainless Steel Plates for the 1% v/v Oleic Acid in Liquid Paraffin-Water System.	136
Table 17. Volume Fraction of the Organic Phase at Inversion at Different Rotational Speeds and Various Gap Widths between Parallel Shearing Stainless Steel Plates for the Dibutyl Maleate-Water System.	137
Table 18. Volume Fraction of the Organic Phase at Inversion at Different Rotational Speeds and Various Gap Widths between Parallel Shearing Glass Plates for the Dibutyl Maleate-Water System.	137
Table 19. Volume Fraction of the Organic Phase at Inversion at Different Rotational Speeds and Various Gap Widths between Parallel Shearing Stainless Steel Plates for the Dibutyl Maleate - 200 ppm Tween 80 in Water System.	138
Table 20. Volume Fraction of the Organic Phase at Inversion at Different Rotational Speeds and Various Gap Widths between Parallel Shearing Glass Plates for the Dibutyl Maleate - 200 ppm Tween 80 in Water System.	138
Table 21. Volume Fraction of the Organic Phase at Inversion at Different Rotational Speeds and 0.5 mm Gap Width between Parallel Shearing Stainless Steel Plates for the Dibutyl Maleate - 20% w/v CaCl_2 aq. soln. System.	139
Table 22. Volume Fraction of the Organic Phase at Inversion at Different Rotational Speeds and Various Gap Widths between Parallel Shearing Stainless Steel Plates for the Escaid-Water System.	139
Table 23. Volume Fraction of the Organic Phase at Inversion at Different Rotational Speeds and Various Gap Widths between Parallel Shearing Glass Plates for the Escaid-Water System.	140
Table 24. Volume Fraction of the Organic Phase at Inversion at Different Total Flow Rates in the Horizontal Glass Tube with the Aqueous Phase through the T-branch at the Inlet for the Escaid-Water System.	141

	Page
Table 25. Volume Fraction of the Organic Phase at Inversion at Different Total Flow Rates in the Horizontal Glass Tube with the Organic Phase through the T-branch at the Inlet for the Escaid-Water System.	142
Table 26. Volume Fraction of the Organic Phase at Inversion at Different Total Flow Rates in the Horizontal Glass Tube with the Aqueous Phase through the T-branch at the Inlet for the Escaid - 200 ppm Tween 80 in Water System.	143
Table 27. Volume Fraction of the Organic Phase at Inversion at Different Total Flow Rates in the Horizontal Glass Tube with the Organic Phase through the T-branch at the Inlet for the Escaid - 200 ppm Tween 80 in Water System.	144
Table 28. Volume Fraction of the Organic Phase at Inversion at Different Total Flow Rates in the Horizontal Glass Tube with the Aqueous Phase through the T-branch at the Inlet for the Escaid - 20% w/v CaCl_2 aq. soln. System.	145
Table 29. Volume Fraction of the Organic Phase at Inversion at Different Total Flow Rates in the Horizontal Glass Tube with the Organic Phase through the T-branch at the Inlet for the Escaid - 20% w/v CaCl_2 aq. soln. System.	146
Table A3.1. Table for Calculation of Shear Stress at Different Shear Rates for the Viscosity Measuring System of Co-Axial Cylinders.	194
Table A3.2. Table for Calculation of Shear Stress at Different Shear Rates for the Viscosity-Measuring System of Double-Gap.	195
Table A3.3. Example of Calculating the Mean Value and Standard Deviation of Φ_i between the Parallel Shearing Plates.	197
Table A3.4. Example of Calculating the Mean Values and Standard Deviations of Q_{Ti} and Φ_i in the Horizontal Glass Tube.	199
Table A3.5. Example of Calculating $\cos\theta\text{We}^{-0.5}\text{Re}^{0.15}$ at the Point of Inversion in the Horizontal Glass Tube.	202

LIST OF FIGURES

	Page
Figure 1. Schematic Diagram of the Continuous-Flow Emulsifying Machine of Parallel Shearing Plates.	148
Figure 2. Details of the System of Parallel Shearing Plates.	149
Figure 3. Schematic Diagram of the Continuous-Flow System of the Horizontal Glass Tube.	150
Figure 4. (a) Details of the Horizontal Glass Tube; (b) Details of the Electrical Connections with the Conductivity Probe.	151
Figure 5. Details of the Settler.	152
Figure 6. Interfacial Tension Measurement: (a) Platinum Ring Method; (b) Drop-Weight Method.	153
Figure 7. Viscosity Measurement: (a) Measuring System of Co-Axial Cylinders; (b) Double-Gap Measuring System.	154
Figure 8. Flow Behaviour of Liquid Paraffin at Room Temperature.	155
Figure 9. Flow Behaviour of Dibutyl Maleate at Room Temperature.	156
Figure 10. Flow Behaviour of Escaid at Room Temperature.	157
Figure 11. Contact Angle with a Solid Surface of: (a) a Liquid Drop; (b) a Liquid-Liquid Interface.	158
Figure 12. Immersed Plate Method of Measuring the Contact Angle with a Solid Surface of: (a) a Liquid; (b) a Liquid-Liquid Interface.	158
Figure 13. Volume Fraction of the Organic Phase at Inversion vs Rotational Speed for the Liquid Paraffin-Water System and Perspex Plates.	159
Figure 14. Volume Fraction of the Organic Phase at Inversion vs Rotational Speed for the Liquid Paraffin-Water System and Stainless Steel Plates.	160
Figure 15. Volume Fraction of the Organic Phase at Inversion vs Rotational Speed for the Liquid Paraffin-Water System and Glass Plates.	161
Figure 16. Volume Fraction of the Organic Phase at Inversion vs Rotational Speed for the Liquid Paraffin-Water System and Different Plates; $s = 0.1 \text{ mm} - 0.5 \text{ mm}$.	162

	Page
Figure 17.	163
Volume Fraction of the Organic Phase at Inversion vs Rotational Speed for Perspex Plates and the Systems:	
a. Liquid Paraffin-Water;	
b. Liquid Paraffin - 60 ppm Tween 80 in Water;	
c. Liquid Paraffin - 200 ppm Tween 80 in Water.	
Figure 18.	164
Volume Fraction of the Organic Phase at Inversion vs Rotational Speed for Stainless Steel Plates and the Systems:	
a. Liquid Paraffin-Water;	
b. Liquid Paraffin - 60 ppm Tween 80 in Water;	
c. Liquid Paraffin - 200 ppm Tween 80 in Water;	
d. 1% v/v Oleic Acid in Liquid Paraffin-Water.	
Figure 19.	165
Volume Fraction of the Organic Phase at Inversion vs Rotational Speed for the Systems:	
a. Dibutyl Maleate-Water with Stainless Steel Plates; ● s = 0.1 mm, ○ s = 0.5 mm;	
Dibutyl Maleate - 200 ppm Tween 80 in Water with Stainless Steel Plates; ◆ s = 0.1 mm, ◇ s = 0.5 mm;	
b. Dibutyl Maleate-Water with Glass Plates;	
■ s = 0.5 mm, □ s = 1 mm;	
Dibutyl Maleate - 200 ppm Tween 80 in Water with Glass Plates; ● s = 0.5 mm, ○ s = 1 mm;	
c. Dibutyl Maleate - 20% w/v CaCl_2 aq. soln. with Stainless Steel Plates; x s = 0.5 mm.	
Figure 20.	166
Volume Fraction of the Organic Phase at Inversion vs Rotational Speed for the Escaid-Water System and	
a. Stainless Steel Plates; ● s = 0.1 mm, ■ s = 1 mm,	
b. Glass Plates; ○ s = 0.2 mm, ◇ s = 0.5 mm	
c. Glass Plates; □ s = 1 mm.	
Figure 21.	167
Volume Fraction of the Organic Phase at Inversion vs Gap Width between the Plates/Radius of Plates for the Liquid Paraffin-Water System and Perspex Plates.	
Figure 22.	167
Volume Fraction of the Organic Phase at Inversion vs Gap Width between the Plates/Radius of Plates for the Liquid Paraffin-Water System and Stainless Steel Plates.	
Figure 23.	168
Volume Fraction of the Organic Phase at Inversion vs Gap Width between the Plates/Radius of Plates for the Liquid Paraffin-Water System and Glass Plates.	
Figure 24.	168
Volume Fraction of the Organic Phase at Inversion vs Gap Width between the Plates/Radius of Plates for the Escaid-Water System and Glass Plates.	
Figure 25.	169
Volume Fraction at Inversion of the Dispersed Phase of the less Preferred Type of Dispersion at High Taylor Numbers vs $\cos\theta$ (θ measured through the phase that preferentially wetted the material of the plates).	
Figure 26.	170
Dependence of the Slope of the Lines in Figure 25 on Interfacial Tension.	

	Page
Figure 27. Volume Fraction of the Organic Phase at Inversion vs Total Flow Rate in the Horizontal Glass Tube with the Aqueous Phase through the T-branch for the Escaid-Water System.	171
Figure 28. Volume Fraction of the Organic Phase at Inversion vs Total Flow Rate in the Horizontal Glass Tube with the Organic Phase through the T-branch for the Escaid-Water System.	172
Figure 29. Volume Fraction of the Organic Phase at Inversion vs Total Flow Rate in the Horizontal Glass Tube with the Aqueous Phase through the T-branch for the Escaid - 200 ppm Tween 80 in Water System.	173
Figure 30. Volume Fraction of the Organic Phase at Inversion vs Total Flow Rate in the Horizontal Glass Tube with the Organic Phase through the T-branch for the Escaid - 200 ppm Tween 80 in Water System.	174
Figure 31. Volume Fraction of the Organic Phase at Inversion vs Total Flow in the Horizontal Glass Tube for the Escaid - 20% w/v CaCl_2 aq. soln.: a. Aqueous Phase through the T-branch; ● Inversion from O/W to W/O dispersion; ○ Inversion from W/O to O/W dispersion; b. Organic Phase through the T-branch; ■ Inversion from O/W to W/O dispersion; □ Inversion from W/O to O/W dispersion.	175
Figure 32. Volume Fraction of the Organic Phase at Inversion vs $\cos\theta\text{We}^{-0.5}\text{Re}^{0.15}$ for the Escaid-Water System in the Horizontal Glass Tube.	176
Figure 33. Volume Fraction of the Organic Phase at Inversion vs $\cos\theta\text{We}^{-0.5}\text{Re}^{0.15}$ for the Escaid - 20% w/v CaCl_2 aq. soln. System in the Horizontal Glass Tube.	177
Figure 34. Volume Fraction of the Organic Phase at Inversion vs $\cos\theta\text{We}^{-0.5}\text{Re}^{0.15}$ for the Escaid - 200 ppm Tween 80 in Water System in the Horizontal Glass Tube.	178
Figure A1.1. Calibration of Rotational Speed Control Box (Variac) in the Parallel Shearing Plates Method.	181
Figure A1.2. Calibration of the Smaller Rotameter for Liquid Paraffin in the Parallel Shearing Plates Method.	182
Figure A1.3. Calibration of the Bigger Rotameter for Liquid Paraffin in the Parallel Shearing Plates Method.	183
Figure A1.4. Calibration of Rotameter for Dibutyl Maleate in the Parallel Shearing Plates Method.	184
Figure A1.5. Calibration of Rotameter for Escaid in the Parallel Shearing Plates Method.	185

	Page
Figure A1.6. Calibration of Rotameter for Escaid in the Horizontal Glass Tube Method.	186
Figure A3.1. Rheogram for Liquid Paraffin.	191
Figure A3.2. Rheogram for Dibutyl Maleate.	192
Figure A3.3. Rheogram for Escaid.	193
Figure A3.4. Example of Change in Conductivity at the Point of Inversion from O/W to W/O Dispersion in the Horizontal Glass Tube.	200
Figure A3.5. Example of Change in Conductivity at the Point of Inversion from W/O to O/W Dispersion in the Horizontal Glass Tube.	200

LIST OF PLATES

- Plate 1. The Continuous-Flow Emulsifying System of Parallel Shearing Plates.
- Plate 2. The Continuous-Flow Emulsifying System of Parallel Shearing Plates under Operation.
- Plate 3. A Typical Example of the Formation of an Oil-in-Water Dispersion in the System of Parallel Shearing Plates.
- Plate 4. A Typical Example of the Formation of a Water-in-Oil Dispersion in the System of Parallel Shearing Plates.
- Plate 5. Phase Inversion of the Liquid Paraffin-Water System with Stainless Steel Plates, $s = 0.1$ mm and $N = 1970$ rpm:
(a) Oil-in-Water Dispersion before Phase Inversion;
(b) Water-in-Oil Dispersion after Phase Inversion.
- Plate 6. The Continuous-Flow System of the Horizontal Glass Tube.
- Plate 7. A Typical Example of Phase Inversion in the Horizontal Glass Tube:
(a) Oil-in-Water Dispersion at the Point of Inversion;
(b) Water-in-Oil Dispersion after Inversion.
- Plate 8. A Typical Example of Phase Inversion in the Horizontal Glass Tube:
(a) Water-in-Oil Dispersion at the Point of Inversion;
(b) Oil-in-Water Dispersion after Inversion.

1. INTRODUCTION

The application of external energy to a mixture of two immiscible liquids leads to the breakup of one liquid into droplets surrounded by the other liquid, forming a liquid-liquid dispersion. The liquid which is in the form of droplets is known as the dispersed phase and the continuum liquid is known as the continuous phase.

In general the term "dispersion" is given to an unstable dispersion in which the phases start separating as soon as the supply of external energy is stopped. A relatively stable liquid-liquid dispersion, which exists even after stopping the supply of external energy, is called an "emulsion". Such a system usually contains a third component, such as a surface-active agent or finely-divided solids, which increases the stability of the system by interfacial action and is known as an emulsifier or emulsifying agent.

The most common method of producing a liquid-liquid dispersion is agitation, which is used for example in liquid-liquid extraction, in devices such as multiple mixer-settlers or counter-current contactors (Sarkar et al., 1980). The breakup of the dispersed phase in agitated systems occurs in the turbulent shear field of the agitator. Since the intensity of the turbulence is not uniform throughout the agitated vessel, colliding droplets may coalesce in the regions of lower intensity and the larger droplets formed will again be sheared and broken up on passing to regions of higher intensity. A dynamic equilibrium between dispersion and coalescence is eventually reached wherein a droplet-size distribution is established throughout the vessel. Besides the conventional agitated vessels, liquid-liquid dispersions can also be produced in static and motionless mixers by the turbulent flow of the two liquid phases in a tube filled with packing material (Tidhar et al., 1986).

Other methods of forming liquid-liquid dispersions are those used in practice for the production of emulsions in devices such as colloid mills and homogenizers (Becher, 1959). In an homogenizer the dispersion is formed by forcing the mixture of liquids to be emulsified through a small orifice under very high pressure. In the standard colloid mill, emulsification is carried out by the shearing action imparted to the liquids when they are forced between two shearing plates, one rotating and one stationary.

In a liquid-liquid system there are two types of dispersion formed depending on the conditions of the system. Usually one of the two immiscible liquids is either water or an aqueous solution and the other one is an organic liquid. When the organic phase is dispersed in the aqueous phase, the dispersion formed is known as an oil-in-water dispersion. When the organic phase is the continuous one, the dispersion is of the water-in-oil type. The phenomenon of the transition from one phase being dispersed to the other is known as phase inversion. When more and more dispersed phase is added to a constant volume of the continuous phase, a point is eventually reached at which the addition of more dispersed phase causes phase inversion to occur. The continuous phase becomes dispersed and the original dispersed phase becomes continuous.

There are many factors affecting the type of dispersion and hence the phase-inversion point, besides the volumetric ratio of the two phases. The method of preparation of the dispersion as well as the various characteristics of the apparatus used, such as the number, shape and position of the impellers in an agitated vessel, the gap width between the plates in a colloid mill or the wettability of the surfaces of the vessel or the plates, exert an influence on the type of dispersion formed. Other important factors are the agitation or rotational speed and the various physical and physico-chemical

properties of the liquids, such as interfacial tension, density and viscosity differences between them as well as the chemical composition and the concentration of the emulsifying agent in the case of emulsions.

Phase inversion is a kind of instability with regard to type of dispersion. It may occur whenever the equilibrium between coalescence and redispersion shifts towards coalescence. Since the stability of the dispersion is least at the phase-inversion point, the phenomenon may be very important in practice. In liquid-liquid extraction in which liquid-liquid dispersed systems are used for speeding up mass transfer between two or more immiscible liquids, phase inversion may effectively be used for the separation of the liquids. On the other hand, in the creation of dispersions in which the opposite effect is desired, a knowledge of the phase-inversion point will enable inversion to be avoided to ensure that the preferred direction of mass transfer is maintained.

In the preparation of many commercial emulsions the knowledge of the phase-inversion point is very important so that the preferred type of emulsion can be produced at any time. It is reported, however, that phase inversion might eventually result in a more stable emulsion based on the fact that emulsions with smaller average particle size were produced by initially preparing the "wrong" type of emulsion and inducing inversion to the desired type by addition of the phase which would ultimately be the continuous one (Becher, 1959).

The importance of the phase-inversion phenomenon has given rise to a considerable amount of work investigating the various parameters which exert an influence on it, so trying to understand the physical mechanism whereby the actual process is carried out and develop mathematical models to predict it. The phenomenon however was not well understood in many respects.

2. LITERATURE REVIEW

2.1. Theories on the Stability of Liquid-Liquid Dispersions and the Mechanism of Phase Inversion

The production of a liquid-liquid dispersion is a result of two competing processes, a breaking-up process and a coagulating process.

The first process consists of the mutual pulverization of the two liquid phases by the formation and subsequent disruption into drops of lamellae and threads of one liquid in the other, either by flow processes or by impact of liquid masses against each other or the walls of the container. In this stage, the dissipation of mechanical energy in the system gives rise to hydrodynamic problems of great complexity which can be better discussed in terms of dynamical quantities like inertial, viscous or surface forces, rather than in terms of thermodynamical parameters like the interfacial energy. The interfacial disruption is a "fast" process in that it occurs in time intervals of the order of seconds or less and that might be the reason why the dispersion processes have not been studied so well as the coagulation kinetics.

The second major process, which occurs simultaneously and subsequently to the breaking-up process, is the coagulation or reunion of the drops of the dispersed phase to form the continuous phase. A liquid-liquid dispersion is thermodynamically unstable and this second process is the natural one. The first step in the coagulation of any dispersed system is a collision process irrespective of consideration of free surface energy. The collision frequency depends on the magnitude of the motion of the drops of the dispersed phase and on the initial separation of the drops, which in turn depends on the

concentration of the dispersed phase. It is to be noted that fine subdivision of the dispersed phase, as is achieved by modern emulsifying machines, introduces randomized motion of the droplets, which is a factor tending to maintain uniform distribution but also increases the probability of encounters between the droplets. The second step of the coagulating process is the adherence of the droplets to each other by the simultaneous draining of the continuous phase film trapped between them, in which each droplet maintains its individuality. The third step which follows collision and adherence is the actual coalescence process which consists of the rupture of the interfacial film and flow of one droplet's content into the other droplet as a result of the elimination of the free interfacial energy.

The type of the dispersion produced must therefore be considered in terms of rates of formation of the two types of dispersion as well as their rates of breaking once formed. Most theories suggest that since the coalescence kinetics are responsible for the stability of a liquid-liquid dispersion, they are also responsible for the type of dispersion formed. In some cases, however, the hydrodynamics of formation play a dominant role in the production of a particular type of dispersion.

The phase-inversion phenomenon, although a subject of considerable investigation, is not well understood in many respects. The most important difficulty resides in the purely conceptual problem of a physical mechanism whereby the phase-inversion process is carried out.

Clowes (1916) presented a widely reproduced diagrammatic representation of the inversion process by following the actual inversion of an oil-in-water dispersion by means of a microscope (Clayton, 1954). The process was initiated by the droplets of the dispersed phase becoming distorted and

elongated near the critical point, while the Brownian motion was very prominent at that stage. At the critical point, larger masses of both phases were in very active movement, probably due to the existence of two continuous phases. When the critical point was passed, the dispersion mainly contained large droplets of the previous continuous phase surrounded by the new continuous phase, while there were still small droplets of the new continuous phase in the drops of the new dispersed phase exhibiting rapid Brownian motion. The phase inversion was regarded as complete when the particular Brownian motion entirely ceased.

Most workers tried to explain the stability of a particular type of dispersion and the mechanism of phase inversion in relation to the action of an emulsifying agent in the interface. The emulsifying agent acted as an energy barrier against coalescence of the drops on collision, so that coalescence would occur only when the momentum of the colliding droplets exceeded the value of the energy barrier. For a substance to act as an emulsifying agent, it should necessarily be adsorbed in the interface and form a coherent interfacial film. The dispersing and the stabilizing effects of that film might have been due, in some extent, to the lowering of the interfacial tension between the phases but the nature of the adsorbed film itself was the most important factor which might depend on the mechanical or electrical properties of the film. According to Clowes, emulsion equilibrium depended on the relative proportions of positive and negative ions adsorbed by the interfacial film so that when negative ions were in excess the oil-in-water type of dispersion was favoured whereas an excess of positive ions had the reverse effect (Clayton, 1954).

Schulman and Cockbain (1940) suggested the formation of inter-molecular complexes of certain types at the oil/water interface as an important factor

in connection with the formation and stability of a particular emulsion type. The complex should consist of at least two components, one of which is appreciably soluble in the aqueous phase and the other one appreciably soluble in the organic phase and it should be a stable one. In relation to that suggestion they presented a somewhat more realistic picture of the mechanism of the phase-inversion process than Clowes for the case of inversion of the oil-in-water type to the water-in-oil one. They suggested that the condition necessary for the formation of oil-in-water emulsions was the interfacial film to be in the liquid condensed state and electrically charged. In order to produce phase inversion of such emulsions, the electric charge on the organic droplets had to be removed first, whereupon the oil-in-water emulsion broke by making coagulation of the droplets possible. In that case it was assumed that amounts of the aqueous phase were trapped among the clumped organic droplets and if, in addition, the compositions of the aqueous and organic phases were such as to enable an uncharged "inter-linked" solid condensed film to be formed at the interface, then an inversion process would occur with the formation of a water-in-oil emulsion. Schulman and Cockbain also observed the irregular shapes of the aqueous droplets under the microscope, appearing to be contained in "sacks" and they attributed that appearance to the rigid nature of the film surrounding the aqueous droplets. On the other hand, they observed that all oil-in-water emulsions contained completely spherical droplets, due to the interfacial film being in the liquid condensed state, so that the organic droplets could easily regain their spherical shape after being deformed in any way. However, those observations cannot be generalized since perfectly spherical droplets have been frequently observed in water-in-oil emulsions.

Despite the stabilizing effect of the interfacial film produced by the emulsifying agent, there might be some other factors that can stabilize a particular type of dispersion even without the presence of the emulsifying

agent. Some workers pointed out the effect of viscosity and molecular structure of the organic phase at the interface determining the type of dispersion formed. According to Clayton (1954), the coalescence of droplets in water-in-oil dispersions could be retarded by a high viscosity of the continuous phase by reducing the chances of contact between the droplets and producing a rigid viscous film between the phases. Speakman and Chamberlain (1933) suggested that the type of dispersion formed in any particular instance would depend, among other things, on the cybotactic state of the liquids concerned so that a well-developed structure of one of the phases would oppose dispersion and the other phase would become the dispersed phase whereas little structure present would not resist dispersion.

All the theories on the stability of a liquid-liquid dispersion and the mechanism of phase inversion are limited and most of them are concerned with the effect of the presence of an emulsifying agent. Little or no work has been done to explain the way in which the actual phase-inversion process is carried out in the simplest case of no emulsifying agent being present.

2.2. Factors Affecting the Droplet size of the Dispersed Phase in Liquid-Liquid Dispersions

The major parameter which is directly related to the equilibrium between breakup and coalescence of the dispersed phase in a liquid-liquid dispersion, determining its dynamic stability, is the droplet size of the dispersed phase. Since phase inversion is the result of breaking the dynamic stability of a certain type of dispersion by stabilizing the opposite type, it was considered important to examine the factors which affect the dispersed phase droplet size of these dispersions.

Since the droplet size of a dispersion depends on the mechanism of formation of the dispersion, the two different mechanisms of shear and turbulent flows are examined separately.

2.2.1. Dispersed-Phase Droplet Size of Dispersions Produced by Shear

Fundamental work on the breaking up of drops in viscous shear flow was done by Taylor (1932, 1934) and Tomotika (1936). It was then revised and continued by Hinze (1955) and Rumscheidt and Mason (1961).

According to their theories justified by their experimental results, when an originally spherical drop was placed in the shear flow of the continuous phase, it was deformed into an ellipsoid before it burst. The drop was deformed in such a way that the stresses generated by the shear flow were balanced by the interfacial tension. It was then concluded that when the maximum pressure difference across the interface, which was generated by the shear stresses and tended to disrupt the drop, exceeded the force due to interfacial tension which tended to hold it together, the drop would burst. When deviations from the spherical shape were neglected, the above suggestions led to the following equation at the breaking up point:

$$\dot{\gamma} \mu_c f(p) > \frac{\sigma}{d}$$

where d : drop size;
 σ : interfacial tension;
 $\dot{\gamma}$: shear rate;
 μ_c : viscosity of the continuous phase;
 μ_d : viscosity of the dispersed phase;
 p : μ_d/μ_c ;

$$f(p): \frac{19p + 16}{16p + 16}$$

Consequently, the maximum droplet size d_{\max} which could resist disruption was given by the equation:

$$d_{\max} = \frac{\sigma}{\gamma \mu_c} \left(\frac{16\mu_d/\mu_c + 16}{19\mu_d/\mu_c + 16} \right) \quad (2.1)$$

Equation (2.1) is based on the suggestions of Taylor (1932,1934) and Tomotika (1936), who examined the breakup of a single drop in shear flow. It does not take into account the volume fraction of the dispersed phase in a dispersion and therefore the interactions between drops which might lead to coalescence. In cases, however, where the hydrodynamics of formation is the dominant factor in the production of a dispersion, the basic model of d_{\max} given by Equation 2.1 can be used to give at least a qualitative picture of the most important parameters affecting the dispersed-phase droplet size in shear flow. It should be noted that elongational flow can also have an important influence on the deformation of the drop (Hinze, 1955), although it is not examined in the present work.

2.2.2. Dispersed-Phase Droplet Size of Dispersions Produced by Turbulence

The theoretical analysis of breakup of drops by turbulent forces was developed by Kolmogoroff (1949) and Hinze (1955). It was then improved and verified by various workers who used experimental results of dispersions produced by agitation (Vermeulen et al., 1955 - Calderbank, 1958 - Coualaloglou and Tavlarides, 1976 - Mersmann and Grossman, 1982 - Davies, 1985, 1987) or turbulent flow in pipes (Sleicher, 1962 - Middleman, 1974).

According to Hinze (1955), the dynamic pressure forces arising from the turbulent velocity fluctuations were the factor determining the size of the largest drops. The dynamic pressure forces tending to break up the drops

would be opposed by both the viscosity of the dispersed phase and the interfacial tension of the liquids. When the dispersed-phase viscosity was low it could be neglected and the maximum droplet size which could resist breakup was given by the following equation:

$$\frac{4\sigma}{d_{\max}} = \rho_c (v')^2$$

where v' : turbulent fluctuation velocity;
 ρ_c : density of the continuous phase;
 σ : interfacial tension.

In the simplest case of isotropic and homogeneous turbulence, there is a range of turbulent eddy spectrum where the Kolmogoroff energy distribution law is valid and the main contribution to the kinetic energy is made by the moderate sized, "energy-containing" eddies. It was shown by Hinze (1955) that in that case the turbulent fluctuation velocity was given by the following equation:

$$v' \propto (\epsilon d_{\max})^{2/3}$$

where ϵ : energy dissipation rate per unit mass. Therefore, assuming isotropic and homogeneous turbulence, d_{\max} was given by the equation:

$$d_{\max} \propto (\sigma/\rho_c)^{3/5} \epsilon^{-2/5} \quad (2.2)$$

Equation (2.2) was only valid when the viscosities of the two liquids were not very different and when the volume fraction of the dispersed phase was small. By taking into account the viscous resistance of the drop to breakup, Davies (1985,1987) modified Equation 2.2 to:

$$d_{\max} \propto (\sigma + \beta \mu_d v')^{3/5} \rho_c^{-3/5} \epsilon^{-2/5} \quad (2.3)$$

where μ_d : viscosity of the dispersed phase
 β : an arithmetical factor of the order unity.

With an increasing volume fraction of the dispersed phase, the droplet size was no longer completely controlled by breakup. On the one hand, there was damping of the turbulence intensity by the dispersed drops, and on the other hand, there was increasing coalescence between the drops. Both effects led to an increase in the maximum droplet size of the dispersed phase and Equation 2.2 was modified (Mersmann and Grossman, 1982) to:

$$d_{\max} \propto (\sigma/\rho_c)^{3/5} \epsilon^{-2/5} (1+c\Phi) \quad (2.4)$$

where Φ : volume fraction of the dispersed phase
 $c \approx 3$.

The assumption of isotropic turbulence is usually valid in the region of wave lengths comparable to the size of the largest drops (Hinze, 1955). The assumption of homogeneous turbulence is valid in turbulent pipe flow and it can also be valid locally in agitated vessels where the dispersion is assumed to occur in a small volume around the impeller (Davies, 1987). Therefore, Equation 2.2 and its modifications (Equations 2.3 and 2.4) give a good representation of the parameters affecting the droplet size of the dispersed phase in turbulent flow.

2.3. Factors Affecting Phase Inversion of Liquid-Liquid Dispersions

The complexity of the phase-inversion phenomenon gave rise to a considerable amount of experimental work investigating the various physical and physico-chemical parameters of different liquid-liquid dispersed systems that might influence the type of dispersion formed and the phase-inversion

point, in an attempt to understand the phenomenon.

Most of the workers tried to examine phase inversion using a mixing vessel, with various kinds and numbers of agitators, in which the dispersion was produced by the breakup of one of the phases in the turbulent shear-field of the agitator. The phase-inversion point was determined either by visual observation and simultaneous use of photographic techniques or by measuring the electrical conductivity of the continuous phase.

There were a few workers, however, who used devices other than mixing vessels, such as simple flasks shaken vigorously by hand or mechanically, with subsequent observation of the coalescence process after stopping the mixing, or the laboratory scale continuous-flow emulsifying machine used by Davies (1960). In that type of machine the dispersion was produced by shearing action between two parallel plates one of which was rotating, the other one being stationary, and the phase-inversion point was determined by visual observation of the continuous phase on a window made of perspex against which the produced dispersion was flung out continuously.

Some workers such as Tidhar et al. (1986) examined the phase-inversion phenomenon in static or motionless mixers in which the dispersion was produced by the flow of the two immiscible liquids against solid elements, made of various materials, packed in a long narrow tube. In that case the phase-inversion point was determined by measuring the conductivity of the aqueous phase by an electroconductivity method.

The parameters investigated by these workers included the volumetric ratio of the two phases in relation to the method of preparation of the dispersion, the agitation or rotational speed, the density and viscosity

differences between the phases, the wettability of the container surfaces, the interfacial tension between the phases, the temperature of the system and the type and concentration of the emulsifying agent in the case of the preparation of emulsions.

2.3.1. Volumetric Ratio of the Liquids in Relation to the Mode of Preparation of the Dispersed System

There is always a volumetric ratio, which can be either one value or a limit of a range of values, of the two immiscible liquids in a dispersed system below or above which there is only one of the liquids that can be the continuous phase, the other one being the dispersed phase, and this is the point of phase inversion.

Traditionally theoretical studies on the phase-volume relationship at the point of inversion have been based either on energy changes or geometric configurations of the spherical droplets of the dispersed phase. In the former case, the frequently quoted value of 0.5 for the volume fraction at inversion assumes minimisation of surface energy as an inversion criterion and equality of drop size distribution before and after inversion. In the latter case, limits are considered of a configuration of spheres or deformed spheres which can exist without the spheres touching each other(Yeh et al.,1964).

It has been observed by many workers that it is very difficult to produce a dispersion containing more than 75% by volume of the dispersed phase. In the range from 25% to 75% by volume either phase can be dispersed depending on the other conditions. The presumption behind this is that the closest packing of spherical droplets of the dispersed phase occurs when the dispersed volume fraction is about 74% of the total volume. In reality the droplets are not

necessarily spherical and of equal size, and dispersions with higher volume fractions of the dispersed phase can be obtained (Clayton, 1954).

The range of phase-volume ratios in which phase inversion may occur is called the "ambivalent region" and it was observed by all the workers who used mixing vessels to produce the dispersed system. The limits of the ambivalent region, however, were influenced by the various factors affecting the type of dispersion.

The best way of representing the phase inversion graphically was plotting the volume fraction of one phase, normally the organic phase, at inversion against agitation speed. The existence of an hysteresis effect was observed, represented graphically by the two inversion curves defining the ambivalent region. In between the two curves, either phase could be dispersed depending on the manner by which the dispersion was initiated. Thus, when at a constant agitation speed the organic liquid was added to a constant volume of water, an oil-in-water dispersion was produced until inversion took place on reaching the upper inversion curve. Conversely, on adding water to a constant volume of organic phase, a water-in-oil dispersion was produced and inversion was indicated by the lower inversion curve. The system could only exist as water-in-oil dispersion above the upper curve and as oil-in-water dispersion below the lower curve.

McClarey and Mansoori (1978) observed the existence of an intermediate inversion curve which was determined by adding certain volumes of both immiscible liquid phases to the mixing vessel and initiating the mixing of the two phases from rest. They produced their results by eliminating the effect of the position and number of the agitators on the phase inversion using a large number of impellers placed at equal distances from the liquid-liquid

interface while at rest, both in the upper and in the lower parts of the mixing vessel. For small number of impellers the phase inversion was dependent on the number of the impellers, and with only one impeller the phase in which the impeller was placed while at rest was the continuous phase during the mixing, provided that the volumetric ratio of the two phases was within the ambivalent region.

Gilchrist et al. (1989) observed that the resulting phase inversion of liquid-liquid dispersions in stirred vessels at the corresponding phase-volume ratio was also a function of time. They observed a delay in phase inversion, when a small increment of the dispersed phase, sufficient to cause inversion at their operating conditions, was added to a system already close to inversion. The delay period depended on the experimental conditions, such as agitation speed, liquid height and baffle-gap. They attributed the phenomenon to the inhomogeneity of turbulence causing different coalescence rates at different regions of the stirred vessel.

Many workers pointed out that the method of preparation of the dispersion had a profound influence on the type of dispersion (Dickinson and Iball, 1948 - Davies, 1960). For instance, mechanical mixing with an impeller gave quite different results from those obtained by passing the liquids through a homogenizer or a colloid mill. Cheesman and King (1938) found that the type of dispersion obtained could be determined by the method of shaking, other conditions being constant.

Davies (1960) reported that the continuous-flow emulsifying system he used had the characteristic of giving the same results with respect to the phase-inversion point no matter from which side that point was approached. Since that system was operated under conditions of continuous flow, certain

volumes of both phases were fed into the system at the same time, so that Davies' inversion curve could be compared to the intermediate inversion curve observed by McClarey and Mansoori. The mode of operation of that machine was such that no ambivalent region could be observed.

Tidhar et al. (1986) reported on a basic difference between dispersions formed in motionless mixers and in conventional mixing vessels, the width of the ambivalent region being much narrower in motionless mixer operations. They pointed out however that in that case the ambivalent region was not a zone where the type of dispersion depended on the way the zone was approached but it rather indicated a region where continuity oscillated from one phase to the other.

2.3.2. Agitation or Rotational speed

Most of the workers who studied phase inversion in mixing vessels agreed that the volume fraction of the oil phase at inversion varied inversely with agitation speed, so that the stable dispersion at low agitation speeds was of the oil-in-water type and as the agitation speed was increased, the system would invert to the water-in-oil type. Hossain et al. (1983) explained the phenomenon in terms of a considerably increased rate of coalescence at high energy input overriding the tendency for smaller mean drop sizes to exist.

Davies' results (1960) for the continuous-flow emulsifying system gave the same kind of dependence of phase inversion on rotational speed.

Quinn and Sigloh (1963) observed that the volume fraction of the organic phase at inversion became constant at high agitation speeds which indicated that the rate of dispersion was the controlling factor at high speeds.

Luhning and Sawistowski (1971) also reported a strong indication of the inversion curves tending asymptotically to a constant value with increasing agitation speed.

The range of agitation speeds used by most of the workers in mixing vessels was chosen to be that of the turbulent mixing regime of the systems studied. McClarey and Mansoori (1978) used a lower range of agitation speeds and observed abrupt changes in the slopes of the intermediate and lower inversion curves of the ambivalent region, suggesting that the phenomenon could be due to transition from laminar mixing to turbulent mixing. They also observed a slight rise, instead of the expected fall, of the upper inversion curve which was insensitive to transition in mixing regimes.

The results of the effect of agitation speed on phase inversion in mixing vessels were obtained with the system starting from rest for each agitation speed. Selker and Sleicher (1964) found that once a dispersion was formed, changing agitation speed without stopping mixing would not cause phase inversion to occur.

2.3.3. Density and Viscosity Differences Between the Phases

Treybal (1951) noted that a large density difference between the phases made the dispersion more difficult to achieve and the same was observed by McClarey and Mansoori (1978) who also reported an uncertainty range of inversion which was diminished when the density difference between the phases was removed.

Rodger et al. (1956) also reported that phase inversion occurred most readily in systems favouring oil-in-water dispersions in which the ratio of

the difference in densities of the phases to the continuous-phase density was large.

Luhning and Sawistowski (1971) noted that at higher speeds a mixture consisting of equal volumes of the two liquids always had the denser liquid as the continuous phase.

Treybal also noted that in immiscible liquid mixtures high viscosity of one of the liquids favoured its forming the continuous phase and hindered coalescence of the dispersed phase by decreasing the rate at which the thin film between drops was removed. The equations developed by some workers (Calderbank, 1958 - Davies, 1985) for the dependence of droplet size of liquid-liquid dispersions on the viscosities of both phases gave a decrease in interfacial area of the dispersed phase with increased dispersed-phase viscosity while an increased continuous-phase viscosity had the opposite effect.

Rodger et al. (1956), however, found that the interfacial area of the dispersed phase was increased slowly with increasing dispersed-phase viscosity. Also, Selker and Sleicher (1965) observed that as the viscosity of a phase increased, its tendency to be dispersed increased as well. They also concluded that the ambivalent region was primarily a function of the viscosity ratio and it was not strongly dependent on vessel characteristics or agitation speed.

McClarey and Mansoori (1978) made experiments using immiscible liquids with the same density and viscosity in order to single out the effect of the viscosity difference on the type of dispersion. They found that in the absence of viscosity difference between the phases, the intermediate inversion

curve was located at the equivolume line for all the impeller speeds reported and they concluded that any deviation of the curve from the equivolume location was indeed due to the viscosity difference between the immiscible liquid phases only, the deviation being always towards higher volume fractions of the more viscous phase. The upper and the lower inversion curves however were not situated at the close-packed locations, as it was previously assumed, and there was an asymmetry between them with respect to the equivolume line, the reason being some other factor or factors involved.

Dickinson and Iball (1948) tried to examine the effect of viscosity of the organic phase on the type of dispersion by shaking the two phases together with an emulsifier to produce stable emulsion. They observed differences in the behaviour of the dispersed system when the viscosity of the organic phase was increased, which were attributed to two main factors, the purely hydrodynamic effect of viscosity on the emulsification process, and the effect of increased viscosity of the organic phase in retarding the diffusion of the emulsifier to the interface during emulsification.

Davies (1960) examined the effect of viscosity on the phase-inversion point in his continuous-flow emulsifying machine and he observed that the increased viscosity of the organic phase increased its tendency to be dispersed but that tendency was decreased at high viscosities. He attributed the phenomenon to the existence of two competitive factors, one being the slow rate of adsorption of the emulsifying agent through the viscous organic phase to the interface, tending to increase the tendency of the organic phase to be dispersed at higher viscosities of that phase. The other factor was suggested to be the hydrodynamic instabilities observed by previous workers (Saffman and Taylor, 1958) in the flow of two immiscible liquids between parallel plates that were preferentially wetted by the more viscous liquid. According to

those workers, the instabilities developed in such a way that long fingers of the less viscous liquid penetrated into the more viscous one. Those fingers could then break up because of high shear gradient and could cause the aqueous phase to become increasingly dispersed in the organic phase as the viscosity of the latter was increased.

Joseph et al. (1984) observed a similar kind of instabilities in the flow of immiscible liquids with different viscosities in their experiments with a rotating rod, inserted through the long planar side of a rectangular box containing the two liquids, the rod being located symmetrically with respect to the interface. In many cases, depending on the wetting properties of the rod and the experimental conditions, they observed fingering of the low-viscosity liquid into the high-viscosity one, the drops being torn off the fingertips leading to the formation of an emulsion of low-viscosity drops in high-viscosity foam. In other cases they observed an encapsulation instability during which the high-viscosity liquid was encapsulated by the low-viscosity one. They attributed the phenomena to the tendency of the low-viscosity liquids to migrate into regions of the greatest shearing in order to minimize the shearing of high-viscosity liquids (see also Chapter 4, Section 4.2.3).

Treybal (1951) reported that a large ratio of the dispersed phase viscosity to the continuous phase viscosity could cause dual dispersions to occur in which part of the continuous phase was encapsulated as small droplets within larger drops of the dispersed phase. The phenomenon could be due to the same kind of hydrodynamic instabilities observed by Joseph et al. (1984). Quinn and Sigloh (1963) observed droplets within droplets in concentrated dispersions which appeared to be water-continuous while Roger et al. (1956) observed oil-continuous dispersions which also indicated droplets within droplets.

Although the results reported for the effect of the density difference between the phases on phase inversion are limited, there is an agreement between the workers investigating the parameter. However, the different results reported by various workers for the effect of the viscosity difference on phase inversion sometimes oppose each other, indicating a complicated mechanism involved including other important factors as well, such as the wettability of the surfaces of the container in which the dispersion was formed or the effect of the emulsifying agent.

2.3.4. Wettability of the Container Surfaces

It has been repeatedly suggested that the wettability of the solid surfaces influences the type of dispersion. Cheesman and King (1934), who tried to produce a dispersion by shaking oil and water in the presence of an emulsifying agent, found that the liquid which first wetted the walls of the tube tended to become the continuous phase. McClarey and Mansoori (1978) suggested that the discrepancies observed in their inversion curves when the effect of other factors, such as density and viscosity differences between the liquid phases, was eliminated could be due to the difference in the wettability of the container surface by the liquid phases. No quantitative measurements of those tendencies were reported.

Davies (1960) obtained some quantitative results with his continuous-flow emulsifying machine. He observed a very marked influence of the material of the shearing plates on phase inversion, oil-wetted plates strongly favouring oil-continuous systems while the roughness of the surfaces had a strong influence as well, since it altered the wettability of the plates.

Guillinger et al. (1988) studied the effect of the tank material on the phase inversion of liquid-liquid dispersions produced by agitation. They also found that the tank material affected the inversion point by promoting the preferentially wetting phase to be the continuous phase. They concluded however that the effect of the tank material became less with increasing agitation speed and increasing size of the mixing tank.

Tidhar et al. (1985) who studied the phenomenon of phase inversion in motionless mixers found that the type of dispersion formed depended strongly on the packing material at low liquid velocities when the turbulence was low, suggesting that the surfaces of the mixing elements had an important role in the processes of drop break-up and coalescence. They suggested, according to their results, that two competing mechanisms were taking part in the coalescence and breakup of drops, and hence were involved with the phenomenon of phase inversion. One was associated with shear forces and turbulence and predominated at high liquid velocities, and the other was associated with surface effects and wetting, consisting of an increased coalescence of the phase that wetted the surface, and predominated at low liquid velocities. They also derived a predictive mathematical model from free energy considerations that described satisfactorily the results reported for motionless mixers.

2.3.5. Interfacial Tension

The effect of interfacial tension on phase inversion has not been fully investigated. It was generally understood that if no other forces were present, interfacial tension would cause phase inversion to occur only for an equivolume mixture of the immiscible liquids.

Selker and Sleicher (1965) assumed in their investigation of the factors affecting the type of dispersion formed that it was unlikely that the magnitude of the interfacial tension could affect which phase would tend to remain continuous. They noted that the opposite would imply that the interfacial tension between a given pair of liquids was a function of the curvature of the interface but no such observation was known to them. They pointed out, however, that interfacially active contaminants as well as differences in polarity of the liquids could markedly affect interfacial properties but they did not have enough data to verify and extend those statements.

Luhning and Sawistowski (1971) and Clark and Sawistowski (1978) made a series of experiments in mixing vessels to investigate the effect of interfacial tension on the type of dispersion by using a solute, such as propionic acid or acetone in phase equilibrium with both liquids, that lowered the interfacial tension of the system. Both groups observed the the width of the ambivalent region was critically affected by the decrease in interfacial tension, indicating a greater resistance of the system to inversion. The presence of propionic acid in phase equilibrium increased the resistance to inversion of the oil-in-water dispersion particularly strongly, probably as a result of the polar nature of the solute.

Davies (1960) also observed, in his experiments with the continuous-flow emulsifying machine, that the type of the organic phase exerted an influence on the type of dispersion, suggesting that the difference in interfacial tension and even the polarity of the system could be the reason.

The presence of impurities, such as minute dust particles, which generally accumulate at the interface when dispersed in two liquid-phase

systems can prevent coalescence (Treybal, 1951). Quinn and Sigloh (1963) reported that the results obtained on phase inversion of liquid-liquid dispersions with impurities present were very irregular. McClarey and Mansoori (1978) also noted that the presence of impurities could exert great influence on the dispersion and cause the ambivalent region to be larger than it would be if pure liquids were used, indicating an increase in the resistance to inversion.

The observations and results obtained in relation to the effect of interfacial tension on the phase inversion of liquid-liquid systems show in general an increase in the resistance to inversion with decreasing interfacial tension. They indicate however that it should be the polarity of the system or the presence of impurities that have the greatest influence rather than the interfacial tension itself.

2.3.6. Temperature

Since the temperature of a liquid-liquid system has an effect on the properties of the liquid phases which affect the type of dispersion, it may also be effective, although data on this subject is meagre.

Most of the workers in mixing vessels tried to keep the temperature of the system constant by using a controlled temperature water bath, in order to eliminate the effect of temperature on the phase-inversion point. McClarey and Mansoori (1978) gave some quantitative results on the effect of temperature on the intermediate inversion curve for an immiscible liquid-liquid system. According to their results the phase inversion occurred at lower fraction of the organic phase with the increase of temperature.

In systems in which an emulsifying agent was added, the temperature at which inversion occurred was sensitive to the concentration of the emulsifying agent, the sensitivity being pronounced at very low concentrations. The phenomenon could be related, to some extent, to the solubility of the emulsifying agent which could also explain the different results obtained by various workers, according to which a rise in temperature favoured the oil-in-water type and a fall in temperature the water-in-oil type or the opposite, depending on the type of the emulsifying agent used (Clayton, 1954 - Shinoda, 1967).

2.3.7. Type and Concentration of the Emulsifying Agent

It has already been mentioned that the stability of a liquid-liquid dispersion is enhanced by the presence of a third component, the emulsifying agent. The nature and the concentration of the emulsifying agent plays an important role in the determination of the type of the emulsion obtained.

Emulsifying agents are classified numerically on the H.L.B. scale which refers to the hydrophilic-lipophilic balance of the emulsifier molecule. The H.L.B. value is a function of the weight percentage of the hydrophilic portion of the molecule of a non-ionic surfactant and can be calculated or determined experimentally. The H.L.B. values, as first reported, represented an empirical numerical correlation of the emulsifying and solubilizing properties of different surface-active agents (Griffin, 1954 - Davies, 1957). Those materials with H.L.B. numbers in the range of 4 to 6 are suitable as emulsifying agents for water-in-oil emulsions, while those with H.L.B. numbers in the range of 8 to 18 are suitable for the preparations of oil-in-water emulsions. Agents with H.L.B. numbers in different ranges, while possessing important surface-active properties cannot be employed as emulsifying agents according to that classification (Becher, 1956).

Dickinson and Iball (1948) used the method of shaking to produce the emulsions in order to examine the effect of the emulsifying agent on emulsion type. They decided to employ two emulsifying agents which separately would produce the opposite emulsion types and together would be expected to give rise to the formation of a molecular complex which would be powerfully adsorbed in the interface and should promote more efficient emulsification than either agent used alone. They found out that they could produce stable emulsions of either type depending on the relative proportions of the agents in the system. Further increase, however, of the concentration of the agents, above the minimum needed to produce the stable emulsion, did not significantly improve the emulsion.

Becher (1959) examined the effect of the chemical structure and concentration of the emulsifying agent using a stirring method to produce the emulsions. The emulsifying agent was dissolved at the same concentration in both phases, so that the total emulsifier concentration remained constant during the entire experiment. When an oil-in-water agent was being studied, aqueous phase was added to a quantity of the organic phase, with good stirring, so that a water-in-oil emulsion was initially formed and the addition continued until inversion occurred. The reverse procedure was followed for a water-in-oil emulsifying agent. Becher found that the volume fraction of the organic phase at inversion fell off with increasing emulsifier concentration for the inversion from oil-in-water type to water-in-oil type and increased for the opposite inversion. For each type of inversion, three different emulsifying agents were used which differed only in the nature of the lipophilic or hydrophilic residue, that is the H.L.B. value, but it did not seem to be any real correlation between structure and performance. His data did not indicate any relation between the composition of the emulsifier and the limits of inversion.

Davies (1960) reported a linear correlation of the volume fraction of the organic phase at inversion with the H.L.B. value of the emulsifying agent under the dynamic conditions of his continuous-flow emulsifying machine, the hold-up of the organic phase at inversion being increased with increasing H.L.B. value. He suggested the measuring of the volume fraction of the organic phase at inversion as a rapid and reliable method of determining the H.L.B. number of any given emulsifying agent. He also reported the importance of the concentration of the emulsifying agent. The tendency to form an emulsion of the type opposite to that favoured by its structure was increased with increasing amounts of it dissolved in the opposite phase, although the stability of the favoured type was enhanced at the higher concentrations of the additive.

2.4. Mathematical Models of the Phase-Inversion Process

The work that has been done on the development of predictive mathematical models of phase inversion is limited and usually restricted to a particular method of production of dispersion, so that the models can only be used in special cases under specific assumptions that cannot be generalized. It is the complicated nature of the phase-inversion phenomenon that needs some sort of simplification in order to be studied mathematically and that is the main reason for no generalized mathematical model to be developed yet.

Yeh et al. (1964) tried to develop a mathematical model of phase inversion, based on the hydrodynamic behaviour of the immiscible liquid system, by modifying the problem of the velocity distribution of two adjacent flows of two immiscible fluids that has been discussed by Bird et al. (1960). They calculated the volume ratio of two immiscible liquids α and β that were flowing in a thin slit of length L and width W under the influence of a

pressure gradient ΔP when the shear at the interface was zero, so that there was no tendency to mix or create a new surface, which was true at the point of inversion. Using the differential equations resulting from momentum balances in phases α and β and the boundary conditions relevant to the phase-inversion point, they found that the volumetric ratio of the two liquids at the point of inversion depended only on the ratio of the viscosities of the liquids according to the relation:

$$\frac{a}{b} = \sqrt{\frac{\eta^\alpha}{\eta^\beta}} \quad (2.5)$$

where a , b , η^α and η^β were the thicknesses and the viscosities of phases α and β respectively.

They suggested however that the correct viscosity ratio should be that of the interfacial viscosities which was believed to be different from bulk viscosities owing to preferential adsorption of certain components at the interface. They treated the system under investigation as consisting of two bulk phases α and β and an interfacial phase γ . Since Equation 2.5 was based on the square root of the ratio of the viscosities at the plane of shear, the latter should be found. Since the energy required to separate or shear two layers of liquid is equal to the work of adhesion, shear under flow conditions should take place at the interface which has the least work of adhesion, which is equal to the sum of the surface tensions of both phases minus the interfacial tension. Therefore the work of adhesion should be least at the α - γ interface because the surface tension of the α phase, which was the organic phase, was usually much less than that of the β phase, which was the aqueous phase. Thus in calculating the volumetric ratio of water to oil in Equation 2.5 η^β was replaced by the interfacial viscosity η^γ :

$$\frac{a}{b} = \sqrt{\frac{\eta^\alpha}{\eta^\gamma}} \quad (2.6)$$

They pointed out however that in the case of the presence of a highly surface-active agent, small quantities of it dissolved in the aqueous phase might lower the surface tension of that phase to the point that shear would take place at the β - γ interface with a corresponding change of Equation 2.6. They also pointed out that it was difficult to estimate the viscosity of the immiscible liquid mixture of the organic and the aqueous phases, namely phase γ , from the compositions and viscosities of pure compounds because the required viscosity data for at least one composition of the mixture was not available. They suggested however a simplified equation for an approximate estimation of the viscosity of phase γ .

It should be remembered that Yeh et al. derived Equations 2.5 and 2.6 based on certain assumptions according to which the two immiscible liquids were Newtonian fluids with negligible differences in densities and they were flowing under conditions in which viscous forces rather than inertia forces played the dominant role in determining the hydrodynamic behaviour of the system. Their experimental results however showed poor agreement with the theoretically estimated values especially in those cases in which the bulk-phase viscosities were used in the calculations. When the interfacial viscosity, calculated using the suggested simplified method, was used the agreement between the experimental and the theoretical values was greatly improved, although in some systems the agreement was still poor, probably due to the simplified assumptions used for estimating the interfacial viscosity.

Davies (1957, 1960) gave a mathematical correlation of the phase-inversion point in relation to the chemical structure of the emulsifying agent, that is the H.L.B. value, by considering the relative rates of coalescence of oil-in-water and water-in-oil systems responsible for the emulsion type. He derived the following equation for the relation of the H.L.B. number to the coalescence rates of the two types:

$$\ln \frac{(C1 \text{ Rate2})}{(C2 \text{ Rate1})} = 2.2\theta(\text{H.L.B.}-7) \quad (2.7)$$

- where
- Rate1 = $C1e^{-W1/RT}$: coalescence rate of the O/W type; (2.8)
- Rate2 = $C2e^{-W2/RT}$: coalescence rate of the W/O type; (2.9)
- $C1 = 4\phi kT/3\eta_w$: coalescence factor of the O/W type; (2.10)
- $C2 = 4(1-\phi)kT/3\eta_o$: coalescence factor of the W/O type; (2.11)
- η_w, η_o : viscosities of aqueous and organic phases respectively;
- ϕ : volume fraction of the organic phase;
- θ : the fraction of the interface covered by the emulsifying agent;
- W_1, W_2 : energy barriers to coalescence for the O/W and W/O types respectively;
- R : gas constant;
- k : Boltzmann constant;
- T : temperature;
- O/W: oil-in-water type of dispersion;
- W/O: water-in-oil type of dispersion.

He noted then that the oil-in-water type was preferentially stable if $\text{Rate2}/\text{Rate1} > 1$ and the water-in-oil type was preferentially stable when $\text{Rate2}/\text{Rate1} < 1$. He observed however a marked difference between his experimental results of the dependence of the volumetric fraction of the oil phase at inversion on the H.L.B. value of the emulsifying agent and those calculated from Equations 2.7, 2.8, 2.9, 2.10 and 2.11. He concluded then that it was not always the rate of coalescence that was the dominant factor in the phase-inversion process and the hydrodynamics of formation of the dispersion could also be very important as in the case of his continuous-flow emulsifying machine.

Arashmid and Jeffreys (1980) tried to predict the ambivalent region and the phase-inversion composition of liquid-liquid dispersions in mixing vessels by combining correlations of the collision frequency and the coalescence frequency of an agitated dispersion with models relating drop size and phase hold-up to agitation speed. They concluded that since phase inversion occurred when the coalescence frequency N_C was equal to the collision frequency N_T , the ratio $T = N_C/N_T$ was equal to 1.0 at the point of inversion and the inversion composition of the system could be predicted from the following equations:

$$T = \frac{K}{\Phi p^2 N^{0.46}} = 1.0 \quad (2.12)$$

$$p = k_3 m_1 N^{-2.88} + m\Phi \quad (2.13)$$

$$m_1 = \left(\frac{\mu_c^3}{\rho_c^2 g}\right) \left(\frac{\rho_c \sigma^3}{\mu_c g}\right)^{0.14} \left(\frac{\rho_c}{\mu_c g}\right)^{-0.32} \quad (2.14)$$

$$m = k_2 \left(\frac{\sigma}{\mu_c g}\right) \left(\frac{\Delta \rho \sigma^3}{\mu_c g}\right)^{-0.62} \left(\frac{\Delta \rho}{\rho_c}\right)^{0.05} \quad (2.15)$$

$$K = 3.65 k_1^{3/4} \quad (2.16)$$

where Φ : volume fraction of the dispersed phase;

p : drop size;

N : agitation speed in rpm;

μ_c : viscosity of the continuous phase;

ρ_c : density of the continuous phase;

$\Delta \rho$: density difference;

σ : interfacial tension;

g : gravitational acceleration;

k_1 : constant characteristic of the type of agitator;

k_2 : geometric constant;

k_3 : combined constant in drop size equation.

Their mathematical model was tested by comparing predicted and experimental phase-inversion compositions of various systems and the agreement was exceptionally good in all cases. The difference between the experimental and predicted inversion concentrations was generally less than 2.0% of volume fraction. Better agreement was obtained when the organic liquid was dispersed and the agreement was improved for each system with increased agitator speed.

Tidhar et al. (1986) developed a predictive model of phase inversion in motionless mixers. The description of their model is given in detail since that model will be compared with the phase inversion results in a horizontal tube, obtained by the present investigator.

Their model was based on their assumption that, since phase inversion was a "spontaneous" phenomenon, the total energy of the system did not change with phase inversion. They also assumed that no change in the mean droplet size occurred after inversion. Assuming further that the surface of the solid was covered by the continuous phase alone, which was acceptable especially at moderate and low turbulence conditions, they derived the following equation:

$$\frac{6\Phi}{d}\sigma_{ow} + a\sigma_{ws} = \frac{6(1-\Phi)}{d}\sigma_{ow} + a\sigma_{os}$$

$$\text{or} \quad \Phi = 0.5 + \frac{a\sigma_{ws}}{12\sigma_{ow}}(b-1) \quad (2.17)$$

where $b = \sigma_{os}/\sigma_{ws}$;

σ_{os} : interfacial tension between the organic phase and the solid;

σ_{ws} : interfacial tension between the aqueous phase and the solid;

σ_{ow} : interfacial tension between the two liquid phases;

a : motionless mixer area per unit volume;

d : mean drop diameter;

Φ : volume fraction of the organic phase at inversion.

Equation 2.17 was reformulated using Young's equation (Chapter 3) which relates the interfacial tensions with the contact angle θ of the liquid-liquid system with the solid surface:

$$\sigma_{os} = \sigma_{ws} + \sigma_{ow} \cos\theta$$

or

$$b = 1 + \frac{\sigma_{ow}}{\sigma_{ws}} \cos\theta \quad (2.18)$$

Equation 2.17 was then transformed by substituting b by Equation 2.18, so that:

$$\Phi = 0.5 + \frac{d}{12} a \cos\theta \quad (2.19)$$

The equation they used for the mean droplet size of the dispersed phase was a modification of that developed by Middleman (1974) for static and motionless mixers, based on the general equation of the maximum droplet size in isotropic and homogeneous turbulence (Equation 2.2). The energy dissipation rate per unit mass in turbulent flow in a pipe was assumed to be given by the following equation (Sleicher, 1962 - Middleman, 1979):

$$\epsilon = \frac{2fV^3}{D} \quad (2.20)$$

where V : average velocity in the pipe;
 D : diameter of the pipe;
 $f = D\Delta P/2\rho_c V^2 L$: friction factor;
 ΔP : pressure difference;
 ρ_c : density of the continuous phase;
 L : length of the pipe.

Assuming $f \propto Re^{-1/4}$ (Bird et al., 1960) and $d \propto d_{max}$, and substituting ϵ in Equation 2.2 by Equation 2.20, Middleman developed the following equation for the mean droplet diameter d of the dispersed phase in turbulent flow of liquids in a pipe:

$$d = C_1 D We^{-3/5} Re^{1/10} \quad (2.21)$$

where $We = \rho_c V^2 D / \sigma$;

$Re = \rho_c V D / \mu_c$;

ρ_c : density of the continuous phase;

μ_c : viscosity of the continuous phase;

σ : interfacial tension;

D : diameter of the pipe;

V : average velocity in the pipe;

C_1 : constant.

He applied Equation 2.21 in static mixers but with a smaller value of the constant C_1 so that the droplet size was reduced by an order of magnitude. Experimental results in motionless mixers (Sembira et al., 1986) were used to introduce a slight modification in Equation 2.21, so that:

$$d = C_1 d_h We^{-0.5} Re^{0.15} \quad (2.22)$$

where the pipe diameter D was replaced by the hydraulic diameter d_h of the motionless mixer.

Substituting d in Equation 2.19 by Equation 2.22 and replacing ρ_c and μ_c by the corresponding properties of the dispersion ρ_m and μ_m , Tidhar et al. derived the following general expression for the volume fraction Φ of the organic phase at inversion:

$$\Phi = 0.5 + C We^{-0.5} Re^{0.15} (d_h a) \cos \theta \quad (2.23)$$

where Weber number: $We = \rho_m V_T^2 d_h / \sigma$; (2.24)

Reynolds number: $Re = \rho_m V_T d_h / \mu_m$; (2.25)

$\rho_m = \Phi \rho_o + (1-\Phi) \rho_w$; (2.26)

$\mu_m = \Phi \mu_o + (1-\Phi) \mu_w$; (2.27)

V_T : total velocity of the dispersion;

- ρ_m, ρ_o, ρ_w : densities of the dispersion, the organic phase and the aqueous phase respectively;
- μ_m, μ_o, μ_w : viscosities of the dispersion, the organic phase and the aqueous phase respectively;
- σ : interfacial tension between the liquids;
- dh : hydraulic diameter of the motionless mixer;
- a : motionless mixer area per unit volume;
- θ : contact angle between the organic liquid drop and the surface of the mixing elements or the wall.

As has already been mentioned, in order to derive Equation 2.23 they assumed that there was no change in the mean droplet size after phase inversion occurred. That was justified as a first approximation because their experimental data indicated that the main factor affecting phase inversion was the nature of the surface of the mixing elements. They also assumed Equation 2.27 to be valid since the viscosities of the two phases were similar and they additionally accepted that energy losses associated with the pressure drop were essentially the same before and after inversion.

The predictive model of Tidhar et al. described satisfactorily the experimental results of the systems they tested. The authors noted however that some of the assumptions made in the derivation of Equation 2.23 were not strong enough and further refinement of the model might have been necessary, based on more extensive experiments.

3. EXPERIMENTAL METHODS AND MATERIALS

3.1. Introduction

The experimental work was based on the determination of the phase-inversion point of various immiscible liquid systems with different physical properties under different operating conditions of the apparatus used. The aim of the experimental work was to examine the effect of as many as possible of the parameters involved in the phase-inversion phenomenon in an attempt to understand its mechanism and develop a predictive mathematical model.

Two different methods of producing the liquid-liquid dispersions were used in the experiments using two different apparatus.

The main work was done in a laboratory scale continuous-flow emulsifying machine (Figure 1) in which the dispersion was produced by shearing the two liquid phases which were fed between two closely placed parallel plates, one rotating and the other being stationary. The phase-inversion point was observed visually on the wall of a cylindrical vessel against which the produced dispersion was thrown continuously permitting instant observation of the continuous phase.

Some work was done using a horizontal glass tube to produce the dispersion by the turbulent flow of the immiscible liquid phases in the tube and the phase-inversion point was determined by a conductivity probe placed at the end of the tube (Figure 3).

Different immiscible liquids were used to examine the effect of the various physical properties of the liquids on phase inversion, always in

relation to the operating conditions of the apparatus used.

3.2. Description of the Apparatus and the Procedure

3.2.1. Parallel Shearing Plates

The continuous-flow emulsifying machine of parallel shearing-plates was a modification of that designed and used by Davies (1960) for the production of liquid-liquid dispersions and the examination of the factors affecting phase inversion with particular emphasis on the wettability of the plates and the H.L.B. value of the emulsifying agent.

The continuous-flow system is shown in Plates 1 and 2 and is presented in the form of a schematic diagram in Figure 1. Some details of the scale and dimensions of the main apparatus are shown in Figure 2.

The main apparatus (Figures 1 and 2) consisted of two parallel horizontal circular plates of 90 mm diameter, the lower one of which was stationary and the upper one was rotating and they were called stator and rotor respectively. The plates were removable, mounted on brass plates, and they could be made of various materials. The rotor was connected by the system of brass plates and a vertical stainless steel shaft to a variable speed motor which was controlled by a Variac control box. The Variac control box was calibrated by measuring the rotational speeds with a tachometer in the range from 750 rpm to 2300 rpm and the calibration line, extrapolated to 500 rpm, is shown in Appendix A1 (Figure A1.1). The rotor was mounted on the shaft with a pin which kept it floating in order to ensure that the centrifugal force would keep it parallel to the stator during rotation. The stator was mounted on the brass bottom of a vessel having a cylindrical perspex wall which surrounded

the whole system. The vessel was 145 mm in diameter and 95 mm in height. In the case of the organic phase affecting perspex, the vessel was replaced by a similar one having a glass wall. The clearance between the plates was very small in comparison with the radius of the plates. It could be controlled by a micrometer screw placed behind the vessel and connected to a horizontal stainless steel bar which was mounted under the bottom of the vessel in order to hold it in the horizontal position. In that way, the position of the vessel and hence the position of the stator was changeable while the position of the rotor was fixed so that the width of the gap between them could be controlled. The calibration of the micrometer screw was standard so that 1 revolution corresponded to 1 mm change in gap width. The gap width could thus be controlled by measuring a 5 mm clearance, which was compared with a scale in mm, and decreasing it to the desired value by using the micrometer screw.

The continuous-flow system consisted of two 1000 ml glass bottles, each one containing one liquid phase and each connected to a centrifugal pump with 1/2in reinforced PVC clear tubes. Each pump was then connected to a rotameter with 5/16in PVC clear tubes. The liquid phases were fed through the system of pumps and rotameters and then through two stainless steel tubes, which were mounted at the bottom of the cylindrical vessel and connected to the rotameters with 5/16in PVC clear tubes. The steel tubes then fed into two holes in the stator, each one having a 2 mm diameter and being at a distance of 6.5 mm from the centre of the stator symmetrically. The dispersion was produced by the shearing action between the rotor and the stator and it was thrown continuously against the wall of the cylindrical vessel and then via the outflow stream into a 3000 ml glass beaker. The dispersion produced was not a stable emulsion and the two phases started separating as soon as they reached the outflow stream. It was possible then to recover most of the organic phase after each run by waiting for the dispersion collected in the

outflow container to settle and take the organic phase which was lighter and gathered at the top.

The pumps used were Stuart-Turner centrifugal pumps of type No.10, each one connected to one of the liquid-phase containers and the corresponding rotameter. Since the flow rates used were quite small in comparison with the quantity of liquid pumped, a bypass was made at the outlet of each pump to recycle the liquid that was not fed into the system through the rotameter, back to the container and so protect the pump from being underloaded. The bypass was made simply by using a 5/16in PVC clear tube and a "Hoffman" clip to control the flow of the liquid being recycled.

The rotameters used were small flowmeters supplied by Platon with glass tubes of 140 mm in length, "plumb bob" stainless steel floats and needle valves at the inlet to control the flow. In the case of the aqueous phase the rotameter had been already calibrated by the suppliers for water flow rates in the range from $10 \text{ cm}^3 \text{ min}^{-1}$ to $80 \text{ cm}^3 \text{ min}^{-1}$. In the case of the organic phase, however, the rotameter had to be recalibrated for each organic liquid used. In the case of the organic liquid being viscous, two rotameters of different scales had to be used, one calibrated for the lower flow rates and the other calibrated for the higher flow rates. The calibration curves of the rotameters used for each organic liquid are presented in Appendix A1 (Figures A1.2-A1.5).

The whole continuous-flow emulsifying system was mounted on a structure of wooden boards and "dexion" frames (Plates 1 and 2), in order to be as steady and flexible as possible and fill the least possible space. However, the vibrations observed especially at high rotational speeds could not be avoided and they could sometimes have a slight effect on the rotameter readings.

Another problem was the degree of accuracy with which the clearance between the plates was measured. The scale of the gap widths used was very small, of the order of 1 mm and less and, although the rotor was floating to ensure parallel gap between the plates during rotation, it was difficult to keep the plates absolutely parallel while measuring it. The problem was partly solved by testing different gap widths, with differences of the order of 0.25-0.4 mm, and examining the effect of the changes on the results.

In each set of experiments the phase-inversion point was detected visually at a given rotational speed and a constant gap width between the plates. The produced dispersion was flung against the wall of the cylindrical vessel and, by keeping the flow rate of one of the liquids constant and increasing the flow rate of the other, a change in its appearance was observed at the phase-inversion point. Because of the difference in the flow properties and the wettability of the material of the wall, between the oil-continuous dispersion and the water-continuous one, it was possible to detect the difference in the nature of the film of the continuous phase on the wall of the vessel before and after inversion. This was either a thin oily film when the organic phase was continuous or an area covered by discrete aqueous drops when the aqueous phase was continuous. When perspex was used as the material of the wall, it was very easy to make the above visual observations since perspex is strongly wetted by organic liquids while it is almost non-wetted by water. When glass was used as the material of the wall, because of perspex being affected by the organic liquid, the difference observed in the appearance of the continuous-phase film on the wall before and after inversion was mainly due to the larger viscosity of the organic continuous phase compared with the viscosity of the aqueous continuous phase.

The mode of operation of the emulsifying machine of parallel shearing plates made the simultaneous use of other techniques for the determination of

phase inversion difficult. It gave, however, the possibility of examining most of the parameters affecting phase inversion accurately and in a short time. Plates 3 and 4 show typical examples of water-continuous and oil-continuous dispersions in the system of parallel shearing plates used. Plate 5 shows an example of visual observation of the phase-inversion point.

The volume fraction of the organic phase at inversion, Φ_i , calculated from the ratio of the flow rate of the aqueous phase to the flow rate of the organic phase at that point, R_i , was the parameter used as a quantitative measure of phase inversion. It was calculated from the following relation (Appendix A2.1);

$$\Phi_i = \frac{1}{R_i + 1} \quad (3.1)$$

where

$$R_i = Q_{wi} / Q_{oi};$$

Q_{wi} : aqueous flow rate at inversion point;

Q_{oi} : organic flow rate at inversion point.

For the various parameters examined, phase inversion was measured for different rotational speeds and it was presented graphically by plotting the volume fraction of the organic phase at inversion against rotational speed. The phase-inversion curves produced could be obtained either by keeping the flow rate of the aqueous phase constant and increasing the flow rate of the organic phase until phase inversion was observed or the opposite without any difference in the results. Since certain amounts of both liquids were fed in the same way at the same time between the plates to produce the dispersion, it did not matter from which side phase inversion was approached and no ambivalent region was observed. The dispersions with organic-phase volume fractions below a particular phase-inversion curve were always water-continuous while those above were always oil-continuous. Since phase

inversion depended only on the volumetric ratio of the two liquid phases, different flow rates could be used under the same conditions without having any effect on the phase-inversion point, resulting always in the same volumetric ratio of the two liquids at inversion{Table A3.3 in Appendix A3.3}.

The experimental method described above had the advantage of giving very quick and significant results, since it was possible to repeat a particular experiment under specified conditions, sometimes using different total flow rates, from 5 to 10 times depending on the degree of reproducibility of the results, and to use the mean value of each set of organic-phase volume fractions at inversion in the interpretation of the results. The reproducibility of the results depended on the operating conditions and the properties of the liquid phases since, in some cases, it was not always very easy to detect the exact point of inversion by distinguishing the continuous phase on the wall of the cylindrical vessel.

Since the presence of contaminants and dust could have a dramatic effect on phase inversion, care was taken to keep the whole system as clean as possible. The plates were washed thoroughly before use, cleaned with acetone (except for the perspex ones which were cleaned with ethanol), and rinsed with distilled water. The cylindrical vessel itself was rinsed with ethanol and distilled water from time to time to take away any dust that could have accumulated on the wall especially when the system was out of use for a long period of time.

3.2.2. Horizontal Glass Tube

The method of producing the liquid-liquid dispersions by the continuous turbulent flow of the immiscible liquids in a horizontal glass tube was used

subsequently to the method of parallel shearing plates.

The whole continuous-flow system is shown in Plate 6 and is presented in the form of a schematic diagram in Figure 3. Details of the glass tube are shown in Figure 4. Details of the settler are shown in Figure 5.

The main apparatus (Figures 3 and 4a) consisted of a horizontal glass tube 70 cm long of 1 cm inside diameter. One of the liquid phases was introduced directly into the glass tube through a T-branch at the inlet. The other liquid phase was introduced into the tube through a small glass tube of 2.5 mm inside diameter which entered the main tube horizontally with its outlet at about 2 cm downstream from the T-branch.

The continuous-flow system (Figure 3) consisted of two 20 ℓ PVC containers each one containing 10 ℓ working volume of each liquid phase and connected to two centrifugal pumps which in turn were connected to two rotameters. Each connection was made with a 1/2in reinforced PVC clear tube from the side at the bottom of each container through a 1/2in gate valve to the corresponding pump and then to the corresponding rotameter. A bypass was made at the outlet of each pump to recycle the liquid that was not fed into the system through the rotameter, back to the container. The bypass was made with a 1/2in reinforced PVC clear tube and a 1/2in gate valve to control the flow of the recycled liquid. Each rotameter was connected either to the T-branch or to the small glass tube at the inlet of the main glass tube with a 3/8in PVC clear tube. The dispersion was produced by the turbulent flow of the two liquid phases in the tube and the produced dispersion was introduced from the outlet of the tube to a settler via a 3/8in PVC clear tube. The two liquid phases were separated in the settler and each one was recycled into the corresponding container via a 1/2in reinforced PVC clear tube.

The pumps used were Stuart-Turner centrifugal pumps of type No.10. The rotameters used were flowmeters supplied by Platon with glass tubes of 140 mm length, "plumb bob" stainless steel floats and needle valves at the inlet to control the flow. In the case of the aqueous phase, the rotameter had been already calibrated by the suppliers for water flow rates in the range from 20 l/h to 270 l/h. In the case of the organic phase, the rotameter had to be recalibrated and the calibration curve is presented in Appendix A1 (Figure A1.6).

The settler (Figure 5) was a 7.65 l perspex rectangular vessel with four fixed weirs and an adjustable one, used for the settling and separation of the two liquid phases. The vessel was 17 cm high, 30 cm long and 15 cm wide. All the parts of the settler were made of perspex and they were mounted on the vessel with araldite. The first weir was 9.5 cm deep, mounted 3 cm from the inlet of the settler and 7.5 cm from the bottom. The second weir was 4 cm deep, placed 24 cm from the inlet of the vessel and 2 cm from the top. The third weir was 15 cm deep, placed 28 cm from the inlet of the vessel and 2 cm from the bottom. A heavy phase trap was made in a small volume between the second and the third weir to trap the flow of the heavy phase and permit the outflow of the light phase alone. An extension of the vessel was made 30 cm from the inlet which had the same width as the main vessel, it was 9 cm high and 6 cm long and placed 8 cm from the bottom of the main vessel. The extension was a light phase trap made to trap the flow of the light phase and permit the flow of the heavy phase only. The adjustable weir was placed between the extension and the main vessel, it was 6 cm deep and it could be moved on a weir guide 9 cm long and adjusted to a given position by means of a screw. The fifth weir was part of the extension, it was 4 cm deep and fixed 2 cm from the heavy phase outlet and 1 cm from the bottom of the extension.

The dispersion was introduced at the top of one of the smaller sides of the main vessel and flowed under the first weir into the volume between the first and the third weir where the separation of the phases took place. The light phase flowed over the second weir to its outlet at the top of one of the larger sides of the vessel. The heavy phase flowed under the third weir and through the adjustable weir into the extension of the vessel and then under the fifth weir to its outlet at the side of the extension of the vessel. The settler was designed to give a minimum total residence time of about 1 minute. The individual residence time of the two phases depended on the position of the adjustable weir. Its optimum position for each set of liquids was determined empirically by checking the separation of the phases at different positions of the weir.

The phase inversion of the dispersion in the glass tube was determined by detecting the electrical conductivity of the continuous phase. A conductivity probe was placed at the end of the glass tube, 65 cm from the inlet (Figures 3 and 4a). It consisted of two pieces of stainless steel wire inserted in the glass tube through two small capillary glass tubes respectively, which were as close to each other as possible on the wall of the glass tube. Each piece of stainless steel wire was fixed with araldite at the outside end of the corresponding capillary tube. The conductivity probe was connected to an analogue electrical bridge box for displaying the conductivity which in turn was connected to a recorder for recording it (Figure 4b).

The whole continuous-flow system was mounted on a structure of wooden boards and "dexion" frames (Plate 6). The glass tube in particular was mounted with two stainless steel pipe clips, at the beginning and the end of the tube respectively, on a vertical wooden board together with the two rotameters in order to be steady and not to be affected by the high flow rates

of the liquids. The settler was placed behind the vertical wooden board mounted with screws between two "dexion" frames so that it could be removed to be cleaned. The containers and the pumps were placed at the bottom of the whole structure while the electrical bridge box and the recorder were placed in front at a height convenient to the investigator.

For the same liquid-liquid system, two different experiments were performed by introducing either phase through the T-branch at the inlet of the glass tube, the other being introduced through the small tube respectively. For each one of the experiments above, phase inversion was determined either by keeping the flow rate of the aqueous phase constant and increasing the flow rate of the organic phase or the opposite. Consequently, phase inversion was approached in two ways, either from an oil-in-water dispersion to a water-in-oil dispersion or the opposite, leading to different results as opposed to the method of parallel shearing plates. The difference in the results was due to the different manner by which each phase was introduced at the inlet of the glass tube.

As was mentioned before, the conductivity probe at the end of the glass tube was used to detect phase inversion by measuring the electrical conductivity of the dispersion in the glass tube. Dispersions in which the aqueous phase is the continuous one show a higher conductivity than those in which the organic phase is continuous because of the polar nature of water. In general, the conductivity of a dispersion is approximately that of the continuous phase, although it might be slightly higher or lower because of the influence of the dispersed phase. A sharp change in conductivity was observed during phase inversion which was either a sharp decrease in conductivity at inversion from an oil-in-water to a water-in-oil dispersion or a sharp increase in conductivity at the opposite inversion (Figures A3.4 and A3.5 in

Appendix A3.4). At the exact point of phase inversion, increased fluctuations in conductivity were observed because of the high instability of the dispersion formed. The exact value of the electrical conductivity of the dispersion was not measured, since it was outside the scope of the experimental work. The change in conductivity was the important factor in detecting phase inversion.

Visual observation of phase inversion was also made, simultaneously to the observed change in conductivity, mainly at lower total flow rates where it was possible to observe the drops of the dispersed phase of the dispersion formed. At the point of inversion, no real dispersion was formed since the two liquid phases were flowing almost separately in the glass tube (Plates 7 and 8).

The parameter used as a quantitative measure of phase inversion was the volume fraction of the organic phase at inversion, Φ_i , determined from the ratio of the flow rates of the two liquid phases as in the method of parallel shearing plates (Equation 3.1). For the various liquid-liquid systems used, phase inversion was measured at different flow rates of the liquid phases and it was presented graphically by plotting Φ_i against total flow rate, Q_T , of the liquid-liquid system.

The method of producing the dispersion in the glass tube was mainly chosen because it was easy to define the liquid flow pattern. In addition, the results obtained using that method were accurate and reproducible, since the exact point of inversion was measured accurately using the conductivity probe. Finally, the whole continuous-flow system was kept free of contaminants and dust since all the vessels, including the glass tube and the settler, were covered in order not to be in contact with the atmosphere.

3.3. Materials and Operating Conditions

The materials and the operating conditions used in the experiments were chosen according to the parameters examined in relation to phase inversion. The parameters examined were as follows:

a. Parallel shearing plates:

- rotational speed;
- gap width between the plates;
- wettability of the surfaces of the plates with the liquid phases;
- viscosity and density differences between the liquid phases;
- interfacial tension;
- addition of an emulsifying agent.

b. Glass tube:

- total flow rate;
- wettability of the surface of the glass tube with the liquid phases;
- density difference between the liquid phases;
- addition of an emulsifying agent.

All experiments were operated at room temperature, 21⁰-22⁰C. The systems of immiscible liquids used in both experimental methods are listed in Tables 1 and 2 respectively together with their physical properties. The viscosity of the aqueous phase was taken to be 1 mPas. Most of the organic liquids used were analytical reagents, supplied by Fisons, except "Escaid" which was a Kerosene type solvent, supplied by Multisol. Distilled water, prepared in the laboratory, was used in the aqueous phase in all cases. The Calcium Chloride used in the parallel shearing plates method was a laboratory chemical, supplied by Griffin and George, while that used in the glass tube method was of technical grade, supplied by I.C.I. The emulsifying agent Tween 80 (polyoxyethylene sorbitan mono-oleate) was a laboratory reagent, supplied by

Sigma, it was hydrophilic with H.L.B. value 15 and it was dissolved in the aqueous phase. The oleic acid was used as a lipophilic emulsifying agent, it was a purified general purpose reagent supplied by Hopkin and Williams with H.L.B. value 1 and it was dissolved in the organic phase.

Liquid paraffin was mainly chosen because of its relatively high viscosity in comparison with that of water, in order to examine the effect of viscosity difference between the liquid phases on phase inversion. Liquid Paraffin was a safe oil which had no effect on the perspex plates and the perspex wall of the cylindrical vessel. Dibutyl Maleate was mainly chosen because of its similar density with that of water, in order to examine the effect of density difference between the liquid phases on phase inversion. However, it was found to exert an even more important property in relation to the aqueous phase, a relatively low interfacial tension. Dibutyl Maleate is irritant to the skin, so care was taken in handling it by using gloves. It also affected perspex and to some extent PVC, so the perspex cylindrical vessel was replaced by one made of glass while the smaller PVC tubes, which were more sensitive, were replaced by fluon tubes which were insensitive to organic chemicals. Escaid was chosen because of its relatively low viscosity, not very far from that of water, and because it was cheap and could be used in large quantities in the case of the glass tube method. Escaid was inflammable, so care was taken to keep it away from any naked flame. It was, however, safe in relation to the materials of the equipment used, mainly in relation to perspex and PVC.

The addition of certain additives in the liquid-liquid systems used was aiming at investigating the effect of certain parameters such as interfacial tension and density difference between the phases on phase inversion. Different types and concentrations of emulsifying agents were chosen in order to examine the effect of their chemical composition, expressed as H.L.B.

value, on phase inversion as well as their effect in relation to lowering the interfacial tension of the system. Calcium Chloride was chosen to be added in the aqueous phase in order to increase its density and so increase the density difference between the phases. The concentrations of the additives were chosen after measuring the effect of different concentrations on changing the corresponding properties of the liquids.

Three different materials of the parallel shearing plates were used, perspex, stainless steel and glass, in order to examine the effect of the wettability of the surfaces of the plates with the liquid phases on phase inversion. All the three different pairs of plates used had rough surfaces, mainly the stainless steel plates, which exerted an additional influence on their wettability. Moreover, the glass plates which were made of ordinary glass that was difficult to cut and handle, had quite rough edges and a few cracks on the surface which were made while mounting them on brass. The contact angles of the actual plates used in the experiments with each liquid-liquid system used were measured as a means of expressing quantitatively the wettability of the materials of the plates with the liquid phases. The values of contact angles for all systems used are presented in Table 4. In the case of the glass tube, the contact angles of glass with the systems of immiscible liquids used were estimated from those measured for the glass plates.

The range of rotational speeds used in the method of parallel shearing plates was between 500 rpm and 2210 rpm. For speeds below 500 rpm and sometimes even up to 750 rpm, depending on the other conditions of the system such as the gap width and the material of the shearing plates, the dispersion produced was not homogeneous, forming an oily film on the cylindrical wall together with discrete aqueous drops, so that the detection of the phase inversion point was difficult. Sometimes at such low rotational speeds, either when the gap width was not small enough or the edges of the plates were

rough, there was not enough centrifugal force for the produced dispersion to be thrown against the perspex wall and that was an additional reason that made the observation of phase inversion difficult. Rotational speeds higher than 2210 rpm were not examined, since the speed range used was large enough to give an indication of the dependence of phase inversion on rotational speed. Moreover, the scale of the apparatus was quite small, so that it could give rise to safety problems if higher rotational speeds were used, because of the small gap widths between the shearing plates and the increase in vibrations.

The effect of the clearance between the shearing plates was tested by changing the gap width in the range from 0.1 mm to 1 mm. Smaller gaps were not used since it was very difficult to measure their width exactly even with the micrometer while larger gaps gave non-homogeneous dispersions. In the case of perspex and stainless steel plates, four different gap widths were tested, namely 0.1 mm, 0.5 mm, 0.75 mm and 1 mm. In the case of glass plates, the gap widths used were 0.2 mm, 0.5 mm and 1 mm. In that case, it was difficult to have a gap smaller than 0.2 mm because of the roughness of the edges of the glass plates.

As was mentioned before, phase inversion did not depend on the actual flow rates of the two liquid phases in the case of parallel plates, but on their flow rates ratio. There was, however, a wide range of flow rates used for each liquid phase, leading always to the same volume fraction of the organic phase at inversion when the rest of the conditions remained the same. The range of flow rates used for the aqueous phase was from $10 \text{ cm}^3 \text{ min}^{-1}$ to $75 \text{ cm}^3 \text{ min}^{-1}$. The range of flow rates used for the organic phase was from $1.75 \text{ cm}^3 \text{ min}^{-1}$ to $50 \text{ cm}^3 \text{ min}^{-1}$. The range of flow rates for both phases was chosen for each liquid-liquid system used in order to be convenient to the observation of phase inversion.

The range of total flow rates used in the glass tube method was between $80 \text{ } \ell\text{h}^{-1}$ and $310 \text{ } \ell\text{h}^{-1}$. The range of flow rates for each liquid phase used was from $30 \text{ } \ell\text{h}^{-1}$ to $150 \text{ } \ell\text{h}^{-1}$ for the aqueous phase and from $48 \text{ } \ell\text{h}^{-1}$ to $185 \text{ } \ell\text{h}^{-1}$ for the organic phase respectively. Flow rates lower than the minimum used would not lead to the production of a dispersion in the glass tube. Moreover, flow rates higher than the maximum used would not lead to a proper separation of the liquid phases in the settler because of the very small residence time in the settler. Besides, the range of total flow rates used was large enough to give an indication of the dependence of phase inversion on total flow rate of the liquid phases in the case of the glass tube.

3.4. Measurement of the Physical Properties of the Liquid Phases

3.4.1. Interfacial Tension Measurement

Two methods of measuring the interfacial tension between the two liquid phases were used, the platinum ring method and the drop-weight method.

The platinum ring method (Figure 6a) is based on determining the force required to detach a platinum ring from a liquid-liquid interface which equals the interfacial tension multiplied by the total perimeter of the ring. It was the method used first to measure the interfacial tension between Liquid Paraffin and water with the "OS" type Torsion Balance. The two liquid phases were put into a small glass dish, placed on a horizontal platform which could be lowered or raised by an adjusting screw. The balance was checked for zero with the platinum ring completely immersed in the lighter of the two phases and clear of both the interface and the surface, so that the small beam pointer on the right hand side of the dial was at the zero point. The platinum ring was then immersed in the heavier liquid phase and the platform

was moved gradually while at the same time the index pointer on the dial was moved in an anticlockwise direction so as to maintain the beam pointer at zero. The value indicated by the index pointer at the moment when the platinum ring parted from the interface was the interfacial tension of the system and it was read directly from the balance dial in Newtons per meter.

The platinum ring method had the disadvantage of giving non-reproducible results in the case of low interfacial tension because of the difficulty in getting a plane interface between the two liquids during the measurement of interfacial tension. The drop-weight method was chosen as the best method of measuring interfacial tension of low values, since the results taken using that method were easily and accurately reproduced.

The drop-weight method of measuring the interfacial tension between two liquids is based on the measurement of the volume of a drop of the heavier liquid which detaches itself from the tip of a vertical tube into the lighter liquid (Figure 6b). Assuming that the drop is formed extremely slowly, it detaches itself completely from the tip when the gravitational pull just reaches the restraining force of interfacial tension:

$$Mg = V\Delta\rho_{\ell}g = 2\pi a\sigma$$

$$\text{or} \quad \sigma = \frac{V\Delta\rho_{\ell}g}{2\pi a} \quad (3.2)$$

where

- g : gravitational acceleration;
- M : apparent mass of the drop;
- V : volume of the drop;
- $\Delta\rho_{\ell}$: density difference between the liquids;
- a : radius of the tip;
- σ : interfacial tension.

These relations, however, require correction because the liquid forming the drop does not completely leave the tip and the interfacial tension seldom acts exactly vertically. The correction factor ψ was found to be a function of the radius of the tip and the volume of the drop only and it can be readily obtained from a plot of ψ against $a/V^{1/3}$ (Davies and Rideal, 1960). Then the interfacial tension is given from the relation:

$$\sigma = \frac{\psi V \Delta \rho_l g}{2\pi a} \quad (3.3)$$

The tube used to form the liquid drops was a glass 1 ml syringe which was mounted firmly on a vertical stand and its tip was connected to a stainless steel needle with a conical end (Figure 6b). The drops were detached from the tip of the conical end which was available in two sizes, 0.27 mm and 0.155 mm in radius. Depending on the density difference between the liquid phases and the expected range of interfacial tensions, the radius of the tip was chosen so as to form a drop with volume that could be measured easily and quickly. A micrometer was placed directly on top of the syringe in order to form the liquid drop very slowly and at the same time measure the volume of the drop formed. The formulation and detachment of the heavier liquid drop took place inside a 5 cm \times 5 cm \times 1 cm glass box filled with the lighter liquid. The exact moment of detachment could be detected accurately using a microscope to observe the formation and detachment of the drop. The mean value of the volumes of the drops formed was taken and the interfacial tension was calculated from Equation 3.3. An example of calculating interfacial tension using the drop-weight method is given in Appendix A3.1.

Both methods were used for measuring the interfacial tension of the Liquid Paraffin-Water system while only the drop-weight method was used for the rest of the systems. Since the results of the drop-weight method were in general more reproducible, the interfacial tension values taken using that method were used for the interpretation of the phase-inversion results.

3.4.2. Viscosity Measurement

The viscosities of the organic liquids used were measured by a Contraves Rheomat 30 rotational rheometer using the measuring system of co-axial cylinders (Figure 7a) for liquid Paraffin and the double-gap measuring system (Figure 7b) for Dibutyl Maleate and Escaid. Different measuring systems for different liquids were used because of the difference in the order of magnitude of their viscosities.

The rotating measuring body was driven by a DC motor, the speed of which was precisely controlled by a programming unit incorporated in the Rheogram recorder which also plotted the speed on the recorder's Y axis. The torque required to maintain the rotational speed of the measuring body was measured and indicated on the torque indicator and it was simultaneously plotted on the recorder's X axis. Since the shear rate was a function of the rotational speed and the dimensions of the measuring system, and the shear stress was a function of the torque, the flow behaviour and the viscosity of the liquid under test could be deduced.

According to the chosen rotational speed programming there was a time-proportional speed increase from standstill up to the preselected peak level which was set to be 350 min^{-1} , then the drive remained on maximum speed for the preselected period of 20 seconds and thereupon it underwent a time-proportional slowing down of speed until it stopped. Measurements were taken at room temperature, $21^{\circ}\text{--}22^{\circ}\text{C}$. From the automatically plotted rheogram, the shear stress was calculated at a particular shear rate by multiplying the scale reading by $\tau\%$ from the tables available for the particular measuring system used and then by the factor corresponding to the selected torque range (Appendix A3.2). There were two lines plotted on each rheogram, which

corresponded to the acceleration and deceleration of speed respectively and were slightly different since they were related to an average of speeds. The acceleration line was used in the calculations assuming that it represented better the flow behaviour of the liquid under-test. The above assumption was based on the fact that if there was a small amount of heat generated by shear during the measurements, despite the fact that the system was temperature-controlled, it would be much less significant during the first part of the measurements.

The flow-type plot was drawn, based on the rheometer measurements, for each liquid used (Figures 8, 9 and 10) and the viscosity was calculated from the slope of the line representing the flow behaviour of the corresponding liquid.

3.4.3. Contact Angle Measurement

The contact angle between a liquid and a solid surface is the angle θ , made by the edge of a drop of the liquid placed on a flat solid surface, with the solid (Figure 11a). Theoretically, the contact angle is given by Young's equation:

$$W_{S/L} = \gamma_{L/A} (1 + \cos\theta) \quad (3.4)$$

where $W_{S/L} = \gamma_{S/A} + \gamma_{L/A} - \gamma_{S/L}$: the work of adhesion between the solid and the liquid;

$\gamma_{L/A}$: surface tension of the liquid;

$\gamma_{S/A}$: surface tension of the solid;

$\gamma_{S/L}$: interfacial tension between the solid and the liquid.

Similarly, the contact angle between an immiscible liquid pair and a solid

surface is the angle θ made by the liquid interface with the flat solid surface (Figure 11b). In this case, the contact angle is given by the modified Young's equation:

$$\cos\theta = (\gamma_{S/L2} - \gamma_{S/L1}) / \gamma_{L1/L2} \quad (3.5)$$

where $\gamma_{L1/L2}$: interfacial tension between
the liquids;
 $\gamma_{S/L1}, \gamma_{S/L2}$: interfacial tensions between the solid
and each of the two liquids respectively.

Both relations apply for contact angles θ less than, equal to, or greater than 90° .

The contact angle between a liquid and a solid or an immiscible liquid pair and a solid is a measure of the wettability of the solid with the liquid or the immiscible liquid pair. It depends however on the roughness of the solid surface and on its adsorption of impurities and water. A solid is completely wet with liquid if the contact angle is zero. An increase in contact angle means a decrease in the wettability of the solid with the liquid. In the case of an immiscible liquid pair, a zero contact angle with the solid means that the solid is completely wetted by one liquid and completely non-wetted by the other liquid. In this case, an increase in contact angle means a decrease in the wettability of the solid with one liquid and an increase in its wettability with the other liquid. In practice, a contact angle of 90° is often regarded as a sufficient criterion of non-wetting. The roughness of the solid surface however has the effect of making the contact angle further from 90° . It must be noted that if the smooth material gives an angle greater than 90° , roughness increases this angle still further, but if the contact angle is less than 90° , roughness decreases the angle.

The measured contact angles of the materials of the parallel shearing plates with both liquid phases was used as a means of examining quantitatively the effect of the wettability of the plates by both liquids on phase inversion. The contact angles of the materials of the plates with each liquid were measured first, in order to give an indication of the wettability of the plates by each liquid phase. However, for the wettability of the plates with the immiscible liquid pair, it was considered more representative to measure the contact angles of each immiscible liquid pair with the materials of the plates and use these for the interpretation of the results.

Since the surfaces of the plates used were quite rough, measurements of contact angles were made on the actual plates used and the results obtained corresponded to the particular surfaces only. Since the adsorption of impurities on the solid surface, especially when it is rough, could cause difficulties in obtaining reproducible contact angle values, both solid and liquid surfaces had to be as clean as possible before measurements of contact angles were made. In the case of the horizontal glass tube, it was not possible to measure the contact angle of the glass tube itself with the liquid phases, so its contact angle was estimated from that measured for the glass plates.

The method used for obtaining the contact angle θ was the immersed plate method, based on the fact that the angle at which a solid surface, in the form of a flat plate a few centimetres across, dips into a liquid or through a liquid-liquid interface can conveniently be altered until the liquid surface or the liquid-liquid interface remains planar right up to the solid surface (Figures 12a and 12b).

The solid surface was held in an adjustable holder capable of being tilted

to any angle and of being raised and lowered. The liquid or the immiscible liquid pair was contained in a glass dish and it was replaced after each measurement, so that the liquid surface or the liquid-liquid interface could be fresh and clean before the following measurement. The solid surface and the glass dish were also cleaned thoroughly before each measurement by washing, rinsing with acetone (except for the perspex plate which was rinsed with ethanol) and then rinsing with distilled water. A travelling microscope was used to study the liquid surface or the liquid-liquid interface where it met the solid. The solid plate was immersed in the liquid or through the liquid-liquid interface at an oblique angle so that a meniscus was made between the solid surface and the liquid surface or the liquid-liquid interface. The angle at which the solid met the liquid surface or the liquid-liquid interface was then increased gradually by tilting the adjustable holder of the solid plate until the meniscus was horizontal. The angle at which the meniscus between the solid and the liquid surface or the liquid-liquid interface became horizontal was the contact angle between them. The angle was measured by comparing it with a scale in degrees. In the case of the immiscible liquid pairs, their contact angles with the solid surfaces were measured always through the aqueous phase. Each measurement was repeated three or four times and the mean value of contact angles was taken (Tables 3 and 4).

4. MODE OF FLOW OF LIQUIDS

4.1. Introduction

The mode of flow of the liquids can have an important influence on the phase-inversion phenomenon, since the mechanism of the production of a dispersion is different under laminar or turbulent flow conditions with subsequent effect on the droplet size of the dispersed phase and hence on coalescence and stability of the dispersion.

So, it was considered very important to calculate some of the parameters and discuss some of the phenomena involved in the type of flow of the liquids and the production of the dispersions. This was done for both the system of parallel shearing plates and the horizontal tube in order to have an idea of how those systems operated.

4.2. Flow between Parallel Shearing Plates

4.2.1. Reynolds and Taylor numbers

In any particular system of parallel shearing plates the mode of flow of a liquid is governed by two dimensionless numbers, the Reynolds number with respect to the radius of the plates and the Taylor number with respect to the clearance between the plates which are defined by the following equations:

$$Re = \frac{N\rho r^2}{\mu}: \text{ Reynolds number} \quad (4.1)$$

$$Ta = \frac{N\rho s^2}{\mu}: \text{ Taylor number} \quad (4.2)$$

where N : rotational speed;
 r : radius of the plates;
 s : gap width between the plates;
 ρ : density of the liquid;
 μ : viscosity of the liquid.

It has been observed (Cooper and Reshotko, 1975) that for the flow of a liquid between a stationary and a rotating disk, transition from laminar to turbulent flow occurred gradually over the range $1.6 \times 10^5 \leq Re \leq 2.5 \times 10^5$. The situation however is more complicated, since the Taylor number is the parameter which denotes the existence or not of boundary layers which might overlap. It was suggested by Benton (1968) that for Taylor numbers up to about 4, the circumferential flow profile was nearly linear, suggesting the existence of a simple rotating Couette flow in which viscous forces dominated throughout. In the intermediate range of Taylor numbers from 4 to about 625, a complicated transition occurred to a state in which a jet-like region of high circumferential flow existed near the stator indicating the beginning of formation of boundary layers that overlapped and therefore interacted strongly. Finally, for Taylor numbers greater than 625, the existence of an asymptotic state was suggested in which the flow near each plate became an asymptotic boundary layer with a well developed core between them.

The range of Reynolds and Taylor numbers used in the experiments were calculated for each liquid phase used assuming that each liquid was flowing on its own between the parallel shearing plates. The calculated Reynolds numbers for each liquid phase used and for the minimum and maximum rotational speeds used in the experiments are presented in Table 5. The calculated Taylor numbers for the minimum and maximum rotational speeds used and for each liquid phase and gap width used are presented in Table 6.

The situation of two liquid phases flowing between the plates was more complicated than that of each liquid flowing on its own, since the physical properties of the liquid-liquid systems depended on the volumetric ratio of the two liquid phases. The density of a liquid-liquid dispersion is usually given by the volume-weighted average of the densities of the two liquid phases (Guilinger et al., 1988 - Tidhar et al., 1986). The viscosity of a liquid-liquid dispersion is closely related to the viscosity of the continuous phase. When the viscosities of the two phases are similar, the viscosity of the dispersion is usually assumed to be the volume-weighted average of the viscosities of the two phases (Tidhar et al., 1986). However, when there is a difference in the viscosities of the two liquid phases, the viscosity of the dispersion is always higher than that of the continuous phase and increases with increasing volume fraction of the dispersed phase. In this case, the equation for the dispersion viscosity which has been found to fit best the experimental data of most workers is the following, proposed by Vermeulen et al. (1955):

$$\mu_m = \frac{\mu_c}{1 - \Phi_d} \left[1 + \frac{1.5\Phi_d\mu_d}{\mu_c + \mu_d} \right] \quad (4.3)$$

where μ_m : viscosity of dispersion;
 μ_c : viscosity of continuous phase;
 μ_d : viscosity of dispersed phase;
 Φ_d : volume fraction of dispersed phase.

However, most workers have reported that all equations proposed by various workers, which relate the viscosity of a liquid-liquid dispersion to these of the continuous and dispersed phase, are mainly valid for low volume fractions of the dispersed phase, usually less than 0.3.

According to the relations mentioned above regarding the density and viscosity of a liquid-liquid dispersion, the Reynolds and Taylor numbers in

the case of two liquids flowing between parallel shearing plates, forming a dispersion, would then fall between those calculated for the aqueous and the organic phase separately, when the viscosities of the two liquids are similar. However, Equation (4.3) shows that when there is a difference in the viscosities of the two liquids towards higher viscosity of the organic phase, the Reynolds and Taylor numbers for a water-in-oil dispersion would be lower than those calculated for the organic phase flowing on its own.

Table 5 shows that the Reynolds number values for the flow of either aqueous or organic phases flowing separately between the two parallel shearing plates were below the transition region from laminar to turbulent flow, indicating that both liquid phases were flowing as a liquid-liquid dispersion under conditions of laminar flow, with Reynolds number values being lowest for a water-in-oil dispersion. The Taylor number values in Table 6 suggest that for each liquid flowing separately between the parallel shearing plates, except for liquid paraffin, transition occurred at a certain gap width between the plates and a certain rotational speed, from a simple rotating Couette flow to a more complicated flow at higher rotational speeds and gap widths, in which merged boundary layers might have started to form on each plate, as was suggested in the literature. In the case of liquid paraffin, with or without the addition of an emulsifying agent, the calculated range of Taylor numbers indicated simple rotating Couette flow with no transition taking place within the range of gap widths and rotational speeds used. In any case, the asymptotic state of separate boundary layers forming near each plate was not reached, since the calculated Taylor numbers were well below the value corresponding to that stage. Regarding the flow of two liquid phases flowing as a liquid-liquid dispersion between the parallel shearing plates, Table 6 indicates that in general, and for the liquid-liquid systems with liquid paraffin as the organic phase in particular, water-in-oil dispersions were

flowing in a rotating Couette flow for most of the rotational speeds and gap widths used. Oil-in-water dispersions, though, were more likely to move to the transitional state of flow at a certain gap width and rotational speed. The difference in the flow between water-in-oil and oil-in-water dispersions was much smaller for the Escaid-Water system, in which case the viscosities of the liquids were similar.

4.2.2. Shear Rate

The shear produced by rotation in the small gap between the stator and the rotor is the parameter responsible for the production of the dispersion between the parallel shearing plates by breaking the liquid phases into drops which either coalesce to form the continuous phase or remain dispersed forming the dispersed phase depending on the conditions of the system. So, it was regarded useful to calculate the shear rates produced between the plates in the range of rotational speeds and gap widths used in the experiments.

The simple relation used to calculate the shear rate produced between parallel shearing plates of radius r and gap width s by rotational speed N was:

$$\dot{\gamma} = Nrs^{-1} \quad (4.4)$$

The above equation was derived for a basic torsional flow geometry (Walters, 1975) assuming that, under the conditions of a very small gap width in comparison to the radius of the plates and very low flow rates of the liquid phases in comparison to the rotational speed, there was no axial flow while the angular velocity depended linearly on gap width. The radial velocity was assumed to be negligible in comparison to the angular velocity, since the estimated maximum ratio of radial to angular velocity was 0.17 (Appendix A2.2).

The calculated values of shear rate are presented in Table 7 for the various rotational speeds and gap widths used to give an idea of the order of magnitude of shear rates produced in the particular system of parallel shearing plates.

Since the flow of both liquid phases between the parallel shearing plates was laminar and the calculated shear rates were high enough to produce a liquid-liquid dispersion, the shear stress was the only factor responsible for the production of the liquid-liquid dispersions and there was no turbulence involved in the system.

4.2.3. Hydrodynamic Instabilities

The main complicating feature which distinguishes two phase gas-liquid and liquid-liquid flows from single phase gas or liquid flows, is the existence of deformable interfaces whose shape and distribution are of critical importance in determining the characteristics of the flow.

It was observed by Saffman and Taylor (1958) that in the flow of two fluids with different viscosities in a flow cell consisting of two closely spaced parallel plates (Hele-Shaw cell) with the less viscous fluid being the driving fluid, hydrodynamic instabilities at the interface led to the formation of fingers of the less viscous fluid penetrating into the more viscous one. The motion of the fluids in a Hele-Shaw cell is mathematically analogous to two dimensional flow in a porous medium. As stated by Wooding and Morel-Seytoux (1976), immiscible displacement of one fluid phase by another in a porous medium implied movement of a fluid-fluid interface through the pore spaces of the solid. If flow boundary conditions were held constant and sufficient time was allowed to elapse, a steady multiphase flow regime

could be established in a porous medium. For a given fluid phase being the driving fluid, the boundaries would consist of solid pore walls broken by "islands" where the driving fluid formed interfaces with other fluids. Such interfaces would be bounded by moving solid-fluid-fluid contact lines, so that the displacing fluid would wet the solid. The interface shape would be expected to be independent of velocity, provided that the parameter $\mu v/\sigma$ would be less than 1 (where σ is the interfacial tension, v the velocity of the moving interface and μ the viscosity of the driving fluid). With increasing $\mu v/\sigma$, the "islands" formed by fluid-fluid interfaces could become elongated and extend through the pores as the displacing fluid would form a core within a film of the other. Fingering formation of the less viscous fluid penetrating into the more viscous one is an instability at the interface which counteracts the steady two-phase flow described above and it is believed to be due to the different wetting properties of the solid walls with the fluids of different viscosities.

Davies (1960), who studied the phenomenon of phase inversion in liquid-liquid dispersions produced between parallel shearing plates, suggested that the hydrodynamic instabilities observed by Saffman and Taylor (1958) in the flow of two immiscible liquids with different viscosities could very well apply in the case of parallel shearing plates, always taking into account the wettability of the surfaces of the plates by the liquid phases. In the flow of two immiscible liquids between parallel plates that were preferentially wetted by the more viscous liquid, the hydrodynamic instabilities could be developed in such a way that long fingers of the less viscous liquid could penetrate into the more viscous one and break up into droplets because of high shear gradients. If, however, the less viscous liquid preferentially wetted the solid walls, it would tend to surround the more viscous liquid forming "islands" of the latter, which would then be dispersed into small drops in the

shear gradient.

Joseph et al. (1983) made a more generalized study of the flow of two immiscible liquids with different viscosities separated by an interface, driven by prescribed forces of the usual type. They suggested that the arrangements of the components that were actually achieved in the flow were certainly connected to the problem of hydrodynamic stability and appeared to be ones which were, in some mathematical sense, extremal. The extremizing configurations were such as to minimize the shearing of the high-viscosity liquid by the spontaneous migration of the low-viscosity liquid into regions where the shearing was greatest. They observed that in some cases the low-viscosity liquid moved into the region of high shear as a sheet leading to encapsulation of the high-viscosity liquid by the low-viscosity one. Sometimes, however, for example when the high-viscosity liquid wetted the moving boundary, the low-viscosity liquid fingered into the high-viscosity liquid. Droplets were then torn off the fingers and moved into the region of high shear as an emulsion of droplets of low-viscosity liquid in a high-viscosity foam.

The above observations of Joseph et al. (1983) agree with the suggestions made by Davies (1960) on the formation of fingers of the less viscous liquid penetrating into the more viscous one and breaking up into droplets, in the flow between parallel shearing plates, preferentially wetted by the more viscous liquid.

4.3. Flow in a Horizontal Tube

4.3.1. Reynolds number

The mode of flow of a liquid in a pipe is governed by Reynolds number, which is defined as follows:

$$Re = \frac{DV\rho}{\mu} \quad (4.5)$$

where D: diameter of pipe;
 V: average velocity of liquid;
 ρ : density of liquid;
 μ : viscosity of liquid.

It is well established that in the flow of a liquid in a pipe, transition from laminar to turbulent flow occurs for $2.1 \times 10^3 < Re < 10^4$.

The range of Reynolds numbers calculated for the minimum and maximum total flow rates in the horizontal glass tube and for each liquid phase used is presented in Table 8. The Reynolds numbers for the immiscible liquid pairs used would fall between those calculated for the aqueous and the organic phase respectively. Table 8 shows that the Reynolds number values for the flow of either aqueous or organic phases flowing separately in the horizontal tube were in general in the transitional region from laminar to turbulent flow. The Reynolds number value calculated in the case of the organic phase flowing on its own at the minimum flow rate at inversion was a little lower than the transitional region, but that was only an exception and it was purely theoretical since at that flow rate the actual Reynolds number value was influenced by the flow of both liquid phases at the appropriate flow rate ratio.

The Reynolds numbers in Table 8 suggest that the flow of both liquid phases in the horizontal tube was not fully turbulent. However, the flow rates of the liquids were high enough to suggest that liquid-liquid dispersions were formed in the horizontal tube by the breakup of one of the liquid phases into droplets under the influence of turbulent eddies.

4.3.2. Flow Patterns

At this stage, it is regarded useful to discuss briefly the flow patterns observed in the flow of two liquid phases in a horizontal tube (Russel et al., 1959, Charles et al., 1961).

It was reported that, in general, two immiscible liquids of different densities tended to stratify when flowing together in a horizontal pipe under laminar flow conditions. As the total flow rate increased, however, different flow patterns could be observed depending on the relative flow rates of the two liquid phases. In the flow of an organic phase and an aqueous phase in the pipe for a relatively high fixed flow rate of the aqueous phase, the flow-pattern changed with decreasing flow rate of the organic phase. The initial water-in-oil dispersion changed to a mixed flow of the water-in-oil dispersion and the two liquid phases, leading to stratified flow. That disappeared with further decrease of the flow rate of the organic phase, giving way to an oil-in-water dispersion. As the flow conditions became more turbulent, the transition from a water-in-oil dispersion to an oil-in-water dispersion was faster with no intermediate stratified flow observed. Other parameters which determined the flow pattern at a given flow rate ratio of the two liquid phases were the densities and viscosities of the liquids, the interfacial tension, which affected the ease of emulsification, and the contact angle of the liquid-liquid interface on the tubing material which

determined the liquid that preferentially wetted the pipe.

Other quantities which are convenient to employ in the treatment of two-phase flow in a horizontal pipe are the input ratio, the in situ ratio and the holdup ratio. The input oil-water ratio, $R_{o/w}$, has been defined as the ratio of the flow rate of the organic phase to the flow rate of the aqueous phase. The in situ ratio is the ratio of the volume of the pipe occupied by the organic phase to the volume occupied by the aqueous phase. It was reported (Charles et al., 1961) that in general the input and in situ ratios differed because the liquid in contact with the pipe wall would tend to accumulate in the pipe, and the ratio of the input oil-water ratio to the in situ oil-water ratio was defined as the holdup ratio. The holdup ratio, then, would differ in general from unity, and would tend to be greater than unity when the aqueous phase was in contact with the pipe wall and less than unity when the organic phase was in contact with the pipe wall. For highly turbulent flow with both liquids thoroughly mixed together, the in situ volumetric ratio would be approximately equal to the input volumetric ratio and the holdup ratio would be almost unity.

5. RESULTS

5.1. Introduction

The results obtained during the investigation of the phenomenon of phase inversion in liquid-liquid dispersions and the parameters which might affect it are presented analytically for both methods used in the experiments.

The effect of each parameter investigated is presented as well as the interactions between the factors involved in phase inversion. An attempt is made to correlate empirically the results of the first method with respect to the effect of wettability on phase inversion and compare the results of the second method with existing theoretical and empirical models.

5.2. Effect of Different Factors on Phase Inversion of Liquid-Liquid Dispersions Produced Between Parallel Shearing Plates

All the results of the investigation of the parameters involved in phase inversion of liquid-liquid dispersions produced between parallel shearing plates are presented in graphical form by plotting the volume fraction of the organic phase at inversion against rotational speed for the various operating conditions used and the various liquid-liquid systems used.

The results represent the mean values of the volume fraction of the organic phase at inversion Φ_1 , at various conditions. The mean values were taken after calculating Φ_1 for each experiment repeated under the same conditions. Each experiment for a particular liquid-liquid system at a given rotational speed and fixed gap width and material of the plates was repeated from 5 up to 10 times depending on how close the results taken were and how easily the phase-inversion point could be detected. Different flow rates were

used in repeating the same experiment but there was no significant effect on phase inversion, since the ratio of flow rate of the aqueous phase to flow rate of the organic phase at inversion remained approximately the same. The degree of reproducibility of the phase-inversion results was estimated by calculating the standard deviation from the mean value of the volume fraction values of the organic phase at inversion taken for each experiment repeated under the same conditions. The standard deviations for the liquid-liquid systems and operating conditions used were found to be in the range from ± 0.002 to ± 0.052 volume fraction with an average standard deviation of ± 0.019 . They are presented in Tables 9-23 for the different liquid-liquid systems used together with the corresponding mean values. An example of calculation of the mean value and standard deviation of the volume fraction of the organic phase at inversion, from the actual flow-rate readings of both liquids at this point, their ratios and the calculated Φ_i for each repeated experiment, is analysed in Appendix A3.3. The highest deviations from the mean value of the volume fraction of the organic phase at inversion were generally observed at low rotational speeds and high gap widths between the plates. At those conditions, it was difficult to observe clearly the phase-inversion point. Aqueous drops together with an oily film were observed on the cylindrical wall of the vessel surrounding the plates, when approaching phase inversion, that made the determination of the exact point of inversion difficult.

The values of the volume fraction of the organic phase at inversion for different rotational speeds and various gap widths between the plates are presented in Figures 13, 14 and 15 for the system Liquid Paraffin-Water and for perspex, stainless steel and glass plates respectively, based on the corresponding results in Tables 9, 10 and 11. Figures 13, 14 and 15 show clearly the dependence of phase inversion on rotational speed for the Liquid Paraffin-Water system while the effect of gap width is shown as well.

The effect of the wettability of the plates with the liquid phases on phase inversion is shown qualitatively in Figure 16 for the Liquid Paraffin-Water system by comparing the values of the volume fraction of the organic phase at inversion at various rotational speeds between the three different materials of the plates used. The results for gap widths up to 0.5 mm were used, since in that range the effect of gap width was very small.

Figures 17 and 18 show the effect on phase inversion of the addition of different types and concentrations of emulsifying agents in the Liquid Paraffin-Water system. With the addition of increasing amounts of Tween 80 in the aqueous phase, namely 60 ppm and 200 ppm in water, the effect of rotational speed and gap width on phase inversion became smaller until it was negligible, over the range of rotational speeds and gap widths used, as shown in Figures 17 and 18 for perspex and stainless steel plates respectively. The graphs in these figures are based on the results in Tables 12, 13, 14 and 15, compared with the results in Tables 9 and 10 for the system Liquid Paraffin-Water without any emulsifying agent present. Figure 18 also presents the effect of the addition of 1% v/v Oleic Acid in the organic phase for the Liquid Paraffin-Water system and stainless steel plates, based on the results in Table 16, in order to compare the effect of different types of emulsifying agents on the volume fraction of the organic phase at inversion.

Figure 19 shows the effects of rotational speed, gap width and material of the plates on phase inversion for the Dibutyl Maleate-Water system. The effects of liquid density difference and addition of an emulsifying agent are also shown. Figure 19 is based on the results in Tables 17 and 18 for stainless steel and glass plates respectively and in Tables 19 and 20 for the addition in the aqueous phase of 200 ppm Tween 80 in the case of stainless steel and glass plates. The results for 20% v/v CaCl_2 aq. soln. as the aqueous phase and stainless steel plates are taken from Table 21. In the system of Dibutyl Maleate-Water, the effects of rotational speed, gap width

and emulsifying agent on phase inversion are negligible but there is an effect of the material of the plates and some change for an increase in density difference between the liquid phases.

Figure 20 shows the dependence of the volume fraction of the organic phase at inversion on rotational speed, gap width and material of the plates in the Escaid-Water system based on the results in Tables 22 and 23 for stainless steel and glass plates respectively. The curve in Figure 20 for stainless steel plates is similar to that for the Liquid Paraffin-Water system. It occurs, however, at much higher values of the volume fraction of the organic phase at inversion, while the effect of gap width is negligible. Moreover, with glass plates, the curves in Figure 20 show an increase in the volume fraction of the organic phase at inversion with increasing rotational speed instead of the decrease observed in other systems. They also show a small dependence of phase inversion on the gap width between the plates.

The effect of the gap width between the plates on phase inversion for the systems Liquid Paraffin-Water and Escaid-Water can also be presented in the form of a plot of the volume fraction of the organic phase at inversion against the ratio of the gap width to the radius of the plates, s/r as in Figures 21, 22, 23 and 24, for three different rotational speeds and for the various materials of the plates. This form of presentation gives a good way of estimating the degree of influence of gap width on phase inversion in these systems in relation to the intensity of rotation and the scale of the apparatus. It shows a small dependence of phase inversion on gap width at lower rotational speeds which is diminished at higher rotational speeds. The same effect is visible in Figures 13, 14, 15 and 20, as well. As has been shown in Figures 17, 18 and 19, the effect of gap width on phase inversion for the systems with added emulsifying agent and decreased interfacial tension was negligible over the range of rotational speeds used.

It has already been mentioned that the absolute determination of the gap width between the plates was difficult to obtain even with the micrometer screw, because of the small scale of the apparatus. The difficulty in keeping the plates absolutely parallel while measuring the gap width as well as the roughness at the edges of the plates, particularly in the case of glass plates, prevented very accurate measurements of it. Testing different gap widths in the small range chosen was the best way of estimating the effect of that inaccuracy on the phase-inversion results. The small dependence of phase inversion on gap width, diminishing at higher rotational speeds, indicated that the dependence of the phase-inversion results on the degree of inaccuracy in the gap-width measurements was negligible. When there was some dependence of phase inversion on gap width, as in the case of Liquid Paraffin-Water and Escaid-Water systems at lower rotational speeds, the maximum degree of inaccuracy in the volume fraction of the organic phase at inversion, estimated from Figures 21, 22, 23 and 24, would be ± 0.04 , assuming that, in the worst case, the inaccuracy in gap width measurement would be $\pm 0.25\text{mm}$.

The contact angles of the various materials of the plates used with both aqueous and organic phases gave a quantitative representation of the effect of the wettability of the plates on phase inversion. The measured contact angles of the plates with each liquid phase used and each liquid-liquid system used (Tables 3 and 4) show that perspex and stainless steel plates were preferentially wetted by the organic phase and they had the least affinity for the aqueous phase. In contrast, although glass plates had almost the same wettability with respect to the aqueous and organic phases separately, they had much more affinity to aqueous than organic phase when in contact with the liquid-liquid interface, suggesting that they were preferentially wetted by the aqueous phase.

Considering that the less preferred type of dispersion formed is the one

which has the liquid that preferentially wets the material of the plates as the dispersed phase, the volume fraction of the dispersed phase of this dispersion at the point of inversion could be related graphically to the contact angle of the liquid-liquid system with the material of the plates. This contact angle, if measured through the phase which preferentially wets the material of the plates, is always less than 90° and its cosine is always positive. Moreover, Young's equation (Equation 3.5) shows that it is the cosine of the contact angle which in fact determines quantitatively the wettability of the liquids with a solid surface. Based on the suggestions made above, Figure 25 represents, quantitatively, the effect on phase inversion of the wettability with the liquid phases of the different materials of the plates at the highest Taylor numbers used, that is the maximum rotational speed and gap width used.

Figure 25 is a logarithmic graphical presentation of the volume fraction at inversion of the dispersed phase of the less preferred type of dispersion, for the maximum rotational speed used (2210 rpm), in which case the effect of gap width was smallest, against the cosine of the contact angle of the material of the plates with the liquid-liquid interface, measured through the phase which preferentially wetted the material of the plates and determined the preferred type of dispersion formed. It presents the phase-inversion results of most of the liquid-liquid systems used and for the various materials of the plates used.

The line in Figure 25, representing the results of the Liquid Paraffin-Water system (line a) has a -5.2 slope, suggesting a big influence of the magnitude of contact angle on phase inversion. However, the results of the same system, with increased concentration of Tween 80 dissolved in the aqueous phase, show deviations from this line. The slopes of the lines corresponding to 60 ppm and 200 ppm Tween 80 dissolved in the aqueous phase of

the Liquid Paraffin-Water system (lines b and c) are -1.2 and -0.4 respectively. These observations suggest that the addition of Tween 80 decreases the effect of the wettability of the plates by the liquid-liquid system on phase inversion, its influence being greater at higher concentrations of Tween 80. Since increased concentration of Tween 80 has the effect of lowering the interfacial tension of the liquid-liquid system, an attempt is made in Figure 26 to correlate using a log-log plot, the slopes of the lines observed in Figure 25 with the decreased interfacial tension. Figure 26 shows that the slope of the line, representing the effect on phase inversion of the contact angle with the plates of the Liquid Paraffin-Water system and of the same system with different concentrations of Tween 80 in the aqueous phase, changes with interfacial tension according to the following relation:

$$a = 8 \times 10^{-5} \sigma^3$$

where a : the slope of lines in Figure 25;
 σ : interfacial tension in dynes cm^{-1} .

The equation then which relates phase inversion with the simultaneous effect of contact angle of the liquid-liquid interface with the material of the plates and interfacial tension, lowered by the addition of Tween 80, for the Liquid Paraffin-Water system, is as follows:

$$\Phi_{d_i} \propto (\cos \theta)^{-8 \times 10^{-5} \sigma^3} \quad (5.1)$$

where Φ_{d_i} : volume fraction at inversion of the dispersed phase of the less preferred type of dispersion, approached asymptotically at high Taylor numbers;
 θ : contact angle of the liquid-liquid interface with the material of the plates, measured through the phase which preferentially wets it;
 σ : interfacial tension in dynes cm^{-1} .

The phase-inversion results in Figure 25 for the Dibutyl Maleate-Water system and the same system with the addition of 200 ppm Tween 80 in the aqueous phase are similar. In this case, the effect of Tween 80 is negligible, as has already been shown in Figure 19. The regression line then in Figure 25 which corresponds to the Dibutyl Maleate-Water system with or without the addition of Tween 80 (line d), has a -6.6 slope, showing a greater influence of contact angle on phase inversion than that in the Liquid Paraffin-Water system without the addition of Tween 80.

The following equation is an attempt to show quantitatively the effect of the magnitude of wettability of the shearing plates by the liquid phases on phase inversion when there is not any effect of an emulsifying agent, based on the results in Figure 25 and within the limitations of the liquid-liquid systems used:

$$\Phi_{d_i} \propto \cos\theta^{-a} \quad (5.2)$$

where Φ_{d_i} and θ are the same as in Equation 5.1 and a is in the range between 5.2 and 6.6.

The phase-inversion results for the Escaid-Water system are not included in the above correlation. As has already been mentioned, the above system with glass plates showed an increase in the volume fraction of the organic phase at inversion with increasing rotational speed, as opposed to the corresponding decrease observed for the rest of the systems examined. Consequently, it was difficult to correlate the wettability of the material of the plates by the immiscible liquid pair with the volume fraction at inversion of the dispersed phase of the preferred type of dispersion formed for the Escaid-Water system.

5.3. Phase Inversion of Liquid-Liquid Dispersions Produced in the Horizontal Glass Tube

5.3.1. Effects of Total Flow Rate and Method of Introducing the Liquids at the Inlet of the Tube for the Liquid-Liquid Systems Used

As has already been mentioned, phase inversion of liquid-liquid dispersions produced in the horizontal glass tube was studied in two ways, being approached either from an oil-in-water dispersion leading to a water-in-oil dispersion or vice versa. The method of introducing the two liquid phases in the tube was also altered by introducing the aqueous phase through the T-branch and the organic phase through the small tube at the inlet or vice versa.

Figure 27 shows how the volume fraction of the organic phase at inversion changed with the total flow rate in the tube for the system Escaid-Water with the aqueous phase being introduced through the T-branch at the inlet while the organic phase was introduced through the small tube at the inlet. The two different curves show that phase inversion depended on the type of the initial dispersion formed, the upper curve representing phase inversion from an oil-in-water dispersion to a water-in-oil dispersion while the lower curve represents phase inversion being approached from a water-in-oil dispersion leading to an oil-in-water dispersion.

Figure 28 shows the dependence of phase inversion on total flow rate and the type of dispersion initially formed for the same liquid-liquid system but for the opposite way of introducing the two liquid phases at the inlet, the organic phase being introduced through the T-branch while the aqueous phase was introduced through the small tube at the inlet. The two curves in Figure 28 are similar to those in Figure 27 but they both lie at lower values

of the volume fraction of the organic phase at inversion than the corresponding curves in Figure 27.

Figures 29 and 30 show the dependence of phase inversion on total flow rate and the initial type of dispersion formed for the same liquid-liquid system with the addition of 200 ppm Tween 80 in the aqueous phase and for either phase being introduced through the T-branch at the inlet respectively. The curves in each figure show a similar dependence of volume fraction of the organic phase at inversion on total flow rate and the type of dispersion initially formed to the corresponding curves for the Escaid-Water system without any emulsifying agent present. The curves in Figure 29 lie, however, at slightly lower values of the volume fraction of the organic phase at inversion than those corresponding to the system without an emulsifying agent (Figure 27). Moreover, the curves in both Figures 29 and 30 are similar and correspond to approximately the same values of volume fraction of the organic phase at inversion.

Finally, Figure 31 shows the behaviour of the Escaid-Water system in relation to phase inversion with the addition of 20% w/v CaCl_2 in the aqueous phase which increased the density of that phase. The curves in Figure 31 show the behaviour of the system with respect to phase inversion with increasing flow rate, type of dispersion initially formed and either phase being introduced through the T-branch at the inlet respectively. These curves are similar to the corresponding curves for the system without the addition of 20% w/v CaCl_2 in the aqueous phase, lying at approximately the same values of volume fraction of the organic phase at inversion as those for the pure liquid-liquid system. The only difference between the two liquid-liquid systems is that the system with the increased density of the aqueous phase showed a dependence of phase inversion on the initial type of dispersion formed which vanished at lower total flow rates than in the original Escaid-Water system.

Figures 27, 28, 29, 30 and 31 are based on the corresponding results in Tables 24, 25, 26, 27, 28 and 29. The results represent the mean values of the volume fraction of the organic phase at inversion, Φ_i , related to the mean values of the total flow rate at inversion, calculated from the corresponding values measured for each experiment repeated under the same conditions. Each experiment for a given liquid-liquid system and a given flow rate of one of the phases was repeated 5 times and the volume fraction of the organic phase at inversion, Φ_i , was calculated from the flow rate ratio of the two phases at the point of inversion while the total flow rate was calculated by adding the flow rates of the two phases at that point.

The standard deviations from the mean value of the volume fraction of the organic phase at inversion and the total flow rate at inversion were also calculated in order to estimate the degree of reproducibility of the phase-inversion results. The standard deviations for the liquid-liquid systems and conditions used were found to be in the range from 0 to ± 0.023 for the volume fraction of the organic phase at inversion with standard deviations of the total flow rate between 0 l/h and ± 7 l/h and with corresponding average standard deviations of ± 0.006 and ± 2 l/h. They are presented in Tables 24-29 together with the corresponding mean values.

An example of calculating the mean values and standard deviations of the volume fraction of the organic phase and the total flow rate at the point of inversion, from the actual flow rate and conductivity readings of both liquid phases at that point, is shown analytically in Appendix A3.4.

5.3.2. Comparison with Predictive Mathematical Models

An attempt is made to correlate the phase-inversion results for liquid-liquid dispersions produced in a horizontal glass tube by modifying the

mathematical predictive model of phase inversion derived and tested by Tidhar et al. (1986) for liquid-liquid dispersion produced in motionless mixers.

As has already been explained (Chapter 2), Tidhar et al. derived the following general expression for the volume fraction of the organic phase at inversion, Φ_i , of dispersions produced in motionless mixers, based on free energy considerations:

$$\Phi = 0.5 + C We^{-0.5} Re^{0.15} (dha) \cos \theta \quad (2.23)$$

where Weber number: $We = \rho_m V_T^2 dh / \sigma;$ (2.24)

Reynolds number: $Re = \rho_m V_T dh / \mu_m;$ (2.25)

$\rho_m = \Phi \rho_o + (1-\Phi) \rho_w;$ (2.26)

$\mu_m = \Phi \mu_o + (1-\Phi) \mu_w;$ (2.27)

V_T : total velocity of the dispersion;

ρ_m, ρ_o, ρ_w : densities of the dispersion, the organic phase and the aqueous phase respectively;

μ_m, μ_o, μ_w : viscosities of the dispersion, the organic phase and the aqueous phase respectively;

σ : interfacial tension between the liquids;

dh : hydraulic diameter of the motionless mixer;

a : motionless mixer area per unit volume;

θ : contact angle between the organic liquid drop and the surface of the mixing elements or the wall.

The equation of the mean viscosity of the dispersion is valid as long as the viscosities of the two phases are similar, which was the case for the liquid-liquid systems used in their experiments and also in these experiments using the horizontal glass tube method.

In the motionless mixer system used by Tidhar et al. the factor $a \cos \theta$ included two areas; the surface area of the mixing elements and the internal

area of the tube, each with its own contact angle. Since the internal surface amounted to 20% of the total solid surface, their experimental data were correlated with the following equation, based on Equation (2.23):

$$\Phi_i = 0.45 + 0.7(0.2\cos\theta_1 + 0.8\cos\theta_2)We^{-0.5}Re^{0.15} \quad (5.3)$$

where θ_1 : contact angle of the liquid-liquid system with the interfacial area of the mixer;

θ_2 : contact angle of the liquid-liquid system with the pipe wall.

They concluded that there was satisfactory agreement between the derived equation and their experimental data. They also pointed out that at high Weber numbers, when the drop diameter decreased and the liquid-liquid interfacial energy took the predominant role, the influence of the type of the solid surface became less important.

Equation (2.23) can be modified in the case of a horizontal glass tube as follows:

$$\Phi_i = 0.5 + C'\cos\theta We^{-0.5}Re^{0.15} \quad (5.4)$$

where $We = \frac{\rho_m V_{Ti}^2 D}{\sigma}$: Weber number; (5.5)

$$Re = \frac{\rho_m V_{Ti} D}{\mu_m}$$
: Reynolds number; (5.6)

D: diameter of the tube;

ρ_m, μ_m : as in Equations 2.26 and 2.27;

V_{Ti} : total average velocity of the dispersion at the point of inversion;

σ : interfacial tension;

θ : contact angle of the liquid-liquid system with the wall of the glass tube (measured through the aqueous phase).

According to Equation 5.3, predicted by Tidhar et al. for motionless mixers, the value of the constant C' should be around 0.7.

The contact angle measurements of the glass plates with the liquid-liquid systems used in the glass tube were also used to estimate the corresponding contact angles in the glass tube, since it was not possible to measure directly the contact angles of the liquid-liquid systems with the surface of the tube. The contact angles of the glass plates with the liquid-liquid systems used (Table 4), measured through the aqueous phase and being less than 90° , show that glass is in general wetted by water or aqueous solutions and has less affinity for the organic liquid used.

The phase-inversion results of the Escaid-Water system in the horizontal glass tube are plotted in Figure 32 as the volume fraction of the organic phase at inversion against the factor $\cos\theta We^{-0.5} Re^{0.15}$, based on Equation 5.4 with $C' = 0.7$. The results represent phase inversion being approached from either an oil-in-water or a water-in-oil dispersion and for either phase being introduced through the T-branch at the inlet respectively. An example of calculating the factor $\cos\theta We^{-0.5} Re^{0.15}$, based on Equations 5.5, 5.6, 2.26 and 2.27, for a range of total flow rates and the corresponding values of the volume fraction of the organic phase at inversion is presented in Appendix A3.5. The phase-inversion results in the horizontal glass tube of the Escaid-Water system with the addition of 20% w/v $CaCl_2$ in the aqueous phase are plotted in a similar way in Figure 33.

The phase-inversion results for the above liquid-liquid systems are compared with the phase-inversion results of Tidhar et al. in motionless mixers, represented by the dotted line in Figures 32 and 33. It can be seen that in both liquid-liquid systems the experimental data which best fit the predictive equation of Tidhar et al. are those in the case of phase inversion being approached from an oil-in-water leading to a water-in-oil dispersion when the organic phase was introduced through the T-branch at the inlet of the tube. For the Escaid-Water system, the results in the case of phase inversion

being approached from a water-in-oil leading to an oil-in-water dispersion, when the aqueous phase was introduced through the T-branch, also fit quite well the predictive equation of Tidhar et al., mainly at higher values of the parameter $\cos\theta We^{-0.5} Re^{0.15}$.

The observed deviations from the predictive equation of Tidhar et al. of the phase-inversion results for the Escaid-Water system and the same system with 20% w/v $CaCl_2$ added in the aqueous phase can be explained in relation to the holdup ratio in the horizontal glass tube, which has already been defined as the ratio of the input oil-water ratio to the in situ oil-water ratio in the tube. The volume fraction of the organic phase at inversion in the tube should have been calculated from the in situ ratio at inversion, which is the volumetric ratio based on the volume of the tube occupied by each liquid phase at the point of inversion. As has already been mentioned, the in situ ratio in the tube is not in general the same as the input flow rate ratio, since the liquid in contact with the tube wall tends to accumulate in the tube. Since it was not possible to measure the volume of the tube occupied by each liquid phase and hence the in situ ratio at the point of inversion, the apparent volume fraction of the organic phase at inversion was used instead, calculated from the input flow rate ratio of the two liquid phases at the point of inversion. The relationship between the apparent and the real volume fraction of the organic phase at inversion can be determined by examining the holdup ratio in the case of the aqueous or the organic phase wetting the tube wall respectively.

As has been reported in the literature (Charles et al., 1961), the holdup ratio tends to be greater than unity when the aqueous phase is in contact with the tube wall and less than unity when the organic phase is in contact with the tube wall. Consequently, the following relations apply in the former case:

$$\begin{aligned}
& Q_o/Q_w > V_o/V_w \\
\text{i.e.} \quad & 1 + Q_w/Q_o < 1 + V_w/V_o \\
\text{i.e.} \quad & 1/(1+Q_w/Q_o) > 1/(1+V_w/V_o) \\
\text{i.e.} \quad & \Phi_{iapp} > \Phi_i \quad (5.7)
\end{aligned}$$

Similarly, the following relations apply in the latter case:

$$\begin{aligned}
& Q_o/Q_w < V_o/V_w \\
\text{i.e.} \quad & 1 + Q_w/Q_o > 1 + V_w/V_o \\
\text{i.e.} \quad & 1/(1+Q_w/Q_o) < 1/(1+V_w/V_o) \\
\text{i.e.} \quad & \Phi_{iapp} < \Phi_i \quad (5.8)
\end{aligned}$$

In the relations above, Q_o/Q_w is the oil-water flow ratio and V_o/V_w is the oil-water in situ ratio while Φ_{iapp} and Φ_i are the apparent and real volume fractions of the organic phase at inversion respectively.

The aqueous phase was in contact with the tube wall when it was introduced through the T-branch and phase inversion was approached from an oil-in-water dispersion. Equation 5.7 shows that in that case the apparent volume fraction of the organic phase at inversion was higher than its real value and can explain the observed deviations in Figures 32 and 33 towards higher volume fractions. Similarly, the organic phase was in contact with the tube wall when it was introduced through the T-branch and phase inversion was approached from a water-in-oil dispersion. In that case, the fact that the apparent volume fraction of the organic phase at inversion was lower than its real value (Equation 5.8) can explain the observed deviations in Figures 32 and 33 towards lower volume fractions.

In cases where phase inversion was approached from the type of dispersion which had the liquid introduced through the T-branch as the dispersed phase, the tube wall was wetted by both liquid phases. In those cases, the observed deviations in the volume fraction of the organic phase at inversion were

negligible for the Escaid-Water system (Figure 32). For the Escaid-20% w/v CaCl_2 aq.soln. system, however, deviations towards higher volume fractions of the organic phase at inversion were observed when the aqueous phase was introduced through the T-branch even with phase inversion being approached from a water-in-oil dispersion (Figure 33). The above observation is related to the observed difference in the slopes of the lines representing phase inversion approached from an oil-in-water and water-in-oil dispersion respectively (Figures 32 and 33), a phenomenon which did not depend on the method of introducing the two phases at the inlet of the tube and cannot be explained by Equations 5.7 and 5.8. The above difference was also observed in Figures 27-31 in relation to the dependence of phase inversion on total flow rate in the glass tube.

The phase-inversion results in the horizontal glass tube for the Escaid-Water system with the addition of Tween 80 in the aqueous phase are presented in Figure 34 as a plot similar to those in Figures 32 and 33. The difference of this liquid-liquid system from those in Figures 32 and 33 is that the dependence of phase-inversion results on the method of introducing the two liquid phases at the inlet of the tube was smaller becoming negligible at higher Weber numbers. Consequently, there is a good agreement of the results in Figure 34 with those of Tidhar et al., represented by the dotted line. The regression analysis, based on all the results of Figure 34, gives 0.65 as the slope and 0.45 as the intersection with the Y axis of the regression line, resulting in the following equation:

$$\Phi_i = 0.45 + 0.65 \cos\theta \text{We}^{-0.5} \text{Re}^{0.15} \quad (5.9)$$

The above equation does not take into account the small difference observed in the slope of the lines representing phase inversion approached from an oil-in-water and water-in-oil dispersion respectively.

6. DISCUSSION OF PHASE-INVERSION RESULTS

6.1. Introduction

The results obtained from the two different experimental methods used to investigate the phase inversion of liquid-liquid dispersions are discussed analytically with respect to the effect of each parameter examined, trying to explain the phenomenon of phase inversion and understand its mechanism.

Comparison is made with the results and theories of previous workers, related to liquid-liquid dispersions and phase inversion in particular. The validity of the mathematical model used to correlate the phase-inversion results of the dispersions produced in the horizontal glass tube is also discussed, mainly in relation to the factors responsible for any discrepancies of the experimental data from the theoretical predictions.

Finally, a comparison between the results from the two different experimental methods is made in order to reach some generalized conclusions on the phenomenon of phase inversion in liquid-liquid dispersions.

6.2. Method of Parallel Shearing Plates

6.2.1. Effect of Viscosity Difference between the Liquids

Since the parameter responsible for the production of a liquid-liquid dispersion in the small gap between two parallel shearing plates, under laminar flow conditions, is the amount of shear in the system, it is evident that the viscosity of each liquid phase has an important role in determining the stability of each type of dispersion formed. Thus, the viscosity

difference between the liquid phases is likely to be a major parameter affecting the type of dispersion formed and its effect on phase inversion was chosen to be examined first.

The dynamic stability of a liquid-liquid dispersion is enhanced when the equilibrium between droplet breakup and coalescence moves towards breakup, leading to a finer dispersion. The breakup of droplets, under shear flow conditions, depends on the shear stress applied to the dispersed phase by the continuous phase, which in turn depends on the shear rate and the viscosity of the continuous phase (Chapter 2, Equation 2.1). Consequently, if the viscosity of the organic phase is higher than the viscosity of the aqueous phase, the shear stress applied to a water-in-oil dispersion is much higher than that applied to an oil-in-water dispersion at the same shear rate, leading to a finer dispersion of the water-in-oil type. The above suggests that higher viscosity of one of the liquid phases increases the dynamic stability of the type of dispersion with this liquid as the continuous phase, since it reduces the droplet size of its dispersed phase. This suggestion agrees with the results of previous workers on the effect of the viscosities of both phases on the droplet size of the dispersed phase, leading to smaller interfacial area of the dispersed phase with increased dispersed-phase viscosity or the opposite with increased continuous-phase viscosity (Treybal, 1951 - Calderbank, 1958 - Davies, 1985).

The phase-inversion results of the liquid-liquid dispersions produced between the parallel shearing plates can be examined by relating phase inversion to the preferred type of dispersion formed. According to the suggestions made above, in the case of substantial viscosity difference between the liquids, the liquid with the higher viscosity determines the preferred type of dispersion formed, since it favours its forming the

continuous phase. Other factors which might have an effect on the preferred type of dispersion formed are the volume ratio of the two phases, the wettability of the material of the shearing plates by the liquids and the type of any added emulsifying agent.

For the liquid-liquid systems with Liquid Paraffin or Dibutyl Maleate as the organic phase, having higher viscosity than the aqueous phase, water-in-oil dispersions were observed with volume fractions of the dispersed phase higher than 0.5. The above water-in-oil dispersions were observed for all the materials of the plates used and for all types of emulsifying agents used (Figures 13, 14, 15, 17, 18 and 19.) In contrast, the volume fraction of the dispersed phase of oil-in-water dispersions formed was less than 0.5 in all cases. Water-in-oil dispersions were obtained with the highest volume fractions of the dispersed phase observed when the shearing plates were strongly wetted by the organic phase. For example, the water-in-oil dispersion with the highest volume fraction of the dispersed phase (0.935) was formed for the Liquid-Paraffin-Water system with perspex plates (Figure 13, Table 9). These observations agree with the suggestions made above on the effect of the higher viscosity of one of the liquids on the preferred type of dispersion formed.

In the case of similar viscosities of the liquid phases, as in the Escaid-Water system, either type of dispersion could be formed at volume fractions of the dispersed phase higher than 0.5, depending on the other conditions of the system (Figure 20). For example, in the case of the Escaid-Water system with stainless steel plates, the highest volume fraction of the dispersed phase of the water-in-oil type of dispersion observed was 0.517. For the same system with glass plates, the highest volume fraction of the dispersed phase of the oil-in-water type of dispersion observed was 0.667

(Figure 20, Tables 22 and 23). The above observations suggest that when the viscosities of the liquids are similar, their effect on the type of dispersion formed in the system of parallel shearing plates is negligible, since the amount of shear stress applied to the immiscible liquid mixture is similar for both types of dispersion formed. Phase inversion, thus, depends only on the other parameters which might affect the preferred type of dispersion formed.

A phenomenon, which might influence the preferred type of dispersion formed when one of the liquids has higher viscosity and preferentially wets the surface of the plates, is the hydrodynamic instabilities observed by Saffman and Taylor (1958) and Joseph et al. (1983) in the flow of immiscible liquids with different viscosities (Chapter 4). If that phenomenon applies in the case of flow of immiscible liquids between parallel shearing plates, as was suggested by Davies (1960), it will be an additional reason for the aqueous phase to be increasingly dispersed in the organic phase. This will apply when the organic phase is the phase with the higher viscosity and preferentially wets the surface of the plates. The formation of water-in-oil dispersions between the parallel shearing plates, preferentially wetted by the organic phase, will then be favoured not only because of higher shear applied when the organic phase, which is the phase with the higher viscosity, is the continuous one but also because of the fingering formation of the aqueous phase, penetrating the organic phase and breaking up because of shear.

Some workers, who studied the formation of liquid-liquid dispersions in agitated vessels (Rodger et al., 1956 - Selker and Sleicher, 1965 - McClarey and Mansoori, 1978), observed an effect of increased viscosity of one of the phases on the type of dispersion formed, which was opposite to that observed in the case of parallel shearing plates. In their case, however, it would be the different mechanism of formation of the dispersion that led to those

results. The formation and the stability of the dispersion depended on the intensity of turbulence of the continuous phase, which decreased with increased viscosity. Consequently, their system favoured the formation of the type of dispersion with the less viscous liquid as the continuous phase. Some cases were also reported, in which the rate of diffusion to the liquid-liquid interface of an emulsifying agent, dissolved in the phase with the higher viscosity, was the controlling factor in determining the type of dispersion formed (Dickinson and Iball, 1948 - Davies, 1960).

6.2.2. Effects of Rotational Speed and Gap Width between the Plates

Since the preferred type of dispersion formed in the small gap between the parallel shearing plates depends on the shear stress applied to the immiscible liquid system, the applied shear rate can also have an important effect on the stability of the preferred type of dispersion formed and hence on phase inversion. The shear rate between the parallel shearing plates is a function of rotational speed and gap width between the plates (Equation 4.4). Its effect on phase inversion will thus be examined by examining the effect of each of the above parameters.

In the case of substantial viscosity difference between the liquids, the effect of rotational speed and gap width on phase inversion will be examined in relation to the preferred type of dispersion formed, which is determined by the higher viscosity of the organic phase as being of the water-in-oil type. For the liquid-liquid systems with Liquid Paraffin as the organic phase, a dependence of phase inversion on rotational speed was observed, so that in general the volume fraction of the organic phase at inversion decreased with increasing speed, favouring water-in-oil dispersions more strongly at higher than at lower rotational speeds. However, the dependence of phase inversion

on rotational speed decreased with increasing speed and increasing gap width between the plates, tending asymptotically at high Taylor numbers to a constant value of the volume fraction of the organic phase at inversion (Figures 13, 14 and 15). Increased concentrations of an emulsifying agent in the aqueous phase led asymptotically to a constant value of the volume fraction of the organic phase at inversion at lower Taylor numbers, that is at lower rotational speeds and gap widths between the plates (Figures 17 and 18). Similarly, liquid-liquid systems with Dibutyl Maleate as the organic phase showed a constant value of the volume fraction of the organic phase at inversion for the whole range of rotational speeds and gap widths used (Figure 19).

The above observations can be explained by relating rotational speed to the effect of shear rate on the stability of the water-in-oil dispersions formed (Equation 2.1). Since higher viscosity of the organic phase favours in general the formation of water-in-oil dispersions between the parallel shearing plates, an increase in rotational speed, that is an increase in shear rate, leads to finer and dynamically more stable water-in-oil dispersions even at higher volume fractions of the dispersed phase, that is lower volume fractions of the organic phase (Figures 13, 14 and 15). If, however, the stability of the dispersions formed is increased by any way other than increasing the rotational speed, such as decreasing the interfacial tension (Equation 2.1), the effect of rotational speed on the type of dispersion formed decreases until it becomes negligible (Figures 17, 18 and 19). The observed asymptotic value of the volume fraction of the organic phase at inversion is related to the closest packing of the dispersed phase droplets of the water-in-oil type of dispersion, that leads to coalescence (Clayton, 1954). At this point the stability of the dispersion formed is only affected by the volume fraction of the dispersed phase and possibly the wettability of the surface of the plates by the liquid phases.

An increase in rotational speed can also increase the rate of collision between the droplets of the dispersed phase, so increasing the rate of coalescence between the droplets (Lawson, 1967 - Howarth, 1967 - Arashmid and Jeffreys, 1980). This mechanism will dominate in the case of the less preferred type of dispersion formed, which is of the oil-in-water type when the viscosity of the organic phase is higher than that of the aqueous phase, so that the stability of this dispersion will decrease with increasing rotational speed (Figures 13, 14 and 15). Although this mechanism could also affect the stability of the water-in-oil type of dispersion, it is suppressed by the greater effect on drop breakup of the increased shear rate with increasing rotational speed, as discussed before.

Since increase in gap width between the plates has the effect of decreasing shear rate, it should also decrease the stability of the water-in-oil dispersions formed in the cases examined above. The phase-inversion results, however, showed exactly the opposite effect, that is an increase in the stability of the water-in-oil dispersions with increasing gap width (Figures 13, 14, 15, 21, 22 and 23). At larger gap widths, the dependence of the volume fraction of the organic phase at inversion on rotational speed decreased, approaching a constant value at all rotational speeds. That constant value was similar to the asymptotic value observed at higher speeds for smaller gap widths. This phenomenon can be explained by the effect of decreased shear rate on the stability of the less preferred type of dispersion, that is the oil-in-water type. When the gap width between the plates is increased, with the viscosity of the organic phase being higher than that of the aqueous phase, the shear stress applied to the liquid-liquid system in order to break up the organic phase into droplets is decreased until it becomes so low that it is not possible for a stable oil-in-water dispersion to be formed. The preferred type of dispersion is then formed, that is the

water-in-oil type, until the volume fraction of the dispersed phase reaches that corresponding to the closest packing of the dispersed phase droplets, above which coalescence is inevitable. The phase-inversion point, in this case, represents the point at which the water-in-oil dispersion cannot be dynamically stable any more and the liquid-liquid system inverts to a mixture of phases, consisting of aqueous phase and water-in-oil dispersion, rather than an oil-in-water dispersion. The above suggestion is supported by the fact that at low rotational speeds and high gap widths between the plates, aqueous drops together with a thin oily film were observed on the wall of the vessel, which surrounded the parallel shearing plates, after inversion of a water-in-oil dispersion or before inversion to a water-in-oil dispersion. When the stability of either type of dispersion is increased by decreasing the interfacial tension or by adding an appropriate emulsifying agent, the effect of gap width on the stability of the dispersions formed becomes negligible (Figures 17, 18 and 19).

As shown in Figures 13, 14, 15, 21, 22 and 23, the effect of gap width on phase inversion became negligible at higher rotational speeds. As has already been mentioned, a constant value of the volume fraction of the organic phase at inversion was approached asymptotically at those speeds which was independent of gap width. That was explained as being due to the closest packing of the dispersed phase droplets of the preferred type of dispersion formed. Therefore, it was a limiting value depending only on the volume ratio of the two phases for each liquid-liquid system and material of the plates and not on the operating conditions of the system. Another phenomenon, which could explain the behaviour of liquid-liquid dispersions in relation to the effect of gap width on phase inversion at high rotational speeds, is the transition state of flow occurring at higher gap widths and rotational speeds, as is suggested by the calculated Taylor numbers (Table 6). In the range of

gap widths and rotational speeds used, the transition from a simple Couette flow to a flow with merged boundary layers forming on each plate is mainly expected to have occurred in the oil-in-water type of dispersions. It could, thus, have had an effect on phase inversion by minimizing the effect of the increased gap width on the stability of this type of dispersions at higher rotational speeds.

When the viscosity difference between the liquids is negligible, as in the case of Escaid-Water system, the dependence of phase inversion on rotational speed and gap width between the plates is no longer related to the effect of the higher viscosity of the organic phase favouring the formation of the water-in-oil type of dispersion. It is related, however, to the wettability of the plates with the liquids, which in this case seems to have the dominant role in determining the preferred type of dispersion formed. When the plates were preferentially wetted by the organic phase, as in the case of Escaid-Water system with stainless steel plates, increased rotational speed favoured water-in-oil dispersions, tending to an asymptotic value of the volume fraction of the organic phase at inversion (Figure 20a). In contrast, when the plates were preferentially wetted by the aqueous phase, as in the case of Escaid-Water system with glass plates, oil-in-water dispersions were favoured at increased rotational speed (Figure 20b). In that case, there was also some effect of increased gap width between the plates which decreased the dependence of phase inversion on rotational speed, favouring more strongly the oil-in-water type of dispersion and tending to a constant value of the volume fraction of the organic phase at inversion (Figures 20c and 24).

The above observations can be explained by relating the wettability of the plates by the liquids to the preferred type of dispersion formed. The liquid which preferentially wets the surface of the plates favours its forming

the continuous phase (Davies, 1960). An increase in rotational speed stabilizes the type of dispersion favoured by this liquid, even at higher volume fractions of the dispersed phase, because of the increase in shear rate. The stability of the less preferred type of dispersion is decreased with increased rotational speed, due to the increase in the collision rate between the droplets of the dispersed phase and with the surface of the plates, which promotes coalescence. In this case, the surface of the plates is preferentially wetted by the dispersed phase. The effect of the increased gap width can be attributed to the decreased stability of this dispersion because of decreased shear rate.

The observations of decreased volume fraction of the organic phase at inversion with increased rotational speed, tending asymptotically to a constant value, agree with the results of most workers who studied phase inversion of liquid-liquid dispersions produced by agitation, including Davies (1960) who used the continuous-flow emulsifying machine of parallel shearing plates (Chapter 2). However, McClarey and Mansoori (1978) observed an increase in the volume fraction of the organic phase at inversion with increasing agitation speed, in cases where the initial conditions of the agitated system favoured the formation of oil-in-water dispersions. Some workers (Quinn and Sigloh, 1963 - Hossain et al., 1983) also pointed out the existence of two competing factors in determining the effect of agitation speed on the type of dispersion formed. Those factors were the increase in coalescence rate of the dispersed phase at high energy input because of increase in collision rate between the droplets and the decrease in the dispersed droplet size with increasing agitation speed. The above agree in general with the suggestions used to explain the effect of rotational speed on phase inversion of liquid-liquid dispersions produced between parallel shearing plates.

6.2.3. Effects of Interfacial Tension, Addition of an Emulsifying Agent and Density Difference between the Liquids

The effect of interfacial tension between the liquid phases on phase inversion of liquid-liquid dispersions between parallel shearing plates is related to the increased stability of the dispersions formed with decreasing interfacial tension.

The phase-inversion results for liquid-liquid systems of low interfacial tension, such as those with Dibutyl Maleate as the organic phase (Table 1), showed no dependence of phase inversion on rotational speed or gap width between the plates over the range of rotational speeds and gap widths used (Figure 19). Those results suggest that in cases where low interfacial tension is the dominant factor in stabilizing the preferred type of dispersion formed, the effect of the operating conditions on the stability of either type of dispersion formed is eliminated. The parameter which finally determines phase inversion in these cases is the volume fraction of the dispersed phase at the closest packing of the droplets of the preferred type of dispersion formed. This point corresponds to the constant value of the volume fraction of the organic phase at inversion, approached asymptotically at higher Taylor numbers in cases of higher interfacial tension (Figures 13, 14 and 15), as has already been discussed.

The phase inversion results regarding the effect of interfacial tension on the stability of the dispersions formed agree with the results of Luhnig and Sawistowski (1971) and Clarke and Sawistowski (1978). They reported that decreased interfacial tension increased the resistance to inversion of the preferred type of dispersion formed, which was favoured by the initial conditions of the agitated system used to produce the dispersions.

The effect of the addition of an emulsifying agent on phase inversion of liquid-liquid dispersions is related to the type of dispersion favoured by the chemical composition of the emulsifying agent, expressed as H.L.B. value. It is also related to the increased stability of this type of dispersion with increased concentration of the emulsifying agent, because of the decreased interfacial tension of the liquids.

As was reported by Becher (1965), emulsifying agents with H.L.B. numbers in the range 8 to 18 are suitable for stabilizing oil-in-water dispersions. The addition of Tween 80, which has an H.L.B. value of 15, in the aqueous phase of the Liquid Paraffin-Water system had the effect of generating phase inversion with higher volume fractions of the organic phase at inversion, which increased with increased concentration of the additive (Figures 17 and 18). That increase was more noticable at higher Taylor numbers. The above observations suggest that increased concentrations of Tween 80 increases the stability of the oil-in-water type of dispersion. Moreover, as has already been discussed, increased concentration of Tween 80 in the aqueous phase of the Liquid Paraffin-Water system had the effect of decreasing the influence of rotational speed and gap width on the type of dispersion formed (Figures 17 and 18). This was due to the decrease of interfacial tension with increased concentration of the additive (Table 1) with the simultaneous effect of approaching a constant value of the volume fraction of the organic phase at inversion, independent of rotational speed and gap width, at lower Taylor numbers.

It was also reported by Becher (1965) that emulsifying agents with low H.L.B. numbers, in the range 4 to 6, were suitable for stabilizing water-in-oil dispersions. He also reported that surface active agents with lower H.L.B. values, although having important surface-active properties, were

not strong emulsifying agents. The addition of Oleic Acid, which has an H.L.B. value of 1, in the organic phase of the Liquid Paraffin-Water system had the effect of generating phase inversion with a low volume fraction of the organic phase at inversion (Figure 18). That value was constant for the whole range of rotational speeds and gap widths used and was the same as the asymptotic value of the volume fraction of the organic phase at inversion for the liquid-liquid system without an emulsifying agent, approached at high Taylor numbers. In that case, the addition of the emulsifying agent, apart from affecting phase inversion by decreasing the interfacial tension of the liquids (Table 1), had no strong effect on favouring the water-in-oil type of dispersion, other than supporting the preference for that type of dispersion of the pure liquid-liquid system itself.

In the case of the Dibutyl Maleate-Water system, which strongly favoured the water-in-oil type of dispersion, addition of Tween 80 in the aqueous phase had no effect on favouring the opposite type of dispersion. It only had the effect of lowering even more the low interfacial tension of the liquids and had no further effect on the stability of the dispersion formed, already stabilized as of the water-in-oil type (Table 1, Figure 19). It seems that, in this case, Dibutyl Maleate itself has strong surface-active properties, which have the effect of lowering its interfacial tension with an aqueous phase and favouring the formation of the water-in-oil type of dispersion, so that its effect dominates when competing with the effect of small concentrations of another surface-active agent.

The phase-inversion results regarding the effect of the type and concentration of the emulsifying agent on phase inversion agree with the results of previous workers, such as Becher (1951) and Davies (1960). The former reported that increased concentration of an emulsifying agent, with an

H.L.B. number that favoured one type of dispersion, increased the volume fraction of the dispersed phase at inversion to the opposite type. The latter reported a linear increase in the volume fraction of the organic phase at inversion with increasing H.L.B. value, under the dynamic conditions of his continuous-flow emulsifying machine.

The effect of the density difference between the liquid phases on phase inversion was tested for the system Dibutyl Maleate-Water and stainless steel plates by adding 20% w/v CaCl_2 in the aqueous phase. The increased density of the aqueous phase (Table 1) caused a small increase in the volume fraction of the organic phase at inversion, when the other conditions remained constant (Figure 19). The above observations suggest that the closest packing of the dispersed phase droplets of the preferred type of dispersion formed is approached at lower volume fractions of the dispersed phase when its density is increased, favouring the formation of the opposite type of dispersion. The asymptotic value of the volume fraction of the organic phase at inversion can thus be affected not only by the viscosities of the liquids or their wetting of the material of the plates but also by their densities.

A similar effect of the density difference between the liquid phases on the type of dispersion formed was observed by previous workers who reported that when the effect of other parameters was diminished, a density difference between the liquids favoured the formation of the dispersion with the denser liquid as the continuous phase (Treybal, 1951 - Rodger et al., 1956 - Luhnig and Sawistowski, 1971 - McClarey and Mansoori, 1978). The phenomenon could be attributed to the effect of gravity on increasing coalescence of the droplets of the denser liquid. This effect might be stronger in dispersions produced by turbulent flow in agitated vessels, as those studied by the workers mentioned above, than in dispersions produced by shear in the small gap

between the parallel shearing plates, depending on the intensity of the "apparent" gravity force produced by the rotating flow.

6.2.4. Effect of Wettability of the Material of Plates by the Liquid Phases

The effect on phase inversion of the parameters discussed so far was always dominated by the effect of the wettability by the liquid phases of the material of the parallel shearing plates, between which the dispersion was formed. It seems that this parameter is the one which finally determines the preferred type of dispersion formed, when the effect of the other parameters is diminished.

It can be seen that the factor which most strongly affected the asymptotic value of the volume fraction of the organic phase at inversion was the wettability of the material of the shearing plates by the liquid-liquid system, by examining the phase-inversion results of the liquid-liquid systems at higher Taylor numbers, so that the effect of rotational speed and gap width was eliminated. The effect of that parameter was easily examined by changing the material of the plates while using the same liquid-liquid system, so that the physical properties of the system, such as viscosity and density differences between the liquids and interfacial tension, remained constant. In all cases, the volume fraction of the organic phase at inversion increased with increased wettability of the material of the plates with the aqueous phase, indicating that increased wettability of the material of the plates with one of the phases favours its forming the continuous phase (Tables 3 and 4, Figures 16, 17, 18, 19 and 20).

When the viscosity of the organic phase favoured the formation of the water-in-oil type of dispersion, the preferential wetting of the material of

the plates by the organic phase, as in the case of perspex and stainless steel plates (Tables 3 and 4), had the effect of favouring even more strongly that type of dispersion (Figures 16 and 19). This phenomenon is related to the combined effect of the higher viscosity of one of the liquids and its wetting the material of the plates on the preferred type of dispersion formed, as was suggested by Davies (1960) and Joseph et al. (1983). However, when the material of the plates was preferentially wetted by the aqueous phase, as in the case of glass plates (Tables 3 and 4), phase inversion to the oil-in-water type of dispersion, was observed at higher volume fractions of the organic phase at inversion (Figures 16 and 19). In that case the preferred type of dispersion was determined by the opposing effects of the higher viscosity of the organic phase and the increased wettability of the plates by the aqueous phase. Although the higher viscosity of the organic phase did not favour the formation of the oil-in-water type of dispersion, the increased wettability of the plates by the aqueous phase favoured the inversion to the oil-in-water type.

When the viscosity difference between the liquids was negligible, the effect of the liquid, which preferentially wetted the material of the plates (Tables 3 and 4), on favouring its forming the continuous phase was more noticable, since it also determined the dependence of phase inversion on rotational speed and gap width between the plates, as had been previously discussed (Figure 20).

The effect of the magnitude of the wettability of the material of the plates with the liquid phases on the volume fraction of the organic phase at inversion could be observed even when the type and concentration of the emulsifying agent strongly affected the preferred type of dispersion formed (Tables 3 and 4, Figures 17 and 18).

Davies (1960) gave some quantitative results about the effect of the wettability of the shearing plates of his continuous-flow emulsifying machine by one of the liquids on favouring its forming the continuous phase, which are in good agreement with the present results. There is also an agreement with other workers who observed the effect of the wettability of the surfaces containing liquid-liquid dispersions on the type of dispersion formed by different methods (Cheesman and King, 1934 - Tidhar et al., 1985 - Guilinger et al., 1988).

A quantitative representation of the effect of the magnitude of wettability of the parallel shearing plates by the liquid-liquid systems on phase inversion is given by empirical relations (Equations 5.1 and 5.2). These relations were derived from the logarithmic plot of the volume fraction, at the point of inversion at high Taylor numbers, of the liquid which preferentially wetted the material of the plates against the cosine of the contact angle of the liquid-liquid interface with the material of the plates, measured through that liquid (Figure 25). The empirically derived equation, when there is no effect of an emulsifying agent on the type of dispersion formed (Equation 5.2), shows a marked influence of the magnitude of the wettability of the plates on phase inversion. The inversion of a dispersion, which has the liquid that preferentially wets the material of the plates as the dispersed phase, is strongly favoured by decreasing the contact angle (that is increasing its cosine) of the liquid-liquid interface with the material of the plates, measured through this liquid.

In the case of an added emulsifying agent affecting the type of dispersion formed (Equation 5.1), there is an effect of the interfacial tension, which is decreased with increased concentration of the additive (Table 1), on the dependence of phase inversion on the magnitude of the

wettability of the plates with the liquids. The effect of the decreased contact angle, as was defined previously, on favouring the inversion of a dispersion which has the liquid that preferentially wets the material of the plates as the dispersed phase, is lowered with decreased interfacial tension (Figures 25 and 26, Equation 5.1). The above suggests that, when increased concentration of an emulsifying agent has an important role in stabilizing one type of dispersion because of decreased interfacial tension, the effect of the wettability of the material of the plates by the liquids on the type of dispersion formed is decreased. In any case, however, both Equations 5.1 and 5.2 suggest that the liquid which preferentially wets the material of the plates preferentially forms dispersions which have this phase as the continuous one and also that the inversion of the opposite type depends quantitatively on the magnitude of the wettability of the plates by this phase.

6.3. Method of the Horizontal Glass Tube

6.3.1. Effect of Total Flow Rate

In the liquid-liquid dispersions produced in the horizontal glass tube, the factor responsible for the breakup of the dispersed phase and hence the production of the dispersion was the intensity of turbulence, caused by the total flow rate of the liquid-liquid system in the tube. Consequently, the effect of total flow rate in the tube was essential in determining the preferred type of dispersion formed in relation to the other factors involved.

A dependence of phase inversion on total flow rate in the tube was observed for all liquid-liquid systems used, which diminished at higher Reynolds numbers, that is at more turbulent conditions, tending asymptotically

to a constant value of the volume fraction of the organic phase at inversion (Figures 27-31). However, the dependence of phase inversion on total flow rate was directly related to the way phase inversion was approached. When phase inversion was approached from an oil-in-water dispersion, the volume fraction of the organic phase at inversion decreased with increasing total flow rate, tending asymptotically to a constant value. In contrast, the approach to phase inversion from a water-in-oil dispersion resulted in lower volume fractions of the organic phase at inversion which increased slightly with increasing flow rate, leading asymptotically to a constant value. That constant value was in general lower but very close to the constant value observed in the former case.

The above observations suggest that the effect of total flow rate on the type of dispersion formed is related to the effect of the liquid phase that initially wets the surface of the tube on favouring its forming the continuous phase. When the aqueous phase initially wets the tube wall, the inversion at low flow rates of the initially formed oil-in-water dispersion takes place at higher volume fractions of the organic phase. In contrast, the inversion of the initially formed water-in-oil dispersion takes place at lower volume fractions of the organic phase, because the tube wall is initially wetted by the organic phase. An increase in the intensity of turbulence, by increasing the total flow rate in the tube, results in minimizing the above effect, by decreasing the volume fraction of the organic phase at inversion in the former case and increasing it in the latter. Finally, the effect of increased total flow rate in the tube results in the volume fraction of the organic phase at inversion being asymptotically constant, although not always identical for both ways of approaching phase inversion. There is thus a zone of ambivalence of phase inversion observed, which is wider at lower total flow rates, and in which either type of dispersion can be formed, depending on the phase which is first introduced into the tube and wets its surface.

The zone of volume fractions of the organic phase in which either type of dispersion can be formed in the horizontal tube, depending on the initial conditions of producing the dispersion, can be compared with the ambivalent region of phase inversion observed by a number of workers (Clarke and Sawistowski, 1979 - McClarey and Mansoori, 1978). It was mainly observed in liquid-liquid dispersions produced by agitation in batch systems, so that a water-in-oil dispersion existed above the upper limit of the ambivalent region and an oil-in-water dispersion existed below its lower limit. Either type of dispersion could be produced in between those limits depending on which phase was introduced first at a constant volume in the container. It was also observed by Tidhar et al. (1986) in liquid-liquid dispersions produced in motionless mixers but it was much narrower and its width was diminished at higher total flow rates. Those workers, however, reported a decrease in the volume fraction of the organic phase at inversion with increasing agitation speed or increasing total flow rate, when phase inversion was approached from a water-in-oil to an oil-in-water dispersion, instead of the slight increase observed in the horizontal tube. Most of them though reported that a constant value of the volume fraction of the organic phase at inversion was approached asymptotically at high Reynolds numbers.

The effect of total flow rate on the type of dispersion formed in the horizontal glass tube could be better understood after examining some of the other factors which affected phase inversion, such as the physical properties of the liquid-liquid systems and the wettability of the horizontal glass tube by each liquid phase.

6.3.2. Effects of Addition of an Emulsifying agent and Density Difference Between the liquids

The phase-inversion results of the liquid-liquid dispersions produced in the horizontal glass tube regarding the effects of total flow rate and the initial type of dispersion formed on the observed ambivalent zone of phase inversion were similar for all liquid-liquid systems used. A difference however was observed, for the various liquid-liquid systems used, in the constant value of the volume fraction of the organic phase at inversion which was approached asymptotically at high total flow rates in the tube.

The addition of Tween 80 in the aqueous phase of the Escaid-Water system (Figures 29 and 30), with the subsequent effect of lowering the interfacial tension of the system (Table 2), had the effect of approaching the asymptotic value of the volume fraction of the organic phase at inversion at lower total flow rates, compared to a similar effect in the same system without the emulsifying agent (Figures 27 and 28). The addition of the emulsifying agent resulted in lowering the effect on phase inversion of the wetting of the tube wall by the initial continuous phase so that the observed zone of ambivalence of phase inversion disappeared when approaching the asymptotic volume fraction of the organic phase at inversion. However, in the case of the aqueous phase being introduced through the T-branch at the inlet of the tube, phase inversion of the Escaid-Water system with the addition of Tween 80 (Figure 29) appeared to occur at a lower volume fraction of the organic phase compared to that observed for the pure system (Figure 27). In this case, the addition of Tween 80 appeared to favour the water-in-oil type of dispersion instead of favouring the opposite type, as was expected. This phenomenon can be explained by examining the effect of the method of introducing the two liquid phases at the inlet of the tube on the observed volume fraction of the organic phase at inversion (see Section 6.3.3).

The phase-inversion results of the Escaid-Water system with the addition of 20% w/v CaCl_2 in the aqueous phase (Figure 31) and the subsequent effect of increased density difference between the liquid phases towards higher density of the aqueous phase, were similar to those observed for the pure system. The only difference was the width of the ambivalent zone of phase inversion at higher total flow rates, which was smaller for the system with the increased density difference, while the asymptotic value of the volume fraction of the organic phase at inversion was approached at lower flow rates compared to that observed for the original system. Moreover, when the aqueous phase was introduced through the T-branch at the inlet of the tube, the ambivalent zone of phase inversion disappeared as the asymptotic value was approached. The above differences could be related to the effect of the density of dispersion on the droplet size of the dispersed phase (Equation 2.2), leading to increased penetration of turbulence into wall regions and reducing the effect of wetting.

Since both interfacial tension and density difference between the phases have an effect on the droplet size of the dispersed phase of both types of dispersion formed in the horizontal glass tube, their effect could be related to the effect of droplet size on phase inversion, as was described by Equation 5.4. However, that equation has been mainly developed to show the effect on phase inversion of the magnitude of wettability of the tube wall by the liquid-liquid systems, and this will be discussed before considering the other terms in the equation.

6.3.3. Effect of Wettability of the Horizontal Glass Tube by the Liquids

One of the effects of the wettability of the surface of the horizontal glass tube by the liquid phases has already been discussed, in relation to the

effect on phase inversion of the continuous phase of the initial type of dispersion formed. An ambivalent zone of phase inversion, which was wider at lower total flow rates, was observed due to the initially continuous phase wetting the tube wall.

Besides the above effect on phase inversion, an effect of the method of introducing the liquid phases at the inlet of the tube was also observed for all liquid-liquid systems used except that with the emulsifying agent added in the aqueous phase. For all those systems, phase inversion was observed at lower volume fractions of the organic phase when that phase was introduced through the T-branch at the inlet of the tube (Figures 27, 28 and 31). The biggest difference observed for the same liquid-liquid system was between the phase inversion results when inversion was approached from an oil-in-water dispersion while the aqueous phase was introduced through the T-branch and the results when inversion was approached from a water-in-oil dispersion while the organic phase was introduced through the T-branch. At a constant total flow rate, phase inversion was observed at a higher volume fraction of the organic phase in the former than in the latter case. That difference, however, decreased with increasing total flow rate of the liquid-liquid system in the tube, approaching an asymptotic value.

The above observations suggest that the effect of the initial wetting of the tube wall by one of the liquids on favouring its forming the continuous phase is enhanced by introducing that liquid through the T-branch, so that it wets the surface of the tube straight from its inlet. A thin layer of that phase could thus be formed on the surface of the tube, which can affect the observations on phase inversion and result in observing an apparent volume fraction of the organic phase at inversion as shown in Figures 32 and 33.

As has already been shown, Figures 32, 33 and 34 represent an attempt to correlate phase inversion in the horizontal glass tube with the magnitude of wettability of the tube by the liquid phases, expressed as contact angle of the liquid-liquid interface with the glass surface of the tube, based on Equation 5.4. This equation is a modification of Equation 2.23 developed by Tidhar et al. (1986) for phase inversion in motionless mixers. The above correlation also relates phase inversion to the droplet size of the dispersed phase which in turn is related to the average velocity of the dispersion in the tube, its density, its viscosity and the interfacial tension between the liquid phases, and is expressed as a function of Weber and Reynolds numbers.

The phase-inversion results for all liquid-liquid systems used show a proportionality of the volume fraction of the organic phase at inversion with the function of Weber and Reynolds numbers which represents the droplet size of the dispersed phase, as predicted by Equation 5.4 (Figures 32, 33 and 34). The above proportionality can partly explain the changes, that have been discussed previously, in phase-inversion results, observed when changing the interfacial tension and the density difference between the liquids (Figures 27-31). Those changes, however, are also related to the effect of the wettability of the glass tube by the liquids. The results in Figures 32, 33 and 34 show a proportionality of the volume fraction of the organic phase at inversion with the cosine of the contact angle of the liquid-liquid interface. Differences, however, are observed in the slopes of the lines representing the different methods of introducing the liquids at the inlet of the tube and the different ways of approaching phase inversion.

For the Escaid-Water system in particular and the same system with the addition of 20% w/v CaCl_2 in the aqueous phase (Figures 32 and 33), deviations from Equation 5.3, predicted by Tidhar et al., are observed, which are higher

at lower Weber numbers, that is lower average velocities in the tube. As has already been mentioned, these deviations are towards higher values of the volume fraction of the organic phase at inversion in the case of the aqueous phase being introduced through the T-branch at the inlet of the tube and inversion being approached from an oil-in-water to a water-in-oil dispersion. In contrast, the deviations are towards lower values of the above parameter in the case of the organic phase being introduced through the T-branch and inversion being approached from a water-in-oil to an oil-in-water dispersion. In the other two cases, phase-inversion results are closer to the line representing Equation 5.3. For the Escaid - 20% w/v CaCl_2 aq. soln. system, however, deviations towards higher volume fractions of the organic phase at inversion are observed in the case of the aqueous phase being introduced through the T-branch even when phase inversion is approached from a water-in-oil dispersion (Figure 33). Moreover, for all liquid-liquid systems used, a difference is observed between the slopes of the lines representing phase inversion being approached from an oil-in-water dispersion and vice versa, regardless of the method of introducing the liquids at the inlet of the tube.

The deviations observed for the different methods of introducing the liquids at the inlet of the tube can be explained by considering that when the initial continuous phase wets the tube wall at the inlet, it tends to accumulate in the tube, mainly when the intensity of turbulence is low (Chapter 4). This phenomenon leads to the observation of an apparent volume fraction of the organic phase at inversion, which is either higher than the real one when the aqueous phase accumulates in the tube or lower than the real one when the organic phase accumulates in the tube (Equations 5.7 and 5.8). The observed effect of the wetting of the tube at the inlet by one of the liquids on favouring its forming the continuous phase is thus related to the

observation of an apparent value of its volume fraction at inversion. When the method of introducing the two liquids at the inlet of the tube and the way of approaching phase inversion results in the wetting of the tube wall at the inlet by both liquids, the accumulation of any of the liquids on the tube wall is minimized. Consequently, the apparent value of the volume fraction of the organic phase at inversion is similar to the real value and the derivations from the slope of the line predicted by Equation 5.3 are not significant. However, even in these cases, the increased magnitude of wettability of the tube wall by one of the liquids might result in small deviation of the observed volume fraction of the organic phase at inversion from the predicted value of Equation 5.3, as shown in Figure 33 for the case of introducing the aqueous phase through the T-branch at the inlet of the tube.

Increased intensity of turbulence minimizes the accumulation of one of the liquids on the tube wall (Chapter 4), so that the difference between the apparent and the real volume fraction of the organic phase at inversion is decreased (Figures 32 and 33). The above suggestion is in accordance with the decrease, with increasing total flow rate, of the difference in phase-inversion results, observed for the two different methods of introducing the liquids at the inlet of the tube (Figures 27, 28 and 31).

The phase-inversion results of the Escaid-Water system with the addition of 200 ppm Tween 80 in the aqueous phase follow quite well the predicted line based on Equation 5.3 for all cases examined (Figure 34). The difference between the slope of that line and the slope of the regression line based on the above results (Equation 5.9) is very small and can be neglected, since the intersection of both lines with the Y axis is the same. The addition of the emulsifying agent to the aqueous phase, with the subsequent effect of decreasing the interfacial tension (Table 2), had an effect similar to the

effect of the increased intensity of turbulence. It decreased the accumulation of the liquid which initially wetted the tube wall at the inlet, so that the observed volume fraction of the organic phase at inversion was much closer to the real value, as predicted by Equation 5.3. That was also the reason for observing an apparent decrease in the volume fraction of the organic phase at inversion with the addition of Tween 80, instead of the expected increase. The above observations are due to the effect of the emulsifying agent, in addition to the increased turbulence, on producing and stabilizing homogeneous liquid-liquid dispersions of both types, while phase inversion in the horizontal tube is determined by the magnitude of the parameters involved, as predicted by Tidhar et al. (Equation 5.3) for motionless mixers.

The difference between the slopes of the lines representing the two ways of approaching phase inversion, observed for all liquid-liquid systems used (Figures 32, 33 and 34), are mainly related to the observed ambivalence in phase inversion. It has already been discussed that the ambivalence in phase inversion is also related to the wetting of the tube wall by the continuous phase. It has been shown that the ambivalent zone is wider at lower total flow rates (Figures 27-31). This observation can explain the difference in the slopes of the lines that relate phase inversion to the predictive Equation 5.4 for the two different ways of approaching phase inversion. The results of Tidhar et al. (1986) also showed a narrow ambivalent zone and some deviation from the predictive slope of the line representing Equation 5.3, which was regarded insignificant.

The validity of Equation 5.3 and therefore Equations 5.4 and 5.9 can best be described by examining the phase-inversion results in the horizontal glass tube in relation to these equations, taking into account the deviations

observed because of the accumulation in the tube of one of the liquids. Deviations of the corresponding results from these equations at high Weber numbers, that is high total flow rates, towards a constant value of volume fraction of the organic phase at inversion (Figures 27-34), show the limitations of these equations.

The equations above are based on the predictive model of phase inversion (Equation 2.23) derived by Tidhar et al. (1986), by taking into account the effect of the solid surface on the total energy of the system before and after inversion. The validity of this model is therefore limited since the influence of the type of solid surface becomes less important at high Weber numbers, as shown by the deviations mentioned above. Moreover, as has already been mentioned, the derivation of this model was based on the assumptions of no change in the mean droplet size of the dispersed phase with phase inversion and of similar viscosities of the liquid phases. The former assumption is not necessarily always true, since it was reported elsewhere (Luhning and Sawistowski, 1971) that phase inversion was accompanied by a change in the droplet size of the dispersed phase. The latter assumption is another limitation of the model, since it does not take into account any substantial viscosity difference between the phases. However, within the limitations of similar viscosities of the liquid phases and a range of Weber numbers in which the influence of the wettability of the surface of the tube by the liquids is important, the predictive model of Tidhar et al. on phase inversion in motionless mixers describes satisfactorily the phase-inversion results in the horizontal glass tube.

6.4. Comparison between the Two Methods

In order to compare phase inversion of liquid-liquid dispersions produced between the parallel shearing plates and those produced in the horizontal

glass tube, the first thing which should be taken into account is the factor responsible for the production of the dispersion by each method used.

Shear stress is the factor responsible for the breakup of the dispersed phase droplets in liquid-liquid dispersions produced between the parallel shearing plates. Consequently, the main factors which affected the dynamic stability of each type of dispersion formed were the viscosity of the continuous phase in comparison to the viscosity of the dispersed phase, the interfacial tension of the liquid phases and the shear rate, being a function of rotational speed and gap width between the plates (Equation 2.1 and 4.4). The breakup of the dispersed phase in liquid-liquid dispersions produced in the horizontal glass tube occurred because of the turbulent eddies produced by the total flow rate in the tube. The dynamic stability of each type of dispersion formed was then affected by the droplet size of the dispersed phase which was a function of the average total velocity in the tube, the densities and viscosities of the two phases, and the interfacial tension between the phases (Equation 2.21). Phase inversion was examined in relation to the factors affecting the droplet size and hence the dynamic stability of both types of dispersion formed by each method used, taking also into account the important influence of the surrounding solid surfaces and the type of any emulsifying agent used.

The important influence of substantial viscosity difference between the liquid phases on the preferred type of dispersion formed between the parallel shearing plates, because of its effect on the amount of shear put in the liquid-liquid system, has already been discussed thoroughly. In contrast, the viscosity difference between the phases was less important in liquid-liquid dispersions produced by turbulent eddies, as shown by Equation 5.4. It was reported, however, that increased viscosity of the dispersed phase could have

a substantial effect on resisting deformation and breakup of the drops in dispersed systems produced by turbulence (Sleicher, 1962 - Davies, 1987). In any case, no comparison can be made between phase-inversion results of the two different methods used, in relation to the effect of viscosity difference between the liquid phases, since no liquid-liquid system with increased viscosity difference between the liquids was used for liquid-liquid dispersions produced in the horizontal glass tube. However, comparison between the phase-inversion results of the two different methods used, for the Escaid-Water system, in which the viscosities of the liquids were similar, shows similar values of the volume fraction of the organic phase at inversion (Figures 20, 27 and 28). Its exact value though depended on the other factors, besides viscosity, which affected phase inversion in each method used.

The effect of rotational speed on phase inversion of liquid-liquid dispersions produced between the parallel shearing plates can be compared with the effect of total flow rate on phase inversion of liquid-liquid dispersions produced in the horizontal tube, since each of those parameters represented the amount of energy put into the liquid-liquid system by the corresponding method. In the parallel shearing plates method, the effect of increased rotational speed was to increase even more the dynamic stability of the type of dispersion favoured by the other factors involved (Figures 13-20). In contrast, in the horizontal tube method, increased total flow rate had the effect of reducing the influence of the other factors on phase inversion (Figures 27-31). In both cases, however, a constant value of the volume fraction of the organic phase at inversion was approached asymptotically with increasing the corresponding parameter. In the former case, that constant value depended on the other factors, which affected phase inversion more strongly than rotational speed. In the latter case, the effect of increased

intensity of turbulence was stronger so that the volume fraction of the organic phase at inversion approached a constant value of about 0.5 for all liquid-liquid systems used (Equation 5.4). The observed deviations from that constant value for some of the systems used were mainly due to the accumulation of one of the liquids in the tube, depending on the method of introducing the liquids at the inlet.

The effect of the magnitude of wettability of the solid surfaces, containing the immiscible liquids, on the type of dispersion formed was quite strong in both methods used. Its effect though was much stronger in the method of parallel shearing plates, as shown in Equation 5.2, compared with Equation 5.4 of the horizontal tube method. Moreover, the wettability of the parallel shearing plates was one of the factors determining the asymptotic value of the volume fraction of the organic phase at inversion whereas the effect of the wettability of the tube wall was stronger at lower total flow rates and decreased with increased turbulence.

Another factor which had an important influence on the preferred type of dispersion formed between the parallel shearing plates was the type and concentration of any emulsifying agent added to the immiscible liquid system. Its effect, besides favouring a certain type of dispersion and reducing the influence of the operating conditions of the system by decreasing the interfacial tension, was to decrease the effect of the wettability of the plates on the type of dispersion formed (Equation 5.1). The effect of the emulsifying agent in liquid-liquid dispersions produced in the horizontal tube was less strong. Its main influence was to decrease the interfacial tension and therefore minimize the effect of wetting of the tube wall by one of the liquids on the observed volume fraction of the organic phase at inversion. Its effect on decreasing the interfacial tension was also related to the

decrease of the droplet size of the dispersed phase which was a function of Weber and Reynolds numbers (Equations 5.4, 5.5 and 5.6).

Finally, the density difference between the liquids had a small effect, by favouring the dispersion with the heavier liquid as the continuous phase in the parallel shearing plates method. It also had a small effect on phase inversion of liquid-liquid dispersions produced in the horizontal glass tube, by affecting the droplet size of the dispersed phase of both types of dispersion formed (Equations 5.4, 5.5 and 5.6).

The comparison of the phase-inversion results of the two different methods used to produce the liquid-liquid dispersions led to the following conclusions regarding the difference between the two methods. In the case of dispersions produced by shearing in the small gap between parallel plates, under laminar flow conditions, the main factors affecting phase inversion were the properties of the liquids, their wettability with the material of the plates and the type and concentration of any added emulsifying agent. The effect of shear rate, when examined as a function of rotational speed at a given gap width between the plates, was less strong and decreased at higher Reynolds and Taylor numbers. In the case of dispersions produced by turbulence in the horizontal tube, the main factor affecting the point of inversion was the interfacial energy between the liquids which was influenced by the properties of the liquids and the intensity of turbulence. Increasing the latter decreased the effect of the wettability of the surface of the tube by the liquids, which had an important influence at lower Weber numbers.

7. CONCLUSIONS

The study of the phenomenon of phase inversion in liquid-liquid dispersions produced by shear or turbulence resulted in drawing some general conclusions regarding the effect of various parameters on it. These conclusions can be helpful in choosing the operating conditions of a given system, so that phase inversion will be either encouraged or avoided depending on the desired outcome.

In liquid-liquid dispersions produced by shear, the point of phase inversion is mainly determined by the properties of the liquids. The viscosity difference between the liquids and their wetting of the shearing surfaces are the main factors which determine the phase-volume ratio that causes inversion. For a liquid-liquid system with substantial viscosity difference, the liquid with the higher viscosity favours its forming the continuous phase. Consequently, it opposes inversion to the opposite type and vice versa. Its influence can become less strong by decreasing its wetting of the shearing surfaces. Choosing a material of the surfaces that is mainly wetted by the less viscous liquid can favour inversion to the type with this liquid as the continuous phase. A substantial viscosity difference between the liquids, however, puts a limitation to the above effect.

The effect of shear rate on the phase inversion point of liquid-liquid dispersions produced by shear is noticable at low rotational speeds. At a given gap width between the shearing plates, increasing the rotational speed, that is increasing the shear rate, decreases any tendency of the preferred type of dispersion formed to invert and vice versa. A point is eventually reached where an increase in rotational speed has no more effect on the point of inversion. Moreover, at low rotational speeds, increasing the gap width

between the plates, that is decreasing the shear rate, can lead to the production of non-homogeneous dispersions, consisting of more than two liquid-phases. Consequently, the shearing system should operate at high shear rates, that is small gap widths between the plates and high rotational speeds, in order to produce homogeneous liquid-liquid dispersions and eliminate any effect of shear rate on phase inversion.

When an emulsifying agent is added in the sheared liquid-liquid system, its type and concentration have a major influence on the preferred type of dispersion formed. The chemical composition of the emulsifying agent, expressed as H.L.B. value, favours strongly only one type of dispersion, depending on this value. Increased concentration of the emulsifying agent decreases the interfacial tension of the liquid-liquid system with the subsequent effect of increasing the stability of the type of dispersion favoured by its H.L.B. value and decreasing any tendency to inversion. However, the wettability of the shearing surfaces by the liquid phases and any substantial viscosity difference between them are still the main factors determining the exact point of inversion, although their influence becomes less strong because of the effects of the emulsifying agent.

In general, low interfacial tension of the sheared liquid-liquid system, even without adding any emulsifying agent, has the effect of stabilizing the type of dispersion favoured by the other conditions of the system. Therefore, it eliminates any effect of shear rate on phase inversion, even at low shear rates. Moreover, increased density difference between the sheared liquids, when the rest of the conditions remain constant, can have a small effect on the point of inversion by favouring the formation of the type of dispersion with the heavier liquid as the continuous phase.

When there is no substantial viscosity or density difference between the liquid phases and there is no added emulsifying agent, the wettability of the shearing surfaces is the only factor determining the point of inversion of a liquid-liquid dispersion produced by shear at high shear rates. Therefore, the choice of the appropriate material of the shearing surfaces will determine the type of dispersion formed at a given phase-volume ratio. It can then be concluded that, when the point of inversion of a liquid-liquid dispersion produced by shear is affected by the liquid properties, such as viscosity or density differences between the liquids, interfacial tension or addition of an emulsifying agent, a careful study of the combined effects of all these factors will determine the choice of the material of the plates and the phase-inversion limits.

In liquid-liquid dispersions produced by turbulence, the phase-inversion point is mainly determined by the intensity of turbulence which, in the case of the production of the dispersion in a horizontal tube, is related to the total flow rate in the tube. Increasing the total flow rate in the tube, that is increasing the intensity of turbulence, leads to the formation of finer dispersions, which are therefore more stable and their tendency to inversion is minimized so that the only factor which controls inversion at conditions of high turbulence is the phase-volume ratio. At low total flow rates, the point of inversion is affected by the liquid properties, such as density difference and interfacial tension between the liquids and their wetting of the material of the tube. Their influence, however, is reduced with increasing total flow rate, leading to a constant point of phase inversion which ideally is the point of equal liquid-phase volumes. The above conclusion as well as those that follow are based on phase-inversion studies of liquid-liquid dispersions produced by turbulence in a horizontal tube, when there was no substantial viscosity difference between the liquids. Therefore, their application is limited to this kind of liquid-liquid systems.

The wetting of the surface of the tube by the continuous phase of a liquid-liquid dispersion initially formed in a horizontal tube reduces its tendency to inversion. Therefore, phase inversion from an oil-in-water to a water-in-oil dispersion occurs at higher volume fractions of the organic phase than the opposite inversion. This phenomenon leads to the existence of an ambivalent region of phase-volume ratios in which either type of dispersion can be formed depending on the phase which initially wets the tube wall and therefore forms the continuous phase. The effect of the wetting of the tube wall by the initial continuous phase is enhanced when this phase wets the tube straight from its inlet. In this case, the initial continuous phase accumulates on the surface of the tube wall leading to the observation of an apparent phase-volume ratio at the point of inversion. The magnitude of the wettability of the tube wall by the liquids, expressed as contact angle between the liquid-liquid interface and the material of the tube wall, affects the phase-inversion point by controlling the range of phase-volume ratios in which inversion can occur. As has been previously mentioned, the effects of the wetting of the surface of the tube by the liquids are minimized with increased intensity of turbulence.

The effect of the addition of an emulsifying agent to the liquid-liquid system is related to the decrease of interfacial tension, leading to the formation of finer dispersions produced by turbulence in a horizontal tube. Increased density of one of the phases has the effect of increasing the density of the dispersion which also leads to the formation of finer dispersions in the horizontal tube. Decreasing the droplet size of the dispersed phase by any way other than increasing the total flow rate in the tube has the same effect as the increase in total flow rate. It therefore reduces the effect of the other parameters on phase inversion, leading to a constant point of phase inversion.

Consequently, in liquid-liquid dispersions produced by turbulence in a horizontal tube, the preferred type of dispersion formed is determined only by the phase-volume ratio when the turbulent conditions or the liquid properties permit the maximum stability of the dispersion formed. When the conditions of the liquid-liquid system do not reach this stage, the phase-inversion point will be determined by the combined effect of the intensity of turbulence, the properties of the liquid-liquid system, the magnitude of wettability of the surface of the tube by the liquids and the initial type of dispersion formed. In this case, care should also be taken when choosing the manner of introducing the liquids at the inlet of the tube, so that the accumulation of one of the liquids in the tube is minimized.

In general, the type of liquid-liquid dispersion formed and the phase-inversion point depend on the method of producing the liquid-liquid dispersion and the corresponding operating conditions. It is, therefore, difficult to develop a generalized mathematical model of phase inversion. For a given method, however, it is possible to develop empirical correlations between phase inversion and the factors affecting it. Equations 5.1 and 5.2 and Equations 5.4 and 5.9, which were developed for the method of producing the dispersions between parallel shearing plates and by turbulent flow in a horizontal tube respectively, represent a first attempt to correlate phase inversion and the most important parameters involved. Further experimental and theoretical work could refine these models and lead to the development of models that can be used to predict phase inversion for a wider range of liquid-liquid systems and operating conditions.

Suggestions for Further Work

Some suggestions on further work can be made regarding both experimental investigation and analysis of the data. The experimental work using the parallel shearing plates method could be extended by investigating more liquid-liquid systems with different physical properties, with main emphasis on viscosity difference, interfacial tension and wettability of the plates. It would be interesting to concentrate on the state of phase inversion which is approached asymptotically at higher Taylor numbers or lower interfacial tensions for this particular method used. Empirical correlations of phase inversion with the physical properties of the liquids in relation to this state could be developed, based on information gathered from further experimental work, possibly involving more detailed statistical analysis of the data. Modifications of the existing apparatus could also be made for further experimental investigation of phase inversion, possibly involving the cone and plate approach or an increase in scale.

More possibilities exist regarding further experimental investigation using the horizontal tube method. The effect on phase inversion of parameters such as viscosity and density differences between the liquids and different materials of the tube could be investigated in more detail. An attempt on investigating conditions of higher turbulence can also be made, possibly by increasing the liquid flow rates or using packing material which would also affect the wettability of the system by the liquids. Further attempts to correlate phase inversion with the parameters involved in this method can then be made by modifying the existing correlations or possibly develop more realistic ones so that they can fit better the experimental results.

TABLES

Table 1

Physical Properties of the Liquid-Liquid Systems used
(Room Temperature) in the Parallel Shearing Plates Method

Organic phase	Aqueous phase	ρ_o [kgm ⁻³]	ρ_w [kgm ⁻³]	$\mu_o \times 10^3$ [Pas]	$\sigma \times 10^3$ [Nm ⁻¹]
Liquid Paraffin	Water	845	1000	27.70	41 (36*)
Liquid Paraffin	60 ppm Tween 80 in Water	845	1000	27.70	26.3
Liquid Paraffin	200 ppm Tween 80 in Water	845	1000	27.70	17.1
1% v/v Oleic Acid in Liquid Paraffin	Water	856	1000	27.70	16.0
Dibutyl Maleate	Water	990	1000	6.25	17.6
Dibutyl Maleate	200 ppm Tween 80 in Water	990	1000	6.25	7.0
Dibutyl Maleate	20% w/v CaCl ₂ aq. soln.	990	1100	6.25	18.5
Escaid	Water	811	1000	1.64	28.7

* measured using the platinum-ring method

Table 2

Physical Properties of the Liquid-Liquid Systems used
(Room Temperature) in the Horizontal Glass Tube Method

Organic phase	Aqueous phase	ρ_o [kgm ⁻³]	ρ_w [kgm ⁻³]	$\mu_o \times 10^3$ [Pas]	$\sigma \times 10^3$ [Nm ⁻¹]
Escaid	Water	811	1000	1.64	28.7
Escaid	200 ppm Tween 80 in Water	811	1000	1.64	21.2
Escaid	20% w/v CaCl ₂ aq. soln.	811	1120	1.64	28.5

Table 3

Contact Angles of the Liquids used with the
Materials of the Parallel Shearing Plates

Material	Perspex	Stainless Steel	Glass
Liquid	Contact angle, θ [deg]		
Water	117	122	59
60 ppm Tween 80 in Water	114	124	-
200 ppm Tween 80 in Water	115	125	-
20% w/v CaCl ₂ aq. soln.	-	121	-
Liquid Paraffin	25	34	47
1% v/v Oleic Acid in Liquid Paraffin	-	0	-
Dibutyl Maleate	-	25	30
Escaid	-	48	30

Table 4

Contact Angles of the Liquid-Liquid Systems used with the Materials of the Parallel Shearing Plates (measured through the aqueous phase)

Material		Perspex	Stainless steel	Glass
Organic Phase	Aqueous Phase	Contact angle, θ [deg]		
Liquid Paraffin	Water	154	143	56
Liquid Paraffin	60 ppm Tween 80 in Water	152	130	60
Liquid Paraffin	200 ppm Tween 80 in Water	151	124	-
1% w/v Oleic Acid in Liquid Paraffin	Water	-	132	-
Dibutyl Maleate	Water	-	146	42
Dibutyl Maleate	200 ppm Tween 80 in Water	-	140	50
Dibutyl Maleate	20% w/v CaCl_2 aq. soln.	-	133	-
Escaid	Water	-	116	71
Escaid	200 ppm Tween 80 aq. soln.	-	-	65
Escaid	20% w/v CaCl_2 aq. soln.	-	-	78

Table 5

Range of Reynolds Numbers for the Liquids used
in the Parallel Shearing Plates Method

Liquid	Re _{min}	Re _{max}
Water (with or without emulsifying agent)	1.7×10^4	7.5×10^4
20% w/v CaCl ₂ aq. soln.	1.9×10^4	8.2×10^4
Liquid Paraffin	515	2.3×10^3
1% v/v Oleic Acid in Liquid Paraffin	521	2.4×10^3
Dibutyl Maleate	2.7×10^3	1.2×10^4
Escaid	8.3×10^3	3.7×10^4

Table 6

Range of Taylor Numbers for the Liquids used
in the Parallel Shearing Plates Method

s[mm]	0.1		0.2		0.5		0.75		1	
Liquid	Ta _{min}	Ta _{max}	Ta _{min}	Ta _{max}	Ta _{min}	Ta _{max}	Ta _{min}	Ta _{max}	Ta _{min}	Ta _{max}
Water (with or without emulsifying agent)	0.083	0.368	0.333	1.473	2.083	9.208	4.688	20.719	8.333	36.833
20% w/v CaCl ₂ aq. soln.	0.091	0.405	0.366	1.620	2.291	10.129	5.157	22.791	9.166	40.516
Liquid Paraffin	2.5×10 ⁻³	0.011	0.010	0.045	0.064	0.281	0.143	0.632	0.254	1.123
1% v/v Oleic Acid in Liquid Paraffin	2.5×10 ⁻³	0.011	0.010	0.046	0.065	0.285	0.145	0.640	0.257	1.138
Dibutyl Maleate	0.013	0.057	0.052	0.234	0.332	1.459	0.743	3.282	1.319	5.831
Escaid	0.041	0.178	0.162	0.731	1.036	4.555	2.320	10.246	4.118	18.204

Table 7**Shear Rates used in the Parallel Shearing Plates Method**

s[mm]	0.1	0.2	0.5	0.75	1
N[rpm]	Shear rate, $\dot{\gamma} \times 10^{-3} [\text{s}^{-1}]$				
500	3.750	1.875	0.750	0.500	0.375
750	5.625	2.813	1.125	0.750	0.563
990	7.425	3.713	1.485	0.990	0.743
1240	9.300	4.650	1.860	1.240	0.930
1480	11.100	5.550	2.220	1.480	1.110
1720	12.900	6.450	2.580	1.720	1.290
1970	14.775	7.388	2.955	1.970	1.477
2210	16.575	8.288	3.315	2.210	1.657

Table 8**Range of Reynolds Numbers for the Liquids used
in the Horizontal Glass Tube Method**

Liquid	Re _{min}	Re _{max}
Water (with or without emulsifying agent)	3.08×10^3	1.068×10^4
20% w/v CaCl ₂ aq. soln.	3.45×10^3	1.196×10^4
Escaid	1.52×10^3	5.28×10^3

Table 9

Volume Fraction of the Organic Phase at Inversion at Different Rotational Speeds and Various Gap Widths between Parallel Shearing Perspex Plates for the Liquid Paraffin-Water System

s[mm]	0.1		0.5		0.75		1	
N[rpm]	$\bar{\Phi}_i$	σ_{Φ_i}	$\bar{\Phi}_i$	σ_{Φ_i}	$\bar{\Phi}_i$	σ_{Φ_i}	$\bar{\Phi}_i$	σ_{Φ_i}
500	0.263	0.014	0.194	0.008	0.100	0.018	0.069	0.003
750	0.198	0.006	0.157	0.015	0.124	0.004	0.064	0.003
990	0.164	0.011	0.154	0.006	0.113	0.007	0.068	0.003
1240	0.125	0.007	0.091	0.003	0.091	0.004	0.065	0.005
1480	0.099	0.007	0.086	0.004	0.083	0.004	0.058	0.005
1720	0.088	0.008	0.072	0.002	0.073	0.005	0.066	0.005
1970	0.064	0.009	0.061	0.003	0.065	0.004	0.065	0.003
2210	-	-	-	-	0.067	0.004	-	-

Table 10

Volume Fraction of the Organic Phase at Inversion at Different Rotational Speeds and Various Gap Widths between Parallel Shearing Stainless Steel Plates for the Liquid Paraffin-Water System

s[mm]	0.1		0.5		0.75		1	
N[rpm]	$\bar{\Phi}_i$	σ_{Φ_i}	$\bar{\Phi}_i$	σ_{Φ_i}	$\bar{\Phi}_i$	σ_{Φ_i}	$\bar{\Phi}_i$	σ_{Φ_i}
500	0.453	0.022	0.381	0.014	0.278	0.037	-	-
750	0.402	0.021	0.375	0.006	0.290	0.020	0.270	0.011
990	0.355	0.016	0.353	0.011	0.282	0.016	0.200	0.015
1240	0.284	0.020	0.310	0.018	0.250	0.025	0.188	0.015
1480	0.219	0.027	0.238	0.019	0.183	0.032	0.196	0.018
1720	0.173	0.015	0.181	0.005	0.151	0.012	0.157	0.009
1970	0.126	0.006	0.123	0.012	0.146	0.030	0.138	0.007
2210	0.116	0.010	0.102	0.015	0.117	0.006	0.119	0.008

Table 11

Volume Fraction of the Organic Phase at Inversion at Different Rotational Speeds and Various Gap Widths between Parallel Shearing Glass Plates for the Liquid Paraffin-Water System

s[mm]	0.2		0.5		1	
N[rpm]	$\bar{\Phi}_i$	σ_{Φ_i}	$\bar{\Phi}_i$	σ_{Φ_i}	$\bar{\Phi}_i$	σ_{Φ_i}
500	-	-	0.480	0.009	0.381	0.025
750	-	-	0.440	0.008	0.386	0.022
990	0.407	0.018	0.435	0.009	0.398	0.019
1240	0.397	0.018	0.370	0.012	0.341	0.052
1480	0.370	0.007	0.355	0.008	0.329	0.033
1720	0.317	0.01	0.328	0.012	0.320	0.040
1970	0.280	0.019	0.288	0.026	0.257	0.043
2210	0.249	0.013	0.280	0.020	0.228	0.015

Table 12

Volume Fraction of the Organic Phase at Inversion at Different Rotational Speeds and Various Gap Widths between Parallel Shearing Perspex Plates for the Liquid Paraffin - 60 ppm Tween 80 in Water System

s[mm]	0.1		0.5		1	
N[rpm]	$\bar{\Phi}_i$	σ_{Φ_i}	$\bar{\Phi}_i$	σ_{Φ_i}	$\bar{\Phi}_i$	σ_{Φ_i}
500	-	-	0.331	0.015	0.311	0.018
750	0.272	0.030	-	-	-	-
990	0.277	0.040	0.280	0.028	-	-
1240	0.272	0.048	-	-	0.286	0.020
1480	0.233	0.039	0.234	0.022	-	-
1720	0.215	0.039	-	-	0.238	0.026
1970	0.189	0.028	0.203	0.014	-	-
2210	0.212	0.020	-	-	0.186	0.015

Table 13

Volume Fraction of the Organic Phase at Inversion at Different Rotational Speeds and Various Gap Widths between Parallel Shearing Perspex Plates for the Liquid Paraffin - 200 ppm Tween 80 in Water System

s[mm]	0.1		0.5	
N[rpm]	$\bar{\Phi}_i$	σ_{Φ_i}	$\bar{\Phi}_i$	σ_{Φ_i}
500	-	-	0.374	0.039
750	0.387	0.029	0.371	0.017
990	-	-	0.354	0.033
1240	0.379	0.023	0.354	0.027
1480	-	-	0.361	0.009
1720	0.383	0.023	0.382	0.027
1970	-	-	0.360	0.025
2210	0.369	0.036	-	-
$\bar{\Phi}_i = 0.370$				

Table 14

Volume Fraction of the Organic Phase at Inversion at Different Rotational Speeds and Various Gap Widths between Parallel Shearing Stainless Steel Plates for the Liquid Paraffin - 60 ppm Tween 80 in Water System

s[mm]	0.1		0.5		1	
N[rpm]	$\bar{\Phi}_i$	σ_{Φ_i}	$\bar{\Phi}_i$	σ_{Φ_i}	$\bar{\Phi}_i$	σ_{Φ_i}
500	0.467	0.027	0.435	0.047	0.427	0.018
750	0.395	0.049	0.415	0.044	0.404	0.034
990	0.411	0.033	0.420	0.015	0.396	0.024
1240	0.365	0.038	0.377	0.030	0.376	0.017
1480	0.364	0.032	0.370	0.037	0.366	0.029
1720	0.356	0.044	0.304	0.028	0.371	0.038
1970	0.343	0.020	0.317	0.042	0.362	0.024
2210	0.300	0.025	0.280	0.051	0.309	0.035

Table 15

Volume Fraction of the Organic Phase at Inversion at Different Rotational Speeds and Various Gap Widths between Parallel Shearing Stainless Steel Plates for the Liquid Paraffin - 200 ppm Tween 80 in Water System

s[mm]	0.1		0.5	
N[rpm]	$\bar{\Phi}_i$	σ_{Φ_i}	$\bar{\Phi}_i$	σ_{Φ_i}
500	-	-	0.467	0.016
750	0.466	0.017	0.465	0.011
990	-	-	0.439	0.037
1240	0.474	0.020	0.427	0.028
1480	-	-	0.426	0.034
1720	0.430	0.041	0.438	0.026
1970	-	-	0.459	0.026
2210	0.440	0.041	0.443	0.031
$\bar{\Phi}_i = 0.448$				

Table 16

Volume Fraction of the Organic Phase at Inversion at Different Rotational Speeds and Various Gap Widths between Parallel Shearing Stainless Steel Plates for the 1% v/v Oleic Acid in Liquid Paraffin-Water System

s[mm]	0.1		0.5	
N[rpm]	$\bar{\Phi}_i$	σ_{Φ_i}	$\bar{\Phi}_i$	σ_{Φ_i}
500	-	-	0.104	0.004
750	0.071	0.005	0.101	0.008
990	0.073	0.004	0.134	0.008
1240	0.070	0.002	0.090	0.008
1480	0.075	0.004	0.099	0.013
1720	0.070	0.005	0.098	0.006
1970	0.064	0.009	0.105	0.006
2210	0.077	0.003	0.091	0.006
$\bar{\Phi}_i = 0.088$				

Table 17

Volume Fraction of the Organic Phase at Inversion at Different Rotational Speeds and Various Gap Widths between Parallel Shearing Stainless Steel Plates for the Dibutyl Maleate-Water Systems

s[mm]	0.1		0.5	
N[rpm]	$\bar{\Phi}_i$	σ_{Φ_i}	$\bar{\Phi}_i$	σ_{Φ_i}
500	-	-	0.194	0.010
750	-	-	0.194	0.009
990	0.189	0.023	0.211	0.018
1240	0.192	0.011	0.185	0.011
1480	0.193	0.009	0.180	0.011
1720	0.204	0.013	0.190	0.014
1970	0.196	0.015	0.177	0.014
2210	0.194	0.013	0.230	0.009
$\bar{\Phi}_i = 0.195$				

Table 18

Volume Fraction of the Organic Phase at Inversion at Different Rotational Speeds and Various Gap Widths between Parallel Shearing Glass Plates for the Dibutyl Maleate-Water System

s[mm]	0.5		1	
N[rpm]	$\bar{\Phi}_i$	σ_{Φ_i}	$\bar{\Phi}_i$	σ_{Φ_i}
500	0.256	0.021	-	-
750	0.265	0.016	-	-
990	0.277	0.024	0.245	0.011
1240	0.225	0.008	0.241	0.009
1480	0.252	0.012	0.232	0.022
1720	0.268	0.017	0.253	0.019
1970	0.240	0.020	0.238	0.015
2210	0.241	0.013	0.254	0.017
$\bar{\Phi}_i = 0.250$				

Table 19

Volume Fraction of the Organic Phase at Inversion at Different Rotational Speeds and Various Gap Widths between Parallel Shearing Stainless Steel Plates for the Dibutyl Maleate - 200 ppm Tween 80 in Water System

s[mm]	0.1		0.5	
N[rpm]	$\bar{\Phi}_i$	σ_{Φ_i}	$\bar{\Phi}_i$	σ_{Φ_i}
750	-	-	0.200	0.005
990	0.190	0.015	-	-
1240	0.204	0.013	-	-
1480	-	-	0.198	0.013
1720	-	-	0.220	0.023
2210	0.204	0.014	-	-
$\bar{\bar{\Phi}}_i = 0.203$				

Table 20

Volume Fraction of the Organic Phase at Inversion at Different Rotational Speeds and Various Gap Widths between Parallel Shearing Glass Plates for the Dibutyl Maleate - 200 ppm Tween 80 in Water System

s[mm]	0.5		1	
N[rpm]	$\bar{\Phi}_i$	σ_{Φ_i}	$\bar{\Phi}_i$	σ_{Φ_i}
1240	0.284	0.025	-	-
1480	-	-	0.272	0.031
1720	0.271	0.013	-	-
2210	0.232	0.014	-	-
$\bar{\bar{\Phi}}_i = 0.265$				

Table 21

Volume Fraction of the Organic Phase at Inversion at Different Rotational
Speeds and 0.5 mm Gap Width between Parallel Shearing Stainless Steel
Plates for the Dibutyl Maleate - 20% w/v CaCl_2 aq. soln. system

N[rpm]	$\bar{\Phi}_i$	σ_{Φ_i}
500	0.232	0.014
750	0.219	0.009
990	0.218	0.009
1240	0.232	0.023
1480	0.230	0.012
1720	0.236	0.015
1970	0.223	0.010
2210	0.231	0.014
$\bar{\Phi}_i = 0.228$		

Table 22

Volume Fraction of the Organic Phase at Inversion at Different Rotational
Speeds and Various Gap Widths between Parallel Shearing Stainless Steel
Plates for the Escald-Water System

s[mm]	0.1		1	
N[rpm]	$\bar{\Phi}_i$	σ_{Φ_i}	$\bar{\Phi}_i$	σ_{Φ_i}
500	0.572	0.021	-	-
750	0.564	0.006	0.548	0.013
990	0.550	0.026	0.573	0.010
1240	0.551	0.013	0.532	0.013
1480	0.530	0.023	0.510	0.020
1720	0.514	0.036	0.481	0.012
1970	0.519	0.021	0.493	0.011
2210	0.483	0.017	0.486	0.024

Table 23

**Volume Fraction of the Organic Phase at Inversion at Different Rotational
Speeds and Various Gap Widths between Parallel Shearing Glass
Plates for the Escaid-Water System**

s[mm]	0.2		0.5		1	
N[rpm]	$\bar{\Phi}_i$	σ_{Φ_i}	$\bar{\Phi}_i$	σ_{Φ_i}	$\bar{\Phi}_i$	σ_{Φ_i}
500	0.553	0.028	0.530	0.026	-	-
750	0.525	0.043	0.498	0.045	0.573	0.018
990	0.519	0.016	0.551	0.032	0.589	0.026
1240	0.578	0.027	0.544	0.024	0.582	0.033
1480	0.600	0.025	0.596	0.020	0.587	0.030
1720	0.641	0.039	0.625	0.031	0.593	0.025
1970	0.648	0.035	0.665	0.035	0.617	0.029
2210	0.665	0.041	0.667	0.042	0.648	0.032

Table 24

Volume Fraction of the Organic Phase at Inversion at Different Total Flow Rates in the Horizontal Glass Tube, with the Aqueous Phase through the T-branch at the Inlet, for the Escald-Water System

Phase Inversion from O/W to W/O dispersion				Phase Inversion from W/O to O/W dispersion			
$\bar{Q}_T[\ell/h]$	$\sigma_{Q_T}[\ell/h]$	$\bar{\Phi}_i$	σ_{Φ_i}	$\bar{Q}_T[\ell/h]$	$\sigma_{Q_T}[\ell/h]$	$\bar{\Phi}_i$	σ_{Φ_i}
113	4.38	0.690	0.012	95	2.55	0.578	0.015
122	1.78	0.673	0.004	105	2.28	0.571	0.012
123	3.62	0.674	0.010	114	2.95	0.578	0.015
142	1.52	0.648	0.004	126	1.67	0.569	0.007
163	3.36	0.632	0.008	135	2.12	0.578	0.009
165	6.87	0.637	0.015	149	2.28	0.563	0.008
180	2.16	0.611	0.004	157	1.30	0.571	0.005
191	2.30	0.608	0.005	172	1.34	0.557	0.004
208	2.07	0.617	0.004	176	0.00	0.574	0.000
210	1.75	0.619	0.004	178	2.12	0.566	0.007
212	2.36	0.600	0.005	184	3.74	0.582	0.012
231	1.48	0.610	0.002	189	3.36	0.565	0.010
247	3.36	0.595	0.006	194	1.30	0.551	0.003
249	3.68	0.600	0.006	196	1.22	0.577	0.003
259	2.30	0.613	0.003	211	1.14	0.565	0.004
281	1.95	0.609	0.003	214	0.00	0.556	0.000
302	3.15	0.602	0.003	227	2.12	0.573	0.006
				231	1.34	0.562	0.003
				243	2.39	0.585	0.006
				249	2.17	0.570	0.005
				260	1.52	0.590	0.004
				264	1.52	0.582	0.003
				288	2.17	0.573	0.004

Table 25

Volume Fraction of the Organic Phase at Inversion at Different Total Flow Rates in the Horizontal Glass Tube, with the Organic Phase through the T-branch at the Inlet, for the Escaid-Water System

Phase Inversion from O/W to W/O dispersion				Phase Inversion from W/O to O/W dispersion			
$\bar{Q}_T[\ell/h]$	$\sigma_{Q_T}[\ell/h]$	$\bar{\Phi}_i$	σ_{Φ_i}	$\bar{Q}_T[\ell/h]$	$\sigma_{Q_T}[\ell/h]$	$\bar{\Phi}_i$	σ_{Φ_i}
110	5.00	0.591	0.023	106	2.26	0.458	0.010
116	3.35	0.568	0.013	120	1.67	0.455	0.006
124	3.13	0.557	0.011	124	2.40	0.485	0.010
128	5.57	0.570	0.019	131	1.34	0.460	0.005
131	0.89	0.540	0.003	134	2.64	0.449	0.009
136	2.60	0.557	0.009	137	2.24	0.482	0.008
144	3.34	0.547	0.011	144	1.87	0.458	0.006
152	2.46	0.541	0.008	152	1.14	0.475	0.003
155	1.41	0.548	0.004	154	3.20	0.501	0.011
158	5.03	0.557	0.015	164	1.10	0.477	0.003
168	2.51	0.552	0.007	166	2.12	0.508	0.006
171	4.75	0.532	0.013	170	2.68	0.494	0.008
187	2.61	0.518	0.007	189	3.81	0.475	0.010
194	0.00	0.535	0.000	194	3.95	0.494	0.010
207	2.05	0.542	0.004	204	1.34	0.468	0.003
212	4.89	0.528	0.011	205	3.27	0.492	0.008
219	0.00	0.543	0.000	214	2.05	0.500	0.005
229	4.30	0.540	0.009	229	3.85	0.467	0.008
239	2.39	0.539	0.005	236	2.95	0.479	0.006
247	5.02	0.535	0.009	238	2.71	0.450	0.004
260	1.50	0.539	0.003	250	5.71	0.448	0.010
270	3.03	0.537	0.005	252	5.20	0.472	0.010
279	5.45	0.534	0.009	264	1.67	0.451	0.002
285	2.49	0.526	0.004	277	5.10	0.469	0.009
				296	4.98	0.480	0.008

Table 26

Volume Fraction of the Organic Phase at Inversion at Different Total Flow Rates in the Horizontal Glass Tube, with the Aqueous Phase through the T-branch at the Inlet, for the Escaid - 200 ppm Tween 80 in Water System

Phase Inversion from O/W to W/O dispersion				Phase Inversion from W/O to O/W dispersion			
$\bar{Q}_T [l/h]$	$\sigma_{Q_T} [l/h]$	$\bar{\Phi}_i$	σ_{Φ_i}	$\bar{Q}_T [l/h]$	$\sigma_{Q_T} [l/h]$	$\bar{\Phi}_i$	σ_{Φ_i}
111	1.10	0.640	0.004	87	0.84	0.561	0.008
128	2.33	0.610	0.007	110	3.21	0.548	0.016
129	1.99	0.611	0.006	113	1.41	0.531	0.007
138	0.55	0.602	0.002	123	1.30	0.533	0.006
148	3.59	0.595	0.010	130	1.14	0.552	0.005
149	2.22	0.600	0.008	133	1.30	0.542	0.006
153	2.02	0.576	0.005	152	0.58	0.554	0.002
159	4.23	0.560	0.012	154	1.41	0.545	0.005
170	2.20	0.559	0.005	176	1.64	0.543	0.005
179	1.22	0.552	0.003	177	1.73	0.541	0.005
192	0.00	0.557	0.000	205	0.84	0.521	0.003
196	1.00	0.541	0.003	205	1.15	0.523	0.003
210	1.76	0.547	0.004	231	2.07	0.516	0.005
221	2.46	0.548	0.005	246	3.36	0.529	0.007
226	1.10	0.535	0.002	263	3.11	0.517	0.006
236	6.81	0.533	0.005				
252	2.85	0.524	0.005				

Table 28

Volume Fraction of the Organic Phase at Inversion at Different Total Flow Rates in the Horizontal Glass Tube, with the Aqueous Phase through the T-branch at the Inlet, for the Escaid - 20% w/v CaCl_2 aq. soln. system

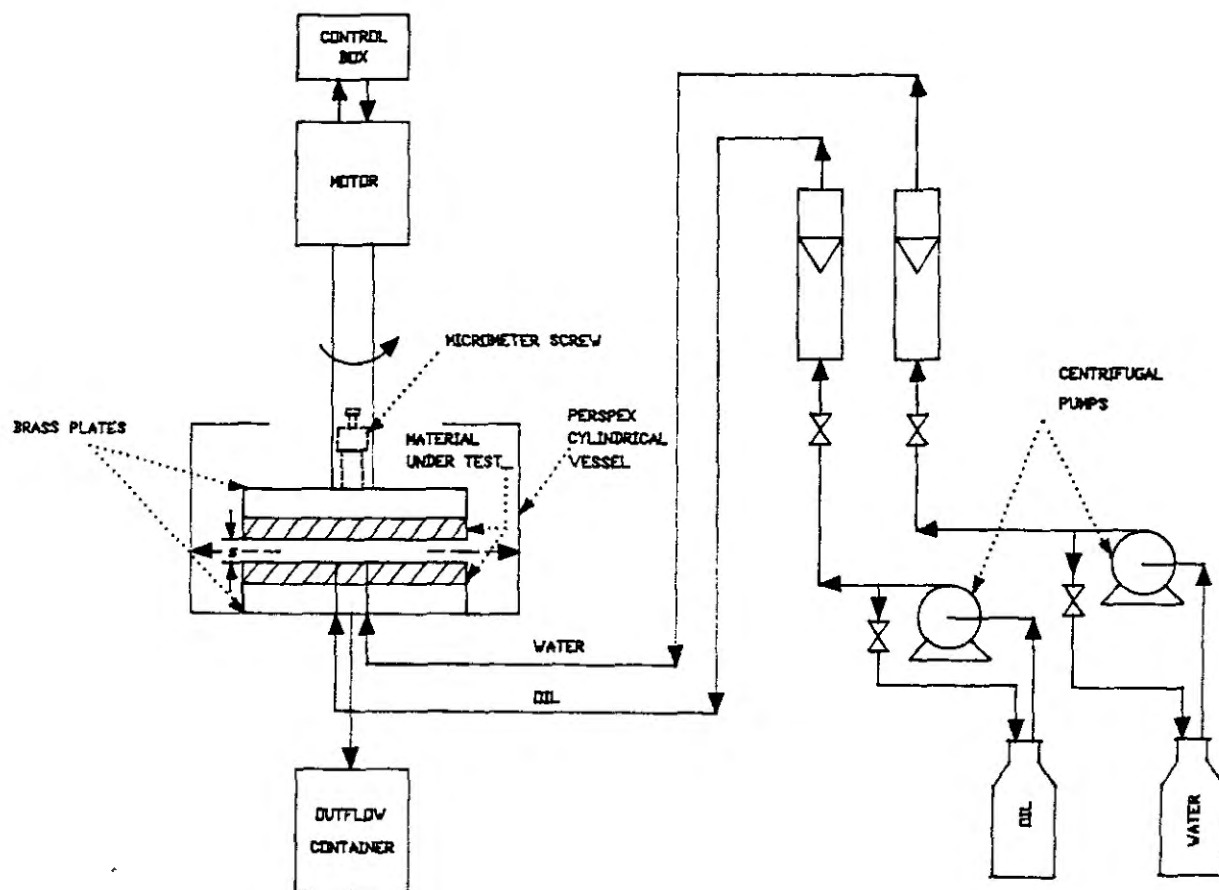
Phase Inversion from O/W to W/O dispersion				Phase Inversion from W/O to O/W dispersion			
$\bar{Q}_T[\ell/h]$	$\sigma_{Q_T}[\ell/h]$	$\bar{\Phi}_i$	σ_{Φ_i}	$\bar{Q}_T[\ell/h]$	$\sigma_{Q_T}[\ell/h]$	$\bar{\Phi}_i$	σ_{Φ_i}
94	2.64	0.682	0.009	96	1.34	0.623	0.009
106	0.89	0.671	0.003	101	3.56	0.599	0.017
119	1.10	0.663	0.003	106	0.84	0.624	0.005
126	2.36	0.643	0.007	117	1.00	0.617	0.005
135	0.98	0.629	0.003	120	2.51	0.602	0.013
136	2.25	0.633	0.006	127	0.55	0.612	0.003
142	1.43	0.613	0.004	136	1.92	0.617	0.009
155	1.10	0.613	0.003	149	0.55	0.606	0.002
156	0.00	0.614	0.000	159	0.89	0.601	0.004
164	0.50	0.603	0.002	169	1.82	0.599	0.006
176	0.84	0.602	0.003	179	1.10	0.599	0.004
180	1.10	0.611	0.002	190	0.55	0.594	0.002
183	1.68	0.591	0.004	199	0.55	0.597	0.002
190	1.76	0.605	0.004	207	0.50	0.601	0.001
197	3.77	0.593	0.008	218	0.55	0.597	0.002
202	3.54	0.604	0.007	226	0.41	0.602	0.008
210	0.00	0.619	0.000	235	1.10	0.604	0.003
218	0.82	0.610	0.002	247	0.50	0.599	0.002
232	0.00	0.612	0.000	253	1.00	0.608	0.002
233	3.52	0.614	0.006				
247	1.10	0.615	0.002				
262	0.00	0.618	0.000				
264	2.51	0.621	0.004				
273	0.55	0.616	0.005				
294	1.34	0.626	0.002				

Table 29

Volume Fraction of the Organic Phase at Inversion at Different Total Flow Rates in the Horizontal Glass Tube, with the Organic Phase through the T-branch at the Inlet, for the Escaid - 20% w/v CaCl_2 aq. soln. system

Phase Inversion from O/W to W/O dispersion				Phase Inversion from W/O to O/W dispersion			
$\bar{Q}_T[\ell/h]$	$\sigma_{Q_T}[\ell/h]$	$\bar{\Phi}_i$	σ_{Φ_i}	$\bar{Q}_T[\ell/h]$	$\sigma_{Q_T}[\ell/h]$	$\bar{\Phi}_i$	σ_{Φ_i}
99	1.10	0.595	0.004	109	0.00	0.447	0.000
103	1.10	0.564	0.004	121	1.10	0.447	0.004
113	2.16	0.558	0.009	129	0.82	0.467	0.003
123	2.12	0.553	0.008	138	0.45	0.479	0.002
133	1.10	0.549	0.004	148	1.63	0.488	0.006
136	0.89	0.524	0.003	157	0.45	0.489	0.001
139	1.39	0.532	0.004	166	0.00	0.506	0.000
149	1.64	0.531	0.005	175	1.10	0.511	0.003
156	2.94	0.551	0.008	186	0.00	0.515	0.000
160	1.92	0.531	0.005	195	1.10	0.517	0.003
161	0.55	0.535	0.002	207	0.45	0.517	0.009
171	1.78	0.531	0.005	214	0.71	0.528	0.002
181	2.14	0.557	0.005	228	0.89	0.521	0.002
185	1.10	0.540	0.003	235	0.00	0.531	0.000
185	1.10	0.540	0.003	248	0.89	0.523	0.002
197	0.00	0.543	0.000	255	1.00	0.533	0.002
200	0.00	0.551	0.000	268	1.1	0.530	0.002
207	1.37	0.541	0.003				
219	2.30	0.544	0.005				
225	1.12	0.556	0.002				
234	3.46	0.552	0.007				
247	2.20	0.554	0.004				
256	2.91	0.552	0.005				
272	0.98	0.558	0.002				

FIGURES

Figure 1

Schematic Diagram of the Continuous-Flow Emulsifying
Machine of Parallel Shearing Plates

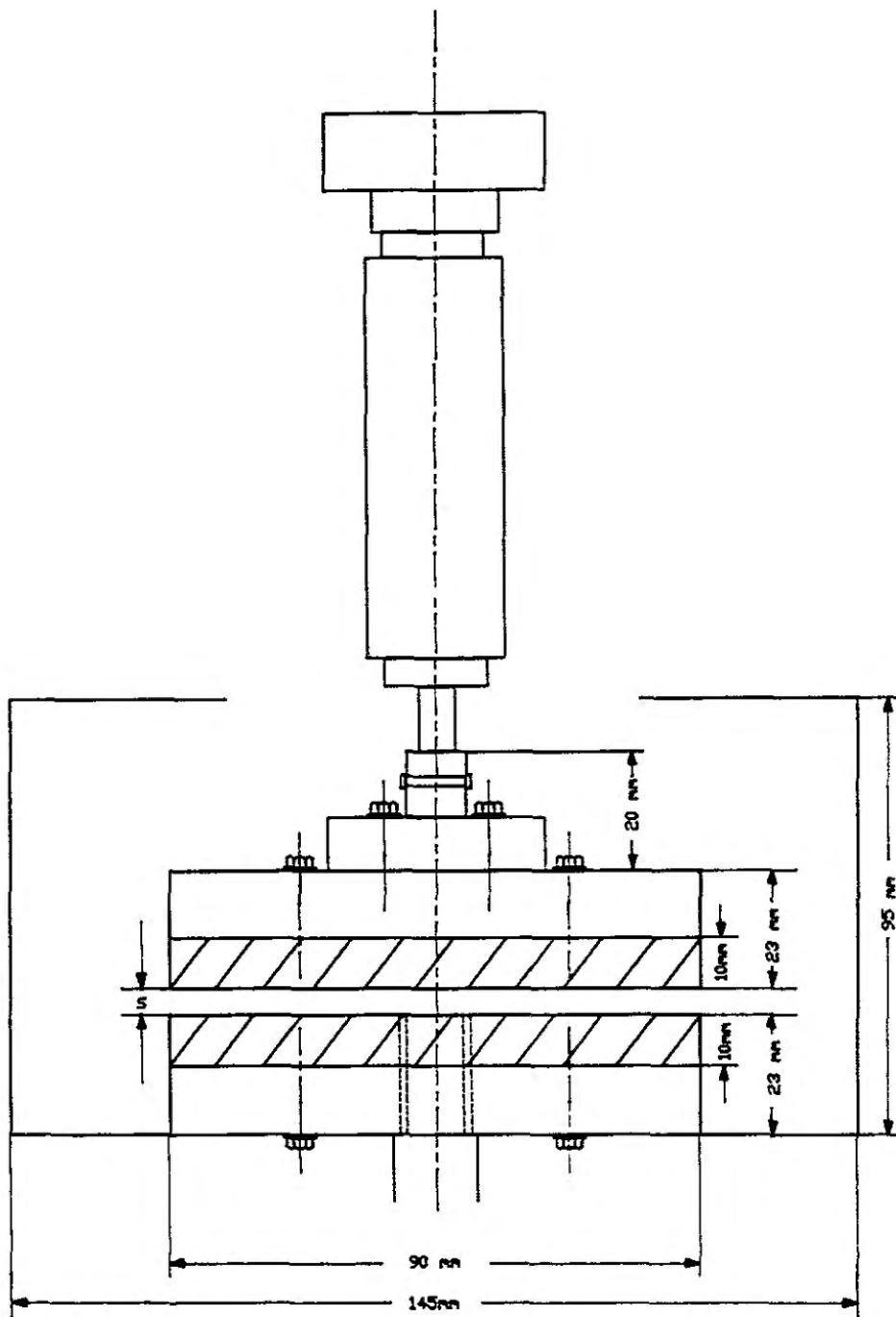
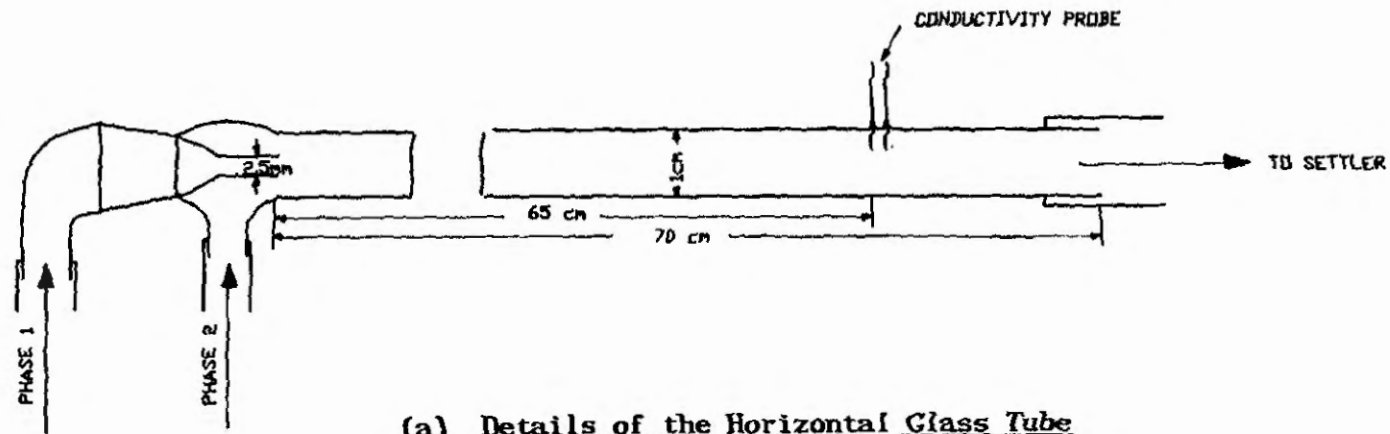
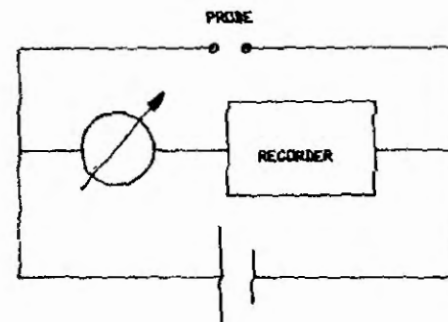
Figure 2Details of the System of Parallel Shearing Plates

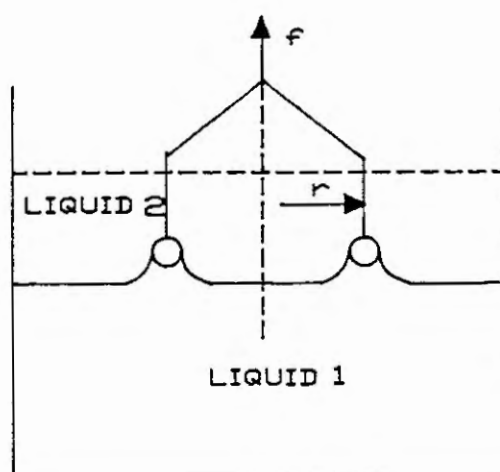
Figure 4



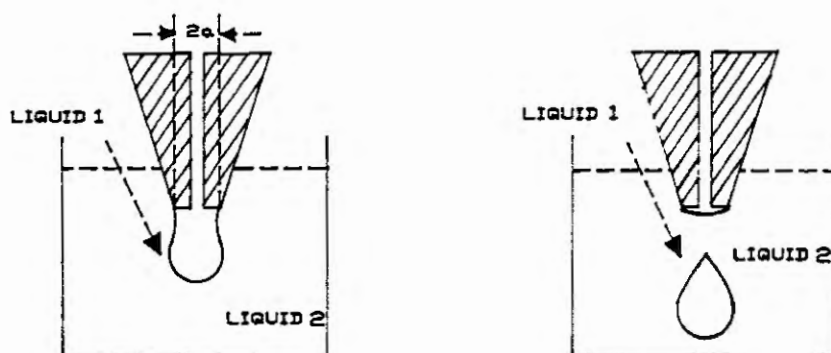
(a) Details of the Horizontal Glass Tube



(b) Details of the Electrical Connections with the Conductivity Probe

Figure 6

(a)



(b)

Interfacial Tension Measurement(a) Platinum Ring Method(b) Drop-Weight Method

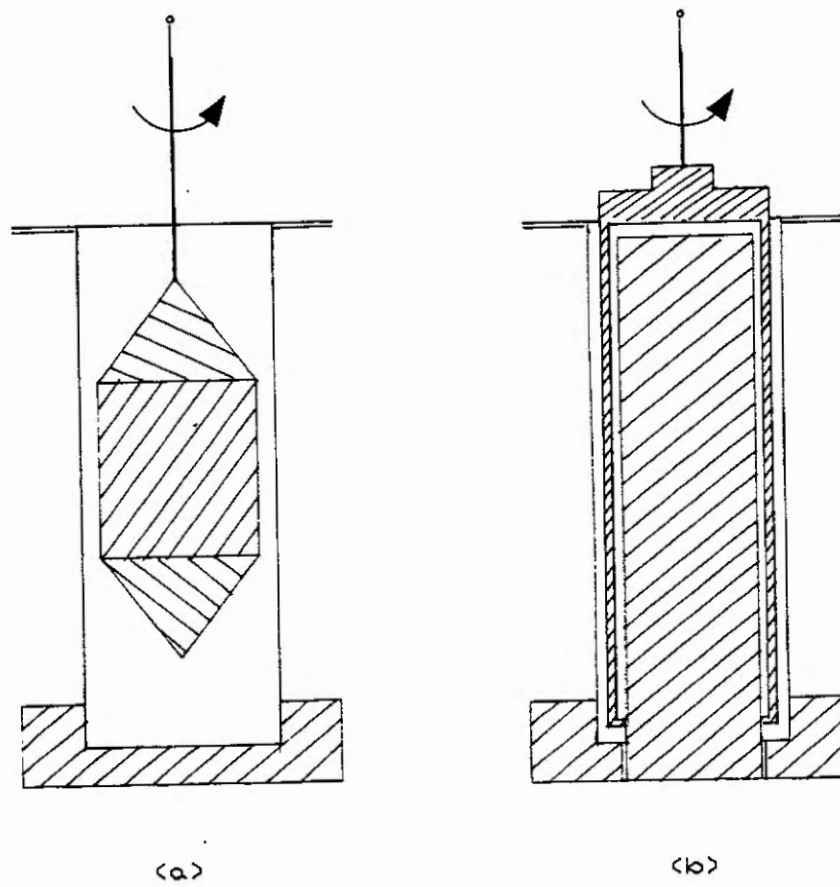
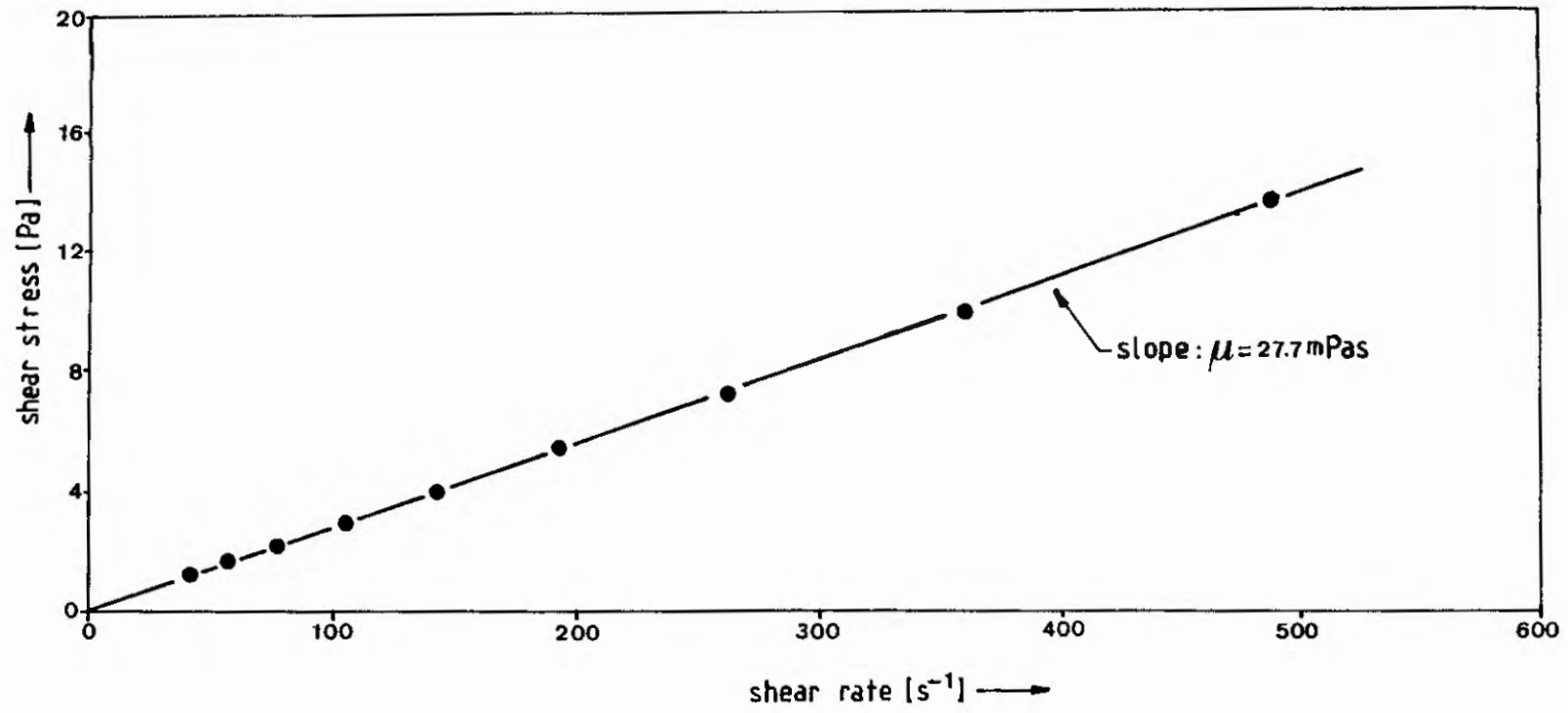
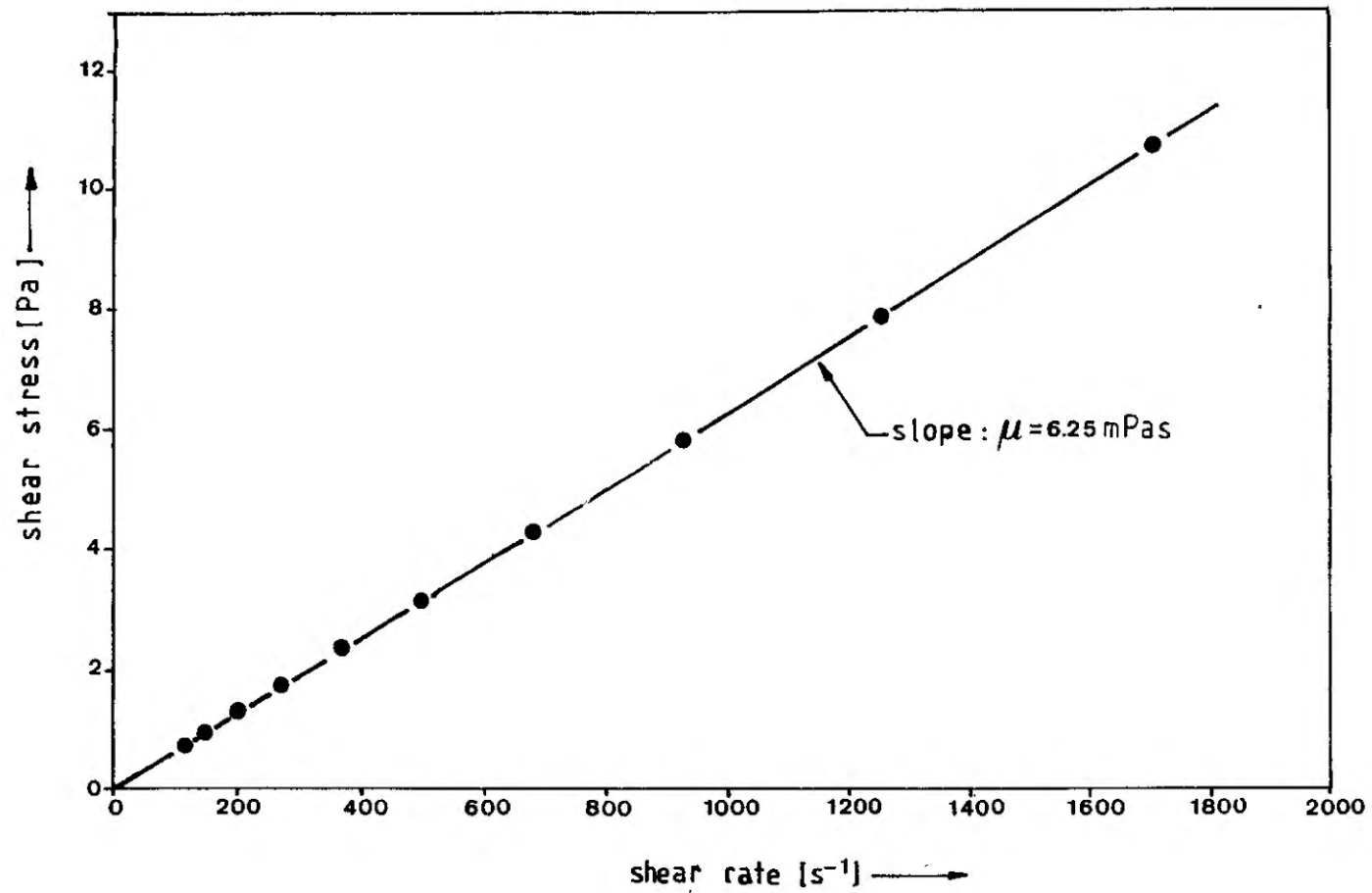
Figure 7Viscosity Measurement(a) Measuring System of Co-Axial Cylinders(b) Double-Gap Measuring System

Figure 8



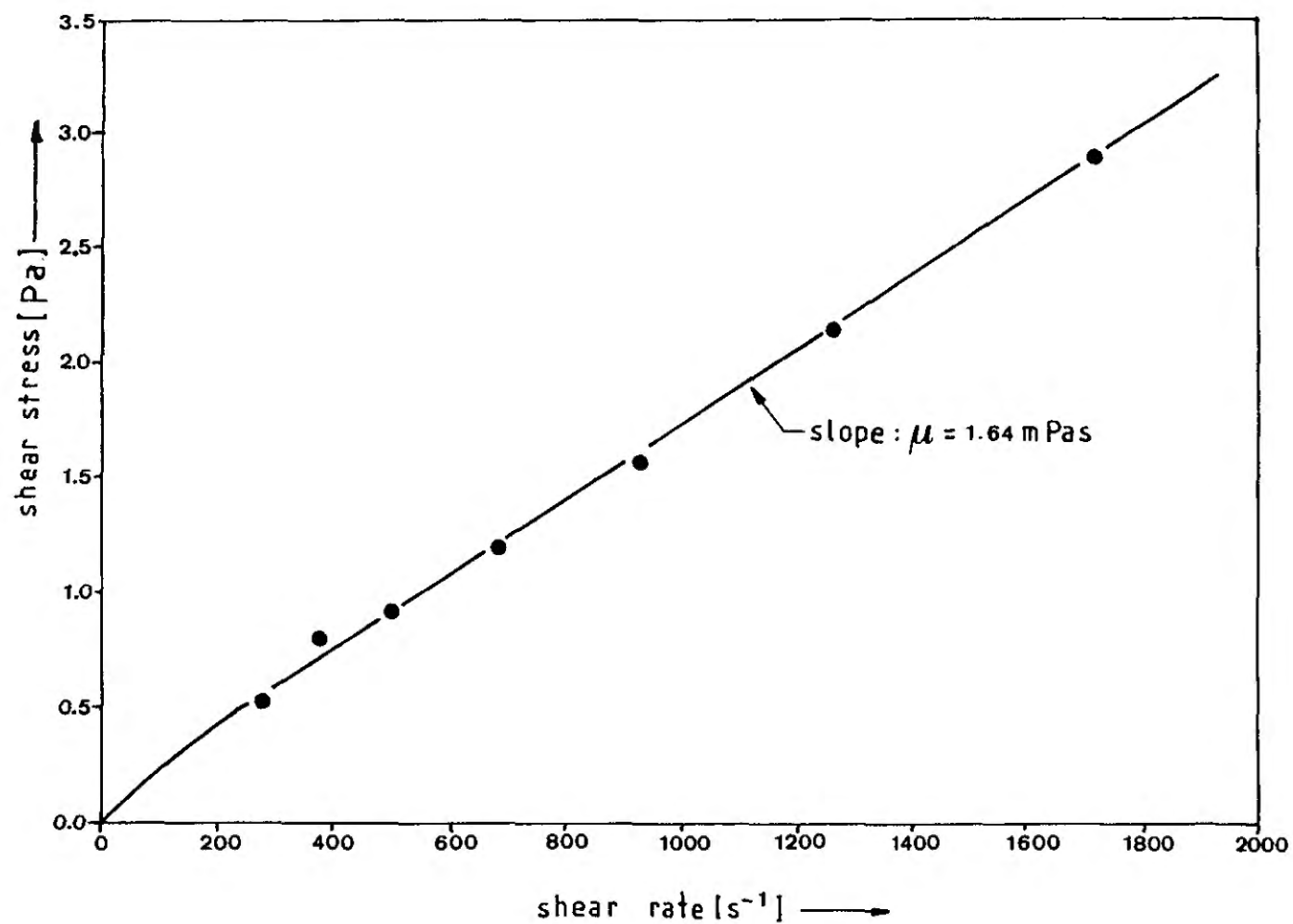
Flow Behaviour of Liquid Paraffin at Room Temperature

Figure 9

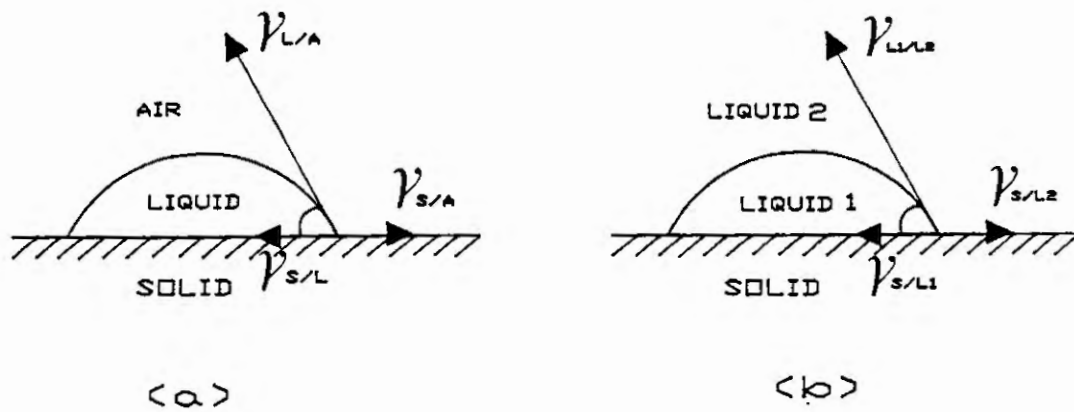


Flow Behaviour of Dibutyl Maleate at Room Temperature

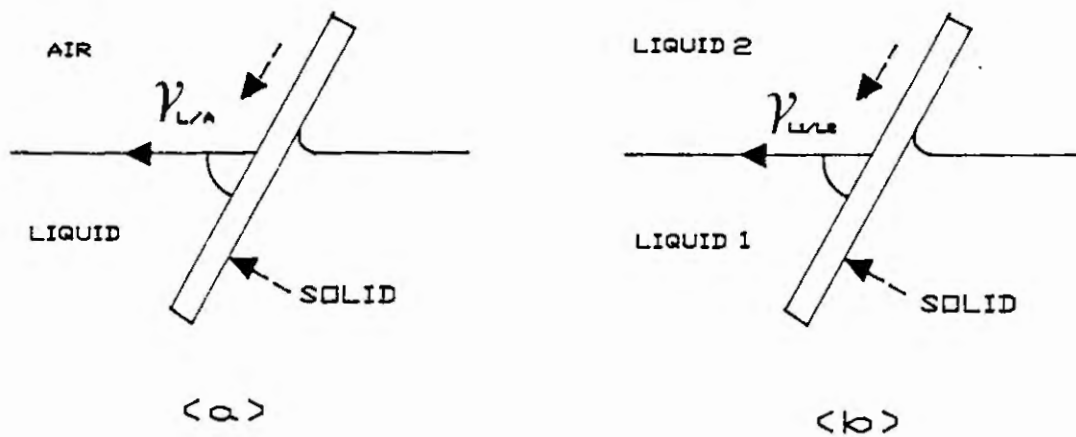
Figure 10



Flow Behaviour of Escaid at Room Temperature

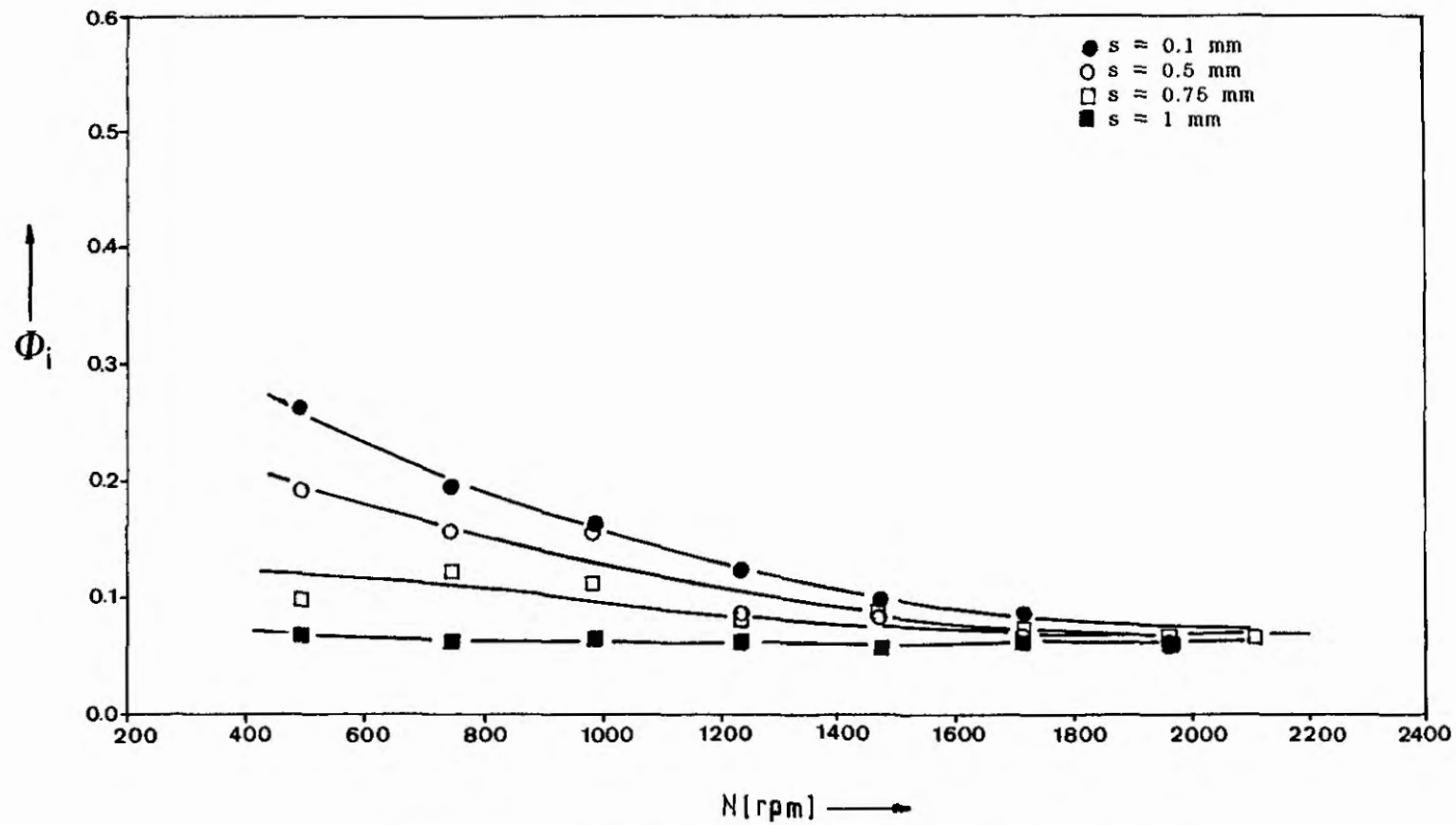
Figure 11

Contact Angle with a Solid Surface of:
(a) a Liquid Drop
(b) a Liquid-Liquid Interface

Figure 12

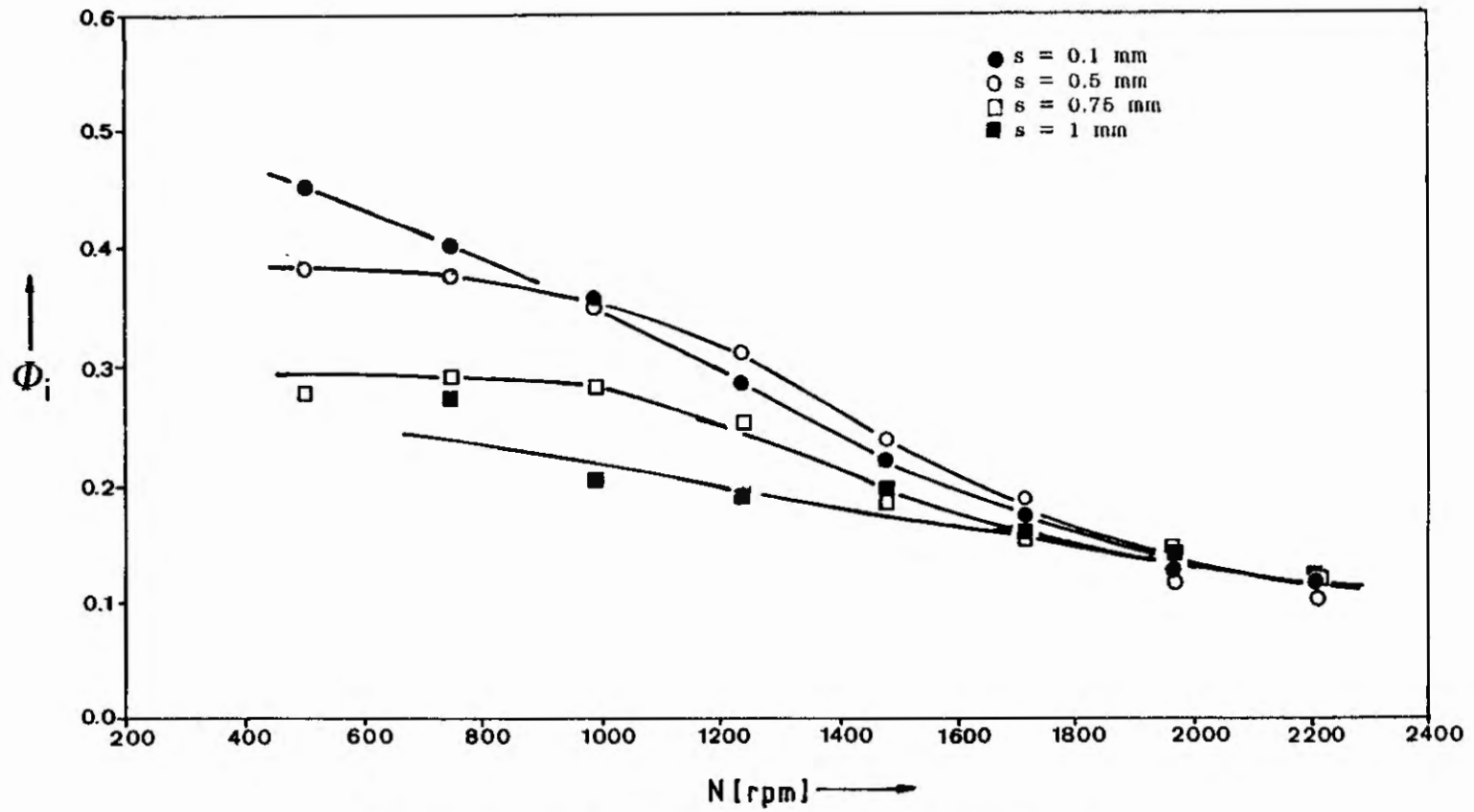
Immersed Plate Method of Measuring the Contact Angle
with a Solid Surface of:
(a) a Liquid
(b) a Liquid-Liquid Interface

Figure 13



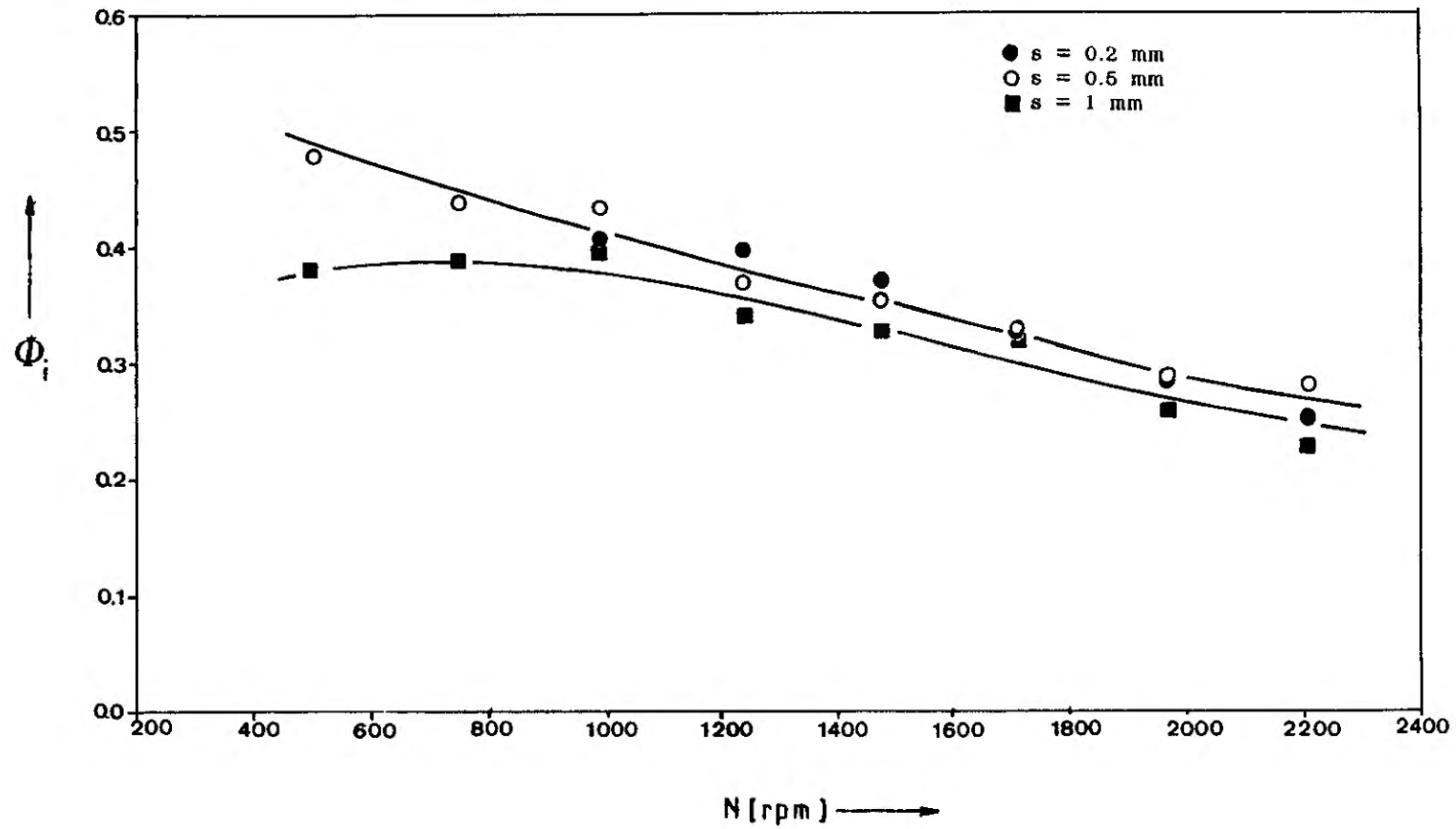
Volume Fraction of the Organic Phase at Inversion vs
Rotational Speed for the Liquid Paraffin-Water System
and Perspex Plates

Figure 14



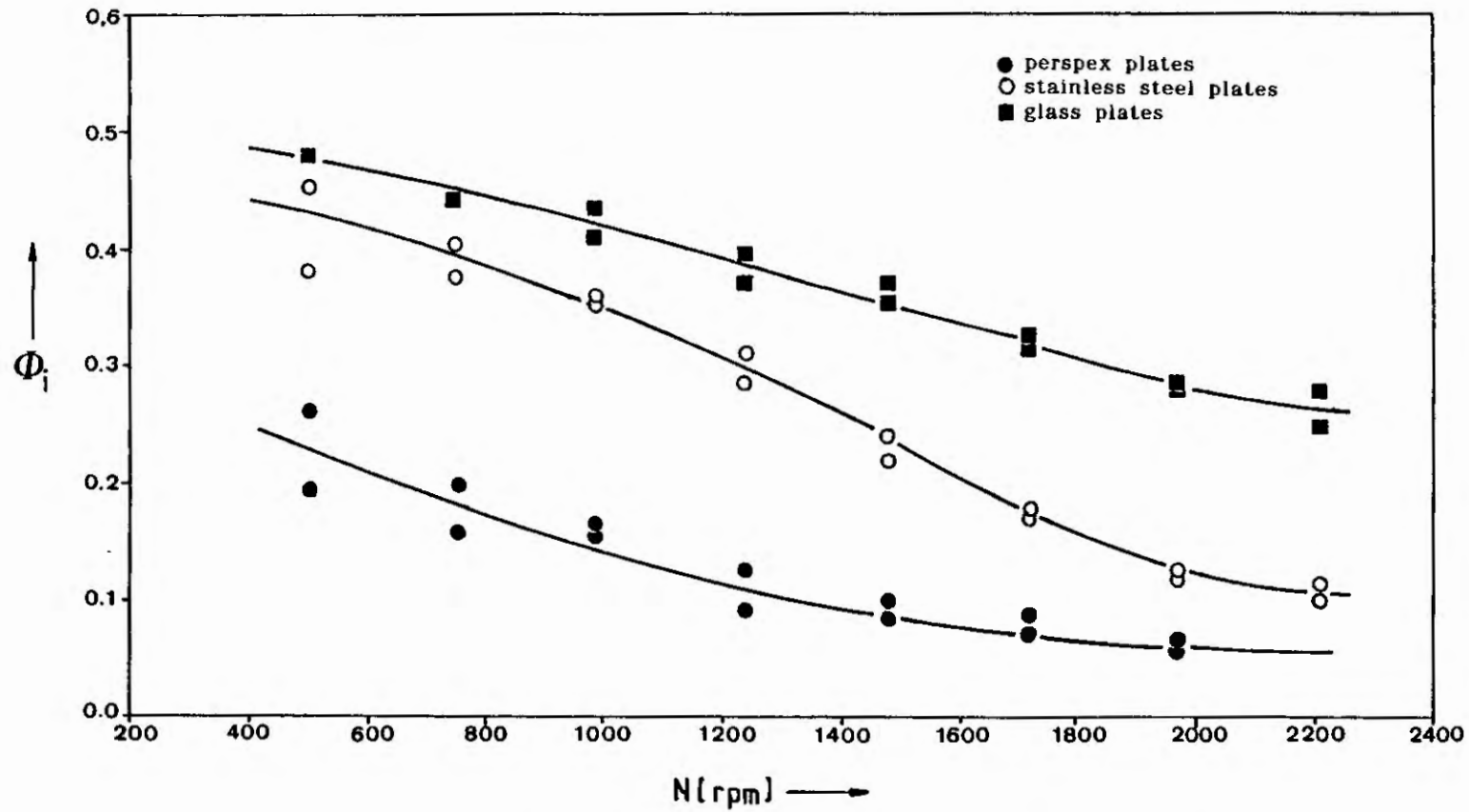
Volume Fraction of the Organic Phase at Inversion vs
Rotational Speed for the Liquid Paraffin-Water System
and Stainless Steel Plates

Figure 15



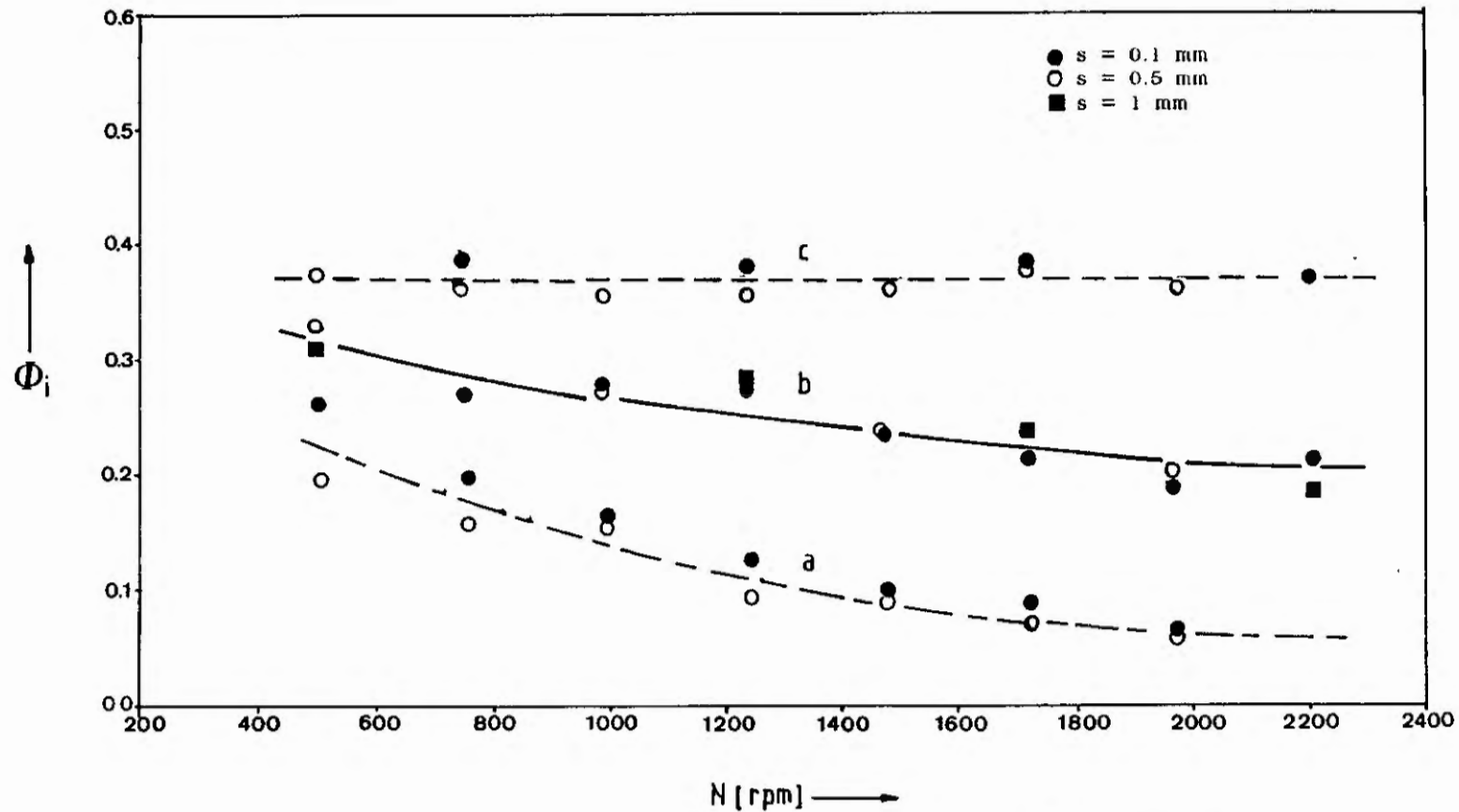
Volume Fraction of the Organic Phase at Inversion vs
Rotational Speed for the Liquid Paraffin-Water System
and Glass Plates

Figure 16



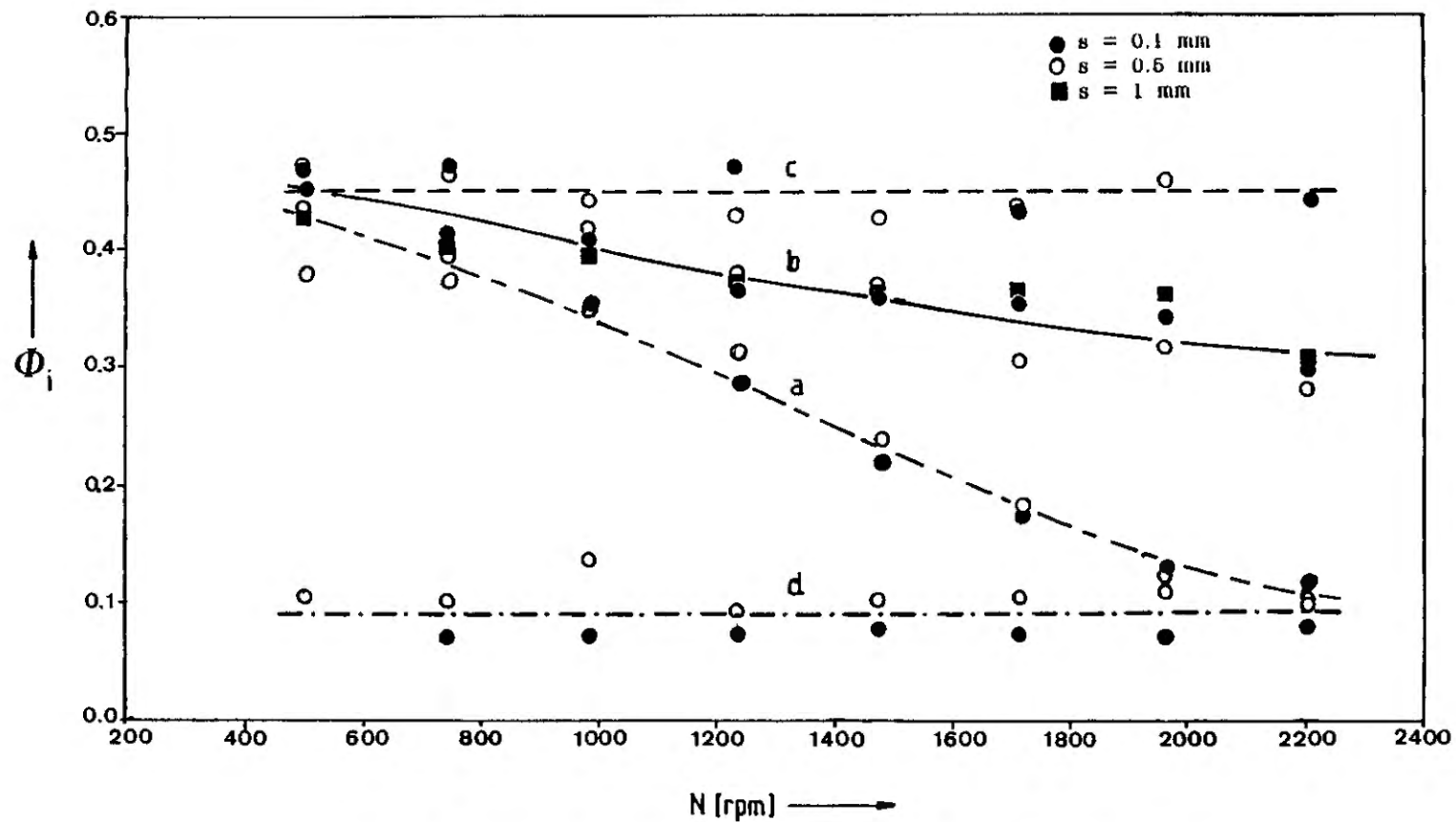
Volume Fraction of the Organic Phase at Inversion vs
Rotational Speed for the Liquid Paraffin-Water System
and Different Plates; $s = 0.1 \text{ mm} - 0.5 \text{ mm}$

Figure 17



Volume Fraction of the Organic Phase at Inversion vs
Rotational Speed for Perspex Plates and the Systems:
a. Liquid Paraffin-Water;
b. Liquid Paraffin - 60 ppm Tween 80 in Water;
c. Liquid Paraffin - 200 ppm Tween 80 in Water.

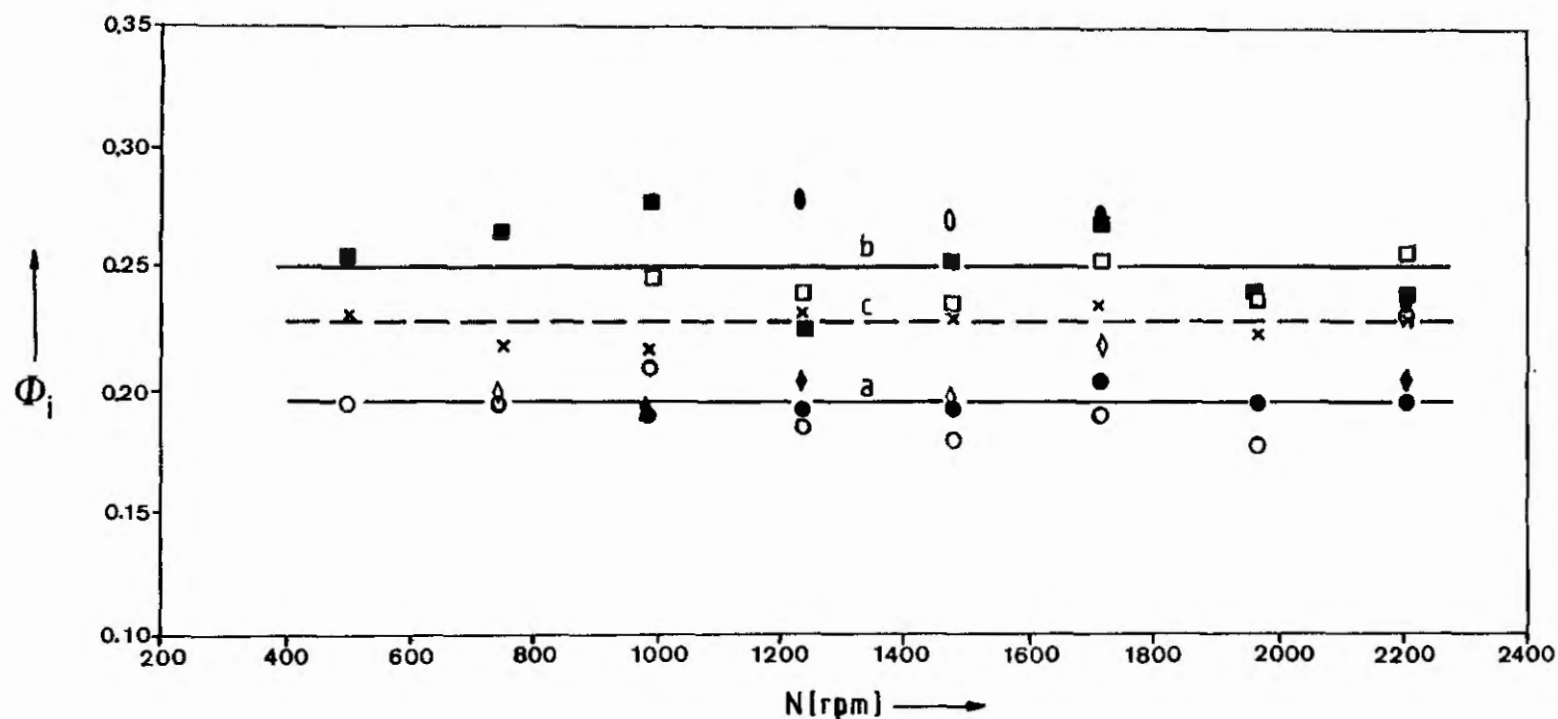
Figure 18



Volume Fraction of the Organic Phase at Inversion vs Rotational Speed for Stainless Steel Plates and the Systems:

- a. Liquid Paraffin-Water;
- b. Liquid Paraffin - 60 ppm Tween 80 in Water;
- c. Liquid Paraffin - 200 ppm Tween 80 in Water;
- d. 1% v/v Oleic Acid in Liquid Paraffin-Water.

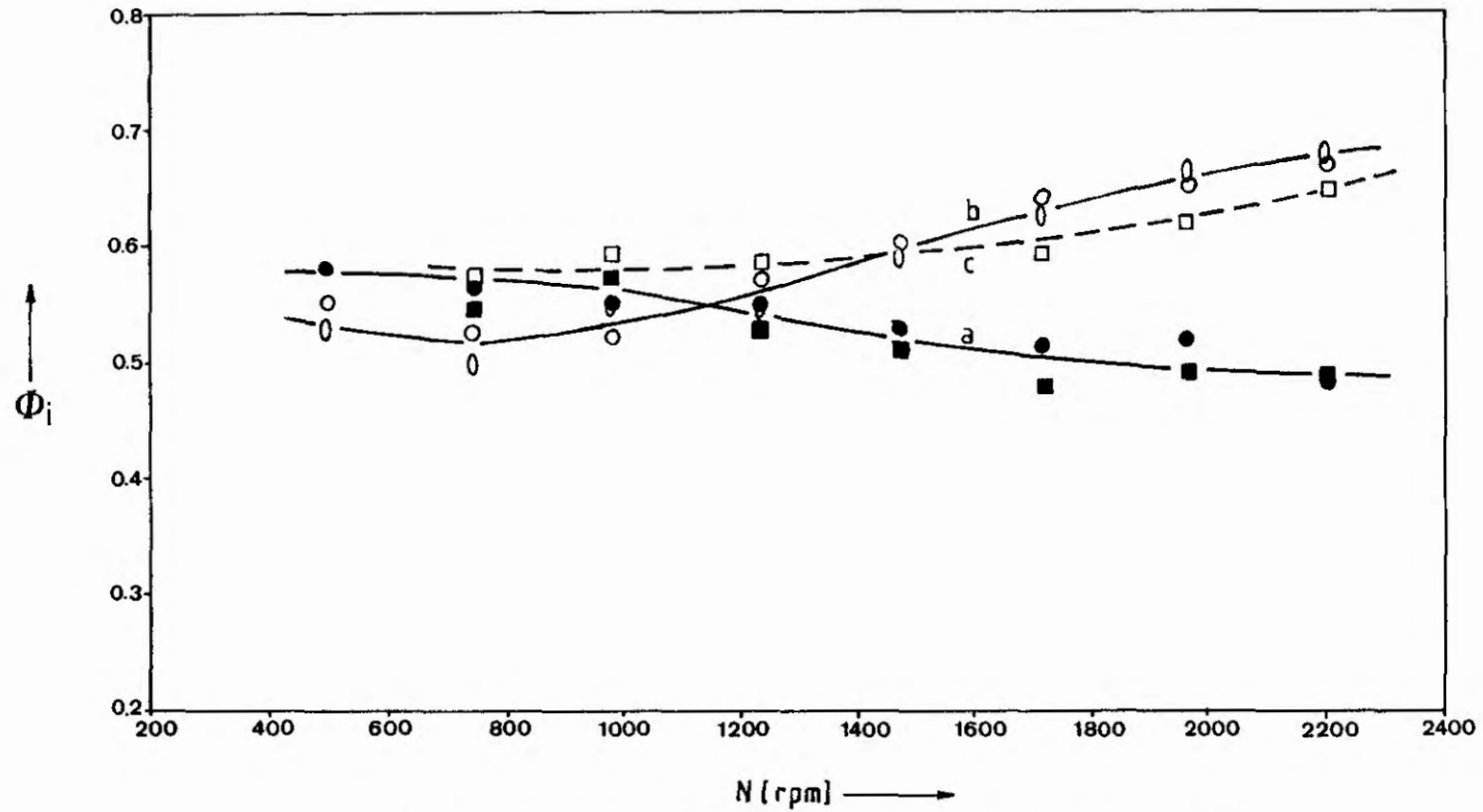
Figure 19



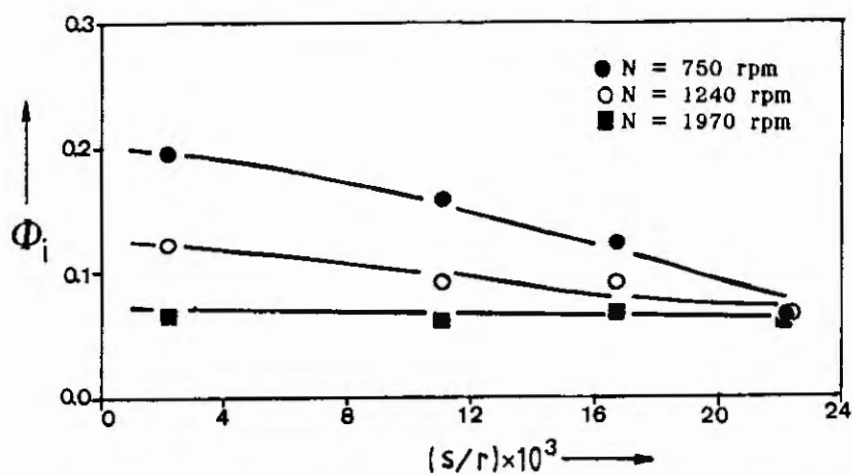
Volume Fraction of the Organic Phase at Inversion vs
Rotational Speed for the Systems;

- a. Dibutyl Maleate-Water with Stainless Steel Plates; ● $s = 0.1$ mm, ○ $s = 0.5$ mm;
Dibutyl Maleate - 200 ppm Tween 80 in Water with Stainless Steel Plates;
◆ $s = 0.1$ mm, ◇ $s = 0.5$ mm;
- b. Dibutyl Maleate-Water with Glass Plates; ■ $s = 0.5$ mm, □ $s = 1$ mm;
Dibutyl Maleate - 200 ppm Tween 80 in Water with Glass Plates;
● $s = 0.5$ mm, ○ $s = 1$ mm;
- c. Dibutyl Maleate - 20% w/v CaCl_2 aq. soln. with Stainless Steel Plates; x $s = 0.5$ mm.

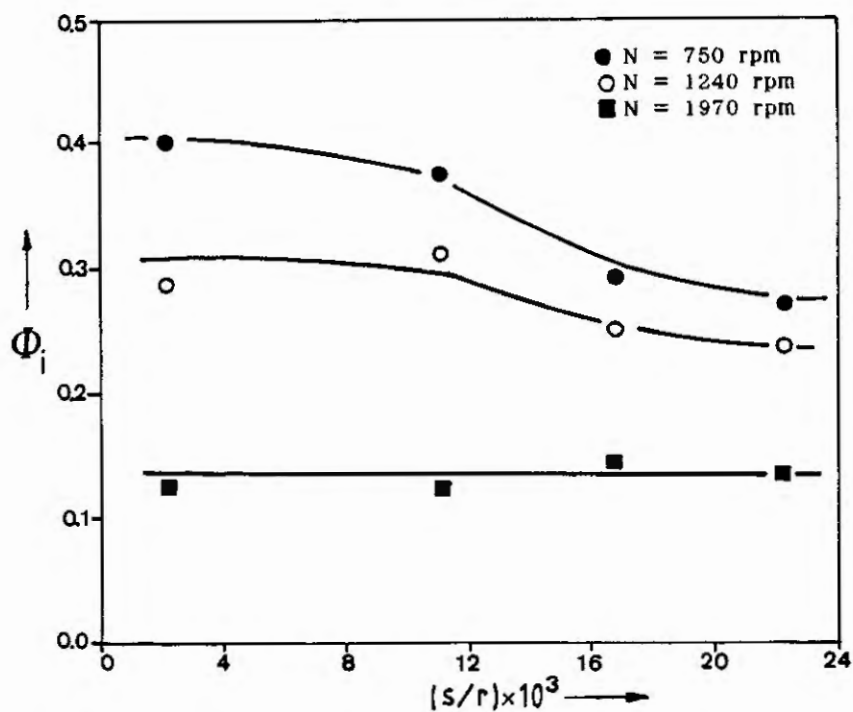
Figure 20



Volume Fraction of the Organic Phase at Inversion vs
Rotational Speed for the Escalid-Water System and
a. Stainless Steel Plates; ● $s = 0.1$ mm, ■ $s = 1$ mm,
b. Glass Plates; ○ $s = 0.2$ mm, □ $s = 0.5$ mm
c. Glass Plates; □ $s = 1$ mm.

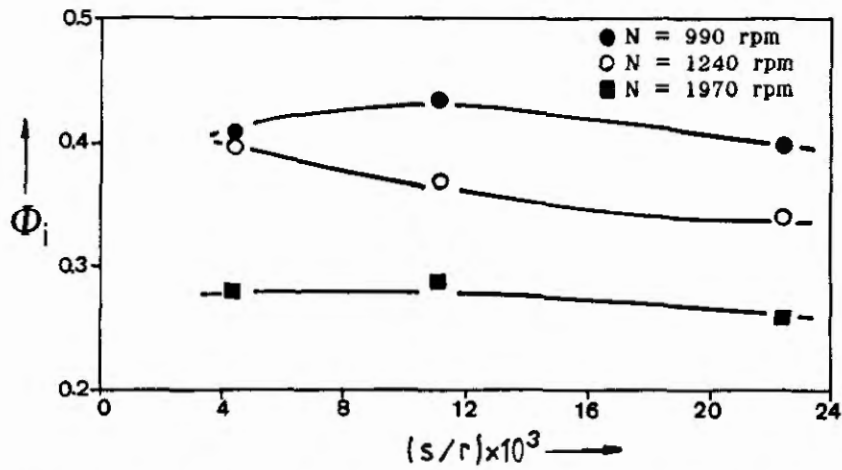
Figure 21

Volume Fraction of the Organic Phase at Inversion vs
Gap Width between the Plates/Radius of Plates for the
Liquid Paraffin-Water System and Perspex Plates

Figure 22

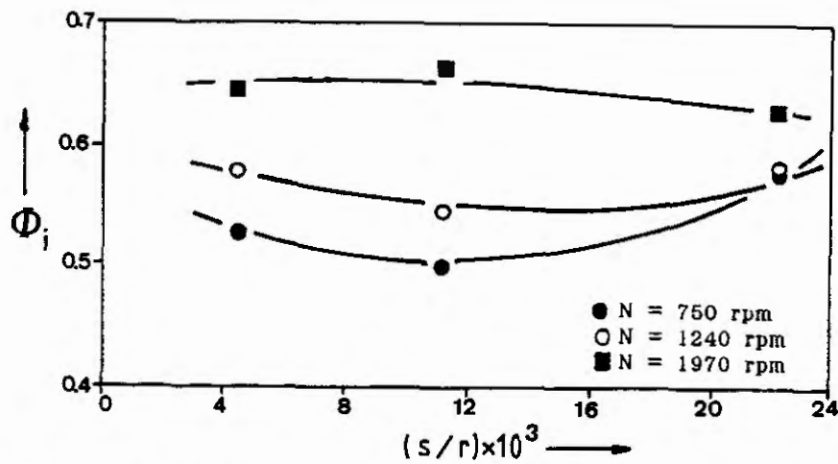
Volume Fraction of the Organic Phase at Inversion vs
Gap Width between the Plates/Radius of Plates for the
Liquid Paraffin-Water System and Stainless Steel
Plates

Figure 23

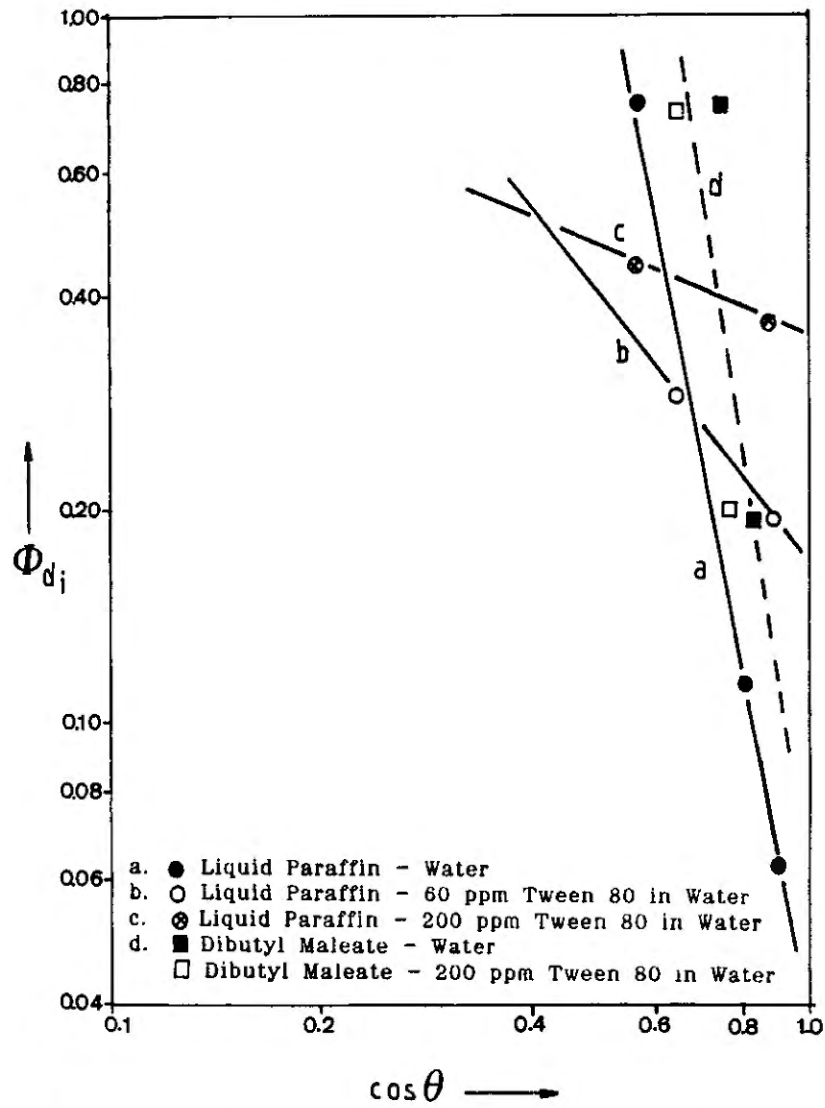


Volume Fraction of the Organic Phase at Inversion vs Gap Width between the Plates/Radius of Plates for the Liquid Paraffin-Water System and Glass Plates

Figure 24

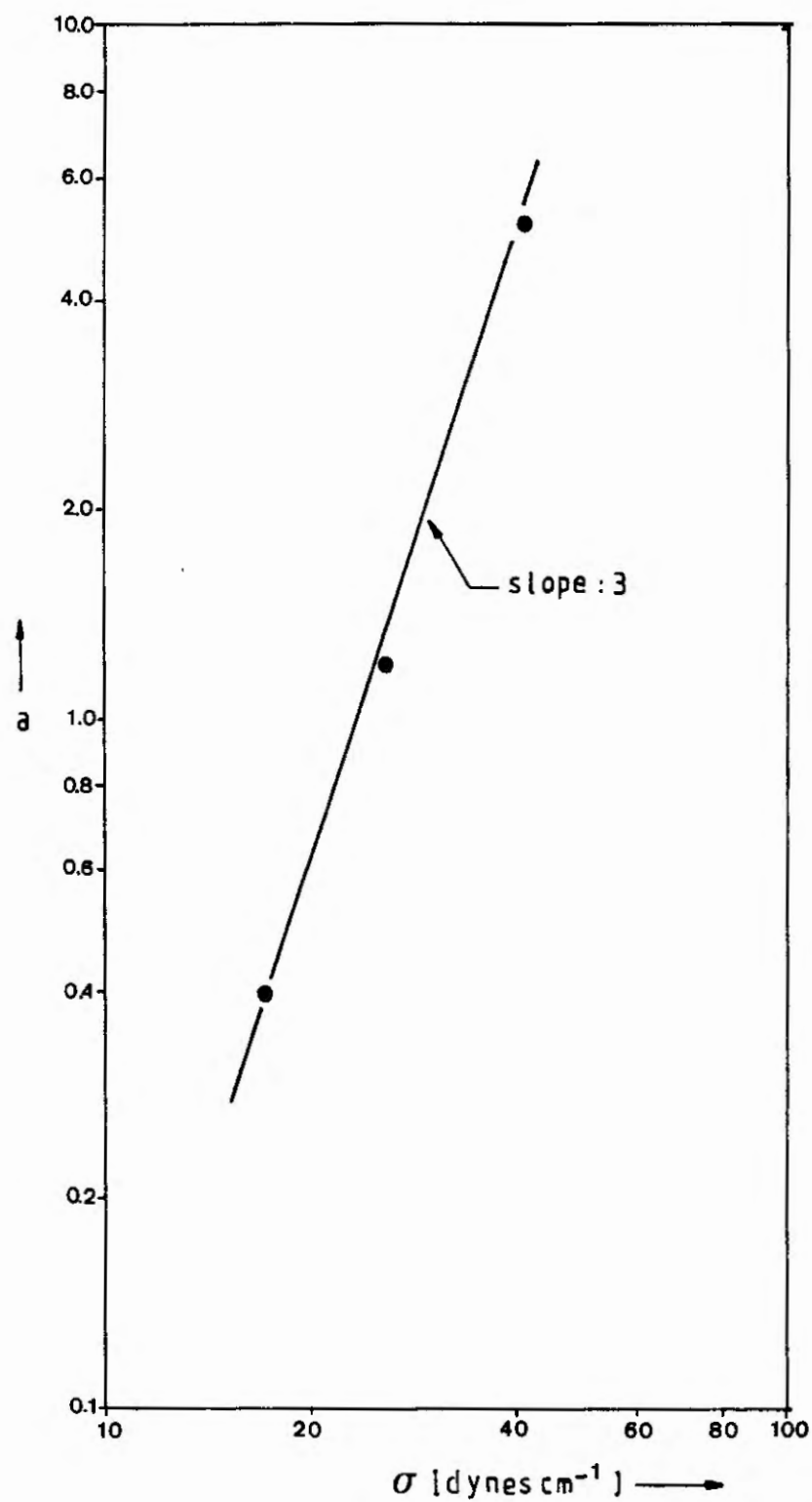


Volume Fraction of the Organic Phase at Inversion vs Gap Width between the Plates/Radius of Plates for the Escalid-Water System and Glass Plates

Figure 25

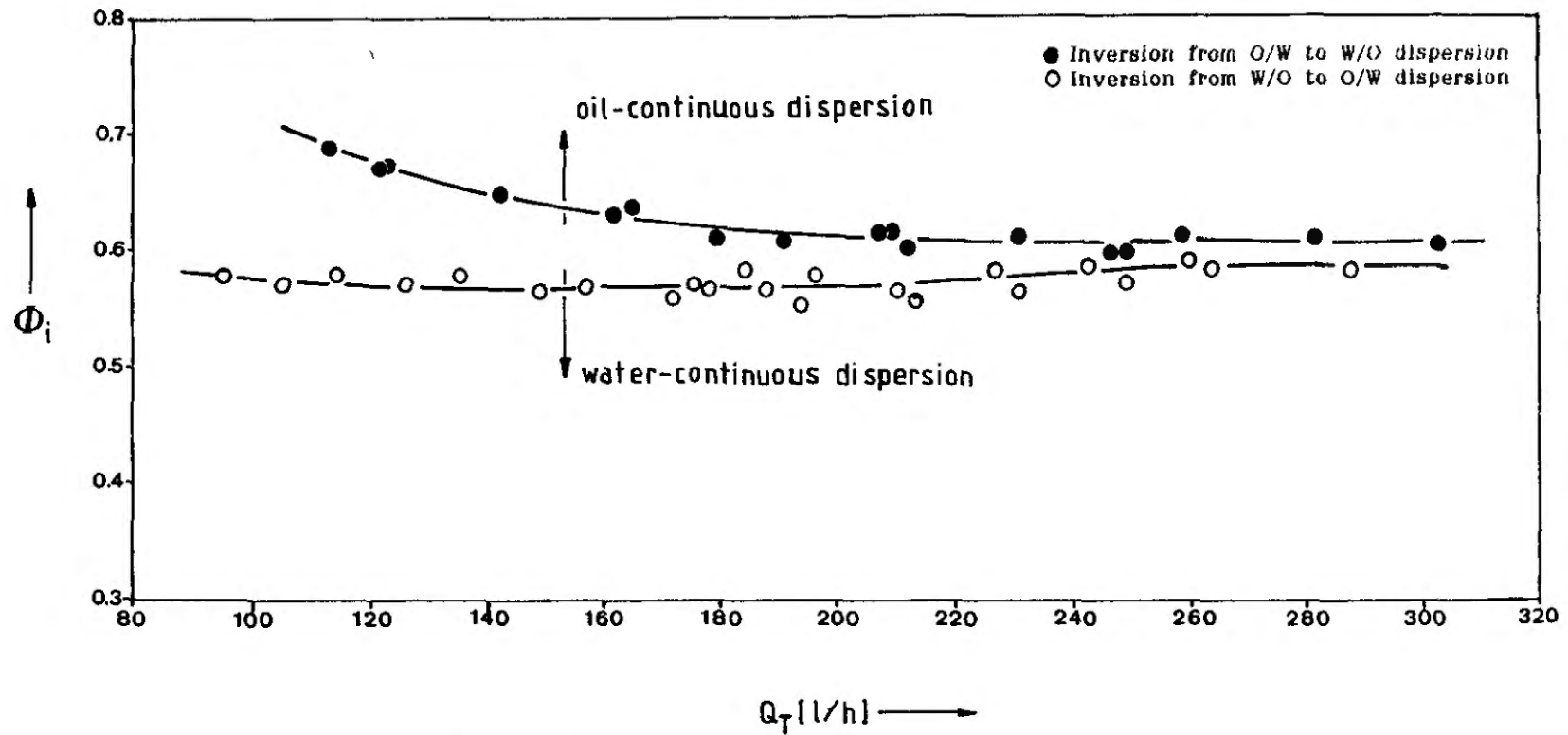
Volume Fraction at Inversion of the Dispersed Phase of the less Preferred Type of Dispersion at High Taylor Numbers vs $\cos \theta$ (θ measured through the phase that preferentially wetted the material of the plates)

Figure 26



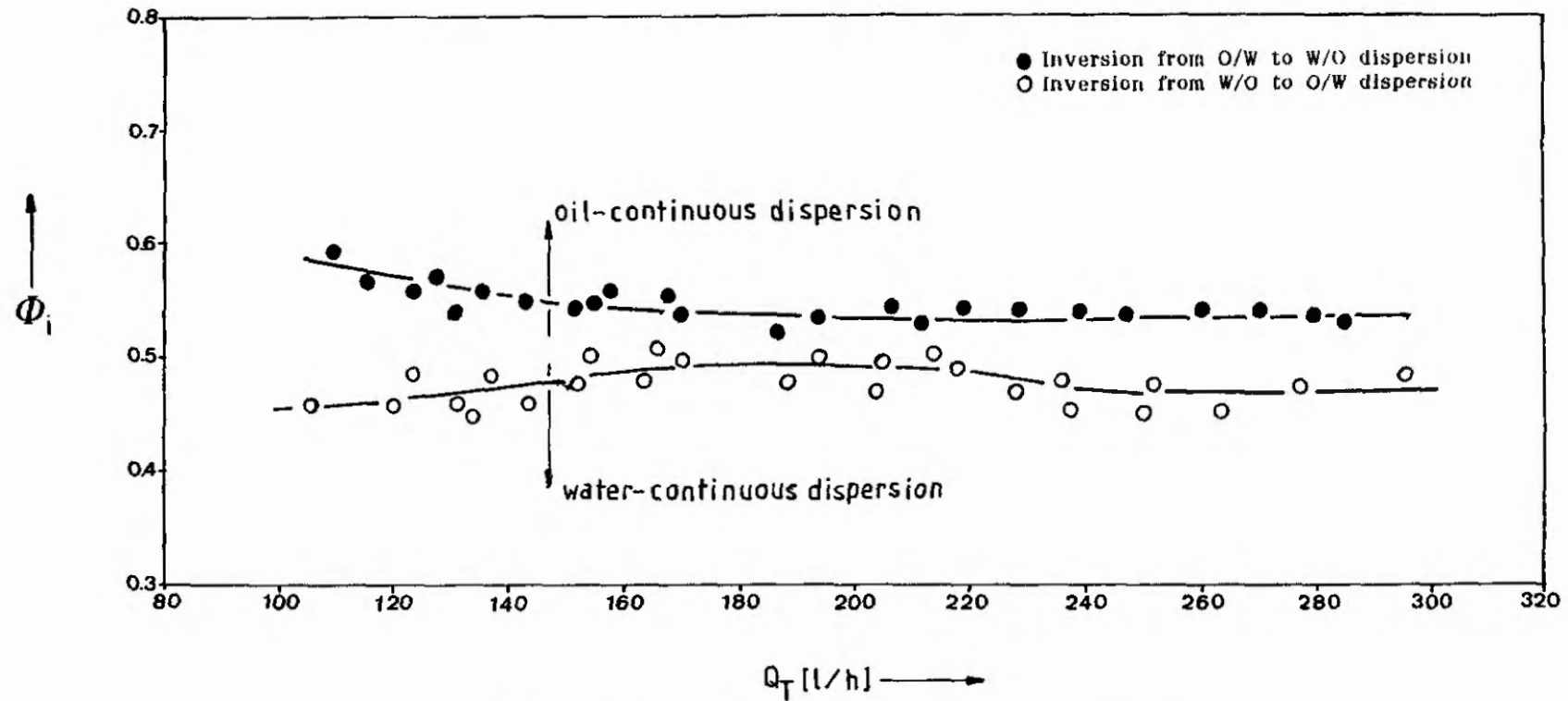
Dependence of the Slope of the Lines in Figure 25 on Interfacial Tension

Figure 27



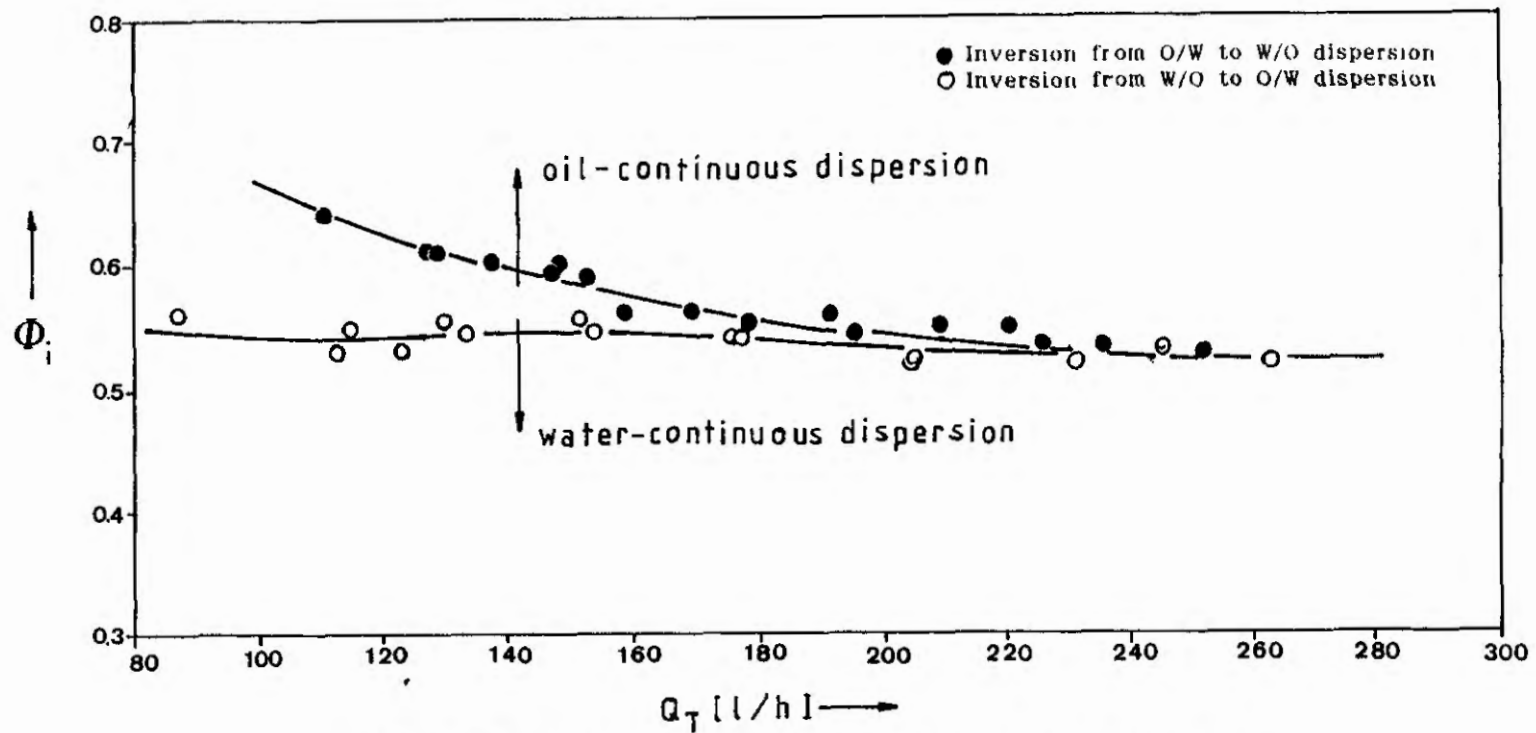
Volume Fraction of the Organic Phase at Inversion vs
Total Flow Rate in the Horizontal Glass Tube with the
Aqueous Phase through the T-branch for the
Escalid-Water System

Figure 28



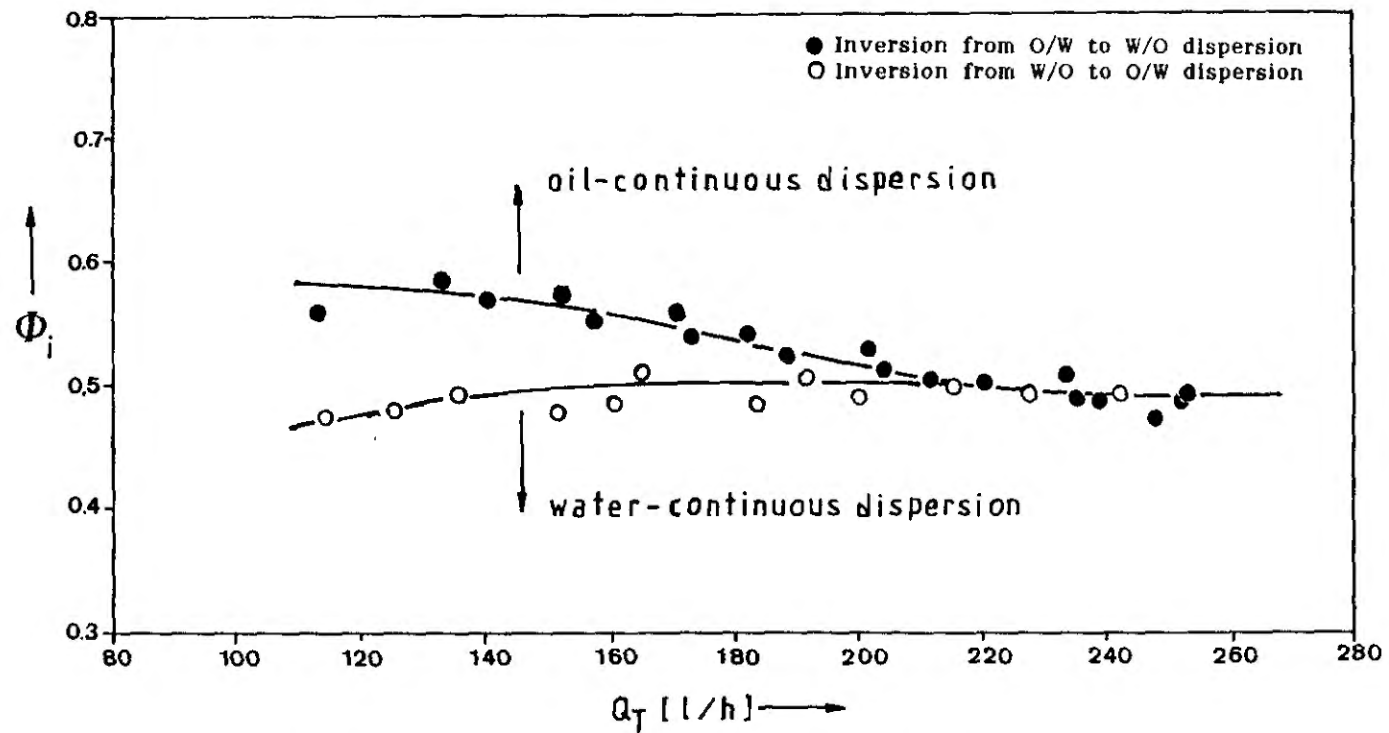
Volume Fraction of the Organic Phase at Inversion vs
Total Flow Rate in the Horizontal Glass Tube with the
Organic Phase through the T-branch for the
Escalid-Water System

Figure 29



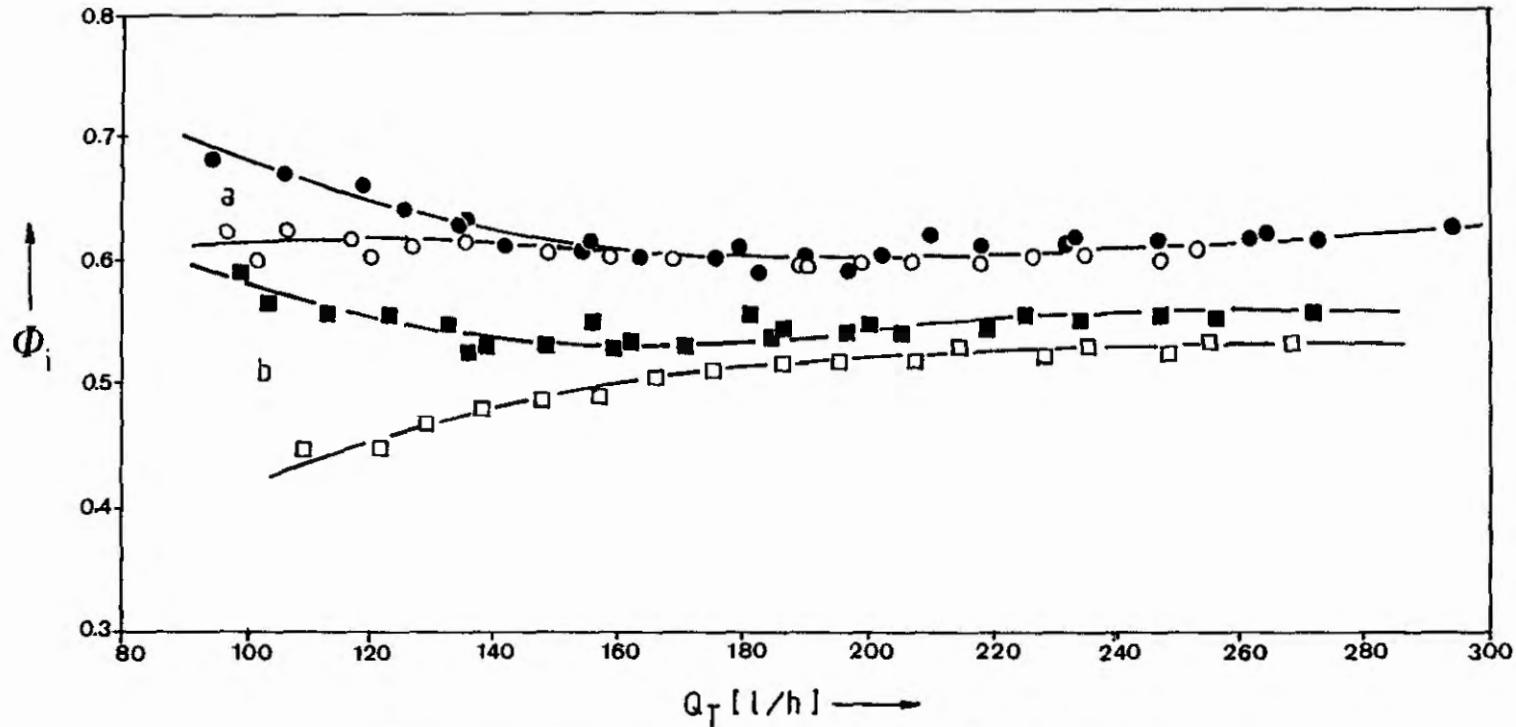
Volume Fraction of the Organic Phase at Inversion vs
Total Flow Rate in the Horizontal Glass Tube with the
Aqueous Phase through the T-branch for the Escaid -
200 ppm Tween 80 in Water System

Figure 30



Volume Fraction of the Organic Phase at Inversion vs
Total Flow Rate in the Horizontal Glass Tube with the
Organic Phase through the T-branch for the Escaid -
200 ppm Tween 80 in Water System

Figure 31



Volume Fraction of the Organic Phase at Inversion vs
Total Flow in the Horizontal Glass Tube for the
Escaid - 20% w/v CaCl_2 aq. soln.:

a. Aqueous Phase through the T-branch;

● Inversion from O/W to W/O dispersion;

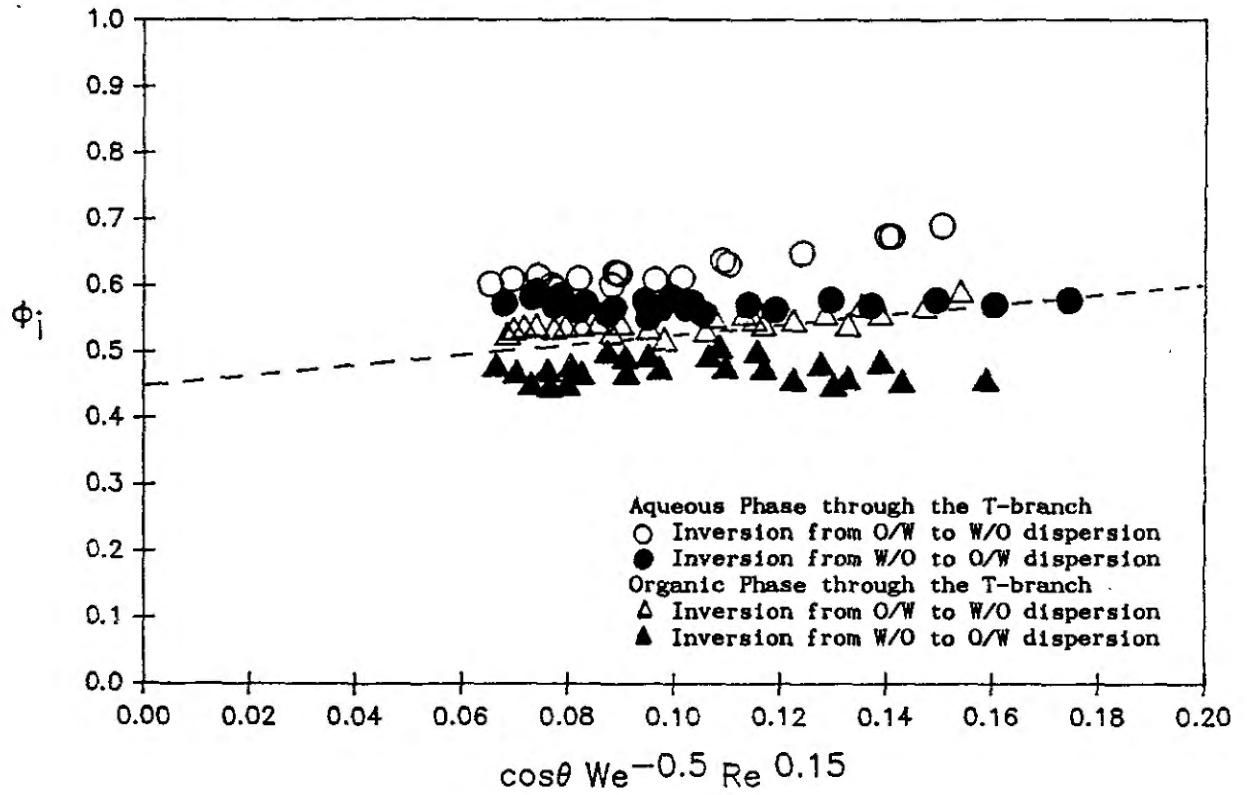
○ Inversion from W/O to O/W dispersion;

b. Organic Phase through the T-branch;

■ Inversion from O/W to W/O dispersion;

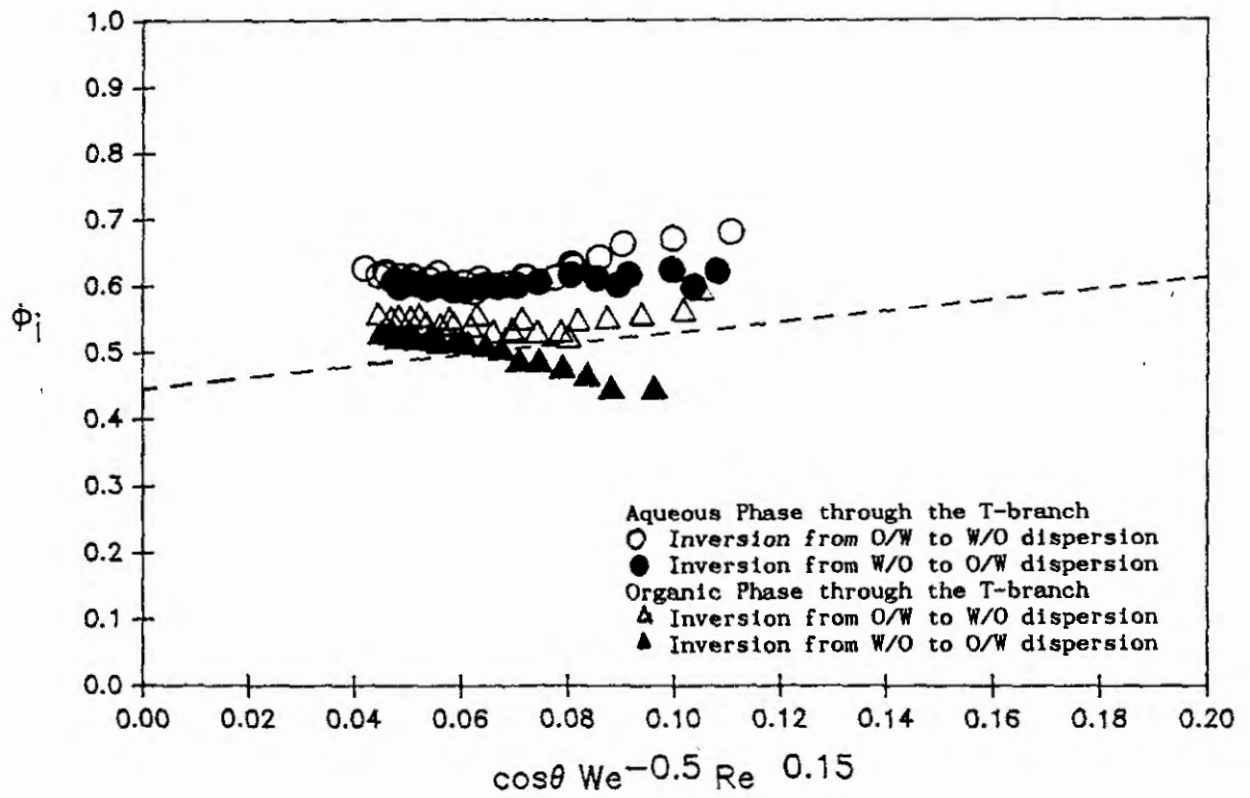
□ Inversion from W/O to O/W dispersion.

Figure 32

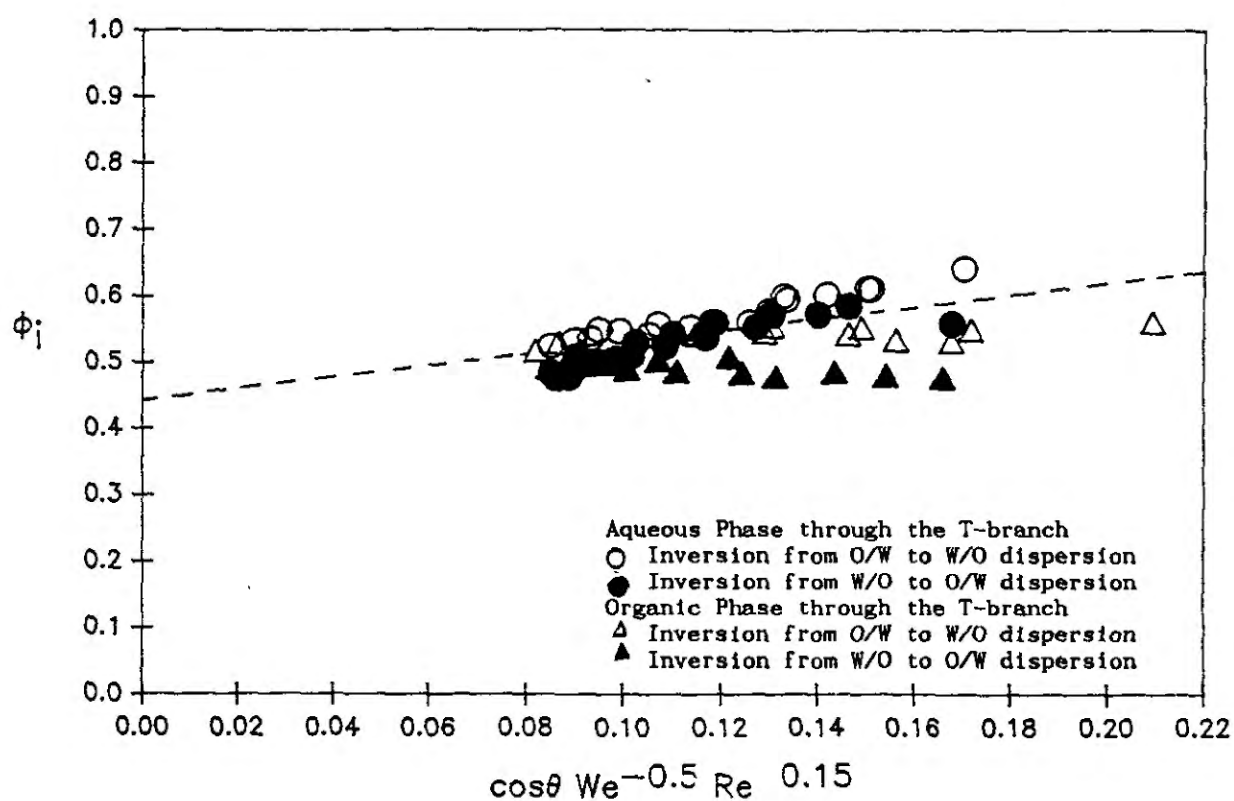


Volume Fraction of the Organic Phase at Inversion vs
 $\cos \theta We^{-0.5} Re^{0.15}$ for the Escaid-Water System in the
Horizontal Glass Tube

Figure 33



Volume Fraction of the Organic Phase at Inversion vs
 $\cos \theta We^{-0.5} Re^{0.15}$ for the Escaid - 20% w/v CaCl_2 aq.
soln. System in the Horizontal Glass Tube

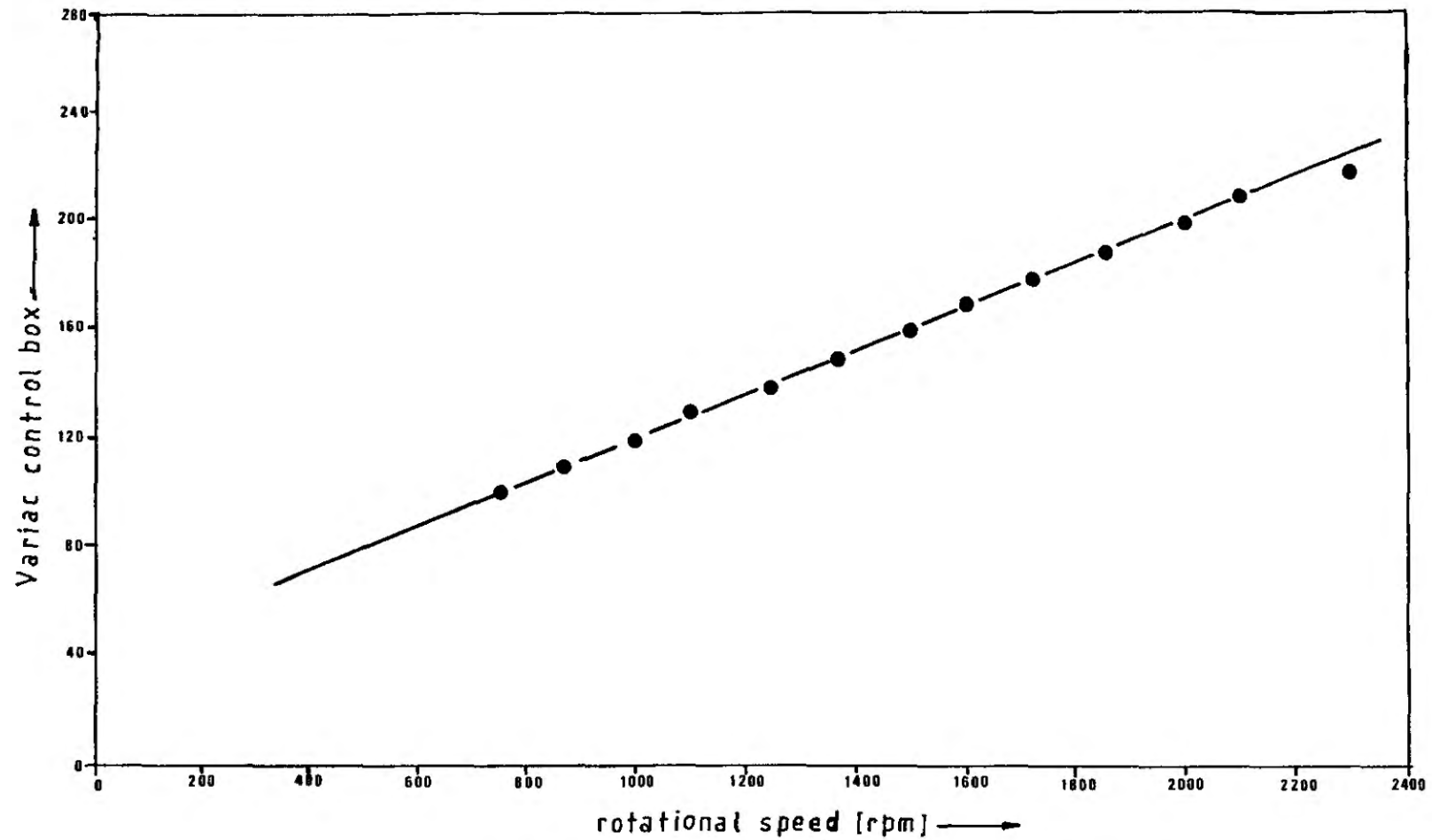
Figure 34

Volume Fraction of the Organic Phase at Inversion vs
 $\cos \theta We^{-0.5} Re^{0.15}$ for the Escaid - 200 ppm Tween 80 in
Water System in the Horizontal Glass Tube

APPENDICES

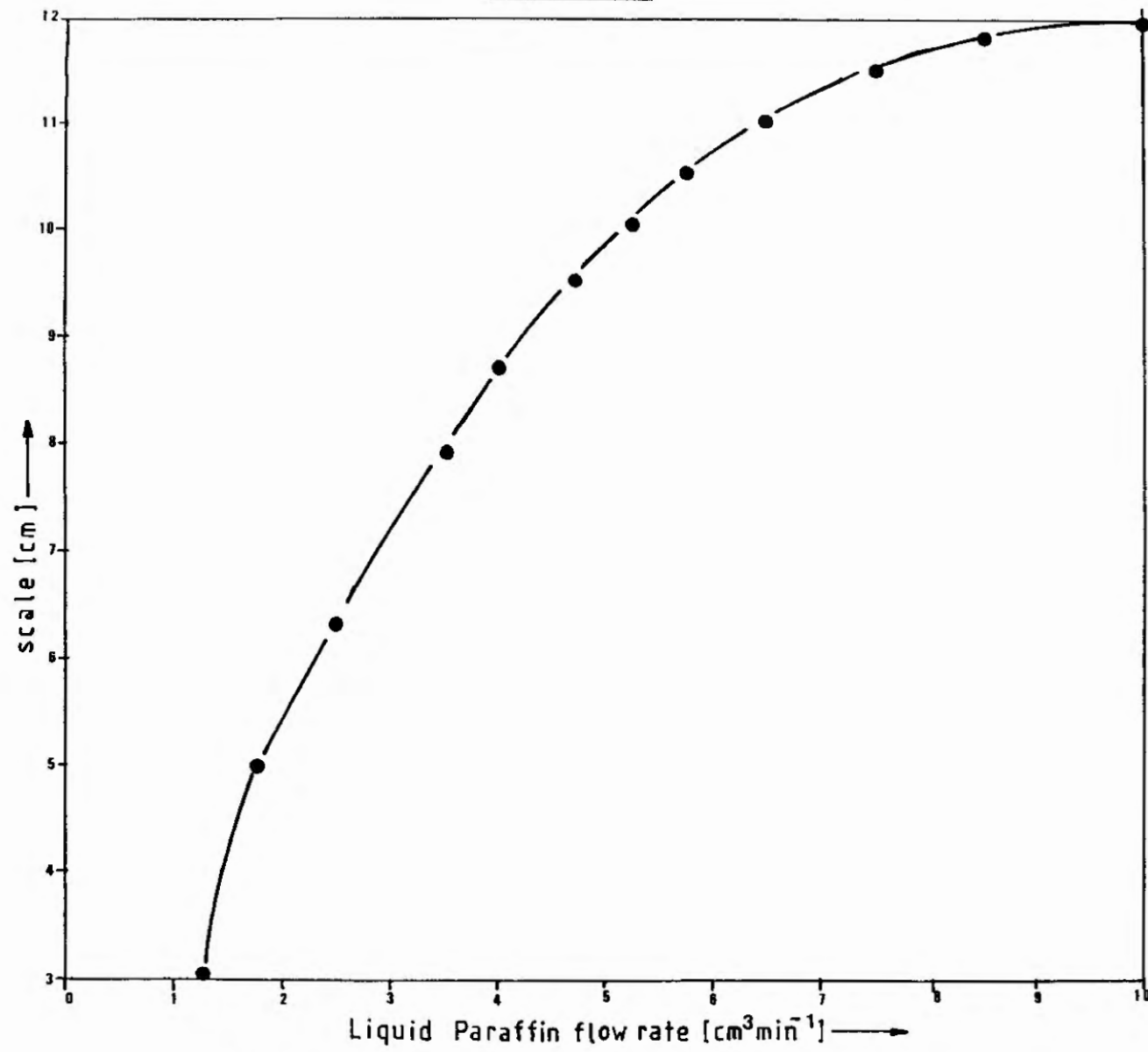
A1. Calibrations

Figure A1.1



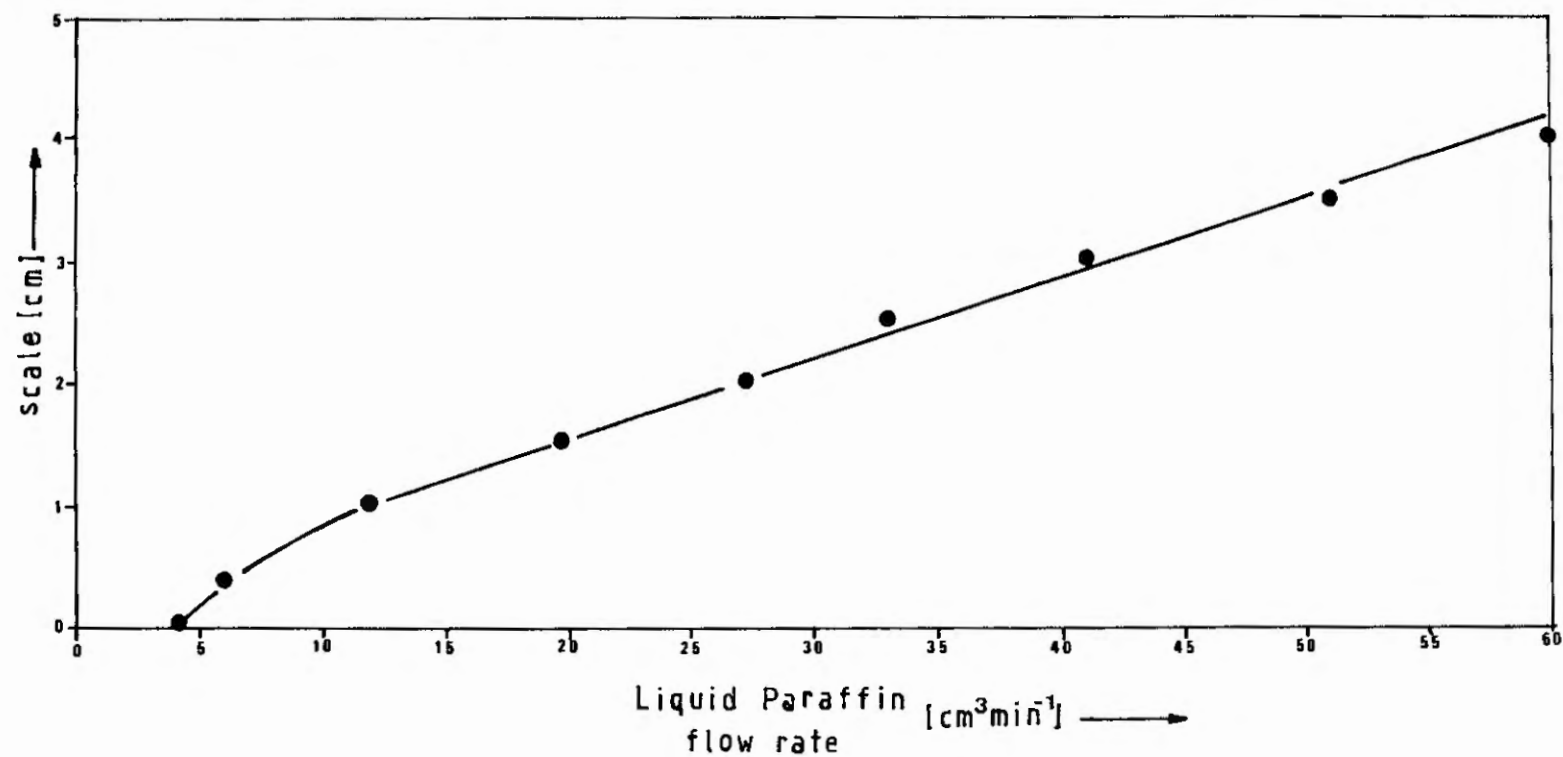
Calibration of Rotational Speed Control Box (Variac)
in the Parallel Shearing Plates Method

Figure A1.2



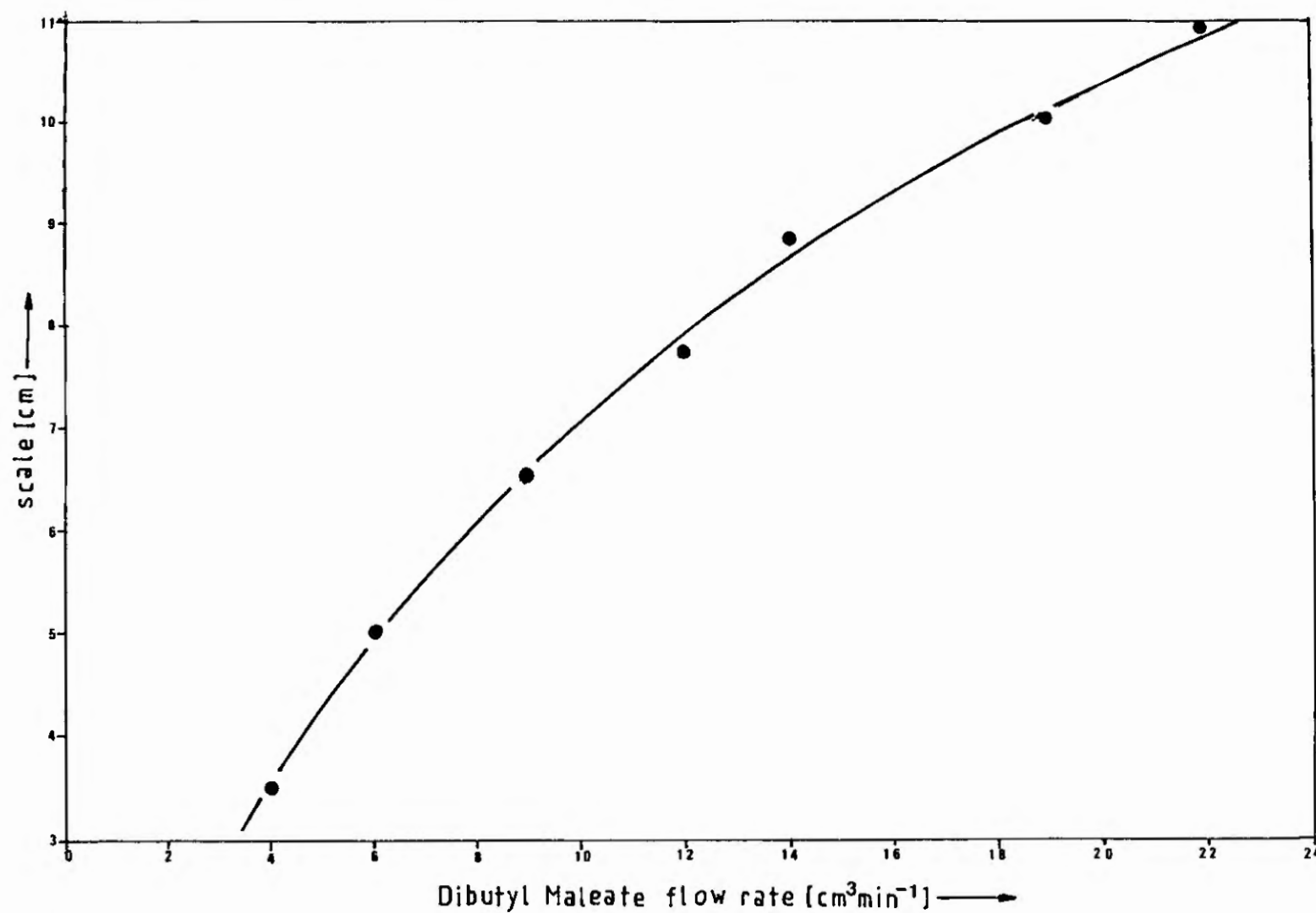
Calibration of the Smaller Rotameter for Liquid Paraffin in the Parallel Shearing Plates Method

Figure A1.3



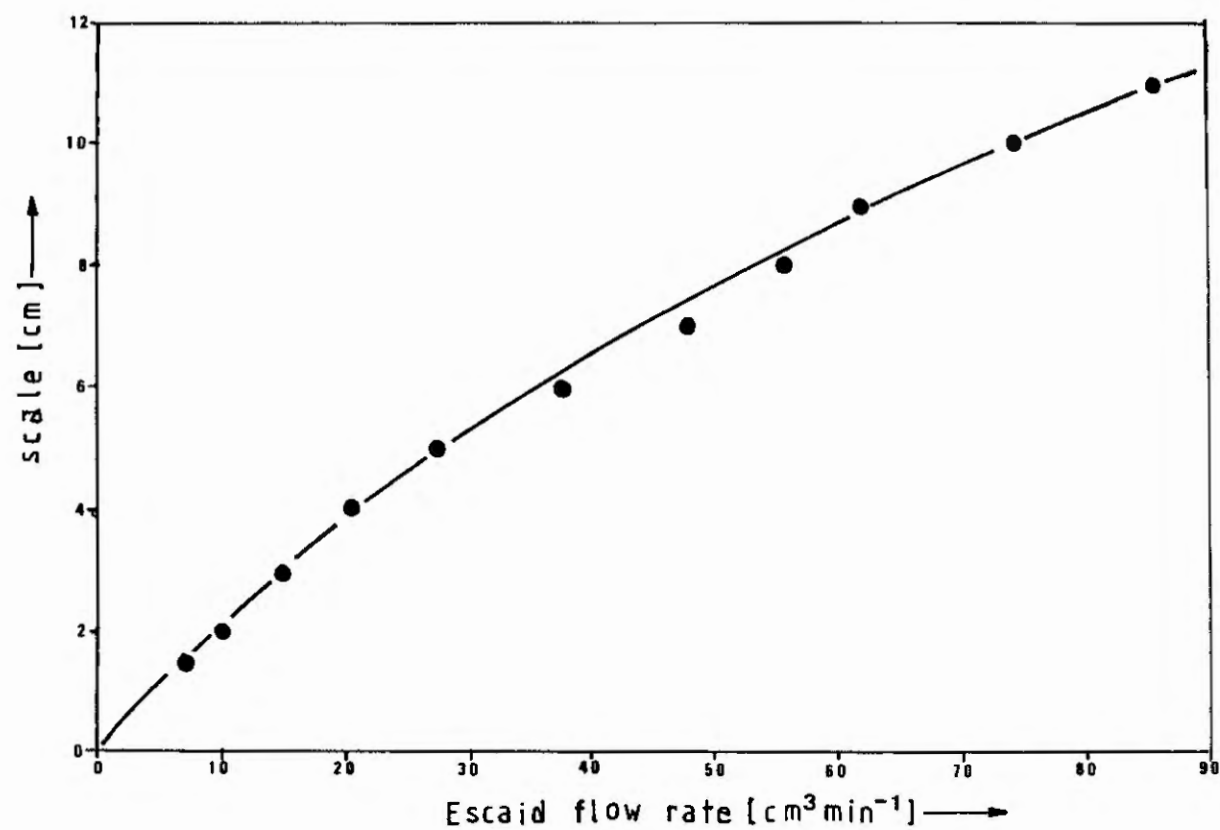
Calibration of the Bigger Rotameter for Liquid Paraffin in the Parallel Shearing Plates Method

Figure A1.4



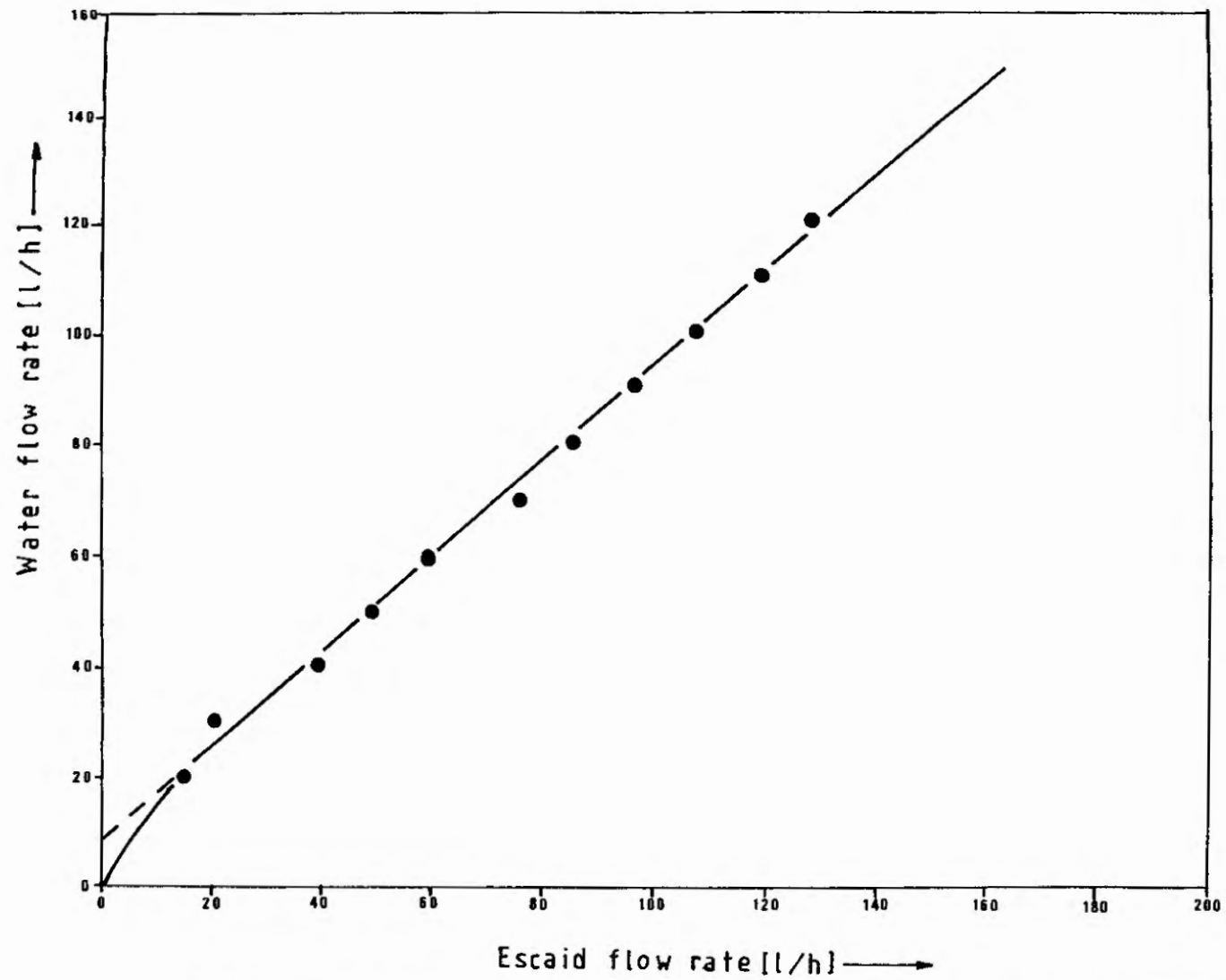
Calibration of Rotameter for Dibutyl Maleate in the
Parallel Shearing Plates Method

Figure A1.5



Calibration of Rotameter for Escaid in the Parallel Shearing Plates Method.

Figure A1.6



Calibration of Rotameter for Escaid in the Horizontal Glass Tube Method

A2. Equations

A2.1. Derivation of Equation 3.1

The volume fraction of the organic phase at inversion, Φ_i , can be calculated from the ratio R_i of the flow rates of the aqueous and the organic phase respectively at the point of inversion:

$$\Phi_i = \frac{Q_{oi}}{Q_{wi} + Q_{oi}}$$

i.e.
$$\Phi_i = \frac{1}{Q_{wi}/Q_{oi} + 1}$$

i.e.
$$\Phi_i = \frac{1}{R_i + 1}$$

where Q_{wi} : flow rate of the aqueous phase at inversion;

Q_{oi} : flow rate of the organic phase at inversion;

R_i : Q_{wi}/Q_{oi} .

A2.2. Derivation of Equation 4.4

In order to calculate the shear rate produced between two parallel plates, one of which is rotating when the other is stationary, with a very small gap width in comparison to the radius of the plates, the following assumptions were made;

1. There was no axial flow, $v(z) = 0$;
2. There was a linear distribution of the rotational velocity, $w = Nzs^{-1}$, and the angular velocity $v_\theta = rw(z)$, where N : rotational speed; r : radius of the plates; s : gap width and z : axial distance from the stationary plate.

The minimum angular velocity at $z = s$ for the minimum rotational speed used was $v_{\theta \min} = 0.375 \text{ ms}^{-1}$ where $N = 500 \text{ rpm}$ and $r = 45 \times 10^{-3} \text{ m}$. The maximum radial velocity, for the maximum flow rates used at the minimum gap width used could be calculated from the following equation:

$$v_{r \max} = \frac{Q_{w \max} + Q_{o \max}}{2\pi r s_{\min}}$$

where $s_{\min} = 0.1 \text{ mm}$: minimum gap width;

$Q_{w \max} = 60 \text{ cm}^3 \text{ min}^{-1}$: maximum flow rate of the aqueous phase at $s = 0.1 \text{ mm}$;

$Q_{o \max} = 50 \text{ cm}^3 \text{ min}^{-1}$: maximum flow rate of the organic phase at $s = 0.1 \text{ mm}$.

$$\text{So, } v_{r \max} = \frac{(60+50) \times 10^{-6}/60}{2\pi \times 45 \times 10^{-3} \times 0.1 \times 10^{-3}} \text{ ms}^{-1}$$

$$\text{i.e. } v_{r \max} = 0.065 \text{ ms}^{-1}$$

Comparing the maximum radial velocity with the minimum angular velocity, having a ratio of $v_{r \max} / v_{\theta \min} = 0.17$, the assumption of a negligible radial velocity could be made.

Following the assumptions made above, the shear rate could be calculated from the following equation:

$$\dot{\gamma} = \frac{dv_{\theta}}{dz} = r \frac{d\omega}{dz}$$

$$\text{i.e. } \dot{\gamma} = rNs^{-1}$$

where N : rotational speed;

r : radius of the plates;

s : gap width between the plates.

A3. Calculations

A3.1. Example of Calculation of Interfacial Tension Measured by the Drop-Weight Method

The Liquid Paraffin-Water system was chosen as an example of calculating the interfacial tension measured by the drop-weight method. The stainless steel needle with the conical end of size $a = 0.027$ cm was chosen for the measurement. The micrometer scale was calibrated by the suppliers so that 1 mm corresponded to a volume of 2×10^{-4} ml. The procedure described in Chapter 3, Section 3.4.1 for the interfacial tension measurement with the drop-weight method was repeated ten times and the mean volume of the drops formed corresponded to 215 mm on the micrometer scale. Therefore, the mean volume of the drops was calculated to be $V = 215 \times 2 \times 10^{-4}$ ml = 0.043 ml. Consequently, $a\sqrt{V}^{1/3} = 0.08$ and the corresponding correction factor was $\psi = 1.1$ (Davies and Rideal, 1960, p.45). The density difference between the liquids was measured by weighing the same volume of both liquids and found to be $\Delta\rho_g = 0.15$ gcm⁻³. The interfacial tension could then be calculated from Equation 3.3 as follows:

$$\sigma = \frac{\psi V \Delta\rho_g g}{2\pi a} \quad (3.3)$$

i.e.
$$\sigma = \frac{1.1 \times 0.043 \times 0.15 \times 981}{2\pi \times 0.027}$$

i.e.
$$\sigma = 41 \text{ dynes cm}^{-1}$$

where the gravitational acceleration is $g = 981$ cm sec⁻². The same procedure was followed for the calculation of interfacial tension of each liquid-liquid system used.

A3.2. Example of Calculation of Shear Stress at a Given Shear Rate from the Contraves Rheomat 30 Rheogram for the Estimation of Viscosity

The Rheogram for Liquid Paraffin (Figure A3.1) was chosen as an example of calculating the shear stress at a give shear rate for the estimation of the viscosity of liquids. In Figure A3.1, the shear stress scale reading is 60.25 for the shear rate scale reading 29. According to the shear stress table available (Table A3.1) for the measuring system used, named A, the shear rate corresponding to this point is 487s^{-1} and the shear stress can be calculated as follows:

$$\tau = 60.25 \times 0.2239 \times 1 = 13.49\text{Pa}$$

where 0.2239 is the $\tau\%$ for the measuring system A (Table A3.1) and 1 is the factor corresponding to the selected torque range mentioned in the rheogram (Figure A3.1).

The same method was followed for the calculation of shear stress at various shear rates and the results were plotted in Figures 8, 9 and 10 for the different organic liquids used. The viscosity of each liquid was then estimated from the slope of the tangent of the corresponding curve.

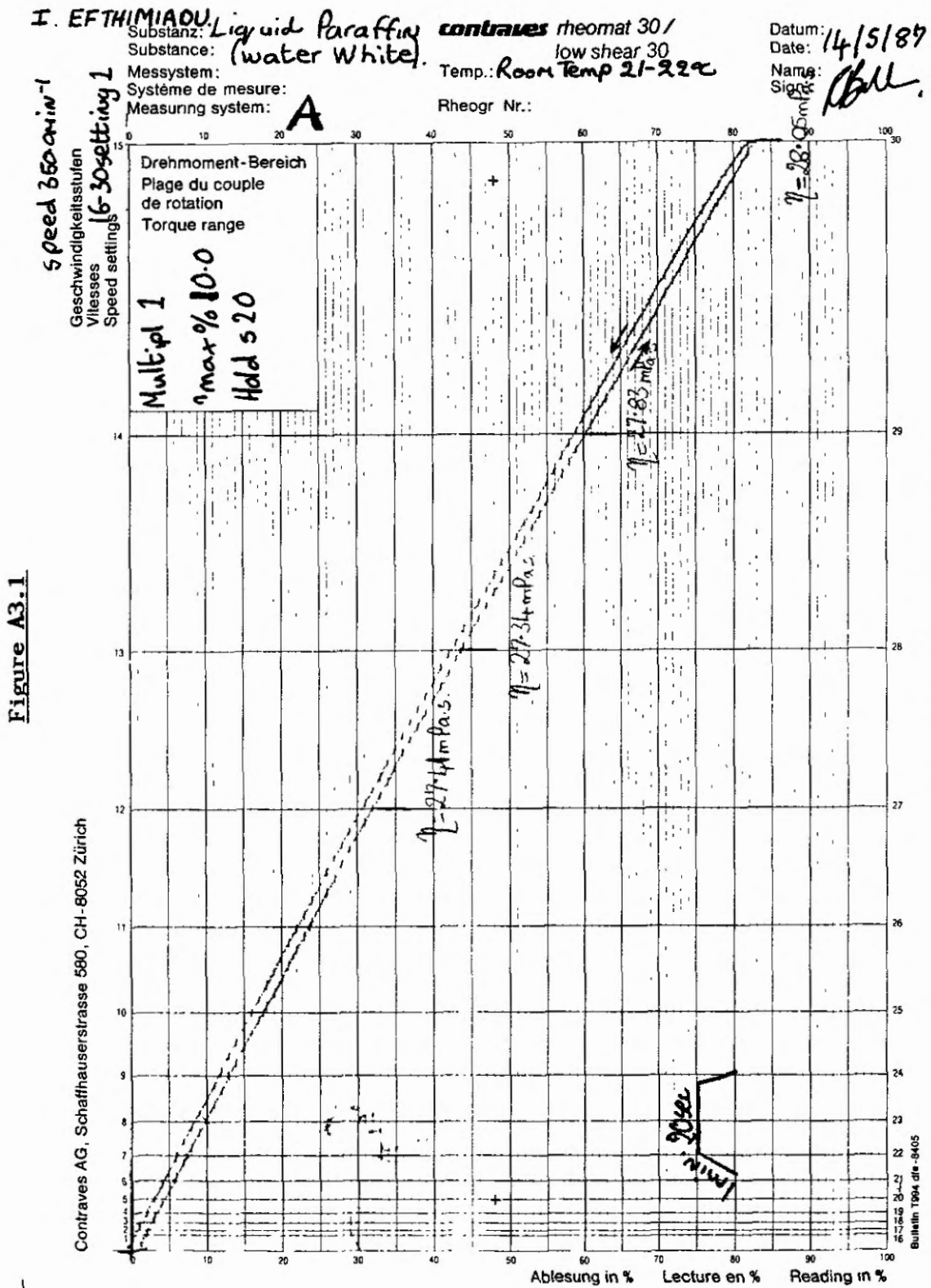
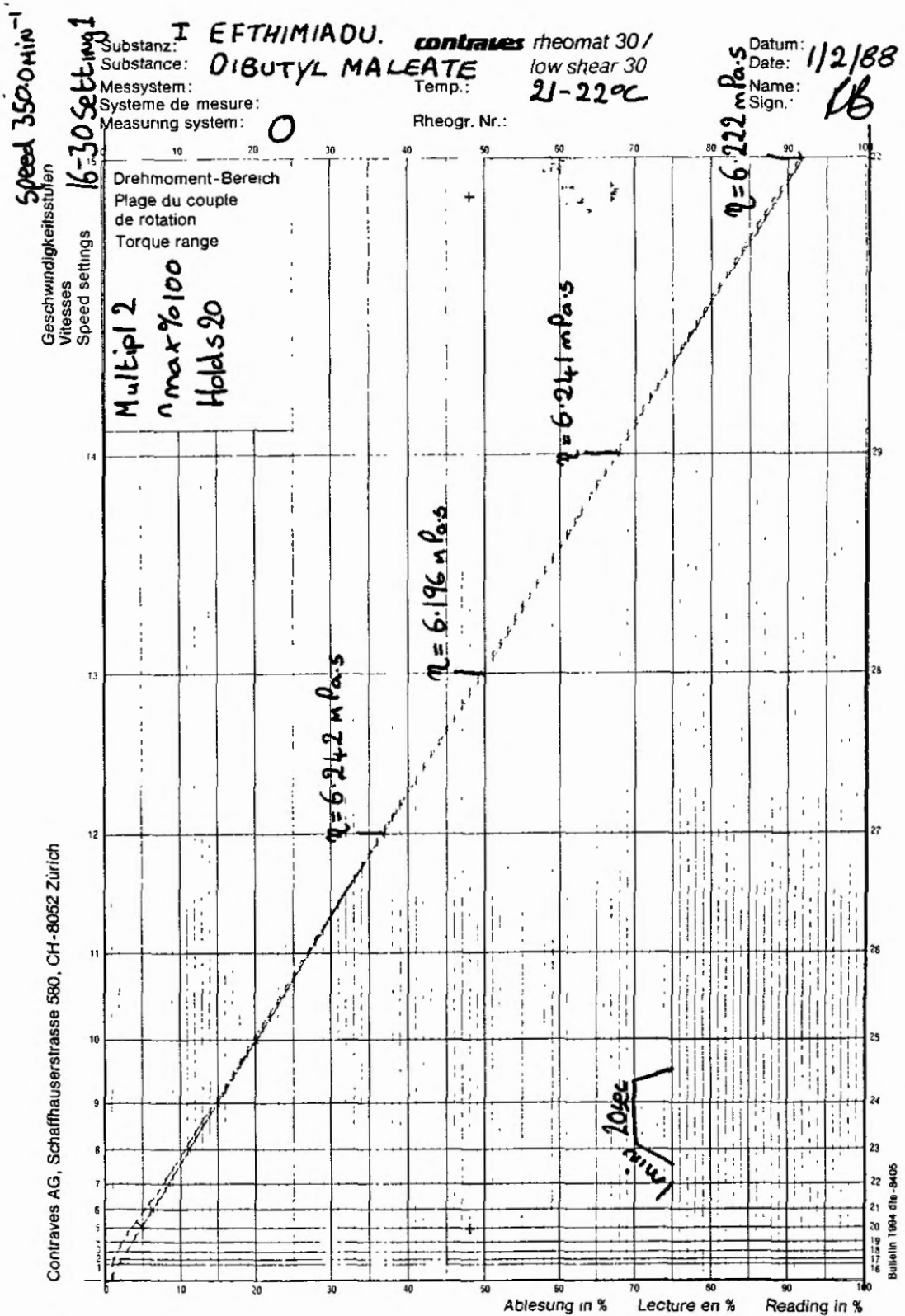
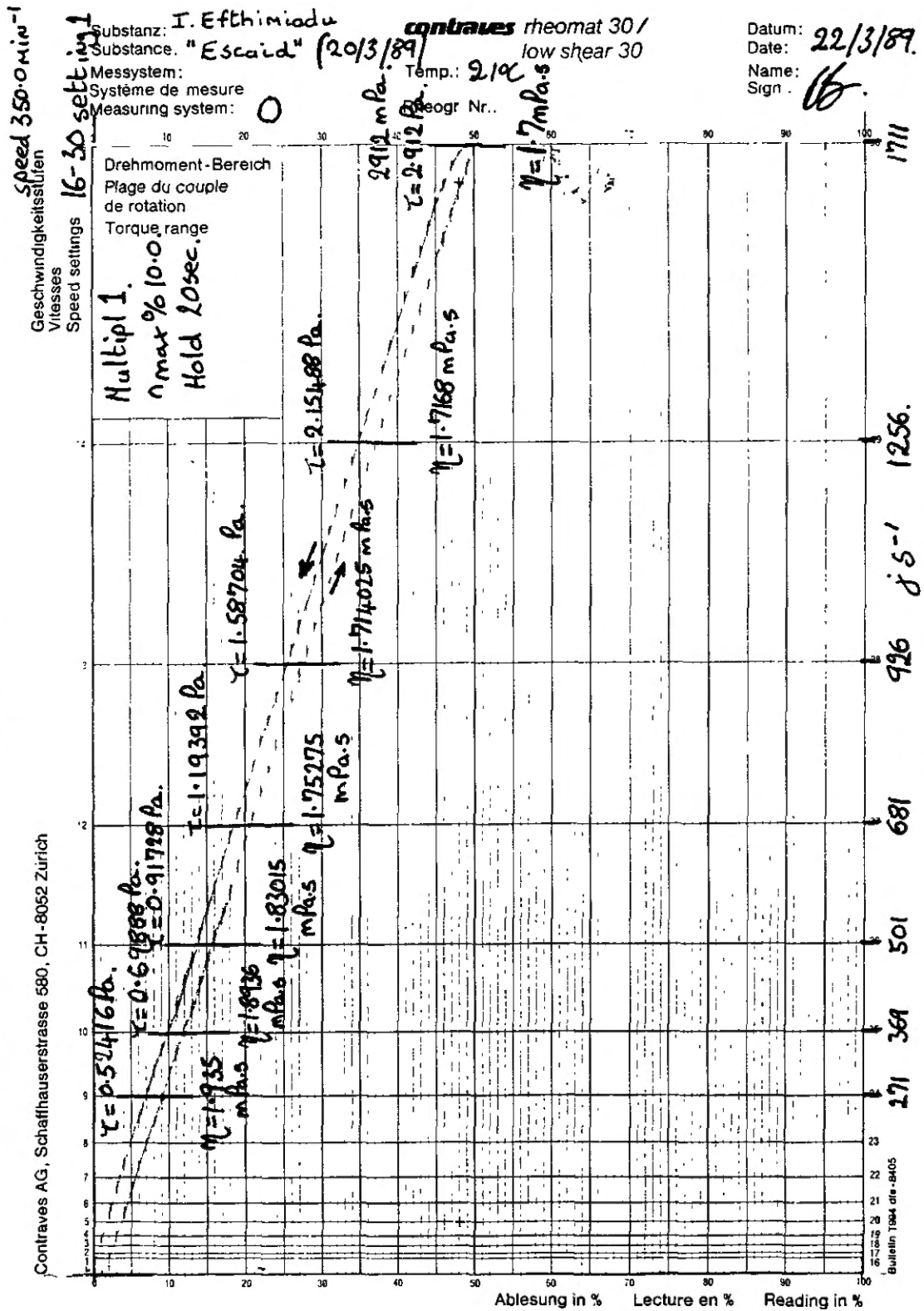


Figure A3.2



Rheogram for Dibutyl Maleate

Figure A3.3



Rheogram for Escaid

Table A3.1

Table for Calculation of Shear Stress at Different
Shear Rates for the Viscosity Measuring System of
Co-Axial Cylinders

Rheomat 30

CONTRAFLEX

MS ABCD/E.

concentric cylinder

D und τ -Tabelle zu Messsystem A-Ee, repräsentative WerteD and τ values table for measuring system A-Ee, representative valuesTableau des valeurs D et τ pour le système de mesure A-Ee, valeurs représentatives

MS	A	B	C	Cb	C2	C4	D	De	D2	D4	E	Ee	n
$\tau_{rep} [Pa]$	0.2239	0.4061	2.384	2.922	2.852	3.083	14.831	19.299	6.860	7.774	73.64	182.59	min.
1	0.0899	0.0215	0.01355	0.0309	0.0392	0.0972	0.00830	0.01779	0.0265	0.0723	0.00575	0.0425	0.0476
2	0.1223	0.0292	0.01842	0.0420	0.0533	0.1322	0.01129	0.0242	0.0360	0.0963	0.00781	0.0578	0.0641
3	0.1662	0.0397	0.0250	0.0571	0.0724	0.1796	0.01534	0.0329	0.0489	0.1337	0.01062	0.0785	0.0877
4	0.226	0.0539	0.0340	0.0777	0.0984	0.244	0.0209	0.0447	0.0665	0.1817	0.01443	0.1067	0.1198
5	0.307	0.0733	0.0463	0.1056	0.1338	0.332	0.0284	0.0608	0.0904	0.247	0.01962	0.1451	0.1622
6	0.417	0.0996	0.0629	0.1435	0.1819	0.451	0.0385	0.0826	0.1230	0.336	0.0267	0.1972	0.221
7	0.567	0.1355	0.0855	0.1951	0.247	0.613	0.0524	0.1123	0.1671	0.456	0.0362	0.268	0.300
8	0.771	0.1841	0.1162	0.265	0.336	0.834	0.0712	0.1526	0.227	0.620	0.0493	0.364	0.408
9	1.049	0.250	0.1580	0.361	0.457	1.133	0.0968	0.207	0.309	0.843	0.0670	0.495	0.555
10	1.425	0.340	0.215	0.490	0.621	1.541	0.1316	0.282	0.420	1.146	0.0911	0.674	0.754
11	1.938	0.463	0.292	0.666	0.844	2.08	0.1789	0.363	0.571	1.566	0.1258	0.916	1.025
12	2.63	0.629	0.397	0.906	1.148	2.85	0.243	0.521	0.776	2.12	0.1683	1.245	1.393
13	3.58	0.855	0.540	1.231	1.560	3.87	0.331	0.708	1.055	2.88	0.229	1.692	1.894
14	4.87	1.162	0.733	1.674	2.12	5.28	0.449	0.963	1.434	3.91	0.311	2.30	2.57
15	6.62	1.579	0.997	2.28	2.88	7.15	0.611	1.308	1.949	5.32	0.423	3.13	3.50
16	8.99	2.15	1.355	3.09	3.92	9.72	0.830	1.779	2.65	7.23	0.575	4.25	4.76
17	12.23	2.92	1.842	4.20	5.33	13.22	1.129	2.42	3.60	9.83	0.781	5.78	6.47
18	16.62	3.97	2.50	5.71	7.24	17.96	1.534	3.29	4.89	13.37	1.062	7.85	8.79
19	22.6	5.39	3.40	7.77	9.84	24.4	2.08	4.47	6.65	18.17	1.443	10.67	11.98
20	30.7	7.33	4.63	10.56	13.38	33.2	2.84	6.08	9.04	24.7	1.962	14.51	16.22
21	41.7	9.96	6.29	14.35	18.19	45.1	3.85	8.26	12.30	33.6	2.67	19.72	22.1
22	56.7	13.55	8.55	19.51	24.7	61.3	5.24	11.23	16.71	45.6	3.62	26.8	30.0
23	77.1	18.41	11.62	26.5	33.6	83.4	7.12	15.26	22.7	62.0	4.93	36.4	40.8
24	104.9	25.0	15.80	36.1	45.7	113.3	9.68	20.7	30.9	84.3	6.70	49.5	55.5
25	142.5	34.0	21.5	49.0	62.1	154.1	13.16	28.2	42.0	114.6	9.11	67.4	75.4
26	193.8	46.3	29.2	66.6	84.4	208	17.89	38.3	57.1	156.6	12.58	91.6	102.5
27	263	62.9	39.7	90.6	114.8	285	24.3	52.1	77.6	212	16.83	124.5	139.3
28	358	85.5	54.0	123.1	156.0	387	33.1	70.8	105.5	288	22.9	169.2	189.4
29	487	116.2	73.3	167.4	212	528	44.9	96.3	143.4	391	31.1	230	257
30	662	157.9	99.7	225	288	715	61.1	130.8	194.9	532	42.3	313	350
Spall mm	1.30	4.03	3.20	1.20	1.30	0.50	3.75	1.25	1.30	0.50	5.50	0.25	
K_{rep}	0.9475	0.8116	0.7312	0.8613	0.8872	0.9513	0.6250	0.7813	0.8417	0.9356	0.5356	0.8951	

Die τ_{rep} -Werte sind gültig für den Drehmomentenbereich 0–4 91 · 10⁻³ Nm (50 cmg)The τ_{rep} values apply to the torque range of 0–4 91 · 10⁻³ Nm (50 cm g)Les valeurs de τ_{rep} sont valables pour la plage de couple de rotation de 0–4 91 · 10⁻³ Nm (50 cm g)

Table A3.2

Table for Calculation of Shear Stress at Different
Shear Rates for the Viscosity-Measuring System of
Double-Cap

<u>Mess-System/Measuring System MS-0</u>						continues rm 30				
D-T- η - Tabelle, repräsentative Werte D-T- η - table, representative values System No. : <u>2041</u>						$D_{rep} = n \cdot 4,889 [s^{-1}]$ $\frac{\tau_{rep}}{K_{rep}} = \tau_i$ $\frac{D_{rep}}{K_{rep}} = D_i$				
$\tau_{rep} \%$ <u>58,24</u> mPa $K_{rep} =$ <u>0,9792</u>						Die $\tau_{rep} \%$ und $\eta_{rep} \%$ Werte sind gültig für den Drehmomentbereich $0 - 4,91 \cdot 10^{-3}$ Nm (50 cmp) $\tau_{rep} \%$ and $\eta_{rep} \%$ values apply to the torque range of $0 - 4,91 \cdot 10^{-3}$ Nm (50 cmg)				

RM 30 Stufe/step	1	2	3	4	5	6	7	8	9	10
$D_{rep} [s^{-1}]$	0,233	0,316	0,430	0,584	0,794	1,080	1,467	1,995	2,71	3,69
$\eta_{rep} \% [mPa \cdot s]$	250	184,3	135,4	99,7	73,4	53,9	39,7	29,2	21,5	15,78
RM 30 Stufe/step	11	12	13	14	15	16	17	18	19	20
$D_{rep} [s^{-1}]$	5,01	6,81	9,26	12,56	17,11	23,3	31,6	43,0	58,4	79,4
$\eta_{rep} \% [mPa \cdot s]$	11,62	8,55	6,29	4,64	3,40	2,50	1,843	1,354	0,997	0,734
RM 30 Stufe/step	21	22	23	24	25	26	27	28	29	30
$D_{rep} [s^{-1}]$	108,0	146,7	199,5	271	369	501	681	926	1256	1711
$\eta_{rep} \% [mPa \cdot s]$	0,539	0,397	0,292	0,215	0,1578	0,1162	0,0855	0,0629	0,0464	0,0340

Datum <u>19.10.84</u> Visum <u>Scht.</u>	CM 301 284-Z
--	--------------

A3.3. Calculation of Mean Value and Standard Deviation of Φ_i between the Parallel Shearing Plates

The phase-inversion results at $N = 1480$ rpm and $s = 0.5$ mm for the Liquid Paraffin-Water system between parallel shearing glass plates was chosen as an example of calculating the mean value and standard deviation of Φ_i . The above values were calculated from the flow rate readings at the point of inversion for the aqueous and the organic phase respectively, taken after repeating the experiment ten times. The following table shows the flow rates at inversion of the aqueous and the organic phases at each repetition, Q_{w_i} and Q_{o_i} respectively, their ratio, R_i , and the corresponding Φ_i , for the example chosen.

The same procedure was followed for each liquid-liquid system used and for the different materials of the plates and different gap widths and rotational speeds.

Table A3.3

Example of Calculating the Mean Value and Standard Deviation of Φ_i
between the Parallel Shearing Plates

Q_{w_i} [cm ³ min ⁻¹]	Q_{o_i} [cm ³ min ⁻¹]	R_i	Φ_i
45	22.50	1.765	0.362
45	24.75	1.818	0.355
42	23.25	1.806	0.356
40	23.25	1.720	0.368
40	22.50	1.778	0.360
35	19.00	1.842	0.352
35	18.00	1.944	0.339
32	17.00	1.882	0.347
30	17.00	1.765	0.362
30	16.25	1.846	0.351
			Mean value, $\bar{\Phi}_i$
			0.355
			Standard deviation, σ_{Φ_i}
			0.008

A3.4. Calculation of Mean Values and Standard Deviations of Φ_i and Total Flow Rate at the Point of Inversion in the Horizontal Glass Tube

Some of the phase-inversion results in the horizontal glass tube for the Escaid - 20% w/v CaCl_2 aq. soln. system were chosen as an example of calculating the mean values and standard deviations of the volume fraction of the organic phase and the total flow rate at the point of inversion. The above values were calculated from the flow rate readings at the point of inversion, which were taken after repeating the experiment five times under the same conditions. The case of the organic phase being introduced through the T-branch was chosen when phase inversion was approached from an oil-in-water leading to a water-in-oil dispersion, since under those conditions the effect of the wettability of the tube on observing an apparent volume fraction at inversion was negligible.

Since the initial type of dispersion was of the oil-in-water type, phase inversion was approached by starting with a constant flow rate of the aqueous phase, Q_w , and increasing the flow rate of the organic phase, Q_o . The following table shows the observed values of the total flow rate at the point of inversion, Q_{T_i} , and the calculated volume fraction of the organic phase at that point, Φ_i , based on the observed changes in conductivity, as in the example shown in Figure A3.4. Φ_i was calculated from the relation

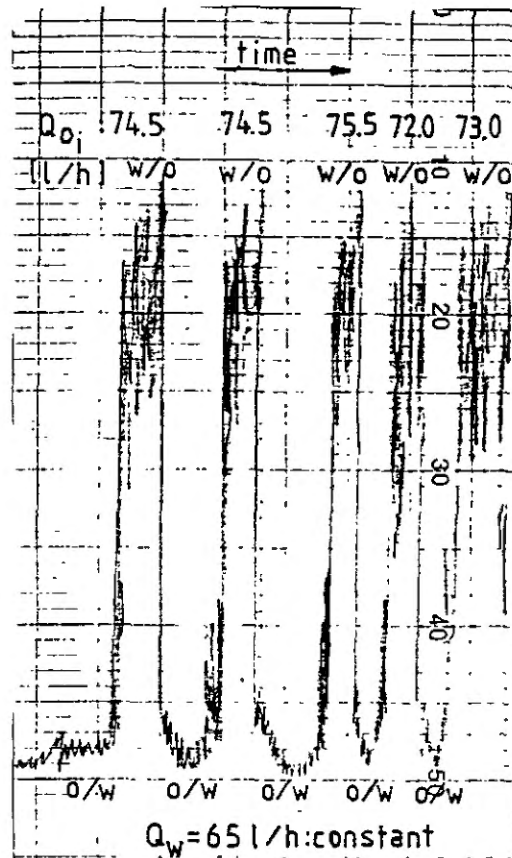
$$\Phi_i = \frac{1}{1 + Q_w/Q_{o_i}}.$$

Table A3.4

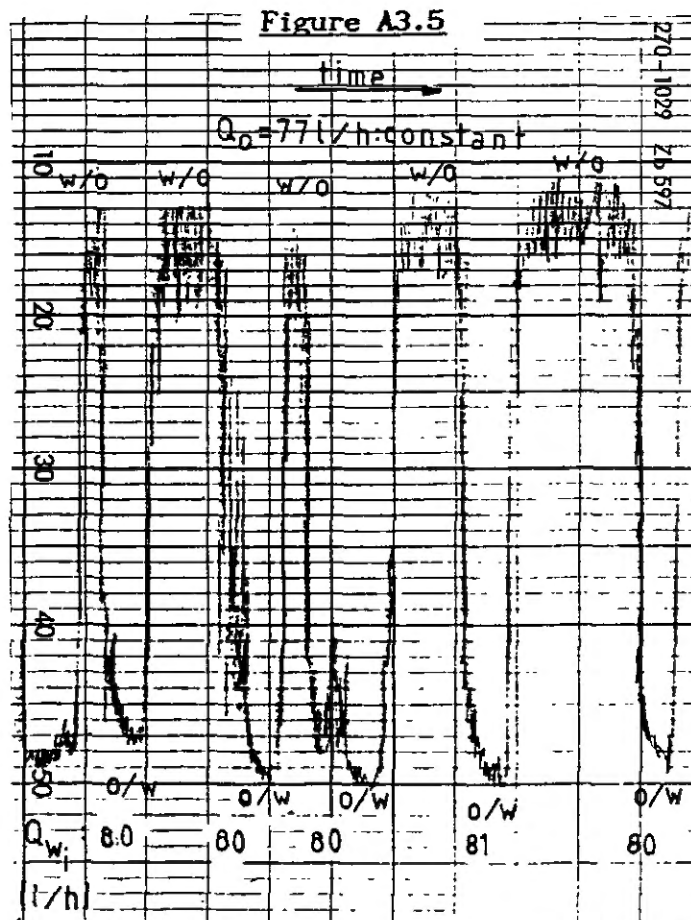
Example of Calculating Mean Values and Standard Deviations
of Q_{T_i} and Φ_i in the Horizontal Glass Tube

Q_w [ℓ/h]	Q_{o_i} [ℓ/h]	Q_{T_i} [ℓ/h]	Φ_i
65	74.5	139.5	0.534
65	74.5	139.5	0.534
65	75.5	140.5	0.537
65	72.0	137.0	0.526
65	73.0	138.0	0.529
		Mean value	
		139	0.532
		Standard deviation	
		1.39	0.004

Figure A3.4



Example of Change in Conductivity at the Point of Inversion from O/W to W/O Dispersion in the Horizontal Glass Tube



Example of Change in Conductivity at the Point of Inversion from W/O to O/W Dispersion in the Horizontal Glass Tube

A3.5. Calculation of the Factor $\cos\theta We^{-0.5} Re^{0.15}$ using Phase-Inversion Results in the Horizontal Glass Tube

An example of calculating the factor $\cos\theta We^{-0.5} Re^{0.15}$ of Equation 5.4 is presented in the following table, based on the phase-inversion results in the horizontal glass tube for the Escaid-20% w/v CaCl_2 aq. soln. system. The case of the organic phase being introduced through the T-branch was chosen when phase inversion was approached from an oil-in-water leading to a water-in-oil dispersion, as in the previous example. The calculation of the factor $\cos\theta We^{-0.5} Re^{0.15}$ is based on the following equations:

$$We = \frac{\rho_m V_{T_i}^2 D}{\sigma} \quad (5.5)$$

$$Re = \frac{\rho_m V_{T_i} D}{\mu_m} \quad (5.6)$$

$$\rho_m = \Phi_1 \rho_o + (1-\Phi_1) \rho_w \quad (2.26)$$

$$\mu_m = \Phi_1 \mu_o + (1-\Phi_1) \mu_w \quad (2.27)$$

where $V_{T_i} = 4Q_{T_i} / \pi D^2$: total average velocity of the dispersion at the point of inversion;

Q_{T_i} : total flow rate at the point of inversion;

D : diameter of the tube;

ρ_o, ρ_w : densities of the organic and aqueous phase respectively;

μ_o, μ_w : viscosities of the organic and aqueous phase respectively;

θ : contact angle of the liquid-liquid interface with the glass tube wall (measured through the aqueous phase);

σ : interfacial tension.

For the Escaid-20%w/v CaCl_2 aq. soln. system $\sigma = 28.5 \times 10^{-3} \text{ Nm}^{-1}$, $\rho_o = 811 \text{ kgm}^{-3}$, $\rho_w = 1120 \text{ kgm}^{-3}$, $\mu_o = 1.64 \times 10^{-3} \text{ Pas}$, $\mu_w = 10^{-3} \text{ Pas}$ and $\theta = 78^\circ$.

Table A3.5

Example of Calculating $\cos\theta We^{-0.5} Re^{0.15}$ at the Point of Inversion in the Horizontal Glass Tube

V_{T_i} [m/s]	Φ_i	ρ_m [kgm ⁻³]	$\mu_m \times 10^3$ [Pas]	We	Re	$\cos\theta We^{-0.5} Re^{0.15}$
0.350	0.595	936	1.4	40	2373	0.105
0.364	0.564	946	1.4	44	2529	0.102
0.400	0.558	947	1.4	53	2793	0.094
0.435	0.553	949	1.4	63	3049	0.087
0.470	0.549	950	1.4	74	3305	0.082
0.481	0.529	958	1.3	78	3451	0.080
0.492	0.532	956	1.3	81	3507	0.079
0.527	0.531	956	1.3	93	3760	0.074
0.552	0.551	950	1.4	101	3876	0.071
0.566	0.531	956	1.3	107	4038	0.070
0.569	0.535	955	1.3	108	4047	0.069
0.605	0.531	956	1.3	123	4316	0.066
0.640	0.557	948	1.4	136	4472	0.063
0.654	0.540	953	1.3	143	4632	0.062
0.654	0.540	943	1.3	143	4632	0.062
0.697	0.543	952	1.3	162	4925	0.058
0.707	0.551	950	1.4	167	4964	0.058
0.732	0.541	953	1.3	179	5181	0.056
0.775	0.544	952	1.3	201	5472	0.053
0.796	0.556	948	1.4	211	5567	0.052
0.828	0.552	949	1.4	228	5809	0.050
0.874	0.554	949	1.4	254	6122	0.048
0.905	0.552	949	1.4	273	6349	0.047
0.962	0.558	948	1.4	308	6717	0.044

NOTATION

- D : diameter of the tube
 d_{\max} : maximum droplet diameter of the dispersed phase
 N : rotational speed
 Q_o : flow rate of the organic phase
 Q_{o_i} : flow rate of the organic phase at inversion
 Q_w : flow rate of the aqueous phase
 Q_{w_i} : flow rate of the aqueous phase at inversion
 Q_{T_i} : total flow rate in the tube at inversion
 Re : Reynolds number (Equations 4.1, 4.5 and 5.6)
 R_i : ratio of the aqueous flow rate to the organic flow rate at inversion
 r : radius of the plates
 s : gap width between the plates
 Ta : Taylor number (Equation 4.2)
 V_{T_i} : total velocity of the dispersion in the tube at inversion
 v' : turbulent fluctuation velocity
 We : Weber number (Equation 5.5)
 O/W : oil-in-water type of dispersion
 W/O : water-in-oil type of dispersion

Greek Symbols

- $\dot{\gamma}$: shear rate
 ϵ : energy dissipation rate per unit mass
 θ : contact angle
 μ_c : viscosity of the continuous phase
 μ_d : viscosity of the dispersed phase
 μ_m : viscosity of the dispersion

- μ_o : viscosity of the organic phase
 μ_w : viscosity of the aqueous phase
 ρ_c : density of the continuous phase
 ρ_d : density of the dispersed phase
 ρ_m : density of the dispersion
 ρ_o : density of the organic phase
 ρ_w : density of the aqueous phase
 σ : interfacial tension
 Φ_i : volume fraction of the organic phase at inversion
 Φ_{d_i} : volume fraction of the dispersed phase at inversion

Statistical Symbols

- \bar{Q}_T : mean total flow rate in the tube at inversion
 σ_{Q_T} : standard deviation of total flow rate in the tube at inversion
 $\bar{\Phi}_i$: mean volume fraction of the organic phase at inversion
 $\bar{\bar{\Phi}}_i$: average of the mean volume fractions of the organic phase at inversion
 σ_{Φ_i} : standard deviation of the volume fraction of the organic phase at inversion
 inversion

REFERENCES

- Allak, A.M.A. and Jeffreys, G.V., 1974. Studies of Coalescence and Phase Separation in Thick Dispersion Bands, A.I.Ch.E.J., 20, 564.
- Arai, H. and Shinoda, K., 1967. The Effect of Mixing of Oils and of Nonionic Surfactant on the Phase Inversion Temperatures of Emulsions, J. Colloid Interface Sci., 25, 396.
- Arashmid, M. and Jeffreys, G.V., 1980. Analysis of the Phase Inversion Characteristics of Liquid-Liquid Dispersions, A.I.Ch.E.J., 26, 51.
- Barnea, E. and Misrahi, J., 1975. Separation Mechanism of Liquid-Liquid Dispersions in a Deep Layer Gravity Settler. Part 3: Hindered Settling and Drop-to-Drop Coalescence in the Dispersion Band, Trans. Inst. Chem. Eng., 53, 75.
- Bayley, F.J. and Conway, L. 1964. Fluid Friction and Leakage between a Stationary and a Rotating Disk, J. Mech. Eng. Sc., 6, 164.
- Bayley, F.J. and Owen, J.M., 1969. Flow between a Rotating and a Stationary Disk, The Aeronautical Quarterly, 20, 333.
- Becher, P., 1959. The Effect of the Nature of the Emulsifying Agent on Emulsion Inversion, J. Soc. Cosmet. Chem., 9, 141.
- Becher, P., 1965. Emulsions, Theory and Practice, Reinhold Publishing Co., N.Y.
- Benton, E.R., 1968. A Composite Ekman Boundary Layer Problem, Tellus, 20, 667.
- Bird, R.B., Stewart, W.E. and Lightfoot, E.N., 1960. Transport Phenomena, John Wiley & sons, New York.
- Brodkey, R.S., 1967. The Phenomena of Fluid Motions, Addison-Wesley, Reading, Massachusetts.
- Broughton, G. and Squires, L., 1938. The Viscosity of Oil-Water Emulsions, J. Phys. Chem., 42, 253.
- Calderbank, P.H., 1958. Physical Rate Processes in Industrial Fermentation, Part I: The Interfacial Area in Gas-Liquid Contacting with Mechanical Agitation, Trans. Instn. Chem. Engrs, 36, 443.
- Charles, M.E., Govier, G.W. and Hodgson, G.W. 1961. The Horizontal Pipeline Flow of Equal Density Oil-Water Mixtures, Can. J. Chem. Eng., 39, 27.
- Cheesman, D.F. and King, A., 1938. The Properties of Dual Emulsions, Trans. Faraday Soc., 34, 594.
- Clarke, S.I. and Sawistowski, H., 1978. Phase Inversion of Stirred Liquid-Liquid Dispersions under Mass Transfer Conditions, Trans. I. Chem. E., 56, 50.
- Clay, P.H., 1940. The Mechanism of Emulsion Formation in Turbulent Flow, I: Experimental Part, K. Nederlandsche Academie van Wetenschappen (Amsterdam), Section of Sciences Proceedings, 43, 852.

- Clay, P.H., 1940. The Mechanism of Emulsion Formation in Turbulent Flow, II: Theoretical Part and Discussion, K. Nederlandsche Academie van Wetenschappen (Amsterdam), Section of Sciences Proceedings, 43, 979.
- Clayton, W., 1954. The Theory of Emulsions and their Technical Treatment, 5th Ed. by C.G. Sumner, J. and A. Churchill Ltd., London.
- Cockbain, E.G. and McRoberts, T.S., 1953. The Stability of Elementary Emulsion Drops and Emulsions, J. Colloid Sci., 8, 440.
- Collins, S.B. and Knudsen, J.G., 1970. Drop-Size Distributions Produced by Turbulent Pipe Flow of Immiscible Liquids, A.I.Ch.E.J., 16, 1072.
- Cooper, P. and Reshotko, E., 1975. Turbulent Flow between a Rotating Disk and a Parallel Wall, AIAA J., 13, 573.
- Coulaloglou, C.A., and Tavlaides, L.L., 1976. Drop Size Distributions and Coalescence Frequencies of Liquid-Liquid Dispersions in Flow Vessels, A.I.Ch.E.J., 22, 289.
- Daily, J.W. and Nece, R.E., 1960. Chamber Dimension Effects on Induced Flow and Frictional Resistance of Enclosed Rotating Disks, Trans. of the ASME, series D: Journal of Basic Eng., 82, 217.
- Davies, J.T., 1957. A Quantitative Kinetic Theory of Emulsion Type, 1: Physical Chemistry of the Emulsifying Agent, Proc. 2nd Int. Congr. Surface Activity, 1, London, 426.
- Davies, J.T., 1960. A Quantitative Kinetic Theory of Emulsion Type, 2: Hydrodynamic Factors, Proc. 3rd Int. Congr. Surface Activity, Cologne, 585.
- Davies, J.T., 1985. Drop Sizes of Emulsions Related to Turbulent Energy Dissipation Rates, Chem. Eng. Sc., 40, 839.
- Davies, J.T., 1987. A Physical Interpretation of Drop Sizes in Homogenizers and Agitated Tanks, including the Dispersion of Viscous Oils, Chem. Eng. Sc., 42, 1671.
- Davies, J.T. and Rideal, E.K., 1963. Interfacial Phenomena, 2nd Ed., Academic Press, N.Y. and London.
- Dickinson, E., 1981. Interpretation of Emulsion Phase Inversion as a Cusp Catastrophe, J. Colloid Interface Sci., 84, 284.
- Dickinson, W., and Iball, J., 1948. Oil/Water Emulsions: Some Physical Factors which Determine the Type of Emulsion, Research Supplement, 1, 614.
- Efthimiadu, I., 1986. Dispersion of Viscous Oils in Turbulent Aqueous Solutions, M.Sc. Thesis, Department of Chemical Engineering, University of Birmingham.
- Garner, F.H. and Mina, P., 1959. Effect of Chain Length and Structure of Organic Compounds in Water, Trans. Faraday Soc., 5, 1616.
- Gilchrist, A., Dyster, K.N., Moore, I.P.T., Nienow, A.W. and Carpenter, K.J., 1989. Delayed Phase Inversion in Stirred Liquid-Liquid Dispersions, Chem. Eng. Sc., 44, 2381.

- Gillespie, T. and Rideal, E.K., 1956. The Coalescence of Drops at an Oil/Water Interface, Trans. Faraday Soc., 52, 173.
- Griffin, W.C., 1954. Calculation of H.L.B. values of Non-Ionic Surfactants, J. Soc. Cosm. Chem., 5, 249.
- Guggenheim, E.A., 1940. The Thermodynamics of Interfaces in Systems of Several Components, Trans. Faraday Soc., 36, 397.
- Guilinger, T.R., Grislingas, A.K. and Erga, C., 1988. Phase Inversion Behaviour of Water-Kerosene Dispersions, Ind. Eng. Chem. Res., 27, 978.
- Hasson, D., Mann, U. and Nir, A., 1970. Annular Flow of Two Immiscible Liquids, I. Mechanism, Can. J. Chem. Engng., 48, 514.
- Hinze, J.O., 1955. Fundamentals of the Hydrodynamic Mechanism of Splitting in Dispersion Processes, A.I.Ch.E.J., 11, 289.
- Hooper, A.P. and Boyd, W.G.C., 1983. Shear-flow Instability at the Interface between Two Viscous Fluids, J. Fluid Mech., 128, 507.
- Hossain, K.T., Sarkar, S., Munford, C.J. and Phillips, G.R., 1983. Hydrodynamics of Mixer Settlers, Ind. Eng. Chem. Process design and development, 22, 553.
- Howarth, W.J., 1964. Coalescence of Drops in a Turbulent Flow Field, Chem. Eng. Sc., 19, 33.
- Howarth, W.J., 1967. Measurement of Coalescence Frequency in an Agitated Tank, A.I.Ch.E.J., 13, 1007.
- Hughmark, G.A., 1971. Drop Breakup in Turbulent Pipe Flow, A.I.Ch.E.J., 17, 1000.
- Jellinek, H.H.G. and Anson, H.A., 1949. α -Monostearin and Sodium Stearate as Emulsifying Agents, J. Soc. Chem Ind., 68, 108.
- Joseph, D.D., Nguyen, K. and Beavers, G.S., 1984. Non-uniqueness and Stability of the Configuration of Flow of Immiscible Fluids with Different Viscosities, J. Fluid Mech., 141, 319.
- Lawrence, A.S.C., and Mills, O.S., 1954. Kinetics of the Coagulation of Emulsions, Disc. Faraday Soc., 18, 98.
- Lawson, G.B., 1967. Coalescence Processes, Chem. and Proc. Eng., 48, 45.
- Levich, V.G., 1962. Physicochemical Hydrodynamics, Prentice Hall, New Jersey.
- Lewis, W.C.M., 1934. On Adherence and Coalescence in Emulsions, Trans. Faraday Soc., 30, 958.
- Lissant, K.J., 1966. The Geometry of High-Internal-Phase-Ratio Emulsions, J. Colloid Interface Sci., 22, 462.
- Lissant, K.J., Peace, B.W., Wu, S.H. and Mayhan, K.G., 1974. Structure of High-Internal-Phase-Ratio Emulsions, J. Colloid Interface Sci., 47, 416.

- Lughning, R.W. and Sawistowski, H., 1971. Phase Inversion in Stirred Liquid-Liquid Systems, Solvent Extraction, Proc. I.S.E.C., 2, 873.
- Madden, A.J. and Damerell, G.L. 1962. Coalescence Frequencies in Agitated Liquid-Liquid Systems, A.I.Ch.E.J., 8, 233.
- Maraschino, M.J. and Treybal, R.E., 1971. The Coalescence of Drops in Liquid-Liquid Fluidised Beds, A.I.Ch.E.J., 17, 1174.
- Merchuk, J.C., Shai, R. and Wolf, D., 1980. Experimental Study of Copper Extraction with LIX-64N by Means of Motionless Mixers, Ind. Eng. Chem. Process Des. Dev., 19, 91.
- Merchuk, J.C., Wolf, D., Shai, R. and White, D.H., 1980. Experimental Study of Dispersion and Separation of Phases in Liquid-Liquid Extraction of Copper by LIX 64N in Various Types of Mixers, Ind. Eng. Chem. Process Des. Dev., 19, 522.
- Mersmann, A. and Grossman, H., 1982. Dispersion of Immiscible Liquids in Agitated Vessels, Int. Chem. Eng., 22, 581.
- Middleman, S., 1974. Drop Size Distributions Produced by Turbulent Pipe Flow of Immiscible Fluids through a Static Mixer, Ind. Eng. Chem. Process Des. Dev., 13, 78.
- Miller, R.S., Ralph, J.L., Curl, R.L. and Towell, G.D., 1963. Dispersed Phase Mixing, II: Measurements in Organic Dispersed Systems, A.I.Ch.E.J., 9, 196.
- Mukherjee, D., Biswas, M.N. and Mitra, A.K., 1988. Hydrodynamics of Liquid-Liquid Dispersion in Ejectors and Vertical Two Phase Flow, Can. J. Chem. Eng., 66, 896.
- McClarey, M.J. and Mansoori, G.A., 1978. Factors Affecting the Phase Inversion of Dispersed Immiscible Liquid-Liquid Mixtures, A.I.Ch.E. Symposium Series, No. 173, 74, 134.
- Nielsen, L.E., Wall, R. and Adams, G., 1958. Coalescence of Liquid Drops at Oil/Water Interfaces, J. Colloid Sci., 13, 441.
- Parke, J.B., 1933. The Phase Volume Theory and the Homogenisation of Concentrated Emulsions, Part I, J. Chem. Soc., 1458.
- Parke, J.B., 1934. Homogenisation of Concentrated Emulsions, Part II, J. Chem. Soc., 1112.
- Paul, H.I. and Sleicher, C.A., Jr., 1965. The Maximum Stable Drop Size in Turbulent Flow: Effect of Pipe Diameter, Chem. Eng. Sc., 20, 57.
- Quinn, J.A. and Sigloh, D.B., 1963. Phase Inversion in the Mixing of Immiscible Liquids, Can. J. Chem. Eng., 41, 15.
- Renardy, Y. and Joseph, D.D., 1985. Couette Flow of Two Fluids between Concentric Cylinders, J. Fluid Mech., 150, 381.
- Rodger, W.A., Trice, V.G., Jr., and Rushton, J.H., 1956. Effect of Fluid Motion on Interfacial Area of Dispersions, Chem. Eng. Prog., 52, 515.

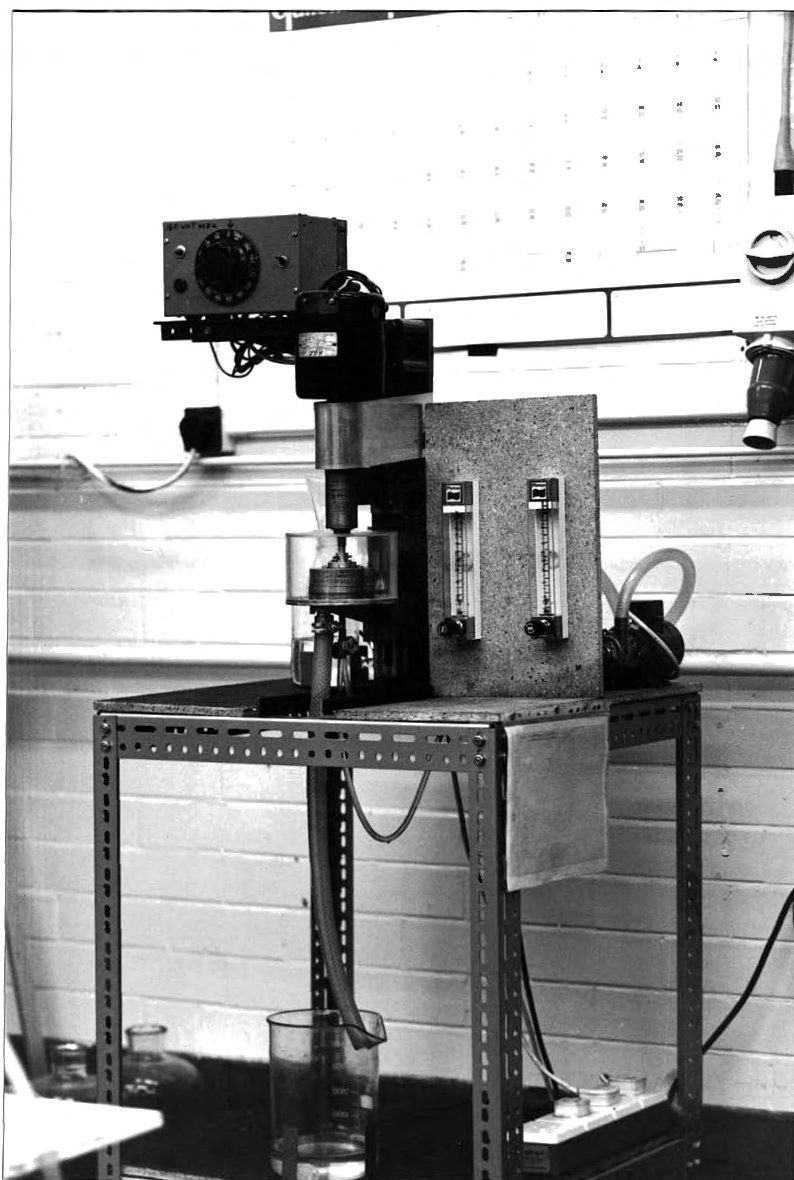
- Rumscheidt, F.D. and Mason, S.G., 1961. Particle Motions in Sheared suspensions, XII: Deformation and Burst of Fluid Drops in Shear and Hyperbolic Flow, J. Colloid Sci., **16**, 238.
- Russell, T.W.F., Hodgson, G.W. and Govier, G.W., 1959. Horizontal Pipeline Flow of Mixtures of Oil and Water, Can. J. Chem. Eng., **37**, 9.
- Saffman, P.G. and Taylor, G.I., F.R.S., 1958. The Penetration of a Fluid into a Porous Medium of Hele-Shaw Cell Containing a More Viscous Fluid, Proc. Roy. Soc. of London A, **245**, 312.
- Saito, H. and Shinoda, K., 1970. The Stability of W/O Type Emulsions as a Function of Temperature and of the Hydrophilic Chain Length of the Emulsifier, J. Colloid Interface Sci., **32**, 647.
- Sarkar, S., Phillips, C.R., Mumford, C.J. and Jeffreys, G.V., 1980. Mechanisms of Phase Inversion in Rotary Agitated Columns, Trans. I. Chem. E., **58**, 43.
- Schlichting, H., 1955. Boundary Layer Theory, 1st Ed., Pergamon Press, London.
- Schulman, J.H. and Cockbain, E.G., 1940. Molecular Interactions at Oil/Water Interfaces, Part I: Molecular Complex Formation and the Stability of Oil-in-Water Emulsions, Trans. Faraday Soc., **36**, 651.
- Schulman, J.H. and Cockbain, E.G., 1940. Molecular Interactions at Oil/Water Interfaces, Part II: Phase Inversion and Stability of Water-in-Oil Emulsions, Trans. Faraday Soc., **36**, 661.
- Selker, A.H. and Sleicher, C.A., Jr., 1965. Factors Affecting which Phase will Disperse when Immiscible Liquids are Stirred Together, Can. J. Chem. Eng., **43**, 298.
- Sembira, A.N., Merchuk, J.C. and Wolf, D., 1986. Characteristics of a Motionless Mixer for Dispersion of Immiscible Fluids, 1: A Modified Electrosensitivity Probe Technique, Chem. Eng. Sc., **41**, 445.
- Sherman, P., 1968. Emulsion Science, 1st Ed., Academic Press, London and N.Y.
- Shinnar, R., 1961. On the Behaviour of Liquid Dispersions in Mixing Vessels, J. Fluid Mech., **10**, 259.
- Shinnar, R. and Church, J.M., 1960. Predicting Particle Size in Agitated Dispersions, Ind. Eng. Chem., **52**, 253.
- Shinoda, K., 1967. The Correlation between the Dissolution State of Nonionic Surfactant and the Type of Dispersion Stabilized with the Surfactant, J. Colloid Interface Sci., **24**, 4.
- Shinoda, K. and Saito, H., 1968. The Effect of Temperature on the Phase Equilibria and the Types of Dispersions of the Ternary System Composed of Water, Cyclohexane and Nonionic Surfactant, J. Colloid Interface Sci., **26**, 70.
- Shinoda, K. and Saito, H., 1969. The Stability of O/W Type Emulsions as Functions of Temperature and the H.L.B. of Emulsifiers. The Emulsification by PIT-method, J. Colloid Interface Sci., **30**, 258.

- Sleicher, C.A., Jr., 1962. Maximum Stable Drop Size in Turbulent Flow, A.I.Ch.E.J., 8, 471.
- Smith, D.H., 1985. The Role of Critical Points and the Phase Inversion Temperature. Evidence from the Cyclohexane/Water/ $i\text{-C}_9\text{H}_{19}\text{C}_6\text{H}_4(\text{OC}_2\text{H}_4)_{9.2}\text{OH}$ /Temperature Diagram, J. Colloid Interface Sci., 108, 471.
- Soo, S.L., 1958. Laminar Flow over an Enclosed Rotating Disk, Trans. ASME, 80, 287.
- Speakman, J.B. and Chamberlain, N.H., 1933. The Emulsification of Mixed Liquids of High Molecular Weight, Trans. Faraday Soc., 29, 358.
- Stamm, A.J. and Kraemer, E.O., 1926. A Note on the Mechanism of Emulsification, J. Phys. Chem., 30, 992.
- Sternling, C.V. and Scriven, L.E., 1959. Interfacial Turbulence: Hydrodynamic Instability and the Marangoni Effect, A.I.Ch.E.J., 5, 514.
- Szeri, A.Z. and Adams, M.L., 1978. Laminar Throughflow between Closely Spaced Rotating Discs, J. Fluid Mech., 86, 1.
- Tartar, H.Y., Dunkan, C.W., Shea, T.F. and Ferrier, W.K., 1929. The Effect of Electrolytes upon Emulsions, J. Phys. Chem., 33, 435.
- Taylor, G.I., F.R.S., 1932. The Viscosity of a Fluid Containing Small Drops of Another Fluid, Proc. Roy. Soc. (London), A138, 41.
- Taylor, G.I., F.R.S., 1934. The Formation of Emulsions in Definable Fields of Flow, Proc. Roy. Soc. (London), A146, 501.
- Tidhar, A.M., Merchuk, J.C., Sembira, A.N. and Wolf, D., 1986. Characteristics of a Motionless Mixer for Dispersion of Immiscible Fluids, 2: Phase Inversion of Liquid-Liquid Systems, Chem. Eng. Sc., 41, 457.
- Tomotika, S., D.Sc., 1935. On the Instability of a Cylindrical Thread of a Viscous Liquid Surrounded by Another Viscous Fluid, Proc. Roy. Soc. (London), A150, 322.
- Tomotika, S., D.Sc., 1936. Breaking up of a Drop of Viscous Liquid Immersed in Another Viscous Fluid which is Extending at a Uniform Rate, Proc. Roy. Soc. (London), A153, 302.
- Treybal, R.E., 1951. Liquid Extraction, 1st Ed., McGraw Hill, N.Y.
- Treybal, R.E., 1958. Estimation of the Stage Efficiency of Simple Agitated Vessels used in Mixer-Settler Extractors, A.I.Ch.E.J., 4, 202.
- Tryggvason, G. and Aref, H., 1983. Numerical Experiments on Hele-Shaw Flow with a Sharp Interface, J. Fluid Mech., 136, 1.
- Tsahalis, D.T., 1979. The Hydrodynamic Stability of Two Viscous Incompressible Fluids in Parallel Uniform Shearing Motion, Trans. ASME, E. J. Appl. Mech., 46, 499.

- Turner, H.E. and McCarthy, H.E., 1966. A Fundamental Analysis of Slurry Grinding, A.I.Ch.E.J., 12, 784.
- Vermeulen, Th., Williams, G.M. and Langlois, G.E., 1955. Interfacial Area in Liquid-Liquid and Gas-Liquid Agitation, Chem. Eng. Progr. 51, 85F.
- Vohra, D.K. and Hartland, S., 1981. Effect of Geometrical Arrangement and Interdrop Forces on Coalescence Time, Can. J. Chem. Eng., 59, 438.
- Walters, K., 1975. Rheometry, 1st Ed., Chapman and Hall, London.
- Weigner, G., 1931. Coagulation, J. Soc. Chem. Ind. (Transactions and Communications), 50, 55T.
- Wooding, R.A. and Morel-Seytoux, H.J., 1976. Multiphase Fluid Flow Through Porous Media, Am. Rev. Fluid Mech., 8, 233.
- Yeh, G.C., Haynie, C.A., Jr. and Moses, R.A., 1964. Phase-Volume Relationship at the Point of Phase Inversion in Liquid Dispersions, A.I.Ch.E.J., 10, 260.

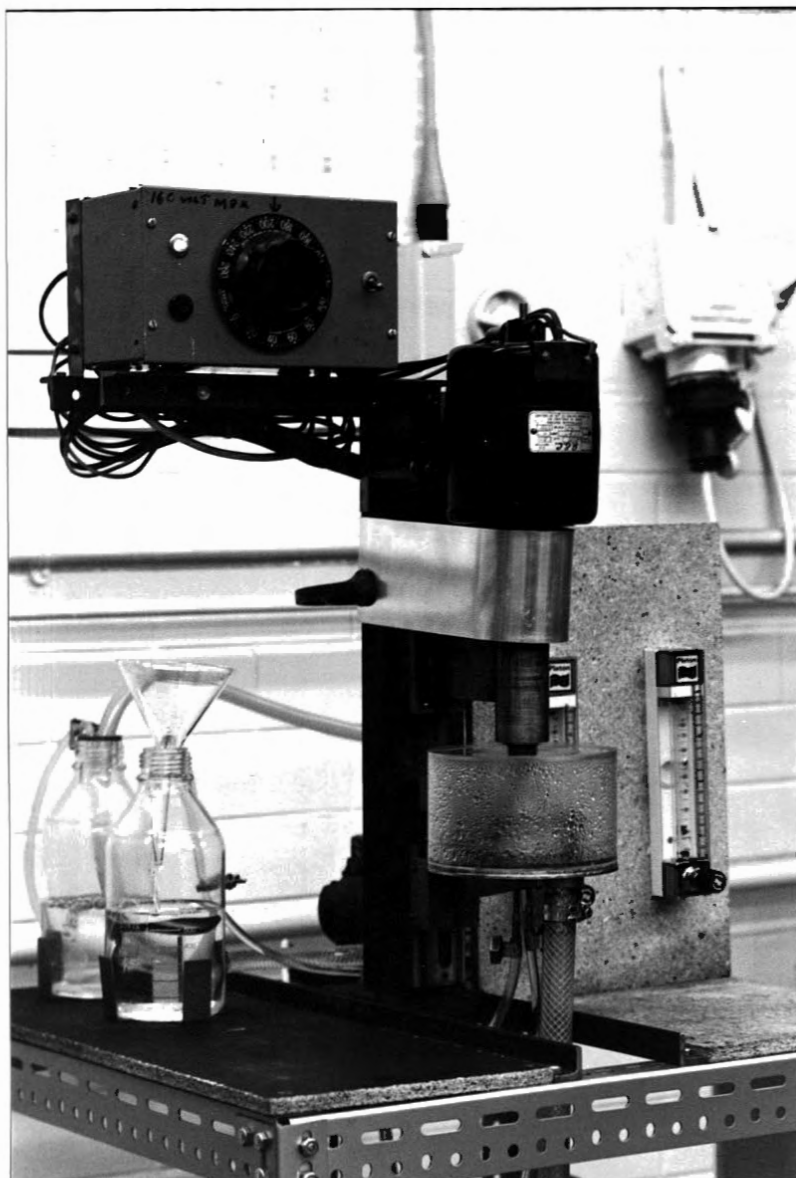
PLATES

Plate 1



The Continuous-Flow Emulsifying System of Parallel Shearing Plates

Plate 2



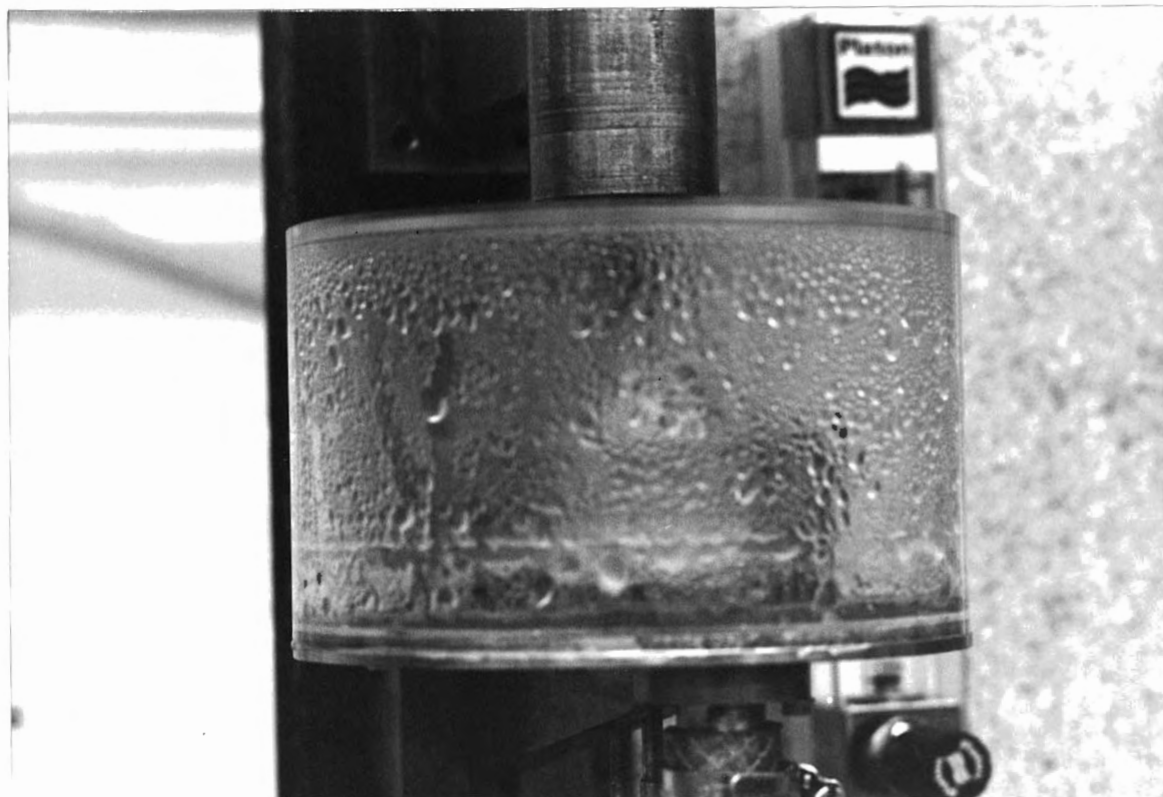
The Continuous-Flow Emulsifying System of Parallel
Shearing Plates under Operation

Plate 3



A Typical Example of the Formation of an
Oil-in-Water Dispersion in the System of Parallel
Shearing Plates

Plate 4

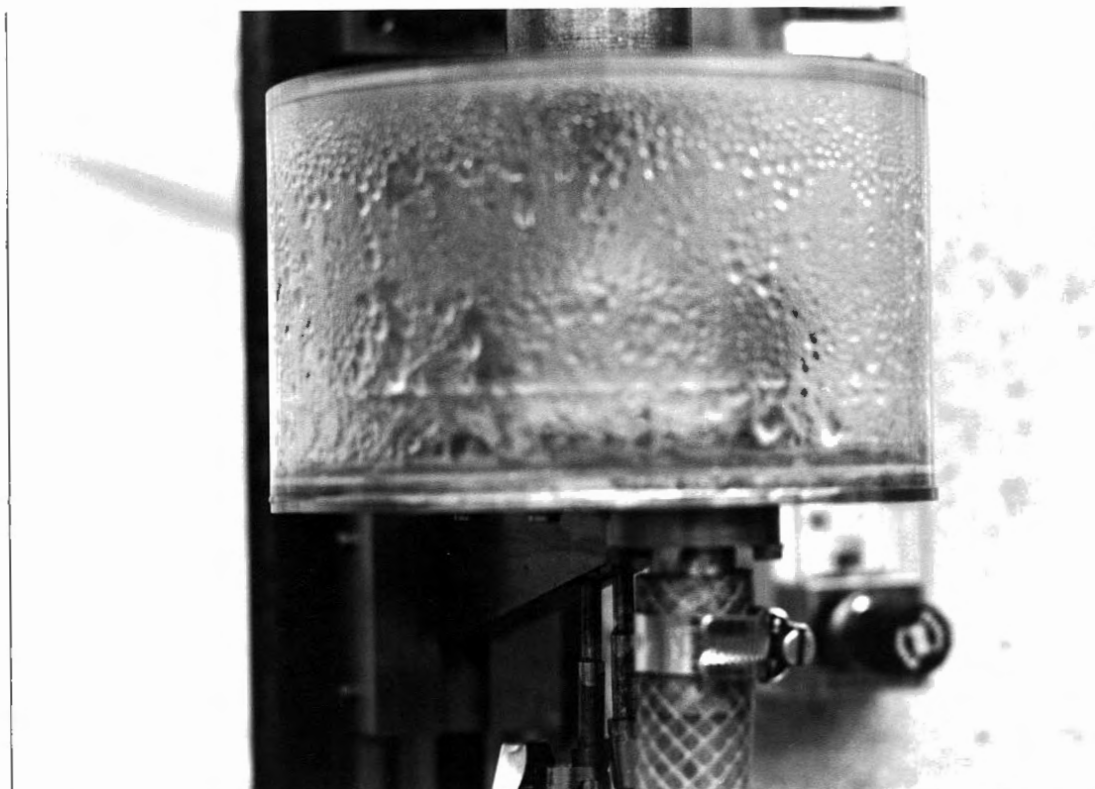


A Typical Example of the Formation of a Water-in-Oil
Dispersion in the System of Parallel Shearing Plates

Plate 5



(a)

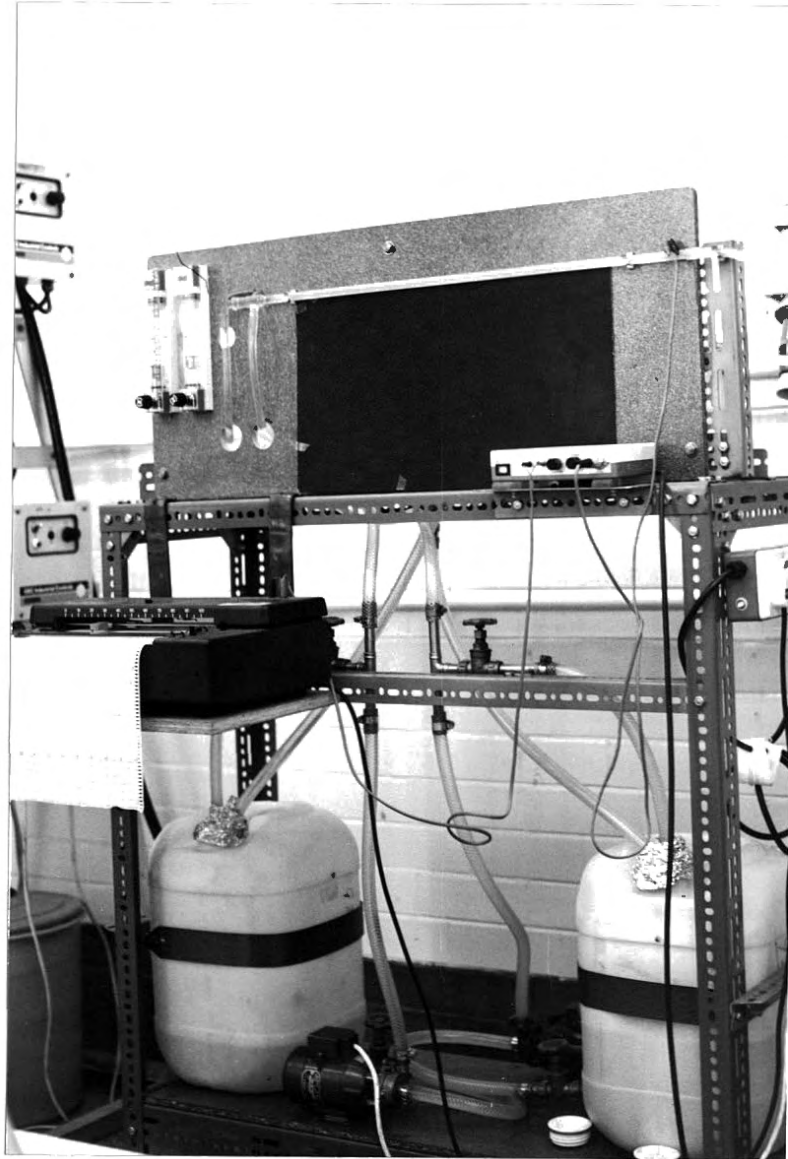


(b)

Phase Inversion of the Liquid Paraffin-Water System
with Stainless Steel Plates, $s = 0.1$ mm and
 $N = 1970$ rpm:

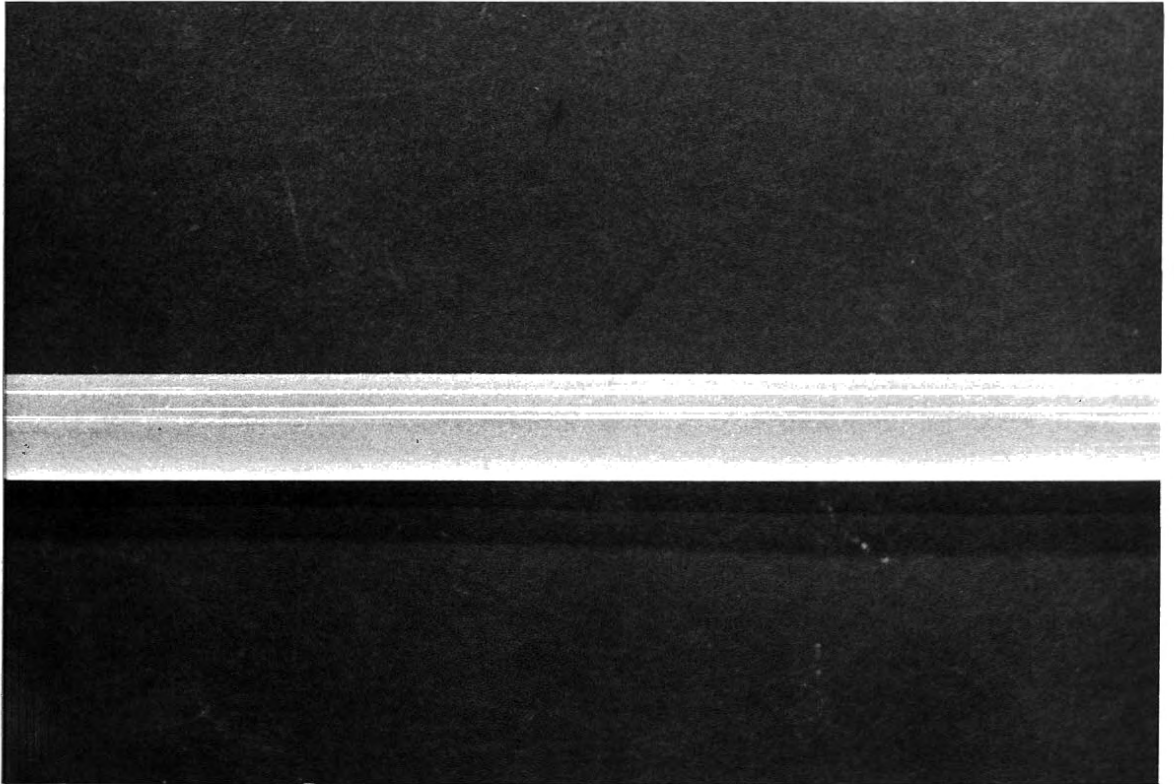
- (a) Oil-in-Water Dispersion before Phase Inversion
(b) Water-in-Oil Dispersion after Phase Inversion

Plate 6

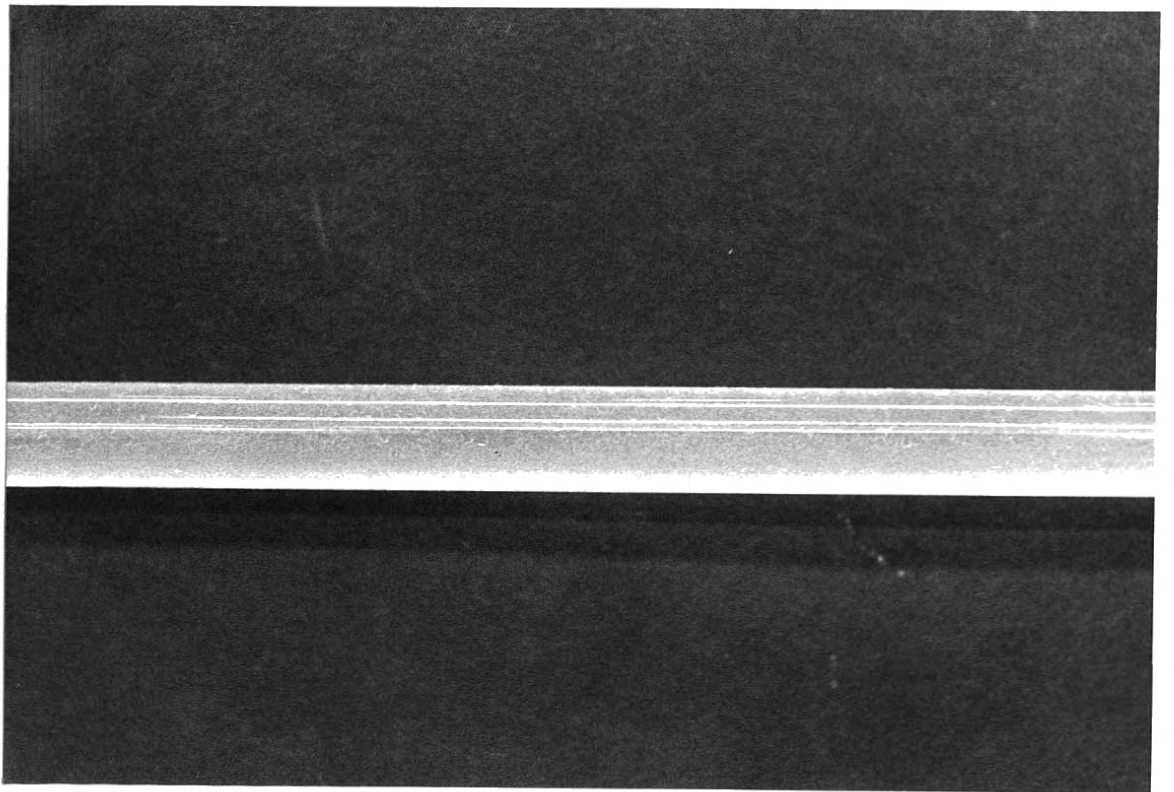


The Continuous-Flow System of the Horizontal Glass Tube

Plate 7



(a)



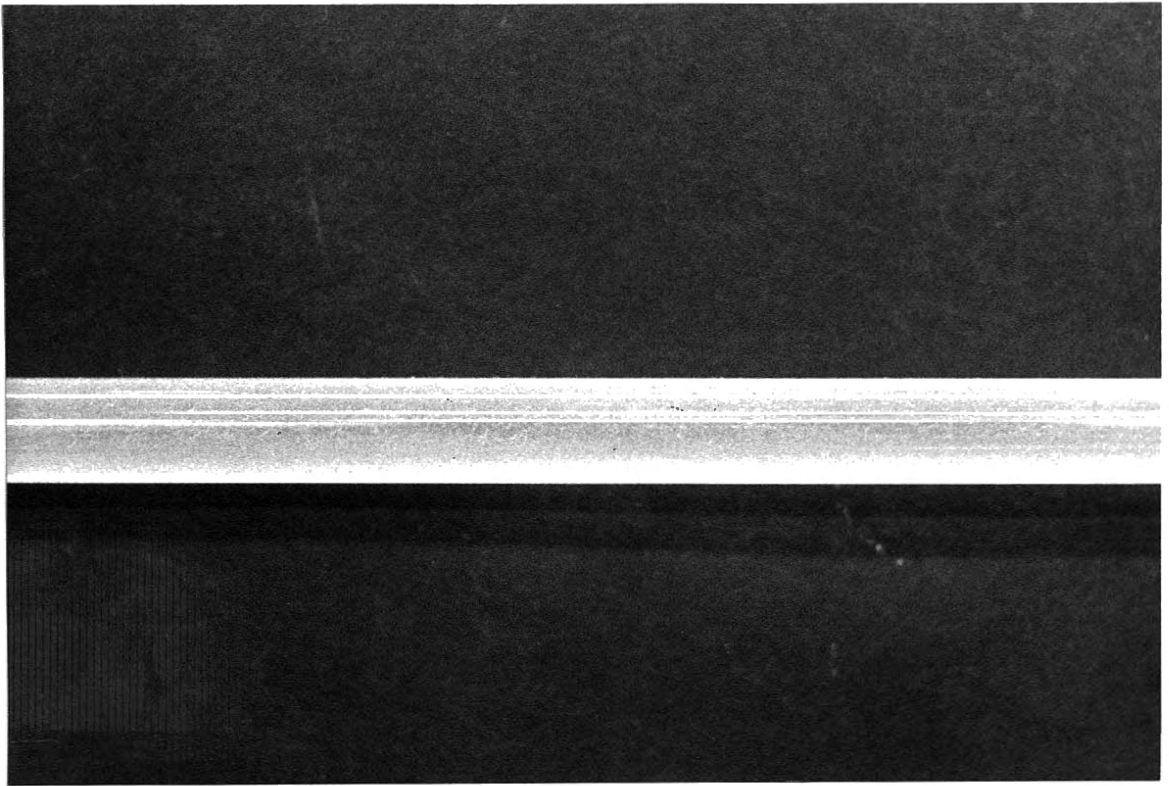
(b)

A Typical Example of Phase Inversion in the Horizontal Glass Tube:

(a) Oil-in-Water Dispersion at the Point of Inversion

(b) Water-in-Oil Dispersion after Inversion

Plate 8



(a)



(b)

A Typical Example of Phase Inversion in the Horizontal Glass Tube:

(a) Water-in-Oil Dispersion at the Point of Inversion

(b) Oil-in-Water Dispersion after Inversion